IRIDIUM CATALYZED C–H BORYLATION OF ARENES WITH N,B-TYPE DIBORON SPECIES AND Ir(I) ANIONIC COMPLEXES

By

Pauline Anna Mansour

A DISSERTATION

Submitted to
Michigan State University
in partial fulfillment of the requirements
for the degree of

Chemistry – Doctor of Philosophy

2024

ABSTRACT

Aryl boronic esters serve as synthetic intermediates for diverse applications in natural products, agrochemicals, and pharmaceuticals due to the abundance of transformations C–B bonds can undergo. These compounds are commonly synthesized in an atom-economical way by directly converting $C(sp^2)$–H bonds into C–B bonds using Ir-catalyzed C–H borylation (CHB) chemistry. Traditionally, this process favors the C–H bond in the least sterically congested position on substituted (hetero)aromatic ring systems. The work described here unveils novel CHB methods that are competent in targeting specific C–H bonds, thereby enabling the synthesis of a diverse set of compounds.

In recent years, a N,B-type dimeric pre-ligand (BB) emerged as the first spectator boryl species capable of steric-directed CHB using a 2:1 ratio of pre-ligand to Ir. Chapter 2 describes how this system was modified to direct borylation *ortho* to directing groups such as amides and esters by decreasing the ligand to metal ratio to 0.5:1, respectively. Additionally, it was found that maintaining the ligand to metal ratio at 2:1 while switching the Ir(I) pre-catalyst from $[Ir(OMe)cod]_2$ to $[IrCl(cod)]_2$ also led to the generation of chelate-directed products. These methods represent the first instances in which regiochemical switching is achieved by altering the reaction conditions as opposed to the ligand system.

The synthesis of the hypothesized pre-assembled catalyst, representing the system where BB loadings are decreased, was isolated and resulted in an Ir(III) cationic species ion pairing with $[IrCl_2(cod)]$ as the counteranion. Chapter 3 studies the role of this Ir(I) anionic species in catalysis, detailing a new mode of Ir-catalyzed CHB. This system demonstrates $[IrCl_2(cod)][NBu_4]$ as a competent catalyst for the transformation of C–H to C–B bonds, independent of external ligand or substrates bearing a directing group. Furthermore, it was found that the site of C–H activation is

influenced by the length of the alkyl chain in the ammonium cation, where $[NPr_4]^+$ increased the amount of *ortho* borylated product. Mechanistic experiments suggest this occurring through a heterogenous process that is distinct from classical homogenous CHB reactions that proceed via an Ir(III)/Ir(V) catalytic cycle.

To my family
Thank you for your unconditional love and support.

ACKNOWLEDGMENTS

I want to express my deepest gratitude to my parents, whose nurturing guidance in cultivating an understanding of culture, respect, and kindness has ultimately shaped the person I am today. Despite them hating how far away their daughter moved away after high school, they have consistently supported my decisions and eased my mental discomfort during difficult times. It is truly a blessing to have such powerful figures in my life, cheering me on every step of the way, and I owe my achievements to their unwavering love and support. Second, I would like to extend my admiration to my older brother, Peter, for being so incredibly strong, intelligent, and humble throughout his journey in life. He is an individual I have followed, and who is an integral part of who I am. I am truly inspired by his tenacity and thank him for always protecting me as his younger sister. During my hardest times in graduate school, he never failed to call me weekly just to make me laugh and find every solution possible to problems I deemed unsolvable.

To Christopher Peruzzi, I thank you for believing in me from the very beginning, and for pushing me into applying to graduate school. Thank you for being such a great companion in the lab, and for being my source of happiness throughout my academic years. Chris defines what it means to be a great chemist and will continue inspiring me and others with his knowledge and compassion for this field. I'm grateful to have grown beside someone who is as special as you are for the past eight years.

Next, I want to express how fortunate I am to have my Nana and Jido in my life. They have played a pivotal role in reinforcing my foundational values instilled. Most importantly, they have taught me that with a pure heart, one can achieve their aspirations. Both have shown me the essence of embracing life and facing the future without fear, as they have dedicated each day to hard work and helping others. I can't individually mention every aunt and uncle, but each one has instilled

something significant and I thank you for being so special and loving (Uncle Alan, I'm sorry I couldn't get the Nobel Prize in Chemistry (bummer..), even though I keep saying the chances are infinitesimally small, I admire your dedication to always asking about my work and believing in me). To Uncle Sammy, Auntie Mouna, and Nana Munera, words cannot describe the impact you have in my life, and I love you. To all my cousins on my father's side (Fr. Andy, Kristina, Chris, Joey, Dominic, Monique, Monica, Micheal, Martin, Lawrence, Lydia), Laurita is my favorite. I thank my cousins on my mom's side for letting me come rest in California every so often, and for being a part of so many childhood memories that shaped who I am today.

I am so proud and thankful of Sandra, my neighbor and best friend since the 3rd grade, for becoming a remarkable lawyer, and for showing me how to follow my dreams. I am so lucky to have had someone that could push me to be the best person I was capable of being, and most importantly, always reassured me that our habits procrastinating is our specialty and that no matter what, we'll get it done. (I don't endorse anyone doing this in life, it's quite a challenge).

Lastly, I would like to thank my advisor, Mitch Smith, for his guidance in shaping me into the chemist I am today. Thank you for encouraging me to always ask questions, to stay focused, and to not be scared to think differently. Your mentorship has cultivated my passion for chemistry, and I am thankful for the opportunity you gave me in your lab. Thank you to my co-advisor, Robert Maleczka, for introducing diverse ideas that helped move my research forward, and for providing essential support that culminated in the completion of my degree. Thank you to my committee members, Aaron Odom, Ned Jackson, Jetze Tepe, and to faculty members Anna Osborn, Dan Holmes, Richard Staples, and so many others for guiding me throughout my academic journey. To Arzoo, Anshu, Thomas, and Chris, thank you for the incredible memories, support, and friendship. (Cliff, you got the next generation of students.. I believe in you.)

TABLE OF CONTENTS

LIST OF TABLES

LIST OF FIGURES

LIST OF SCHEMES

LIST OF ABBREVIATIONS

[Ir]	$[IrCl_2(cod)]^-$
[M]	molar concentration of species
$[M]^+$	molecular ion peak
μL	microliters
BB	1,1'-di(pyridin-2-yl)-1,1',3,3'-tetrahydro-2,2'-bibenzo[d][1,3,2]diazaborole
Bn	benzyl
bpy	bipyridine
Bu	butyl
cat	catechol
CHB	C–H activation/borylation
cod	1,5-cyclooctadiene
Cp	cyclopentadienyl
Cy	cyclohexyl
dab	diaminobenzene
DCM	dichloromethane
DFT	density functional theory
dppe	1,2-bis(diphenylphosphino)ethane
dtbpy	4,4’-di-tert-butyl-2,2’-bipyridine
eg	ethylene glycol
EI	electron ionization
equiv	equivalents
Et	ethyl
FWHM	full width at half maximum

GC-MS	Gas Chromatography-Mass Spectrometry
h	hours
HOTf	triflic acid
J	coupling constant
KIE	kinetic isotope effect
m	*meta*
M	metal
Me	methyl
MHz	megahertz
min	minutes
mL	milliliters
mol	moles
mp	melting point
NMR	nuclear magnetic resonance
o	*ortho*
p	*para*
Ph	phenyl
pin	pinacolate
pKa	acid dissociation constant at logarithmic scale
ppm	parts per million
Pr	propyl
Py	pyridine
R	remaining attachment to molecule

RDS	rate determining step
rt	room temperature
THF	tetrahydrofuran
tmphen	3,4,7,8-tetramethyl-1,10-phenanthroline
TON	turnover number

CHAPTER 1.
INTRODUCTION

1.1: Aryl Boronic Esters and Acids

1.1.1: Practical Applications

Boronic esters and acids have been proven to be useful intermediates in natural product synthesis, pharmaceuticals, and other disciplines for decades.[1,2] These compounds are reactive due to the unique electronic properties in C–B bonds where boron possesses an empty *p*-orbital, is less electronegative than carbon, and holds Lewis acidic character. Overall, these characteristics open a plethora of chemical reactions that transform aryl boronic esters or acids into C–R moieties, where R = C, O, N, Si bonds. Examples of common general reactions that utilize these substrates are transition metal or oxidative cross coupling, 1,2-migration, or nucleophilic attack of boryl anions.[3,4] Of the many routes in creating organoboranes, iridium-catalyzed C–H borylation (CHB) has found its way as an atom economical approach in making this important class of compounds. Generally, the regioselectivity of iridium catalysts ligated with commonly used bipyridine or phenanthroline ligands is complimentary to electrophilic and nucleophilic aromatic substitution in that the product regioselectivity is determined by steric effects rather than electronics.[5–7]

1.1.2: Synthetic Methods

An extensive amount of research has been done on the development of methods for the synthesis of boronic esters and acids. These methods include transforming C–X (X = Cl, Br, I) or C–H to C–B bonds. Metalation is an indirect way to achieve this where an aryl halide is necessary to reach a Grignard or organolithium intermediate, which then adds to a boronic ester reagent (**Scheme 1.1, Method A**). Miyaura borylations became a popular, and more practical way of doing this where C–X bonds could be directly transformed via Pd-catalyzed cross-coupling with base activated boron reagents (**Scheme 1.1, Method B**).[8,9] Though these methods get to the desired

product, they depend on the availability of specifically substituted aryl halides, which inevitably limits the extent of where this type of chemistry can be applied.

Scheme 1.1: Methods to Prepare C(sp^2)–B Bonds.

I. C–B Transformations from Aryl Halide

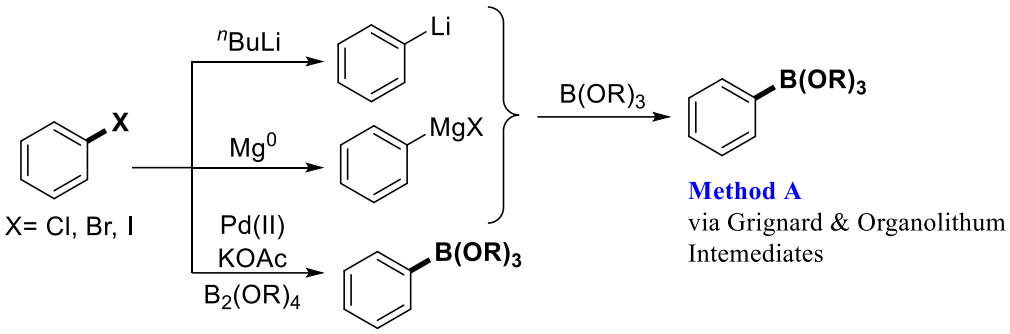

Method A
via Grignard & Organolithum Intemediates

Method B
Direct C–X to C–B Transformation

II. Direct C–H Borylation

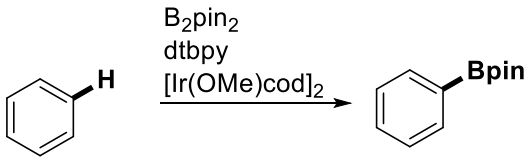

Method C
Direct C–H to C–B Transformation

Approaching the 21st century, direct C–H borylation (CHB) became the most common and effective way to yield aryl boronic esters and acids. After Smith and Iverson's discovery of the first thermal catalytic CHB reaction of benzene and an Ir complex,[10] rapid improvements were made to increase the Ir turnover numbers. Initial findings found that diphosphine and bipyridyl ligands sufficiently directed catalysis towards the least sterically hindered C–H bond with $[Ir(X)cod]_2$ (X = Cl, OMe) as the Ir(I) pre-catalyst and B_2pin_2 or HBpin as the boron source (**Scheme 1.1**, **Method C**).

1.2: Ir-Catalyzed CHB Mechanism

The mechanism for Ir-catalyzed CHB was studied in the early 2000's where Smith and co-workers initially discovered that Ir(I) catalysts were inadequate for catalyzing these reactions. This provided a crucial insight into the underlying mechanism.[11] Hartwig later carried out a plethora of mechanistic studies that solidified the understanding that CHB occurs through an Ir(III)/Ir(V) catalytic cycle (**Figure 1.1**).[12]

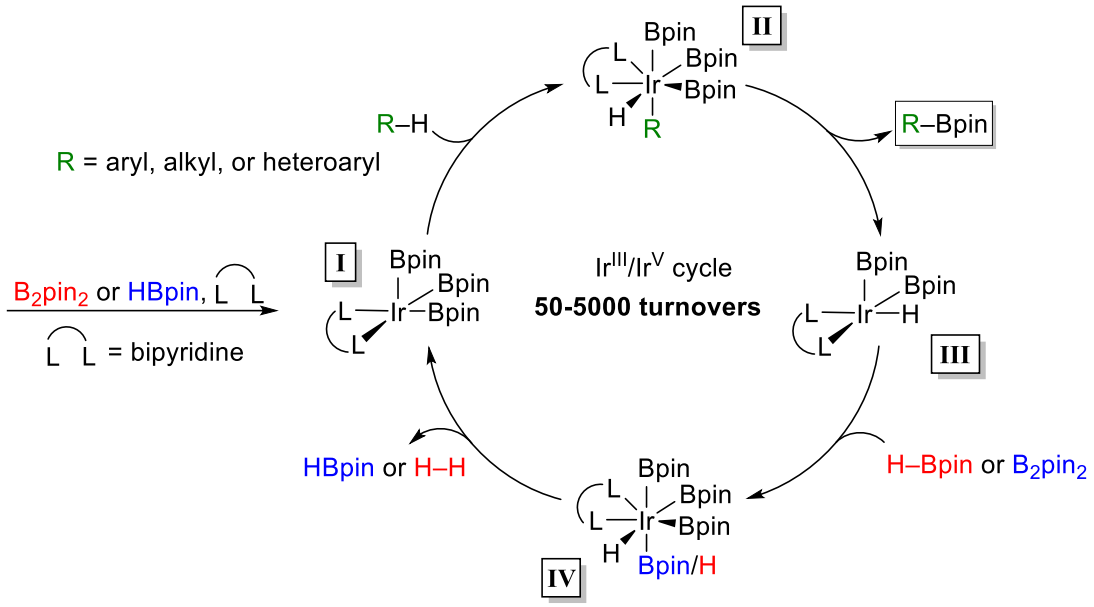

Figure 1.1: Ir(III)/Ir(V) Catalytic Cycle.

These studies primarily utilized Ir(III) tris-boryl species [Ir(dtbpy)(COE)(Bpin)$_3$] as the pre-assembled catalyst entering the catalytic cycle (**I**). The rate determining step (RDS) was found to be oxidative addition of **I** into the C(sp^2)–H bond of the substrate to give Ir(V) species **II**. Isotopic labeling and kinetic studies showed a primary kinetic isotope effect and overall rate constants as first order in arene, zero order in B_2pin_2, and half order in catalyst due to the reversible association of COE yielding equimolar amounts of the tris-boryl complex with and without bound COE. The mechanism was also supported by computational studies done by Sakaki.[13] After reductive elimination of the borylated product, the boron source oxidatively adds to the resulting

species **III** to give the Ir(V) complex **IV** to complete the catalytic cycle after reductive elimination of HBpin or H_2 depending on the boron source used, regenerating tris-boryl complex **I**.

1.3: Methods to Control Regioselectivity in CHB

1.3.1: Ligand Types for ortho-CHB

C–H activation generally occurs at the least sterically hindered position on the substrate when using bidentate bipyridine or diphosphine ligands.[6,11] Oxidative addition of the C–H bond will occur on the open coordination site of the aforementioned Ir-trisboryl species, where the site of C–B bond formation is typically governed by bulkiness of the substrate or ligand.[5,14] Borylation *ortho* to directing groups such as amides and esters has been achieved by opening up an additional coordination site for a directing group on the substrate to chelate and direct CHB.[15,16] This has commonly been done by designing a ligand that enables direct inner-sphere coordination between a Lewis-basic directing group on aryl substrates and metal center (**Figure 1.2**).

Sawamura found that Si-SMAP-Ir, a silica-supported monodentate phosphine-iridium system, was viable to *ortho* borylate aryl esters, amides, and phenols derivatives in high yields and selectivites.[17,18] This system differed from previously reported Ir-catalyzed CHB systems as this catalyst was heterogenous, however, the reaction of Si-SMAP and $[Ir(OMe)cod]_2$ to yield this species was difficult to reproduce and synthesize. Miryaura has also selectively borylated *ortho* to aryl esters using a triaryl monodentate phosphine ligand.[19] Soon after, Lasaletta screened *N*,*N* ligands having the potential to be hemilabile and found aromatic *N*,*N*-dimethylhydrazones to be suitable for *ortho* borylation of isoquinolines and aryl hydrazones.[20,21] Clark also discovered picolylamine can be used as a hemilabile ligand to borylate *ortho* to benzylamines under mild conditions.[22] The evidence regarding the hemilabile nature of these ligands during catalysis has

not yet been secured, though it is hypothesized that the weaker donor substituents tethered to the pyridyl backbone will dissociate and allow the coordination of a directing group.[23]

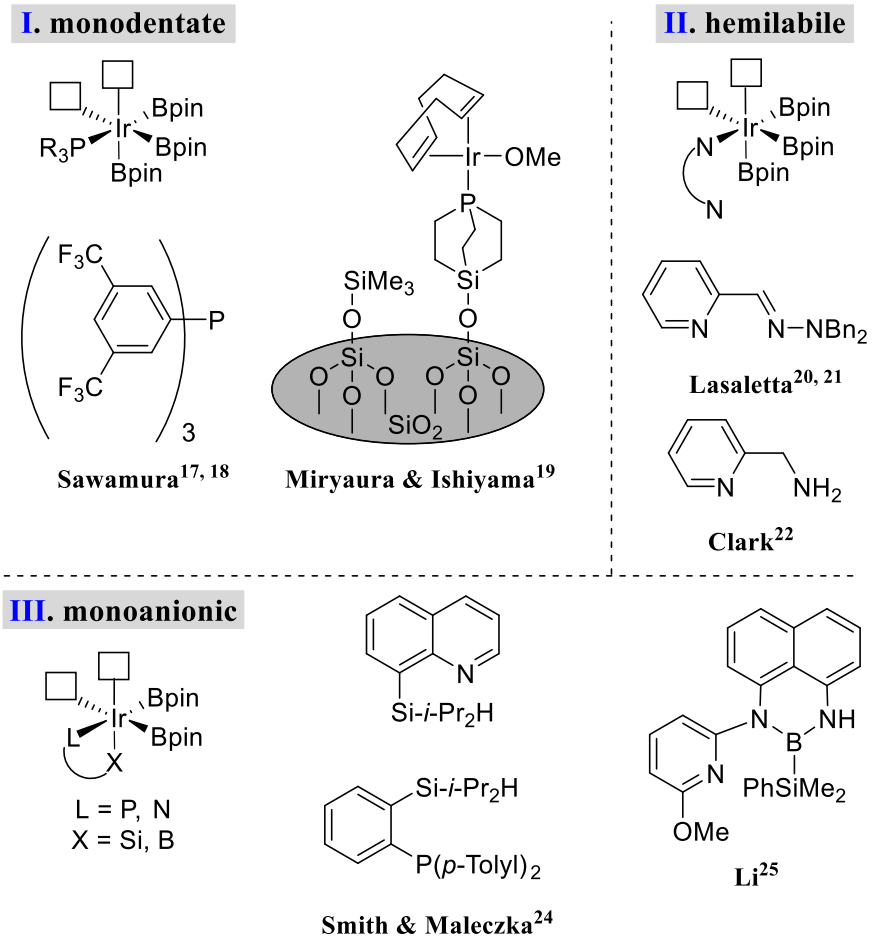

Figure 1.2: Ligand Designs for *ortho*-CHB.

Inspired by the highly reactive Si-SMAP-Ir system, our group designed P,Si- and N,Si-monoanionic ligands capable of *ortho* borylating to a variety of substituted (hetero)arenes bearing amide and ester directing groups in a homogenous fashion.[24] Following the mechanism for Ir-catalyzed CHB mentioned previously, replacing bipyridine with a L-X type ligand would allow the silyl group to take the place of a spectator boryl and yield a bisboryl Ir(III) intermediate with two open coordination sites. Interestingly, the first *ortho* CHB reported by Hartwig and co-workers

found that dtbpy could be used as the ligand as long as the silyl group was tethered to the substrate.[25] This method is limited given the necessity of hydrosilane directing groups.

Li and co-workers later reported monoanionic pre-ligand N,B-Si, expecting that the B–Si bond would oxidatively add to the metal center and the silyl ligand would be removed via reductive elimination or ligand exchange with -Bpin.[26] This system was efficient at *ortho* borylating a plethora of substrates in high yields and selectivities.

1.3.2: Non-Covalent Interactions

The ligand types discussed previously are predominantly compatible with directing groups that can strongly coordinate to Ir. As borylation is not only limited from a regioselective perspective, where borylation is directed *ortho* vs *meta* and *para*, but in most cases the substrate scope is confined to derivatives of aryl esters, amides, and carbamates. To overcome this limitation, non-covalent or outer-sphere interactions between the ligand on the catalyst and substrates, some of which are categorized under electrostatic interactions,[27] have been explored where the proximity of the C–H bond to the metal center is determined by the resulting geometry of the catalyst intermediate during C–H activation (**Figure 1.3**).

H-bonding interactions have been advantageous in directing catalysis in the *ortho* and *meta* positions of aryl substrates bearing a hydrogen bond acceptor. Kanai and Kuninobu were the first to report catalyst controlled *meta*-selective CHB's by utilizing a bipyridine ligand substituted with a pendent urea moiety.[28] Mechanistic studies indicated an important role of the hydrogen bonding interaction between the urea and aryl esters, amides, and phosphonates to direct catalysis specifically at the *meta* site, avoiding substrate-metal coordination. Years later, Reek and co-workers showed *ortho*-CHB of *N*-methylbenzamide derivatives using a similar ligand framework, where DFT calculations support that the selectivity is controlled via H–bonding interactions.[29]

Phipps has expanded on this idea by attaching a pendent sulfonate anion to bpy, aimed to hydrogen bond with benzyl-amine derived amides as the hydrogen bond acceptor and resulted in *meta* borylated products.[30]

Our group discovered a method to achieve *ortho* selectivity through *N*-borylated intermediates of a wide variety of substituted anilines, employing dtbpy as the ligand.[31] Computational studies revealed a hydrogen bonding interaction occurring between the Ir-Beg ligand and the anilines N(Beg)H, where transition states of other electrostatic interactions had higher Gibbs' free energies.

Lewis-acid base interactions is another method employed to control the regiochemical outcome in CHB. This was first observed by Kanai and Kuninobu, demonstrating successful *ortho* borylation on aryl sulfides when using an aryl boronic ester tethered to bpy as the ligand.[32] The authors carried out control experiments to study ligand-substrate interactions, discovering that *ortho* borylation could only be achieved when the boronic ester was in the *ortho* position of the pendent arene. However, when the boronic ester was in the *para* position, only *meta* and *para* borylated products were observed. This suggested that *ortho* selectivity was influenced by a Lewis-acid base interaction between the boron of the ligand and sulfur atom of the substrate.

Recent work done by Kuninobu and co-workers revealed that using a derivative of this ligand, where the boronic ester is removed from the pendent arene, also led to the formation of *ortho* borylated aryl sulfides.[33] The authors carried out computational studies demonstrating that regioselectivity is determined by a hydrogen bonding interaction between the methyl group of dimethyl sulfide and a spectator boryl on the Ir catalyst.

Other notable work by Nakao and co-workers shows *para*-selective CHB of benzamides can be achieved through cooperative Ir/Al catalysis, where a bulky aluminum additive is added

H–Bonding

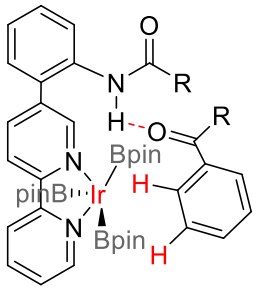

Kanai, Kuninobu[28] (*m*)
Reek[29] (*o*)

Lewis Acid-Base

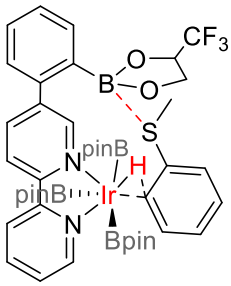

Kanai, Kuninobu[32, 33] (*o*)

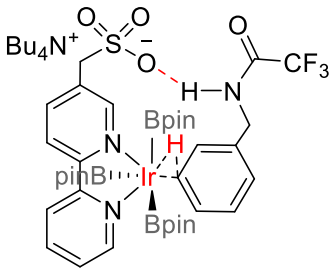

Phipps[30] (*m*)

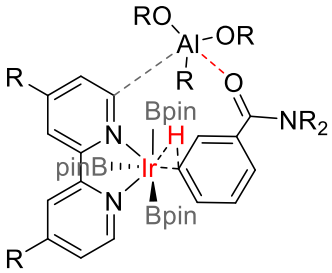

Nakao[34, 35] (*m*)

Ion-Pairing Electrostatic Interactions

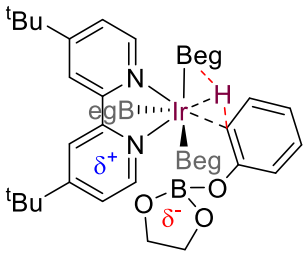

Smith, Maleczka[27] (*o*)

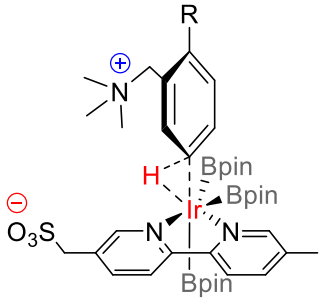

Phipps[37] (*m*)

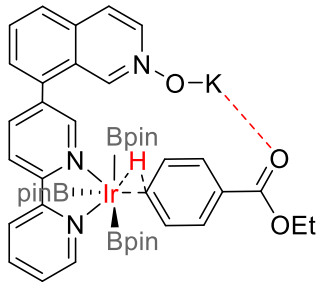

Chattopadhyay[43] (*p*)

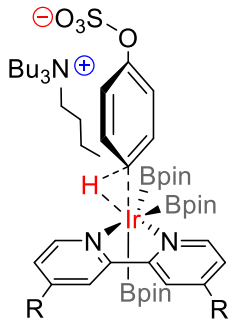

Smith & Maleczka,[40] Phipps [41] (*p*)

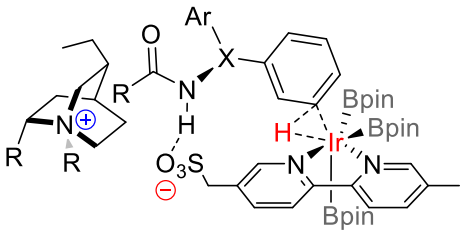

Phipps[42] (*m*)

Figure 1.3: Directed *ortho* (*o*), *meta* (*m*), and *para* (*p*) CHB via Non-Covalent Interactions.

to the reaction and directs catalysis as a Lewis acid with the substrate.[34] His group later reported *meta*-selective CHB of benzamides and pyridines by incorporating a derivative of this aluminum species directly on the ligand.[35] Further investigation in the structure and applications of such Ir/Al bifunctional catalysts in CHB, as well as *ortho* borylated products of dimethyl-benzyl amine derivatives using similar systems, has been detailed by Yamashita and Suzuki in recent years.[36]

Phipps, a pioneer in discovering this type of mechanism, showed that their anionic bipyridine ligand (previously discussed to direct CHB via hydrogen bonding)[30] can also be used with cationic quaternary ammonium and phosphonium salts as the aryl substrate to direct the catalysis at the *meta* position through ion-pairing.[37–39] In the following years, our group in tandem with Phipps investigated sulfated phenols, benzyl alcohols/sulfonates, and anilines that were synthesized with tetraalkyl ammonium counter-cations.[40,41] Employing these substrates in CHB reactions resulted in *para* borylated products as the major regioisomer. Control reactions showed that as the alkyl chain length decreases, *para* selectivity diminishes, supporting the idea that *ortho* and *meta* positions are blocked when tetrabutyl ammonium is ion-pairing with the substrate. In most recent years, Phipps has elevated this concept by showing the use of a common organocatalyst as a chiral cation to desymmetrize benzhydrylamides via remote CHB with anionic iridium bpy complexes.[42] Work has also been done by Chattopadhyay and co-workers showing outer-sphere $O^{-}K^{+}$---O ion-pairing interactions between a bpy derived L-shaped ligand and aryl esters compatible for *para* selective CHB.[43]

REFERENCES

(1) Yamaguchi, J.; Yamaguchi, A. D.; Itami, K. C-H Bond Functionalization: Emerging Synthetic Tools for Natural Products and Pharmaceuticals. *Angew. Chem. Int. Ed Engl.* **2012**, *51* (36), 8960–9009.

(2) Guillemard, L.; Kaplaneris, N.; Ackermann, L.; Johansson, M. J. Late-Stage C-H Functionalization Offers New Opportunities in Drug Discovery. *Nat Rev Chem* **2021**, *5* (8), 522–545.

(3) Hall, D. G. *Boronic Acids, 2 Volume Set: Preparation and Applications in Organic Synthesis, Medicine and Materials*; Wiley, 2011.

(4) Kadu, B. S. Suzuki–Miyaura Cross Coupling Reaction: Recent Advancements in Catalysis and Organic Synthesis. *Catal. Sci. Technol.* **2021**, *11* (4), 1186–1221.

(5) Ishiyama, T.; Takagi, J.; Ishida, K.; Miyaura, N.; Anastasi, N. R.; Hartwig, J. F. Mild Iridium-Catalyzed Borylation of Arenes. High Turnover Numbers, Room Temperature Reactions, and Isolation of a Potential Intermediate. *J. Am. Chem. Soc.* **2002**, *124* (3), 390–391.

(6) Hassan, M. M. M.; Guria, S.; Dey, S.; Das, J.; Chattopadhyay, B. Transition Metal-Catalyzed Remote C─H Borylation: An Emerging Synthetic Tool. *Sci Adv* **2023**, *9* (16), eadg3311.

(7) Mahamudul Hassan, M. M.; Mondal, B.; Singh, S.; Haldar, C.; Chaturvedi, J.; Bisht, R.; Sunoj, R. B.; Chattopadhyay, B. Ir-Catalyzed Ligand-Free Directed C-H Borylation of Arenes and Pharmaceuticals: Detailed Mechanistic Understanding. *J. Org. Chem.* **2022**, *87* (6), 4360–4375.

(8) Miyaura, N.; Yamada, K.; Suzuki, A. A New Stereospecific Cross-Coupling by the Palladium-Catalyzed Reaction of 1-Alkenylboranes with 1-Alkenyl or 1-Alkynyl Halides. *Tetrahedron Lett.* **1979**, *20* (36), 3437–3440.

(9) Miyaura, N. *Cross-Coupling Reactions*; Springer Berlin Heidelberg, 2002.

(10) Iverson, C. N.; Smith, M. R., III. Stoichiometric and Catalytic B−C Bond Formation from Unactivated Hydrocarbons and Boranes. *J. Am. Chem. Soc.* **1999**, *121* (33), 7696–7697.

(11) Cho, J.-Y.; Tse, M. K.; Holmes, D.; Maleczka, R. E., Jr; Smith, M. R., III. Remarkably Selective Iridium Catalysts for the Elaboration of Aromatic C-H Bonds. *Science* **2002**, *295* (5553), 305–308.

(12) Boller, T. M.; Murphy, J. M.; Hapke, M.; Ishiyama, T.; Miyaura, N.; Hartwig, J. F. Mechanism of the Mild Functionalization of Arenes by Diboron Reagents Catalyzed by Iridium Complexes. Intermediacy and Chemistry of Bipyridine-Ligated Iridium Trisboryl Complexes. *J. Am. Chem. Soc.* **2005**, *127* (41), 14263–14278.

(13) Tamura, H.; Yamazaki, H.; Sato, H.; Sakaki, S. Iridium-Catalyzed Borylation of Benzene with Diboron. Theoretical Elucidation of Catalytic Cycle Including Unusual Iridium(V) Intermediate. *J. Am. Chem. Soc.* **2003**, *125* (51), 16114–16126.

(14) Mkhalid, I. A. I.; Barnard, J. H.; Marder, T. B.; Murphy, J. M.; Hartwig, J. F. C-H Activation for the Construction of C-B Bonds. *Chem. Rev.* **2010**, *110* (2), 890–931.

(15) Haldar, C.; Hoque, M. E.; Chaturvedi, J.; Hassan, M. M. M.; Chattopadhyay, B. Ir-Catalyzed Proximal and Distal C-H Borylation of Arenes. *Chem. Commun.* **2021**, *57* (97), 13059–13074.

(16) Wright, J. S.; Scott, P. J. H.; Steel, P. G. Iridium Catalysed C-H Borylation of Heteroarenes: Balancing Steric and Electronic Regiocontrol. *Angew. Chem. Int. Ed Engl.* **2020**.

(17) Kawamorita, S.; Ohmiya, H.; Hara, K.; Fukuoka, A.; Sawamura, M. Directed Ortho Borylation of Functionalized Arenes Catalyzed by a Silica-Supported Compact Phosphine-Iridium System. *J. Am. Chem. Soc.* **2009**, *131* (14), 5058–5059.

(18) Yamazaki, K.; Kawamorita, S.; Ohmiya, H.; Sawamura, M. Directed Ortho Borylation of Phenol Derivatives Catalyzed by a Silica-Supported Iridium Complex. *Org. Lett.* **2010**, *12* (18), 3978–3981.

(19) Ishiyama, T.; Isou, H.; Kikuchi, T.; Miyaura, N. Ortho-C-H Borylation of Benzoate Esters with Bis(Pinacolato)Diboron Catalyzed by Iridium-Phosphine Complexes. *Chem. Commun.* **2010**, *46* (1), 159–161.

(20) Ros, A.; Estepa, B.; López-Rodríguez, R.; Álvarez, E.; Fernández, R.; Lassaletta, J. M. Use of Hemilabile N,N Ligands in Nitrogen-Directed Iridium-Catalyzed Borylations of Arenes. *Angew. Chem. Int. Ed Engl.* **2011**, *50* (49), 11724–11728.

(21) López-Rodríguez, R.; Ros, A.; Fernández, R.; Lassaletta, J. M. Pinacolborane as the Boron Source in Nitrogen-Directed Borylations of Aromatic N,N-Dimethylhydrazones. *J. Org. Chem.* **2012**, *77* (21), 9915–9920.

(22) Roering, A. J.; Hale, L. V. A.; Squier, P. A.; Ringgold, M. A.; Wiederspan, E. R.; Clark, T. B. Iridium-Catalyzed, Substrate-Directed C-H Borylation Reactions of Benzylic Amines. *Org. Lett.* **2012**, *14* (13), 3558–3561.

(23) Ros, A.; Fernández, R.; Lassaletta, J. M. Functional Group Directed C-H Borylation. *Chem. Soc. Rev.* **2014**, *43* (10), 3229–3243.

(24) Ghaffari, B.; Preshlock, S. M.; Plattner, D. L.; Staples, R. J.; Maligres, P. E.; Krska, S. W.; Maleczka, R. E., Jr; Smith, M. R., III. Silyl Phosphorus and Nitrogen Donor Chelates for Homogeneous Ortho Borylation Catalysis. *J. Am. Chem. Soc.* **2014**, *136* (41), 14345–14348.

(25) Boebel, T. A.; Hartwig, J. F. Silyl-Directed, Iridium-Catalyzed Ortho-Borylation of Arenes. A One-Pot Ortho-Borylation of Phenols, Arylamines, and Alkylarenes. *J. Am. Chem. Soc.* **2008**, *130* (24), 7534–7535.

(26) Wang, G.; Liu, L.; Wang, H.; Ding, Y.-S.; Zhou, J.; Mao, S.; Li, P. N,B-Bidentate Boryl Ligand-Supported Iridium Catalyst for Efficient Functional-Group-Directed C-H Borylation. *J. Am. Chem. Soc.* **2017**, *139* (1), 91–94.

(27) Chattopadhyay, B.; Dannatt, J. E.; Andujar-De Sanctis, I. L.; Gore, K. A.; Maleczka, R. E., Jr; Singleton, D. A.; Smith, M. R., III. Ir-Catalyzed Ortho-Borylation of Phenols Directed by

Substrate-Ligand Electrostatic Interactions: A Combined Experimental/in Silico Strategy for Optimizing Weak Interactions. *J. Am. Chem. Soc.* **2017**, *139* (23), 7864–7871.

(28) Kuninobu, Y.; Ida, H.; Nishi, M.; Kanai, M. A Meta-Selective C-H Borylation Directed by a Secondary Interaction between Ligand and Substrate. *Nat. Chem.* **2015**, *7* (9), 712–717.

(29) Bai, S.-T.; Bheeter, C. B.; Reek, J. N. H. Hydrogen Bond Directed *Ortho* -selective C−H Borylation of Secondary Aromatic Amides. *Angew. Chem. Weinheim Bergstr. Ger.* **2019**, *131* (37), 13173–13177.

(30) Davis, H. J.; Genov, G. R.; Phipps, R. J. Meta-Selective C-H Borylation of Benzylamine-, Phenethylamine-, and Phenylpropylamine-Derived Amides Enabled by a Single Anionic Ligand. *Angew. Chem. Int. Ed Engl.* **2017**, *56* (43), 13351–13355.

(31) Smith, M. R., III; Bisht, R.; Haldar, C.; Pandey, G.; Dannatt, J. E.; Ghaffari, B.; Maleczka, R. E., Jr; Chattopadhyay, B. Achieving High Ortho Selectivity in Aniline C-H Borylations by Modifying Boron Substituents. *ACS Catal.* **2018**, *8* (7), 6216–6223.

(32) Li, H. L.; Kuninobu, Y.; Kanai, M. Lewis Acid--Base Interaction-Controlled Ortho-Selective C- H Borylation of Aryl Sulfides. *Angew. Chem. Int. Ed Engl.* **2017**, *129* (6), 1517–1521.

(33) Zeng, J.; Naito, M.; Torigoe, T.; Yamanaka, M.; Kuninobu, Y. Iridium-Catalyzed Ortho-C–H Borylation of Thioanisole Derivatives Using Bipyridine-Type Ligand. *Org. Lett.* **2020**, *22* (9), 3485–3489.

(34) Yang, L.; Semba, K.; Nakao, Y. Para-Selective C-H Borylation of (Hetero)Arenes by Cooperative Iridium/Aluminum Catalysis. *Angew. Chem. Int. Ed Engl.* **2017**, *56* (17), 4853–4857.

(35) Yang, L.; Uemura, N.; Nakao, Y. Meta-Selective C-H Borylation of Benzamides and Pyridines by an Iridium-Lewis Acid Bifunctional Catalyst. *J. Am. Chem. Soc.* **2019**, *141* (19), 7972–7979.

(36) Nakamura, T.; Suzuki, K.; Yamashita, M. Aluminabenzene-Rh and -Ir Complexes: Synthesis, Structure, and Application toward Catalytic C-H Borylation. *J. Am. Chem. Soc.* **2017**, *139* (49), 17763–17766.

(37) Davis, H. J.; Mihai, M. T.; Phipps, R. J. Ion Pair-Directed Regiocontrol in Transition-Metal Catalysis: A Meta-Selective C-H Borylation of Aromatic Quaternary Ammonium Salts. *J. Am. Chem. Soc.* **2016**, *138* (39), 12759–12762.

(38) Lee, B.; Mihai, M. T.; Stojalnikova, V.; Phipps, R. J. Ion-Pair-Directed Borylation of Aromatic Phosphonium Salts. *J. Org. Chem.* **2019**, *84* (20), 13124–13134.

(39) Mihai, M. T.; Davis, H. J.; Genov, G. R.; Phipps, R. J. Ion Pair-Directed C–H Activation on Flexible Ammonium Salts: Meta-Selective Borylation of Quaternized Phenethylamines and Phenylpropylamines. *ACS Catal.* **2018**, *8* (5), 3764–3769.

(40) Montero Bastidas, J. R.; Oleskey, T. J.; Miller, S. L.; Smith, M. R., III; Maleczka, R. E. Para-Selective, Iridium-Catalyzed C–H Borylations of Sulfated Phenols, Benzyl Alcohols, and Anilines Directed by Ion-Pair Electrostatic Interactions. *J. Am. Chem. Soc.* **2019**, *141* (39), 15483–15487.

(41) Mihai, M. T.; Williams, B. D.; Phipps, R. J. Para-Selective C–H Borylation of Common Arene Building Blocks Enabled by Ion-Pairing with a Bulky Countercation. *J. Am. Chem. Soc.* **2019**, *141* (39), 15477–15482.

(42) Genov, G. R.; Douthwaite, J. L.; Lahdenperä, A. S. K.; Gibson, D. C.; Phipps, R. J. Enantioselective Remote C–H Activation Directed by a Chiral Cation. *Science* **2020**, *367* (6483), 1246–1251.

(43) Hoque, M. E.; Bisht, R.; Haldar, C.; Chattopadhyay, B. Noncovalent Interactions in Ir-Catalyzed C-H Activation: L-Shaped Ligand for Para-Selective Borylation of Aromatic Esters. *J. Am. Chem. Soc.* **2017**, *139* (23), 7745–7748.

CHAPTER 2.

REGIOCHEMICAL SWITCHING IN Ir-CATALYZED C–H BORYLATION USING N,B–TYPE DIBORON SPECIES

2.1: Altering Pre-ligand Loadings

2.1.1: Introduction

In 2015, Pengfei Li and co-workers introduced a new spectator tetra-N-substituted diboron complex with an N^1-(pyridin-2-yl)benzene-1,2-diamine backbone (**BB**) that was competent for steric-directed iridium catalyzed CHB (**Scheme 2.1**, **A**). The ligand is designed to stabilize the typically reactive boryl ligand through chelation[1] where the lone pairs of the adjacent nitrogen atoms can donate into the p-orbital of boron and reduce its predisposition of being removed from the metal.[2–4] As reaction conditions followed the classical 2:1 ratio of ligand to Ir(I) dimer,[5] Li's group synthesized the hypothesized pre-catalyst by reacting 2 equiv of **BB** with $[IrCl(cod)]_2$. The product $[Ir(\mathbf{BB})_2(cod)][Cl]$ was characterized by X-ray diffraction and features an Ir(III) cation where two boryl pyridine chelating ligands are installed by B–B oxidative addition to Ir(I).[6]

Scheme 2.1: General Reactions of Steric and Chelate-Directed CHB Using **BB**.

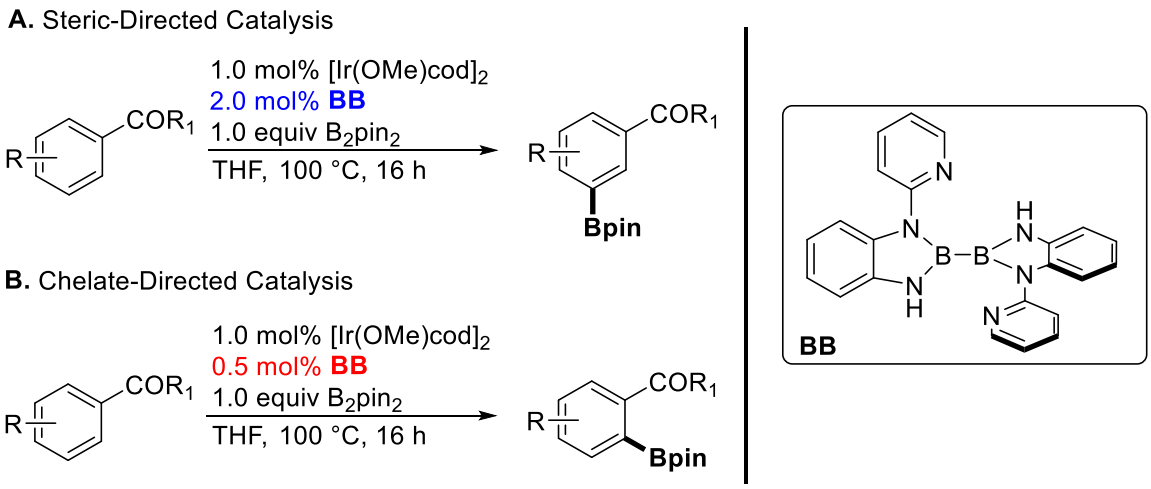

Given the use of a dimeric pre-ligand, it was hypothesized that this catalyst could be altered by reducing the number of B,N ligands attached to the metal center, thereby creating an open coordination site to yield chelate-directed *ortho* products. We have found that when decreasing the pre-ligand loading in the reaction to **BB**:$[Ir(X)(cod)]_2$ = 0.5:1 (X = Cl, OMe), aryl amides and esters are selectively *ortho*-borylated with B_2pin_2 (**Scheme 2.1**, **B**). In this work, the method of changing the regioselectivity of a traditionally steric-directing catalyst for *ortho* C–H borylation is described.[7]

2.1.2: Preliminary Results

The results of **Table 2.1** demonstrate that using the **BB** pre-ligand in lower loadings resulted in higher *ortho* selectivity. In fact, as the loading decreased, more chelate product was formed (Entries 1-5).

Table 2.1: Comparison of **BB** and dtbpy at Various (Pre)ligand Loadings.

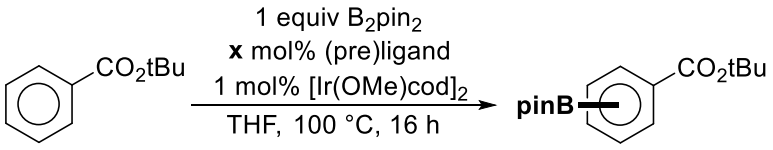

entry	(pre)ligand	**x mol%**	selectivity (*o*:(*m*+*p*))	conversion
1	BB	2	1:>99	>99%
2	BB	1	60:40	80%
3	BB	0.75	90:10	74%
4	BB	0.50	95:5	67%
5[a]	BB	0.50	96:4	90%
6	dtbpy	2	1:>99	99%
7	dtbpy	0.50	1:>99	74%
8[a]	dtbpy	0.50	1:>99	76%

Conversions and selectivities were calculated using ^{1}H NMR of crude reaction mixture. [a]Entries 5 and 8 were run using 1 mol % $[Ir(Cl)cod]_2$ as precatalyst.

These results did not follow typical CHBs using iridium catalysts. Stoichiometrically, traditional catalyst systems like Hartwig, Ishiyama, and Miyaura's use of dtbpy and $[Ir(OMe)cod]_2$

require a 2:1 ratio of ligand to precatalyst.[8] Previous work done by our group on ligand to pre-catalyst ratio showed that optimal catalytic activity was achieved when the pre-ligand is in slight excess of the pre-catalyst, where attempts using a 1:1 ligand to pre-catalyst ratio with dtbpy or tmphen and $[Ir(OMe)cod]_2$ resulted in lower catalytic activity.[9] Similarities are found in this work where we observe that decreasing the amount of dtbpy to pre-catalyst lessens the reactivity of the system, but has no effect on regioselectivity (Entries 6-8).

2.1.3: Hypothesized Pre-assembled Catalysts

In Li's report displaying **BB** as a competent pre-ligand for steric-directed borylations, he successfully isolated the hypothesized pre-assembled catalyst by reacting 2 equivalents of **BB** with 1 equivalent of $[IrCl(cod)]_2$.[6] This resulted in oxidative addition of the B–B bond and produced the Ir(III) cationic salt, $[Ir(BN)_2(cod)][Cl]$, where two B,N-ligands are chelated to the Ir metal center with COD (**Figure 2.1**, Complex **1**).

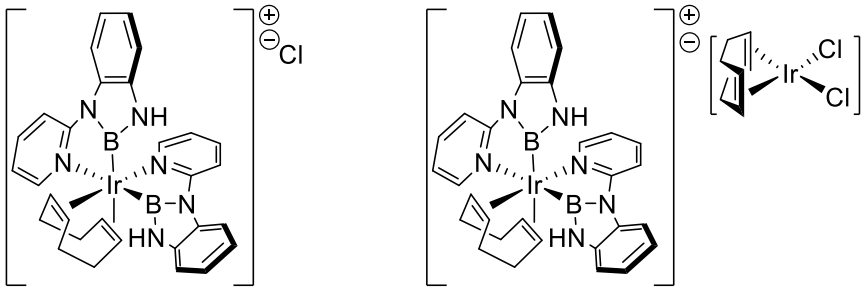

1 **2**

Figure 2.1: Isolated Pre-Catalysts Using a 2:1 ratio (**1**) vs. 1:1 (**2**) ratio of **BB**:$[IrCl(cod)]_2$.

To better understand why we see a switch from steric to chelate-directed CHB at decreased **BB** pre-ligand loadings, we attempted to isolate the pre-assembled catalyst that best represents our system. Mimicking the reaction conditions that yield the highest *ortho* selectivity, we reacted 0.5 equivalents of **BB** with 1 equivalent of $[IrCl(cod)]_2$, though this gave inconclusive results. Reacting equimolar amounts of **BB** and $[IrCl(cod)]_2$ produced the structurally characterized salt

[$Ir(BN)_2(cod)$][$IrCl_2(cod)$], where the Ir(III) cation is identical, however, the key distinction is the Ir(I) counterion instead of the chloride (**Figure 2.1**, Complex **2**) seen in Li's work.

To identify the role of Complex **2** in this system, we used it in chelate-directed CHBs under standard reaction conditions with substrate and B_2pin_2. Though this complex was not catalytically competent at room temperature, we observed *ortho*-borylation of tert-butyl benzoate (*o*:(*m*+*p*) = 95:5) with 77% conversion at 100 °C. At temperatures of 80 °C and lower, reactivity dropped significantly though *ortho*-borylation was still preferred. These data suggest the possibility of the pre-assembled catalyst playing a key role in the catalytic cycle and regioselective outcome.

Initial attempts to change the regioselectivity of Complex **1** for *ortho* CHB used a base additive, KO-*t*-Bu, to setup a Lewis acid-base interaction with one of boron's *p* orbitals and initiate cleavage of the bidentate ligand. Similar reactions have precedent in our research group.[10] This method was not successful; In fact, it inhibited borylation in proportion to the amount of KO-*t*-Bu used based on both conversion and *ortho* selectivity.

2.1.4: Substrate Scope Comparison Under Chelate and Steric Conditions

Based on the promising results in **Table 2.1**, a substrate scope study was carried out using the reaction conditions from **Entry 4** for achieving *ortho* regioselectivity. To fully assess how the pre-ligand loading differs in this catalytic system, reactions were run in parallel to Li's original system[6] (**Table 2.1, Entry 1**), alongside our optimized reaction conditions of 0.5 mol% **BB** and $[Ir(Cl)cod]_2$ (**Scheme 2.2**).

Scheme 2.2: CHBs of Arenes using Conditions for Steric- and Chelate-Directed Catalysis.

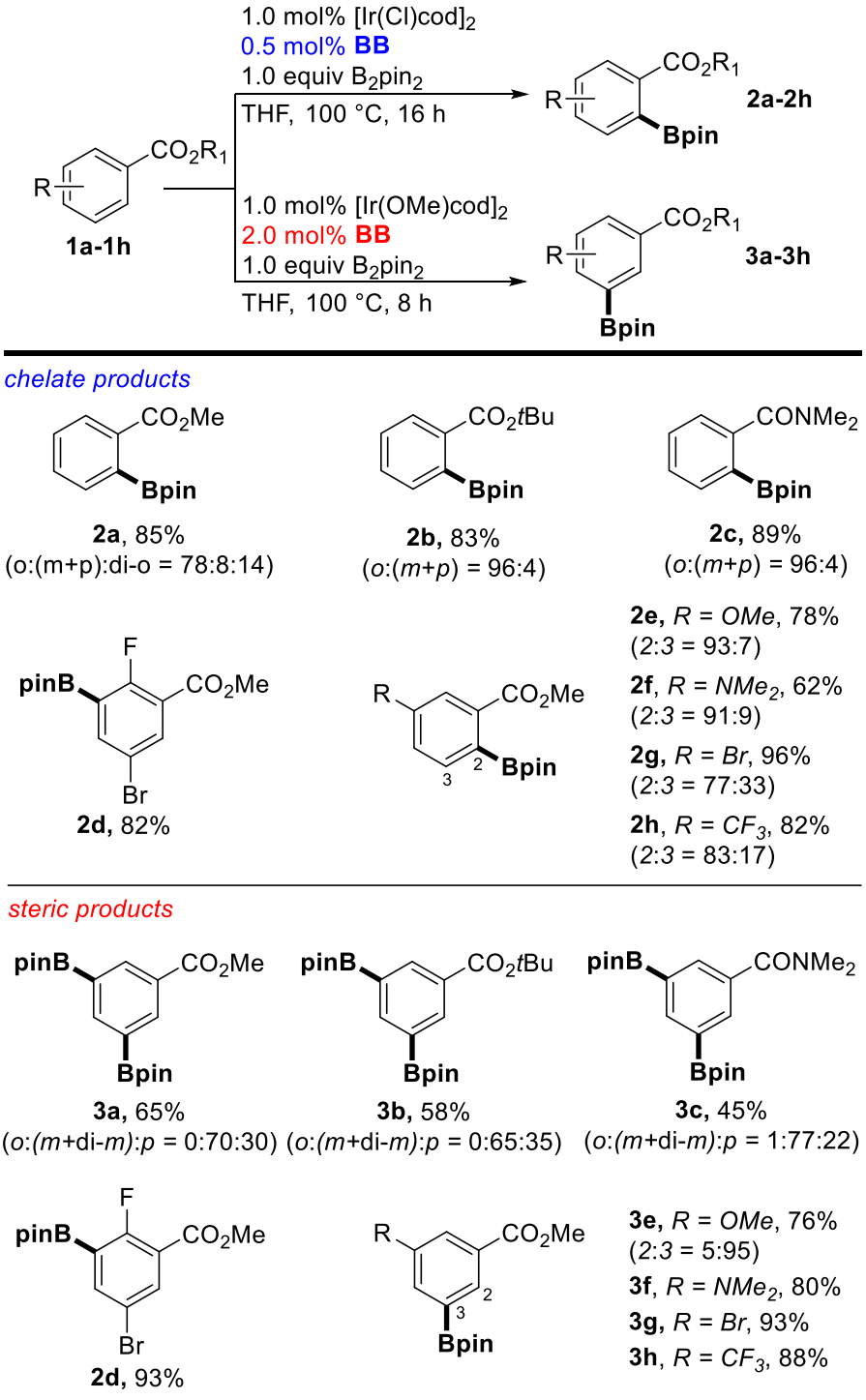

Conversions and selectivities were calculated using ^{1}H NMR of crude reaction mixture.
Note: N,N-dimethylbenzamide was used in the generation of 2c and 3c.

For the esters and amide tested, it was found that changing the ligand loading flips the regioselectivity, with *ortho*-selectivity ranging from 60-96% being observed with 0.5 mol % **BB**.

Steric controlled conditions with 2 mol % **BB** gave almost exclusively the meta and para steric products (**3a–3h**). CHB reactions for both conditions were effective for a variety of functional groups, both electron withdrawing and donating. To see the efficacy of the chelate-directed conditions, *ortho* borylation was attempted for substrate **1d**, which has only one *ortho* site to the ester directing group and a bulky substituent in the position *meta* to the ester. The borylation of this substrate was in the steric position regardless of the pre-ligand loading conditions, illustrating the limits for switching regioselectivity with multiple substituents present.

Scheme 2.3 shows mono and di-substituted thiophene (**1i** and **1j**) and furan (**1k** and **1l**) heterocycles that were tested for their competency under both borylation conditions. Monosubstituted heteroarenes **1k** and **1l** showed that the ester was incapable of directing *ortho* as it could not overcome the borylation of the more reactive 5-position of each substrate.[11] By blocking the 5-position with a methyl group (**1j** and **1l**), the heterocycle could be borylated adjacent to the ester under chelate conditions. Interestingly, we found major differences in disubstituted heterocyclic products **2i** and **2j**, the latter showing steric preference regardless of the decreased pre-ligand loading. Steric conditions gave products borylated in the 4-position for both heterocycles. Borylating substrates **1a-1l** using 0.5 mol % **BB** and $[Ir(OMe)cod]_2$ resulted in modest if any changes in reactivity or regioselectivity relative to using $[Ir(Cl)cod]_2$ (see *section 2.5.7* for direct comparisons). In contrast, following Li's reaction conditions with 2 mol % **BB** and $[Ir(OMe)cod]_2$ gave higher yields and almost solely the steric product for all substrates in **Schemes 2.2 and 2.3**.

Scheme 2.3: CHBs of Heteroarenes using Conditions for Steric- and Chelate-Directed Catalysis.

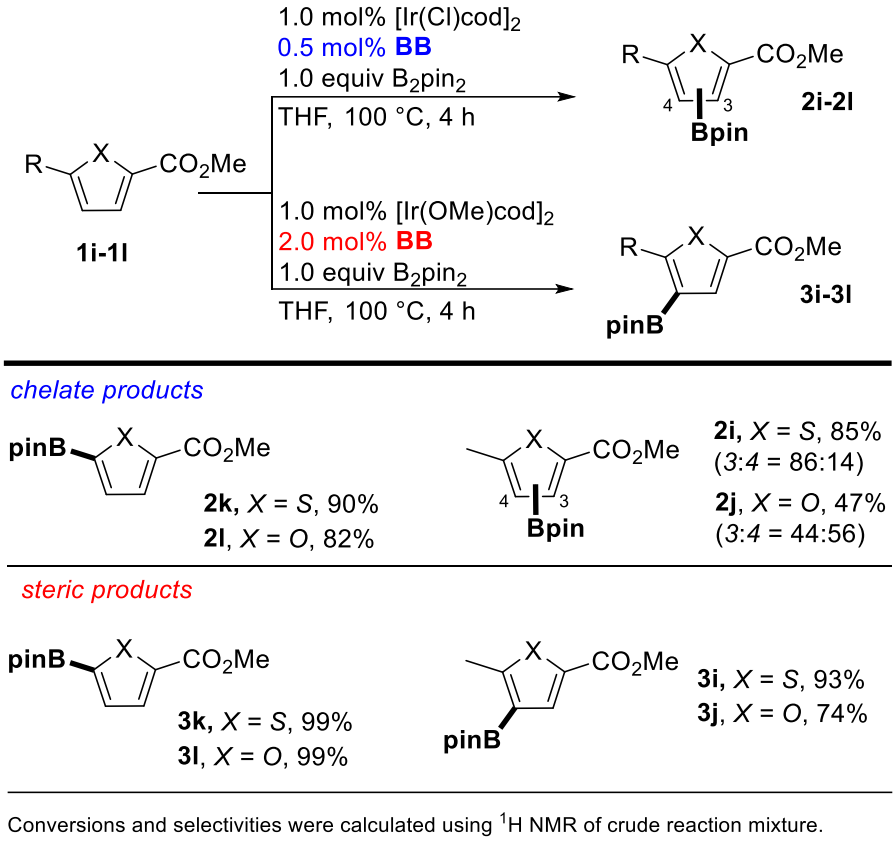

Conversions and selectivities were calculated using ^{1}H NMR of crude reaction mixture.

Given that spectator boryl ligands have found their way as a powerful and versatile ligand class in CHBs for both C(sp^2)–H and C(sp^3)–H, as evidenced by the prominent work done by the Li and Xu groups,[12–17] the insights on potential modifications using dimer boron pre-ligands like **BB** can be valuable in future iterations of this ligand type. Although alternative ligand systems (specifically those with B–Si linkages instead of B–B dimers) can produce chelate-directed products, the **BB** ligand at lower loadings is more appealing to use for catalyzed CHBs. Its synthesis can be done within two steps starting from commercially available materials and its simpler workup and purification does not produce as large a waste stream as the B–Si ligand syntheses. **Figure 2.2** displays the synthetic route in obtaining **BB** and **BSi** ligand used by Li.[12]

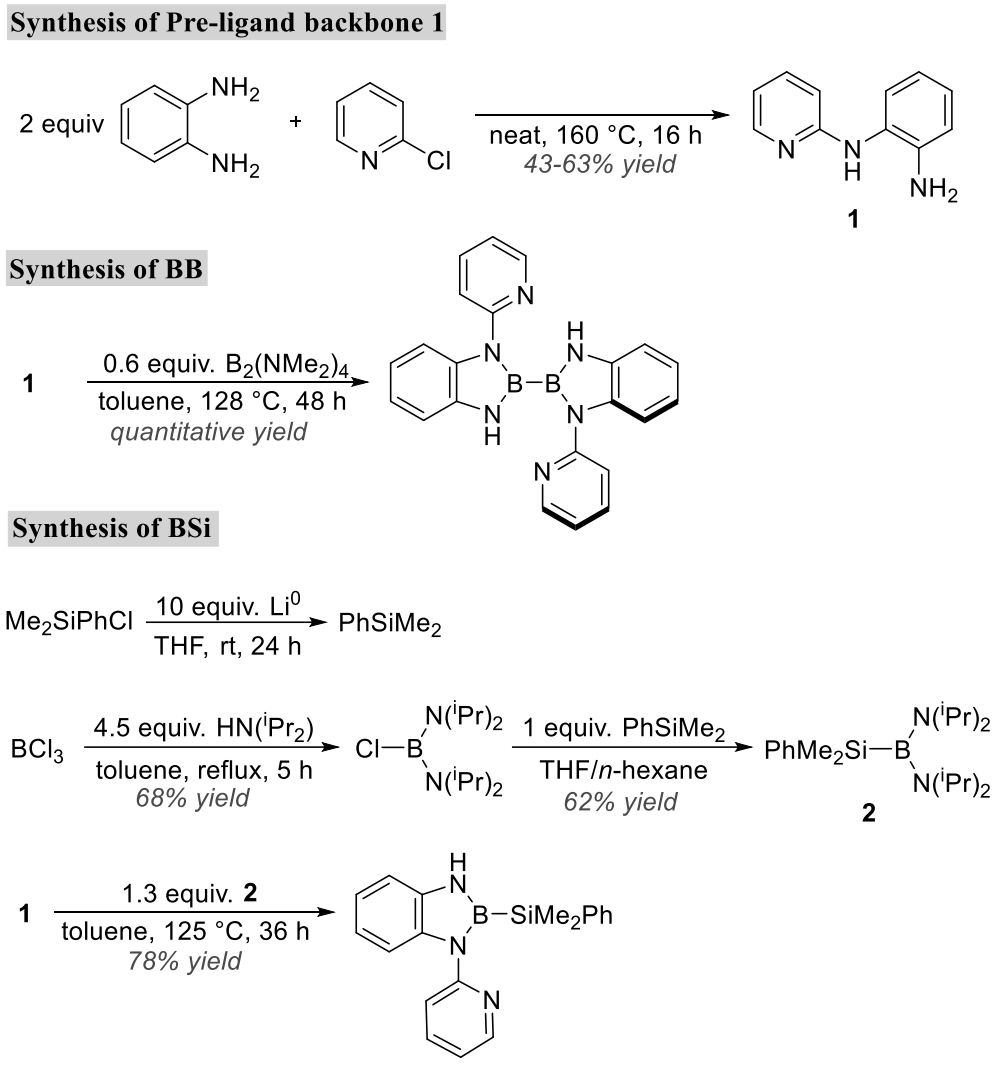

Figure 2.2: Synthetic Routes to Obtain **BB** and **BSi** Pre-ligands.

2.2: Borane Syntheses for Catalyst Control

2.2.1: Purpose

Currently, the only structural difference regarding why *ortho* selectivity is preferred as the amount of **BB** decreases is based on the counter anion difference in the isolated pre-assembled catalysts shown in **Figure 2.1**. However, it is not clear why Complex **2** would change the selectivity in this way given that the ligands on the metal center of the Ir(III) cation are the same as in Li's case. A hypothesis is that one of the B,N ligands is transferring to the Ir(I) counter anion after oxidative addition which in turn could allow coordination of the directing group into the

newly opened site. As **BB** is a dimeric compound, confidently knowing the reactivity of every B,N unit, or **BB** molecule that did not oxidatively add would be difficult (e.g. defining the number of ligands on the metal for every Ir center). To reach a more well-defined pre-catalyst, we sought to synthesize borane derivative of **BB** and react it with $[IrCl(cod)]_2$. In this way we could better control the number of B,N-units on the metal center, and identify further structural differences at ligand loadings between 0.5 and 2 mol % with higher certainty.

2.2.2: Reaction Optimization

The synthesis of the diamino-pyridyl borane was initially attempted under reaction conditions similar to those used to yield HBdab by Robinson,[18] where borane dimethyl sulfide is reacted with the pre-ligand backbone with dichloromethane as the solvent (**Table 2.2,** Entries 1-2). This yielded the Lewis-base borane adduct (product **2**), confirmed by the crude ^{11}B NMR (δ –17.2 (q, J = 95.3 Hz, BH_3) regardless of heating. We expected this synthesis to be a challenge as the pyridinyl nitrogen is a stronger Lewis base in respect to the primary and secondary amine on the aromatic ring,[19,20] and thus adduct formation is more favorable with BH_3. In addition, there are no reports synthesizing derivatives of borane product **1** when there is a pyridine in the molecule. We hypothesized that adding a catalytic amount could help form the borane through a different mechanism that would be driven by the release of H_2 gas after the azinyl BH_3 would coordinate with the protonated secondary amine in proximity. After the acid is reformed, the same reactivity could occur with the primary amine. However, adduct was exclusively formed when testing this with HOTf (**Entry 3**). As Lewis acid-base adducts are governed by the reaction's equilibrium constant (Kb),[20] we attempted to push the thermodynamics towards the less favorable product **2** by refluxing the reaction in toluene (Entries 4-7).

Table 2.2: Reaction Optimization of Borane Synthesis.

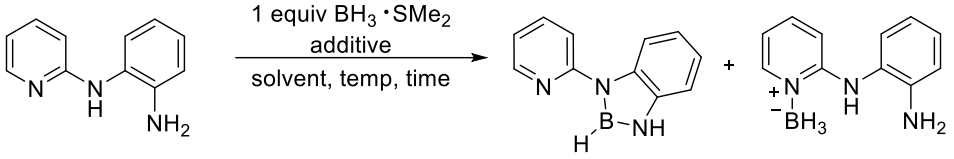

entry	solvent	temp (°C)	time (h)	additive[a]	[M] of rxn	conversion[b]	ratio of **1:2**
1	CH_2Cl_2	rt	24 h	--	0.621	>99%	1:>99
2	CH_2Cl_2	50	5 h	--	0.305	>99%	1:>99
3	CH_2Cl_2	rt	24 h	0.1 equiv HOTf	0.893	>99%	1:>99
4	toluene	115	24 h	--	0.625	32%	94:6
5[c]	toluene	115	24 h	--	0.947	--	--
6	toluene	115	13 h	--	0.089	40%	98:2
7[c,d,e]	toluene	-5 to 115	12 h	--	0.150	--	--
8	THF	-78 to rt	16 h	1.05 equiv *n*BuLi	0.285	>99%	1:>99
9[f]	THF	-78 to rt	12 h	1 equiv $BrBH_2 \cdot SMe_2$ 1.05 equiv *n*BuLi	0.144	>99%	1:>99[g]

Conversions and selectivities were calculated using ^{1}H NMR of crude reaction mixture. [a]$BH_3 \cdot SMe_2$ was used as a 1 M solution in CH_2Cl_2, *n*BuLi was used as a 2.5 M solution in hexanes.[b]Conversion is based on starting material was calculated by the crude ^{1}H NMR integrations. [c]The aromatic region in the crude ^{1}H could not give conclusive results, though ^{11}B shows minimal formation of **1** and no unreacted $BH_3 \cdot SMe_2$.[d]Borane was added at -5 °C then refluxed. [e]1.05 equiv of $BH_3 \cdot SMe_2$ was used. [f]$BrBH_2 \cdot SMe_2$ was used as the borane source. [f]Crude reaction mixture contained 30% adduct (**2**) to 70% of an unknown boron compound shown in ^{11}B NMR (C_6D_6) δ 2.5 ppm.

Initial results from **Entry 4** show that the desired product **1** was formed, confirmed by the crude ^{11}B NMR (δ 25.4 (d, J = 149.9 Hz, BH) and ^{1}H NMR, though only 32% of starting material was converted. However, the ^{11}B NMR showed another minor species in solution (δ 3.79 ppm) that appeared to be a doublet, though this could not be confirmed. It was believed that this was due to poor shimming, but this resonance continuously appeared as described in later experiments, where the sample was well-shimmed. After removing solvent under vacuum, the ^{1}H NMR of the isolated solid showed additional peaks in the aromatic region between 8.6 and 6.4 ppm in $CDCl_3$ that were not distinguishable as this region was broader, with the new resonances coalescing. In addition, new minor peaks appeared in the ^{11}B NMR (δ 9.2, 5.8, 2.4 ppm) with unclear splitting. Tetrahedral boron species typically appear as sharp peaks upfield of 10 ppm,[21] and we suspect these new peaks to represent tetra-coordinate boron given their chemical shift and calculated

FWHM to be between ~96-180 Hz. The initial hypothesis was that either a) decomposition occurred as the solid was exposed to air after the solvent was evaporated under vacuum to weigh and obtain NMR data outside of the glovebox or b) the product is only stable in solution. As this was the first experiment showing that borane formation is possible, we assume that the boron is bonding with the aryl amines over the pyridyl nitrogen as a) this 5-membered ring formation would be preferred over the four-membered ring and b) only one N-H resonance is seen at δ 3.75 ppm in the ^{1}H NMR integrating to one. Obtaining crystallographic data in the future would be ideal to support where the boron atom is covalently bonding.

Though product **1** was not isolated, we wanted to test the reproducibility and ensure that all manipulations were done under nitrogen (**Entry 5**). The ^{1}H NMR of the crude reaction mixture showed the same type of broadness of peaks even prior to solvent evaporation and was considerably worse as peaks could not be distinguished from one another. Thus, no conclusive results could be recorded even after the solvent evaporation. As everything was done under Schlenk techniques, and NMRs were prepared inside of a glovebox, it was thought that the higher [M] of this reaction (in respect to **Entry 4**) could be promoting inter/ or intra-molecular reactions and forming oligomers, or that the compound was disproportioning.

The reaction in **Entry 6** was thus carried out at a lower concentration and monitored hourly. Though conversion of the starting material did not improve, we saw that product **2** was initially formed but over the course of 12 hours, >98% of this was converted to desired product **1** with only 40% of starting material converted. We also observed the same minor species from **Entry 4** forming in the ^{11}B NMR (δ 3.79 ppm) at the start of this transformation.

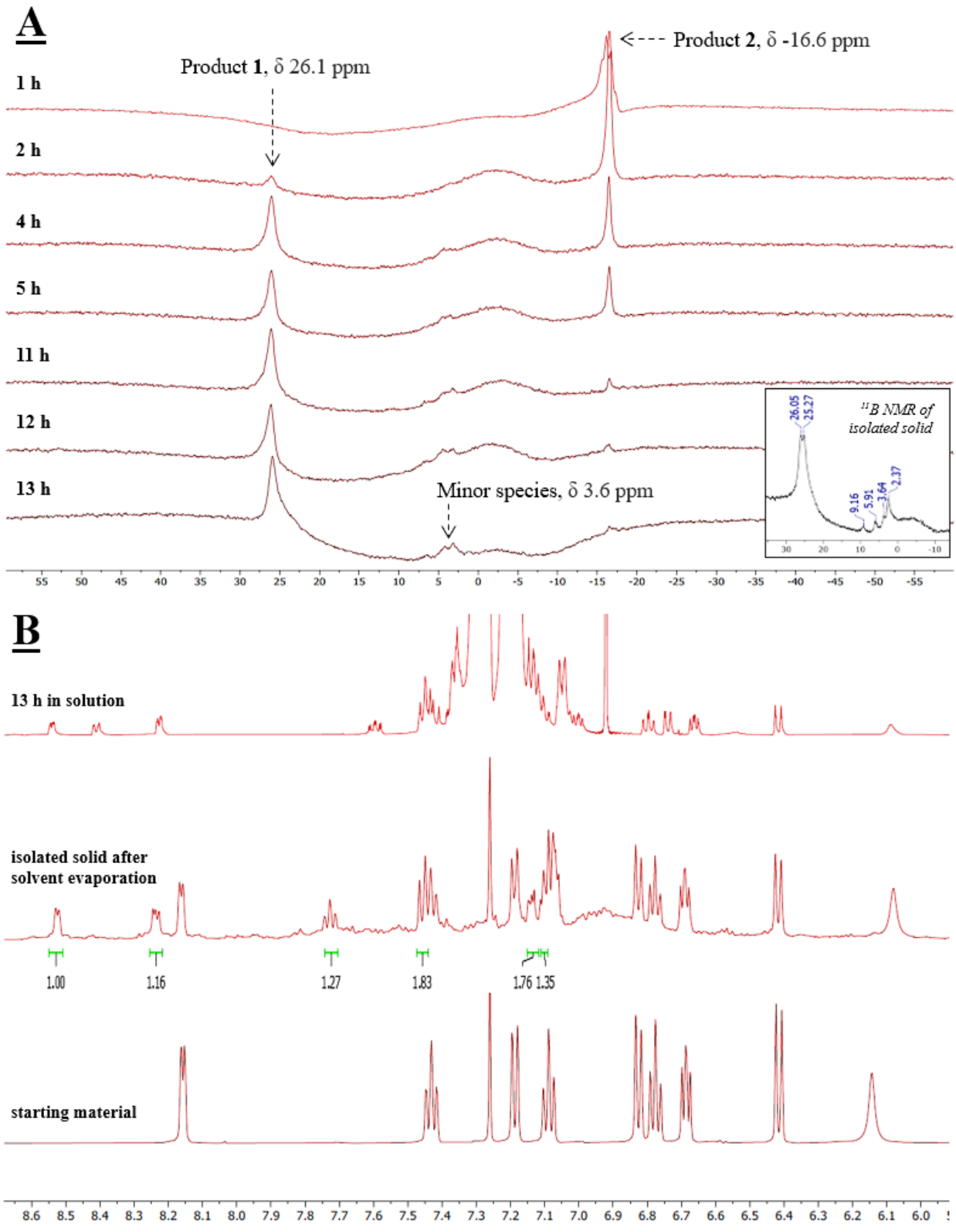

Figure 2.3: Formation of Borane Product **2** Over time.

The new boron impurities in the isolated solid after solvent evaporation are also consistent with previous experiments (**Figure 2.3, A**). When analyzing the ^{1}H NMR of the crude reaction mixture, the baseline was much smoother, and the peaks could be distinguished from one another. After solvent evaporation, the aromatic region shows those new impurities represented in the broader baseline, though the integration of the borane resonances represented the 8 protons in the molecule, including the N–H (**Figure 2.3, B,** *see pg. 120 for spectral assignment*). Various purification techniques such as Kugelrohr distillation, sublimation, solvent extractions, were attempted to isolate the borane from the other boron species and starting material, though this was unsuccessful as the sample grew with more impurities. These experiments suggest that the borane is not stable in its solid-state and was stabilized in solution with toluene. This could be due to intermolecular interactions with the B–H and other Lewis basic atoms such as the pyridyl nitrogen, though we believe this is due to the disproportionation of the compound under vacuum which is common with boranes such as HBeg and HBcat.[22,23]

Given the poor conversions in **Entries 4** and **6** of **Table 2.2**, we attempted adding the borane reagent at -5 °C to ensure full reactivity of the borane with the starting material. Again, the NMR spectrum matched what was previously described for **Entry 5** and thus no conclusive results could be obtained (**Entry 7**). Using ^{n}BuLi to deprotonate the primary amine in the starting material to influence the reactivity of BH_3·SMe_2 away from the pyridine was also unsuccessful (**Entry 8**). Using $BrBH_2$·SMe_2 to react with the deprotonated organo-lithium intermediate, where the driving force to form the desired borane would be release of LiBr and H_2 gas, only yielded the adduct (**Entry 9**). Though not shown in this table, we attempted refluxing the isolated material of product **2** in toluene based on the knowledge that adduct is initially formed then converted into product **1**.

However, the crude reaction mixture consisted of a 1:1 ratio of unreacted starting material to the diamino-pyridyl compound, where the adduct was broken up.

2.2.3: NMR Tube Reaction with Borane and [IrCl(cod)]$_2$

Focusing on the initial goal of synthesizing a well-defined catalyst by controlling the number of B,N-units on the metal center, we tested the viability of the borane as a ligand with [IrCl(cod)]$_2$ where we hypothesized oxidative addition of the B–H bond would occur to form the Ir(III), 18 electron pre-assembled catalyst (**Figure 2.4**). Using the conditions that gave the best results (**Table 2.2**, **Entry 6**), the borane synthesis was carried out in a J-young tube with C_7D_8 and monitored (**Figure 2.4, A)**. As opposed to the optimized conditions, this was heated in a closed system under nitrogen where 65% conversion of the starting material was reached after only 5 hours. As previous reactions were done in an open system to bubble the dimethyl sulfide gas into a bleach trap, the reactivity was poor and conversions could only reach < 40%. The ^{1}H NMR shows the starting material and some of the impurities observed previously (also evidenced by the ^{11}B spectrum), and the product was successfully made.

Following this, [IrCl(cod)]$_2$ was dissolved in methylene chloride and added directly to the borane solution (**Figure 2.4, B)**. Instantaneous reactivity between the two reagents was observed at room temperature with minor amount of unreacted borane evidenced by ^{11}B NMR. The ^{1}H NMR spectrum shows oxidative addition of the B–H bond (δ -10.68 ppm, s, Ir–H). This was confirmed by ^{11}B NMR where the Ir–B resonance is seen as a broad singlet at +36.7 ppm. As seen with **BB** oxidative addition to Ir in *section 2.1*, the proton adjacent to the pyridyl nitrogen is shifted downfield once chelated to the metal center (δ 9.05 ppm) in the ^{1}H NMR. The integration of the remaining protons match the compound, and the N–H resonance is shown at δ 6.24 ppm integrating

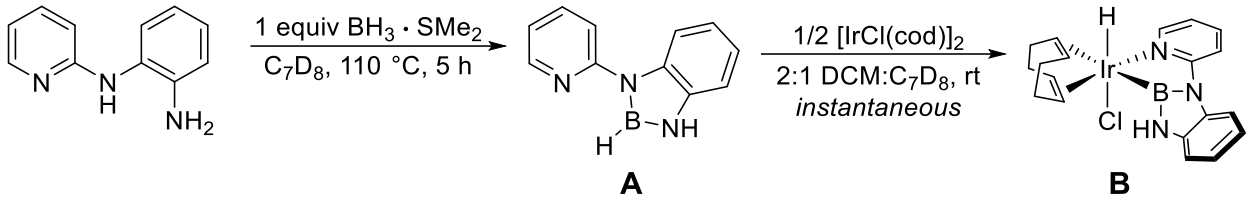

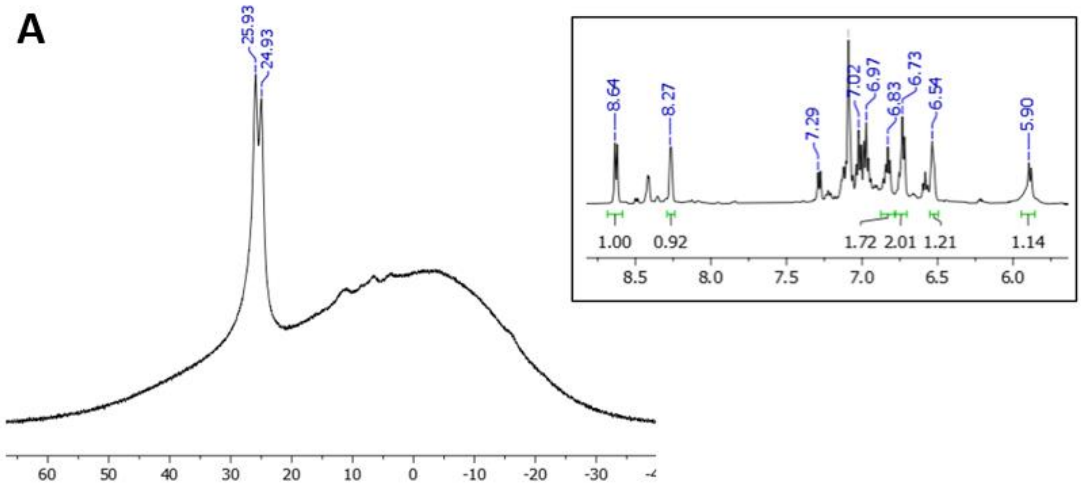

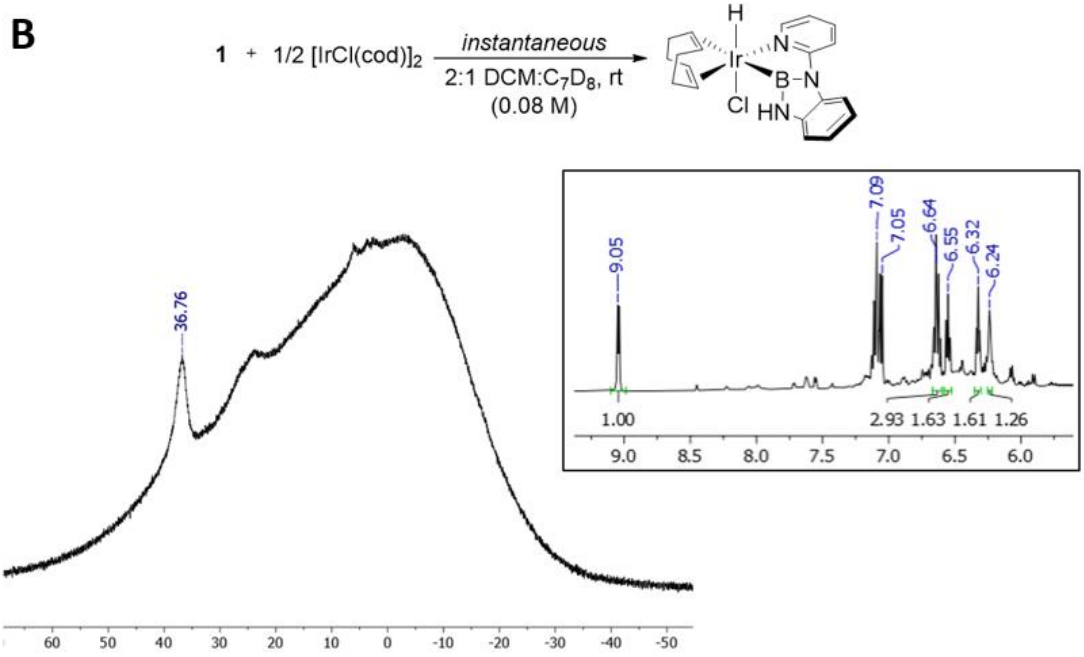

Figure 2.4: NMR Tube Reaction of Borane and $[IrCl(cod)]_2$.

to 1 as a broad singlet. The upfield region of this spectrum shows all methylene protons distinct from one another as expected in an asymmetric metal complex.

As seen in iridium and titanocene borane σ-complexes,[24,25] it is possible the B–H bond acts as two-electron donor ligand over oxidative addition where Ir(I) 16e$^-$ compound would be formed over Ir(III) 18e$^-$ species **B**, respectively. As we observe a sharp singlet representing the Ir–H in the ^{1}H NMR, it is likely that the B–H bond oxidatively adds to Ir as resonances representing agnostic B–H interactions are extremely broad due to the quadrupolar relaxation of ^{11}B.

2.3: [Ir(X)cod]$_2$ Influence on Regioselectivity

2.3.1: Direct Comparisons Between Ir(I) Pre-catalysts

The original publication from Li's group[6] showcased that using 2 mol% pre-ligand was compatible to borylate the least sterically hindered C(sp^2)–H bonds with [Ir(OMe)cod]$_2$ and B_2pin_2. When optimizing reaction conditions with 1-methoxyanisole, they show that [IrCl(cod)]$_2$ gave <20% yield and conversions (**Scheme 2.4**, **A**).

Scheme 2.4: [Ir(X)cod]$_2$ Comparison at 0.5 and 2 mol% **BB**.

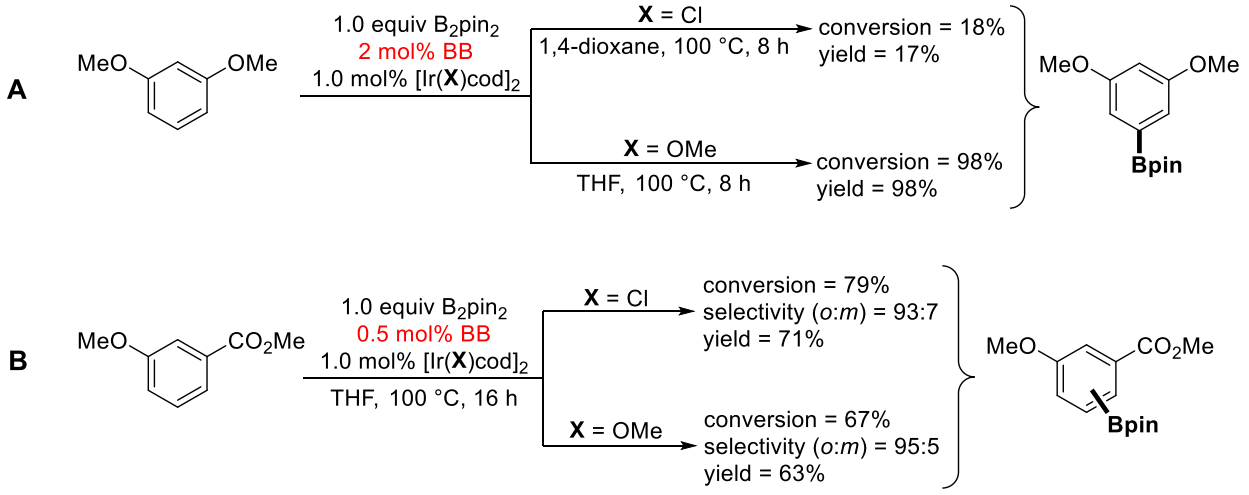

Comparing these reaction conditions with our work in *section 2.1*, accessing positions *ortho* to directing groups was preferred as the pre-ligand loading decreased to as little as 0.5 mol %. In addition, we found that using $[IrCl(cod)]_2$ did not affect the selectivity but did result in better conversions and yields. However, the reactivity was not nearly as poor as it was for Li when switching between Ir(I) pre-catalysts (**Scheme 2.4**, **B**). It was originally hypothesized that because arenes substituted with Lewis-basic directing groups were used as the substrate, versus the one example Li shows with 1-methoxyanisole, the chelation of the directing group helped facilitate catalysis regardless of the metal source. Thus, the Ir(I) pre-catalyst would not show as drastic of a difference in reactivity.

To evaluate whether a directing group on the substrate would improve reactivity with 2 mol % **BB**, we monitored the reaction of methyl 3-(trifluoromethyl)benzoate where the only variable changed from Li's optimized reaction conditions is the Ir(I) pre-catalyst (**Table 2.3**).

Table 2.3: Li's Steric Conditions with an Ester-containing Arene and $[IrCl(cod)]_2$ in CHB.

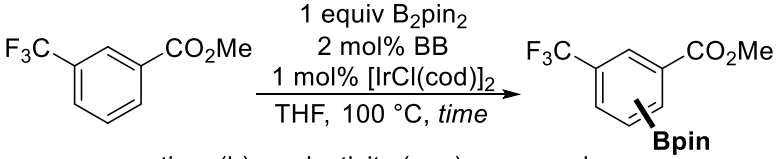

time (h)	selectivity (*o*:*m*)	conversion
1	82:18	44%
2	79:21	56%
3	79:21	68%
5	76:24	81%
7.5	71:29	81%
11	75:25	85%
24	75:25	87%

Conversions and selectivities were calculated using ^{1}H NMR of crude reaction mixture.
o = *ortho* to the ester.

Results did show greater reactivity, but more surprising, the chelate product was the major regioisomer, where borylation occurred *ortho* to the ester. Given the variety of substrates tested by

our group and Li's when 2 mol % **BB** is used, observing this regiochemical switching by changing the Ir(I) pre-catalyst alone was unprecedented. Additionally, a) the *ortho*-borylated product was not the only regioisomer yielded, where a 25% of the regioisomeric mixture was *meta* borylated product and b) *ortho* product slowly decreased from 82% to 75% over 11 hours.

Reported CHB's in the literature have used either $[IrCl(cod)]_2$ or $[Ir(OMe)cod]_2$ depending on which pre-catalyst gives the highest conversion. Selectivity differences between these two pre-catalysts have not been explicitly reported but were observed by Li and co-workers in their work with functional-group directed CHB using a N,B-Bidentate Si-containing boryl ligand. Here they found that $[IrCl(cod)]_2$ worked best for their system showing 84% conversion from >99:1 *o*:(*m*+*p*) product. When screening [Ir(OMe)cod]2, they showed that the conversion is lower, but the selectivity is flipped to 35:65 *o*:(*m*+*p*) (**Figure 2.5**). They reported that "$[Ir(OMe)cod]_2$….led to inferior results".[12]

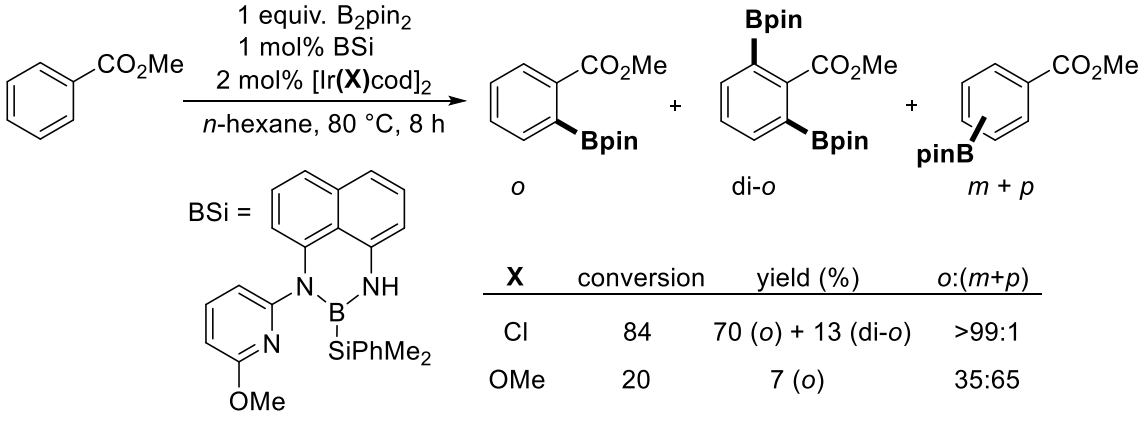

X	conversion	yield (%)	*o*:(*m*+*p*)
Cl	84	70 (*o*) + 13 (di-*o*)	>99:1
OMe	20	7 (*o*)	35:65

Figure 2.5: Literature Example of Regiochemical Switching with Ir(I) pre-catalysts.

A direct comparison between $[IrCl(cod)]_2$ and $[Ir(OMe)cod]_2$ was carried out with 2 mol % **BB** to investigate a clear chelate or steric preference of borylated products (**Table 2.4**). 1,3-Disubstituted methyl benzoate derivatives were used as the substrate, where bromo and methoxy

substituents *meta* to the methyl ester were tested against the model substrate, methyl 3-(trifluoromethyl)benzoate.

Table 2.4: Comparison of [Ir(X)cod]$_2$ Pre-catalysts at 2 mol % **BB**.

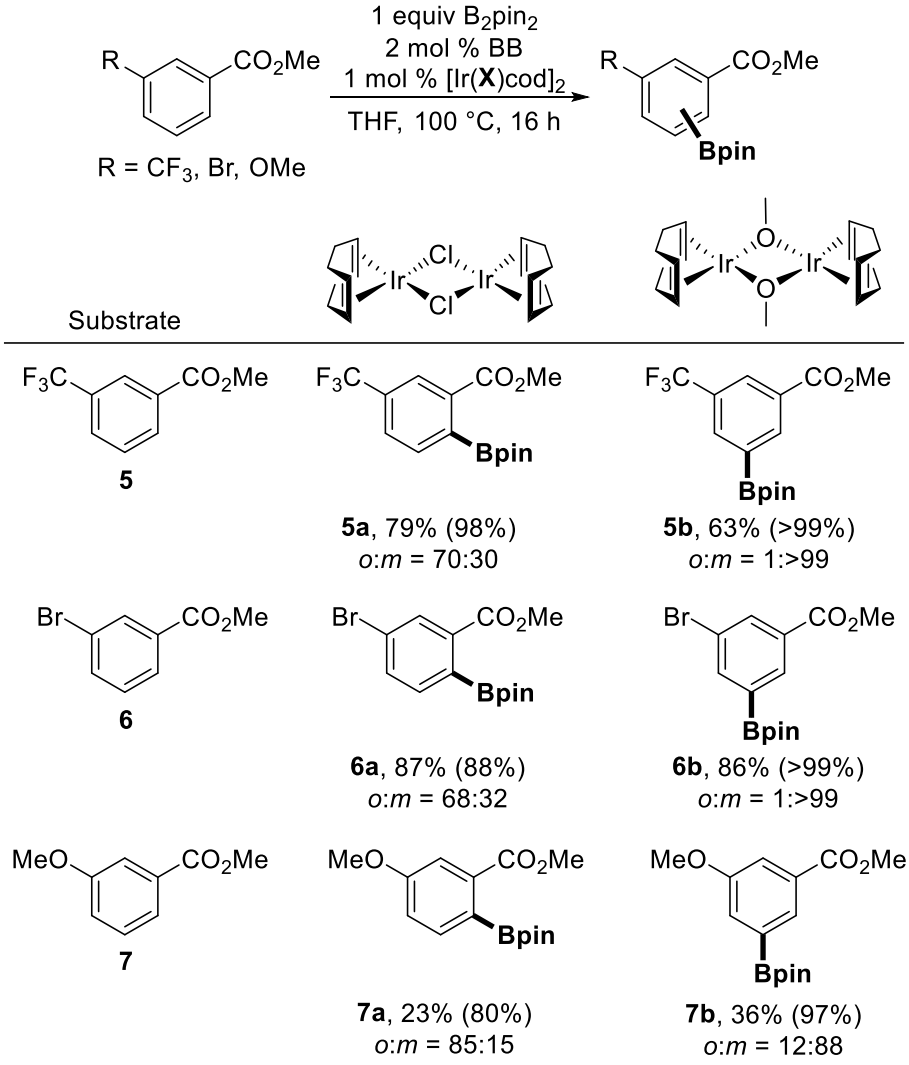

Conversions and selectivities were calculated using ^{1}H NMR of crude reaction mixture. Isolated yields are shown in parentheses.

Using [Ir(OMe)cod]$_2$, we observe a clear preference for borylation in the least sterically hindered position as the major product. This was as expected given these reaction conditions are identical to those used by Li and our group in *section 2.1*. Substrates **5** and **6** yielded >99% *meta*-borylation, though testing the more electron rich aromatic system (substrate **7**) yielded a modest

12% *ortho* to ester borylation. When using $[IrCl(cod)]_2$, the CHB of all substrates showed great preference for *ortho* to ester borylation, all exceeding >75% *ortho* selectivity.

2.3.2: Mechanistic Insights and Hypotheses

In *section 2.1.3*, **Figure 2.1** shows Li's isolated pre-assembled catalyst responsible for steric borylations (Complex **1**) which was made using a 2:1 ratio of **BB**:Ir. When comparing our isolated pre-assembled catalyst (Complex **2**) hypothesized to be responsible to yield *ortho*-borylated products, the main difference between the two structures is the $[Ir(cod)Cl_2]^-$ counter-anion versus the [Cl]. The **BB** pre-ligand oxidatively adds to yield two monoanionic ligands on the metal with COD resulting in an Ir(III) cation with 18 electrons. However, if only 1 equivalent of **BB** is used, the balanced reaction gives the Ir(I) counter anion instead of the chloride which is what we observed.

In respect to the regioselective switching when $[IrCl(cod)]_2$ was used in **Table 2.4**, it is speculated that the same $[IrCl_2(cod)]$ anionic complex is responsible for the *ortho*-selectivity even though 2 mol % of pre-ligand is used. This would suggest that Complex **1** forms quicker, potentially entering the catalytic cycle before the one equivalent of **BB** remaining can oxidatively add. This may relate to the results from **Table 2.3** where complete *ortho* C–H activation is not preferred over the *meta* position, as *ortho* product decreases over time. If the Ir(I) anion is initially formed and participates in *ortho*-borylation, it can be thought that over time one equivalent of unreacted **BB** reacts with the Ir(I) counter-anion forming Li's complex **2**. Furthermore, a reason for not yielding the full *ortho* product may be due to the mixture of anions in catalysis, where there are competing reactions between **BB** oxidative addition to the Ir(I) anion.

There is only one report in the literature showing this mixture of anions, in which Ozerov and co-workers attempted to isolate an iridium complex that could show the activation of N–C or

C–H bonds of PNP pincer ligands. Upon reacting 1 equivalent of PNP ligand and 0.5 equivalents of $[IrCl(cod)]_2$, a cationic Ir(III) species was formed with the two exact counter anions being chloride and $[IrCl_2(cod)]$, along with excess ligand.[26] We suggest this is a possibility in this work as after analyzing Li's ^1H NMR spectra of his isolated complex **2**, there are unidentified and unreported peaks that are consistent with the chemical shifts representing the Ir(I) anion reported by Ozerov.[6] It should be noted that we have attempted to repeat Li's experimental procedure to synthesize complex **2** though >92% purity could not be obtained as minor amounts of the Ir(I) anion was yielded, supporting the idea of having a mixture of anions in solution.

With respect to the results with $[IrCl(cod)]_2$, we have shown *ortho* borylated products are yielded when using 0.5-2.0 mol % **BB**, and only *meta* borylated products are formed with 2.0 mol % **BB** and $[Ir(OMe)cod]_2$. To test the hypothesis of the faster formation of complex **1** over complex **2**, we carried out experiments with increased pre-ligand loadings of **BB** (**Table 2.5**).

Table 2.5: Increased Pre-ligand Loadings of **BB** in CHB with $[IrCl(cod)]_2$.

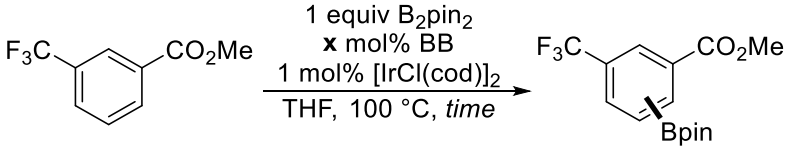

x mol%	time (h)	selectivity (*o*:*m*)	conversion	yield
2	1	82:18	31%	--
2	16	70:30	84%	73%
4	1	41:56	45%	--
4	16	25:75	95%	72%
6	16	1:>99	86%	74%

Conversions and selectivities were calculated using ^1H NMR of crude reaction mixture.

If there is a 2-3 fold excess of **BB** molecules in the reaction, it is possible that Li's isolated preassembled complex (complex **2**) will be formed faster, thus generating another equivalent of $[Ir(BN)_2(cod)]$ in the reaction and thereby yielding steric borylated products. Methyl 3-

(trifluoromethyl)benzoate was the substrate chosen for these experiments due to more accurate ^{19}F NMR integrations, as well as the expected higher reactivity in CHB from the electronic withdrawing effects of -CF_3. The experiments in **Table 2.5** showed that as the ligand loading increased, the *meta* product also increased. This supports the hypothesis that if more **BB** is present in the initial reaction mixture at t = 0, the Ir(I) anion will not be able to enter the catalytic cycle, or more generally, possess the appropriate amount of time to help direct the *ortho*-borylation.

2.4: Conclusions

In conclusion, a catalyst system was modified from steric- to chelate-directed CHB by decreasing the pre-ligand loading from 2 to 0.5 mol % respectively with 1 mol % $[Ir(X)cod]_2$ (X = Cl, OMe), where borylation occurred *ortho* to esters and amides of (hetero)arenes. Though the "X" substituent of the iridium dimer pre-catalyst did not affect selectivity at the lower pre-ligand loadings, regiochemical switching was made possible using the same 2:1 ratio of **BB**:Ir Li used to achieve steric-directed products, where when X = Cl instead of -OMe, the selectivity is flipped from to yield *ortho*-borylated products. Both systems are the first cases reported in Ir-catalyzed CHB where desired regioselectivity can be achieved by altering the amount of ligand, or by changing the Ir(I) pre-catalyst. Throughout the beginnings of iridium catalyzed CHBs,[27] boron has typically been an actor ligand, but through new developments has shown to be a promising support ligand that can be used for regiochemical switching.

When comparing the isolated, hypothesized preassembled catalysts formed when reacting with **BB**:Ir ratios that mimicked the steric- and chelate directed CHB systems, we observe an Ir(I) counteranion, $[IrCl_2(cod]$, at the lower pre-ligand loadings as opposed to the $[Cl]^-$ found in Li's steric directed system. In an attempt to understand further why regioselectivity changes at lower ligand loadings, syntheses of the borane derivative of **BB** were carried out to better control the

number of B,N units on Ir and isolate a more well-defined catalyst. Though this compound was not stable after solvent evaporation, adding $[IrCl(cod)]_2$ to the reaction solution showed oxidative addition of the B–H bond, evidenced by ^1H and ^{11}B NMR. In Chapter 3, we investigate the role of $[IrCl_2(cod)]^-$ in CHB and its effect on regioselectivity.

2.5: Experimental Data

2.5.1: General Information

All reactions were carried in a nitrogen-filled glovebox with oven-dried glassware. THF and toluene were obtained from a wet still refluxing over sodium benzophenone ketyl, and pentane was obtained from a wet still refluxing over CaH_2. Methylene chloride was obtained from a dry still. $[Ir(OMe)cod]_2$ was prepared according to the literature.[28] Reagents for ligand syntheses, along with reagents for CHB reactions that include $[IrCl(cod)]_2$, B_2pin_2, and all starting materials were obtained commercially and used as received unless otherwise noted. ^1H NMR spectra were recorded on a Varian 500 MHz instrument. ^{13}C and ^{11}B NMR were recorded on 126 MHz and 160 MHz instruments, respectively. Borylation reactions were set up in a nitrogen-filled glovebox and carried out in 3.0 mL Wheaton microreactor vials equipped with a stir bar and pressure cap, where stock solutions of the ligand and pre-catalyst were freshly made.

High-resolution mass spectra (HRMS) were obtained at the Michigan State University Mass Spectrometry Service Center using electrospray ionization (ESI+ or ESI-) on quadrupole time-of-flight (Q-TOF) instruments. Melting points were measured in a capillary melting point apparatus and are uncorrected.

2.5.2: Synthesis of N^1-(pyridin-2-yl)benzene-1,2-diamine

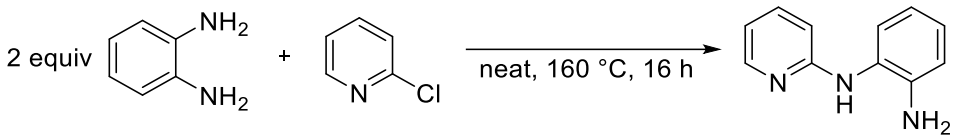

Following the literature procedure,[6] 1,2-Diaminobenzene (1.0 g, 9.26 mmol, 2.0 equiv) along with 2-chloropyridine (0.42 mL, 4.63 mmol, 1.0 equiv) were added to a 100 mL round bottom flask containing a magnetic stir bar. A condenser was attached, the system was purged with N_2, and the flask was heated in an oil bath at 160 °C for 16 hours while under nitrogen. After the allotted time, the black solid formed was cooled to room temperature, after which the reaction flask was opened to air. Water and acetone were then added in equal amounts to the solid until it completely dissolved. The pH of the solution was adjusted to 10 by adding a saturated Na_2CO_3 solution. Brine was then added, and the crude product was extracted with ethyl acetate. Organic layers were combined, dried over Na_2SO_4, filtered, and concentrated under reduced pressure. The residue was washed with hexanes (3 x 10 mL) on a filter frit. The solids were then transferred to a Soxhlet thimble, and a Soxhlet extraction was performed with DCM for 20 hours. Solvent was removed from the filtrate by rotary evaporation, yielding the product as a pale violet solid (528 mg, 62%). ^{1}H NMR (500 MHz, $CDCl_3$) δ 8.16 (ddd, *J* = 5.1, 1.9, 0.9 Hz, 1H), 7.44 (td, *J* = 7.9, 1.9 Hz, 1H), 7.20 (dd, *J* = 7.8, 1.5 Hz, 1H), 7.10 (td, *J* = 7.7, 1.5 Hz, 1H), 6.83 (dd, *J* = 8.0, 1.4 Hz, 1H), 6.78 (td, *J* = 7.6, 1.4 Hz, 1H), 6.69 (ddd, *J* = 7.1, 5.0, 0.9 Hz, 1H), 6.42 (dt, *J* = 8.4, 0.9 Hz, 1H), 6.27 – 6.12 (s, 1H), 3.88 (s, 2H); ^{13}C{H} NMR (126 MHz, $CDCl_3$) δ 157.7, 148.3, 143.0, 137.9, 127.2, 125.8, 118.9, 116.2, 114.4, 107.2. Spectral data are in accordance with literature values.[6] *See pg. 78 for NMR spectra.*

2.5.3: Synthesis of 1,1'-di(pyridin-2-yl)-1,1',3,3'-tetrahydro-2,2'-bibenzo[d][1,3,2]diazaborole (BB)

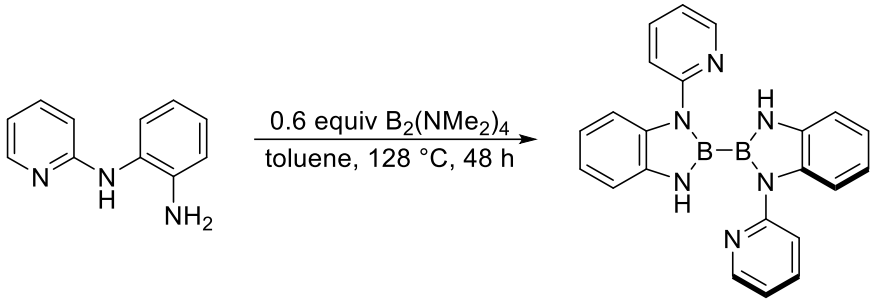

Inside a glovebox, N^1-(pyridin-2-yl)benzene-1,2-diamine (0.3700 g, 2 mmol, 1 equiv) was added to a 10 mL Schlenk flask equipped with a magnetic stir bar. Tetrakis(dimethylamino)diboron (0.24 mL, 1.2 mmol, 0.6 equiv) was added, along with 5 mL of toluene. The flask was then sealed and taken outside of the glovebox. Under a positive flow of nitrogen, a water condenser was attached to the flask and placed in an oil bath. The contents were stirred and heated at 128 °C for 48 hours while under nitrogen. After 48 hours, volatiles were removed, and a light tan solid was obtained (0.390 g, 99%). ^{1}H NMR (500 MHz, $CDCl_3$) δ 8.53 (d, J = 4.9 Hz, 1H), 7.64 – 7.56 (m, 2H), 7.50 (bs, 1H), 7.30 (d, *J* = 8.0 Hz, 1H), 7.15 (dd, *J* = 7.5, 1.5 Hz, 1H), 7.10 (ddd, *J* = 7.3, 4.9, 1.0 Hz, 1H), 7.03 (dtd, *J* = 22.0, 7.4, 1.3 Hz, 2H); ^{13}C{H} NMR (126 MHz, $CDCl_3$) δ 155.1, 148.7, 137.9, 137.3, 135.8, 120.6, 120.3, 119.5, 118.6, 111.5; ^{11}B NMR (160 MHz, $CDCl_3$) δ 29.1 (br, s). Spectral data are in accordance with literature values.[6] *See pg. 80 for NMR spectra.*

2.5.4: Synthesis of N,B-Double Bidentate Iridium Complex (IrBB)

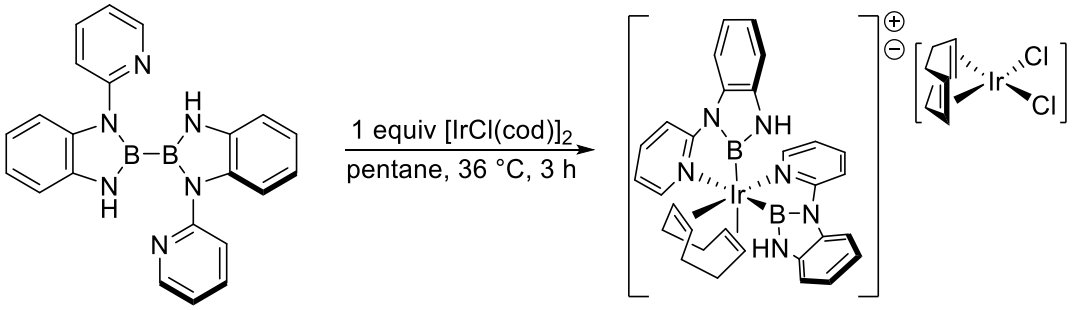

[Ir(Cl)cod]$_2$ (0.0375 g, 0.056 mmol, 1 equiv) and **BB** (0.0205 g, 0.053 mmol, 1 equiv) were added to a Schlenk flask containing a magnetic stir bar and dissolved in pentane. The flask was placed in an oil bath and stirred at 36 °C for 3 hours, then allowed to cool to room temperature before removing solvent by reduced pressure. A bright yellow solid was obtained (58 mg, quantitative yield) that was catalyst (**IrBB**).[7] ^{1}H NMR (500 MHz, DMSO-d_6) δ 9.63 (s, 1H), 9.44 (d, *J* = 5.6 Hz, 1H), 8.34 (t, *J* = 5.6 Hz, 1H), 8.15 (d, *J* = 8.4 Hz, 1H), 8.07 (d, *J* = 4.2 Hz, 1H), 8.05 (s, 1H), 7.90 (t, *J* = 8.7 Hz, 1H), 7.86 (t, *J* = 8.0 Hz, 2H), 7.75 (d, *J* = 8.1 Hz, 2H), 7.56 (t, *J* = 6.4 Hz, 1H), 7.39 (d, *J* = 7.8 Hz, 1H), 7.17 (t, *J* = 7.5 Hz, 1H), 7.07 (d, *J* = 8.7 Hz, 1H), 7.01 (t, *J* = 7.8 Hz, 1H), 6.92 – 6.82 (m, 3H), 4.84 – 4.78 (m, 1H), 4.74 – 4.68 (m, 1H), 4.29 (t, *J* = 8.6 Hz, 1H), 3.97 (S, 4H), 3.40 (t, *J* = 8.5 Hz, 1H), 3.00 (q, *J* = 11.6 Hz, 1H), 2.55 – 2.35 (m, 3H), 2.26 – 1.99 (m, 1H), 2.16 (m, 4H), 2.09 – 1.99 (m, 1H), 1.57 (m, 4H). *See pg. 83 for NMR spectra.* *Note: HRMS and elemental analysis data could not be obtained due to quick decomposition outside of the glovebox.*

Single Crystal X-ray Diffraction Data for IrBB

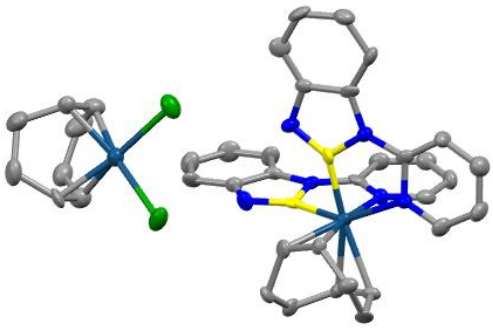

Crystals suitable for x-ray analysis were made via solvent diffusion. **IrBB** was dissolved in minimal DCM inside a 20 mL vial. The vial was then placed in a larger vessel containing pentane and sealed in a nitrogen-filled glovebox. Golden sheet-like crystals formed from this method. A suitable crystal with dimensions 0.22 × 0.16 × 0.09 mm^3 was selected and mounted on a nylon loop with paratone oil on a Saxi-CrysAlisPro-abstract goniometer imported SAXI images

diffractometer. The crystal was kept at a steady T = 173.15(10) K during data collection. The structure was solved with the ShelXT (Sheldrick, 2015) solution program using dual methods and by using Olex2 1.5 (Dolomanov et al., 2009) as the graphical interface. The model was refined with ShelXL 2018/3 (Sheldrick, 2015) using full matrix least squares minimization on F2. The CCDC number is 2236745 for this structure and contains the supplementary crystallographic data for this paper. *Notes: Crystal was grown by Alex O'Connell; Dr. Richard Staples performed the crystallographic analysis at Michigan State University.*

Crystal data and structure refinement for IrBB.

CCDC	2236745
Empirical formula	$C_{42}H_{50}B_2Cl_4Ir_2N_6$
Formula weight	1186.70
Crystal size/mm3	0.22 × 0.16 × 0.09
Temperature/K	173.15(10)
Crystal system	monoclinic
Space group	$P2_1/n$
a/Å	16.6813(8)
b/Å	15.0350(5)
c/Å	17.8182(9)
α/°	90
β/°	112.889(6)
γ/°	90
Volume/Å^3	4117.0(4)
Z	4

Radiation	MoKα (λ = 0.71073)
Reflections collected	33345
Independent reflections	7424

Fractional Atomic Coordinates (×10^4) and Equivalent Isotropic Displacement Parameters (Å^2×10^3) for AlexOBN. U_{eq} is defined as 1/3 of the trace of the orthogonalized U_{IJ} tensor.

Atom	***x***	***y***	***z***	**U(eq)**
Ir(1)	7236.5(4)	5647.4(4)	7401.3(3)	20.38(17)
N(1)	7270(8)	6032(9)	5603(7)	27(3)
N(2)	6389(7)	4930(8)	5746(7)	20(3)
N(3)	6358(8)	4577(7)	6965(7)	20(3)
N(4)	6008(8)	7244(8)	6326(7)	27(3)
N(5)	5822(8)	6774(8)	7473(7)	22(3)
N(6)	6724(8)	5797(8)	8364(7)	23(3)
C(1)	6852(9)	5603(10)	4852(9)	23.1(16)
C(2)	6316(9)	4945(10)	4927(9)	23.1(16)
C(3)	5839(10)	4436(10)	4243(10)	31(4)
C(4)	5923(11)	4611(11)	3527(10)	37(4)
C(5)	6463(12)	5278(12)	3480(10)	37(4)
C(6)	6939(10)	5806(10)	4142(9)	26(3)
C(7)	6054(9)	4405(10)	6158(10)	28(4)
C(8)	5427(10)	3747(10)	5820(9)	28(4)
C(9)	5134(11)	3264(11)	6318(10)	32(4)
C(10)	5482(10)	3418(10)	7138(10)	30(4)

C(11)	6081(9)	4072(10)	7437(9)	24(3)
C(12)	5348(9)	7759(10)	6436(9)	23.1(16)
C(13)	5228(9)	7473(10)	7124(9)	23.1(16)
C(14)	4599(10)	7879(11)	7337(11)	35(4)
C(15)	4109(11)	8557(11)	6835(11)	37(4)
C(16)	4241(11)	8831(10)	6158(10)	32(4)
C(17)	4851(11)	8423(11)	5966(10)	33(4)
C(18)	6028(9)	6330(10)	8193(9)	24(3)
C(19)	5591(10)	6399(11)	8710(10)	33(4)
C(20)	5883(12)	5954(12)	9425(11)	43(5)
C(21)	6612(11)	5428(10)	9636(9)	31(4)
C(22)	7001(11)	5348(10)	9094(8)	29(4)
C(23)	8346(9)	4776(10)	8282(9)	23(3)
C(24)	8328(9)	4663(11)	7522(9)	28(4)
C(25)	8929(10)	5086(10)	7183(9)	26(4)
C(26)	9059(10)	6074(10)	7338(10)	28(4)
C(27)	8251(9)	6546(10)	7367(9)	27(4)
C(28)	8112(10)	6686(11)	8088(9)	28(4)
C(29)	8718(10)	6326(10)	8905(9)	25(3)
C(30)	9002(9)	5366(10)	8904(9)	27(4)
B(1)	7032(10)	5609(11)	6193(10)	21(3)
B(2)	6300(11)	6619(11)	6960(10)	21(3)
Ir(2)	7449.6(4)	8307.8(4)	4318.8(4)	27.02(18)

Cl(1)	8410(3)	7865(3)	5632(2)	41.6(11)
Cl(2)	6363(3)	8554(3)	4834(3)	39.5(10)
C(31)	8492(10)	8566(10)	3994(10)	29(4)
C(32)	8192(10)	7718(12)	3764(9)	31(4)
C(33)	7692(12)	7408(12)	2898(10)	43(5)
C(34)	6730(13)	7542(14)	2626(11)	53(5)
C(35)	6502(10)	8210(11)	3152(9)	30(4)
C(36)	6801(11)	9087(12)	3283(10)	37(4)
C(37)	7404(12)	9453(13)	2897(13)	52(5)
C(38)	8350(12)	9312(12)	3410(11)	43(4)
Cl(3)	6750(60)	7700(200)	10580(60)	136(14)
Cl(3A)	6920(60)	7800(200)	10760(60)	136(14)
Cl(4)	7179(5)	8186(4)	9261(3)	77.4(19)
C(1S)	7500(20)	7910(20)	10224(13)	105(10)
C(2S)	9390(20)	5510(30)	5178(18)	138(16)
C(3S)	10266(18)	5330(20)	5841(17)	95(9)
C(4S)	10770(50)	4710(50)	5660(80)	80(30)
C(4T)	10400(50)	4460(40)	5680(80)	80(30)

Anisotropic Displacement Parameters ($\times 10^4$) for AlexOBN. The Anisotropic displacement factor exponent takes the form: $-2\pi^2[h^2a^{*2}U_{11}+2hka^*b^*U_{12}+\ldots]$.

Atom	**U_{11}**	**U_{22}**	**U_{33}**	**U_{23}**	**U_{13}**	**U_{12}**
Ir(1)	18.3(3)	22.2(3)	16.1(3)	-0.4(2)	1.8(2)	-0.9(2)
N(1)	21(7)	31(7)	21(7)	-7(6)	0(6)	-16(5)

N(2)	18(6)	22(6)	18(6)	0(5)	3(5)	-8(5)
N(3)	21(6)	8(6)	26(7)	-3(5)	5(5)	-4(5)
N(4)	23(7)	36(8)	20(7)	-3(6)	6(6)	5(6)
N(5)	24(7)	20(6)	19(6)	8(5)	5(5)	8(5)
N(6)	28(7)	23(7)	21(7)	1(5)	12(6)	1(6)
C(1)	13(4)	23(4)	22(4)	-4(3)	-5(3)	-5(3)
C(2)	13(4)	23(4)	22(4)	-4(3)	-5(3)	-5(3)
C(3)	27(8)	24(8)	35(9)	3(7)	5(7)	-8(7)
C(4)	43(11)	29(9)	31(10)	-4(7)	5(8)	-8(8)
C(5)	53(11)	42(10)	16(8)	0(7)	12(8)	16(9)
C(6)	32(9)	23(8)	20(8)	-5(6)	6(7)	-2(7)
C(7)	18(8)	23(8)	43(10)	-9(7)	13(7)	2(6)
C(8)	29(9)	30(9)	18(8)	-5(7)	2(7)	6(7)
C(9)	32(9)	26(9)	37(10)	-11(7)	11(8)	-11(7)
C(10)	27(8)	28(9)	36(9)	4(7)	12(7)	-7(7)
C(11)	21(8)	25(8)	26(8)	-7(7)	9(7)	-1(6)
C(12)	13(4)	23(4)	22(4)	-4(3)	-5(3)	-5(3)
C(13)	13(4)	23(4)	22(4)	-4(3)	-5(3)	-5(3)
C(14)	31(9)	31(9)	41(10)	11(8)	11(8)	-4(8)
C(15)	26(9)	34(10)	49(11)	8(8)	13(8)	3(7)
C(16)	39(10)	16(8)	29(9)	10(7)	-1(8)	8(7)
C(17)	35(9)	34(9)	23(8)	-3(7)	5(7)	0(8)
C(18)	14(7)	27(8)	23(8)	-2(6)	-1(6)	-7(6)

C(19)	26(9)	44(10)	26(9)	8(8)	7(7)	7(8)
C(20)	54(12)	42(11)	37(10)	5(9)	22(9)	14(9)
C(21)	42(10)	32(9)	11(7)	9(6)	1(7)	7(8)
C(22)	41(10)	29(8)	10(7)	-5(6)	2(7)	-8(7)
C(23)	18(8)	20(8)	26(8)	1(6)	1(6)	1(6)
C(24)	17(8)	32(9)	28(9)	16(7)	2(7)	10(7)
C(25)	28(9)	32(9)	16(8)	4(6)	5(7)	11(7)
C(26)	24(8)	34(9)	27(9)	2(7)	9(7)	-8(7)
C(27)	20(8)	28(9)	25(8)	1(7)	2(7)	-15(7)
C(28)	24(8)	35(9)	19(8)	5(7)	3(7)	-8(7)
C(29)	20(8)	33(9)	18(8)	0(6)	2(6)	3(7)
C(30)	14(7)	41(9)	19(8)	-10(7)	-2(6)	-8(7)
B(1)	19(6)	18(6)	22(6)	1(5)	5(5)	8(5)
B(2)	19(6)	18(6)	22(6)	1(5)	5(5)	8(5)
Ir(2)	30.1(4)	29.1(3)	22.4(3)	-1.5(3)	10.8(3)	-4.1(3)
Cl(1)	44(3)	46(3)	23(2)	6.8(19)	0.4(19)	-11(2)
Cl(2)	43(3)	47(3)	38(2)	-12(2)	26(2)	-12(2)
C(31)	22(8)	34(9)	44(10)	11(8)	28(8)	3(7)
C(32)	25(8)	60(12)	13(7)	8(8)	12(7)	8(8)
C(33)	59(12)	38(10)	30(10)	-4(8)	16(9)	9(9)
C(34)	66(14)	54(12)	31(10)	7(9)	9(10)	3(11)
C(35)	28(9)	38(10)	16(8)	13(7)	0(7)	10(7)
C(36)	34(10)	45(11)	32(9)	14(8)	14(8)	2(8)

C(37)	42(11)	48(12)	60(13)	24(10)	15(10)	8(9)
C(38)	44(11)	47(11)	46(11)	-2(9)	26(9)	-13(9)
Cl(3)	170(30)	204(14)	50(40)	-10(50)	70(30)	0(40)
Cl(3A)	170(30)	204(14)	50(40)	-10(50)	70(30)	0(40)
Cl(4)	109(5)	78(4)	47(3)	-15(3)	32(3)	-39(4)
C(2S)	140(30)	210(40)	80(20)	0(20)	50(20)	120(30)
C(3S)	77(19)	140(30)	67(18)	-12(18)	24(15)	19(19)
C(4S)	80(60)	110(40)	39(15)	-10(40)	-10(50)	50(40)
C(4T)	80(60)	110(40)	39(15)	-10(40)	-10(50)	50(40)

Bond Lengths in Å for AlexOBN.

Atom	**Atom**	**Length/Å**	**Atom**	**Atom**	**Length/Å**
Ir(1)	N(3)	2.111(11)	C(1)	C(2)	1.37(2)
Ir(1)	N(6)	2.206(12)	C(1)	C(6)	1.36(2)
Ir(1)	C(23)	2.312(14)	C(2)	C(3)	1.40(2)
Ir(1)	C(24)	2.291(15)	C(3)	C(4)	1.36(2)
Ir(1)	C(27)	2.185(14)	C(4)	C(5)	1.37(2)
Ir(1)	C(28)	2.163(15)	C(5)	C(6)	1.39(2)
Ir(1)	B(1)	2.045(17)	C(7)	C(8)	1.39(2)
Ir(1)	B(2)	2.059(16)	C(8)	C(9)	1.38(2)
N(1)	C(1)	1.402(18)	C(9)	C(10)	1.36(2)
N(1)	B(1)	1.41(2)	C(10)	C(11)	1.35(2)
N(2)	C(2)	1.418(19)	C(12)	C(13)	1.39(2)
N(2)	C(7)	1.340(19)	C(12)	C(17)	1.36(2)

N(2)	B(1)	1.47(2)	C(13)	C(14)	1.39(2)
N(3)	C(7)	1.351(19)	C(14)	C(15)	1.39(2)
N(3)	C(11)	1.341(19)	C(15)	C(16)	1.37(2)
N(4)	C(12)	1.420(19)	C(16)	C(17)	1.34(2)
N(4)	B(2)	1.40(2)	C(18)	C(19)	1.38(2)
N(5)	C(13)	1.411(18)	C(19)	C(20)	1.35(2)
N(5)	C(18)	1.366(18)	C(20)	C(21)	1.38(2)
N(5)	B(2)	1.45(2)	C(21)	C(22)	1.36(2)
N(6)	C(18)	1.345(18)	C(23)	C(24)	1.35(2)
N(6)	C(22)	1.376(18)	C(23)	C(30)	1.506(19)
C(24)	C(25)	1.50(2)	C(33)	C(34)	1.50(3)
C(25)	C(26)	1.51(2)	C(34)	C(35)	1.52(2)
C(26)	C(27)	1.54(2)	C(35)	C(36)	1.40(2)
C(27)	C(28)	1.41(2)	C(36)	C(37)	1.52(2)
C(28)	C(29)	1.51(2)	C(37)	C(38)	1.50(2)
C(29)	C(30)	1.52(2)	Cl(3)	C(1S)	1.63(2)
Ir(2)	Cl(1)	2.360(4)	Cl(3A)	C(1S)	1.63(2)
Ir(2)	Cl(2)	2.358(4)	Cl(4)	C(1S)	1.641(18)
Ir(2)	C(31)	2.073(14)	C(2S)	C(3S)	1.51(4)
Ir(2)	C(32)	2.063(15)	C(2S)	C(4S)	11.46(12)
Ir(2)	C(35)	2.070(15)	C(2S)	C(4T)	11.70(13)
Ir(2)	C(36)	2.097(16)	C(3S)	C(4S)	1.37(4)
C(31)	C(32)	1.37(2)	C(3S)	C(4T)	1.37(4)

C(31)	C(38)	1.49(2)		C(32)	C(33)	1.51(2)	

Bond Angles in ° for AlexOBN.

Atom	Atom	Atom	Angle/°	Atom	Atom	Atom	Angle/°
N(3)	Ir(1)	N(6)	86.6(5)	C(18)	N(5)	C(13)	130.9(13)
N(3)	Ir(1)	C(23)	94.4(5)	C(18)	N(5)	B(2)	121.0(12)
N(3)	Ir(1)	C(24)	87.4(5)	C(18)	N(6)	Ir(1)	116.5(10)
N(3)	Ir(1)	C(27)	153.6(5)	C(18)	N(6)	C(22)	116.7(13)
N(3)	Ir(1)	C(28)	168.0(5)	C(22)	N(6)	Ir(1)	126.6(10)
N(6)	Ir(1)	C(23)	88.9(5)	C(2)	C(1)	N(1)	109.8(13)
N(6)	Ir(1)	C(24)	121.8(5)	C(6)	C(1)	N(1)	126.1(13)
C(24)	Ir(1)	C(23)	34.2(5)	C(6)	C(1)	C(2)	124.0(13)
C(27)	Ir(1)	N(6)	119.8(5)	C(1)	C(2)	N(2)	108.2(12)
C(27)	Ir(1)	C(23)	86.8(6)	C(1)	C(2)	C(3)	118.8(14)
C(27)	Ir(1)	C(24)	78.8(6)	C(3)	C(2)	N(2)	133.0(14)
C(28)	Ir(1)	N(6)	82.4(5)	C(4)	C(3)	C(2)	118.7(15)
C(28)	Ir(1)	C(23)	80.7(6)	C(3)	C(4)	C(5)	120.5(15)
C(28)	Ir(1)	C(24)	94.4(6)	C(4)	C(5)	C(6)	122.6(16)
C(28)	Ir(1)	C(27)	37.7(6)	C(1)	C(6)	C(5)	115.3(15)
B(1)	Ir(1)	N(3)	77.5(6)	N(2)	C(7)	N(3)	114.0(13)
B(1)	Ir(1)	N(6)	149.9(6)	N(2)	C(7)	C(8)	125.7(15)
B(1)	Ir(1)	C(23)	117.4(6)	N(3)	C(7)	C(8)	120.2(15)
B(1)	Ir(1)	C(24)	83.2(6)	C(9)	C(8)	C(7)	119.4(14)
B(1)	Ir(1)	C(27)	78.6(6)	C(10)	C(9)	C(8)	119.3(15)

B(1)	Ir(1)	C(28)	114.5(6)	C(11)	C(10)	C(9)	119.1(15)
B(1)	Ir(1)	B(2)	80.1(6)	N(3)	C(11)	C(10)	123.1(14)
B(2)	Ir(1)	N(3)	94.9(6)	C(13)	C(12)	N(4)	109.8(13)
B(2)	Ir(1)	N(6)	76.0(6)	C(17)	C(12)	N(4)	129.4(15)
B(2)	Ir(1)	C(23)	161.7(6)	C(17)	C(12)	C(13)	120.7(15)
B(2)	Ir(1)	C(24)	162.2(6)	C(12)	C(13)	N(5)	107.7(13)
B(2)	Ir(1)	C(27)	91.8(6)	C(12)	C(13)	C(14)	119.3(14)
B(2)	Ir(1)	C(28)	87.1(6)	C(14)	C(13)	N(5)	133.0(14)
C(1)	N(1)	B(1)	109.0(12)	C(13)	C(14)	C(15)	117.6(16)
C(2)	N(2)	B(1)	107.4(11)	C(16)	C(15)	C(14)	121.9(16)
C(7)	N(2)	C(2)	133.4(12)	C(17)	C(16)	C(15)	119.0(15)
C(7)	N(2)	B(1)	119.0(12)	C(16)	C(17)	C(12)	121.3(16)
C(7)	N(3)	Ir(1)	117.2(10)	N(5)	C(18)	C(19)	125.8(14)
C(11)	N(3)	Ir(1)	124.1(10)	N(6)	C(18)	N(5)	112.6(13)
C(11)	N(3)	C(7)	118.7(12)	N(6)	C(18)	C(19)	121.7(14)
B(2)	N(4)	C(12)	107.3(12)	C(20)	C(19)	C(18)	120.1(16)
C(13)	N(5)	B(2)	107.8(12)	C(19)	C(20)	C(21)	119.9(17)
C(22)	C(21)	C(20)	118.1(15)	C(35)	Ir(2)	Cl(2)	89.9(5)
C(21)	C(22)	N(6)	123.3(15)	C(35)	Ir(2)	C(31)	97.4(7)
C(24)	C(23)	Ir(1)	72.1(8)	C(35)	Ir(2)	C(36)	39.1(6)
C(24)	C(23)	C(30)	122.6(14)	C(36)	Ir(2)	Cl(1)	161.7(5)
C(30)	C(23)	Ir(1)	109.0(10)	C(36)	Ir(2)	Cl(2)	92.5(5)
C(23)	C(24)	Ir(1)	73.7(9)	C(32)	C(31)	Ir(2)	70.2(8)

C(23)	C(24)	C(25)	126.3(15)	C(32)	C(31)	C(38)	123.5(16)
C(25)	C(24)	Ir(1)	108.6(10)	C(38)	C(31)	Ir(2)	114.5(11)
C(24)	C(25)	C(26)	114.5(13)	C(31)	C(32)	Ir(2)	71.0(9)
C(25)	C(26)	C(27)	113.1(12)	C(31)	C(32)	C(33)	125.7(15)
C(26)	C(27)	Ir(1)	114.4(10)	C(33)	C(32)	Ir(2)	115.2(11)
C(28)	C(27)	Ir(1)	70.3(8)	C(34)	C(33)	C(32)	112.7(15)
C(28)	C(27)	C(26)	123.8(14)	C(33)	C(34)	C(35)	112.5(15)
C(27)	C(28)	Ir(1)	72.0(8)	C(34)	C(35)	Ir(2)	112.9(11)
C(27)	C(28)	C(29)	122.7(14)	C(36)	C(35)	Ir(2)	71.5(9)
C(29)	C(28)	Ir(1)	109.7(10)	C(36)	C(35)	C(34)	124.5(16)
C(28)	C(29)	C(30)	115.5(13)	C(35)	C(36)	Ir(2)	69.4(9)
C(23)	C(30)	C(29)	115.1(12)	C(35)	C(36)	C(37)	121.4(17)
N(1)	B(1)	Ir(1)	142.3(12)	C(37)	C(36)	Ir(2)	113.2(12)
N(1)	B(1)	N(2)	105.4(12)	C(38)	C(37)	C(36)	113.4(15)
N(2)	B(1)	Ir(1)	112.2(11)	C(31)	C(38)	C(37)	112.1(14)
N(4)	B(2)	Ir(1)	139.2(12)	Cl(3)	C(1S)	Cl(4)	117(5)
N(4)	B(2)	N(5)	107.3(12)	Cl(3A)	C(1S)	Cl(4)	128(6)
N(5)	B(2)	Ir(1)	113.3(10)	C(3S)	C(2S)	C(4T)1	103(4)
Cl(2)	Ir(2)	Cl(1)	89.25(16)	C(4S)1	C(2S)	C(3S)	120(3)
C(31)	Ir(2)	Cl(1)	90.5(5)	C(4S)1	C(2S)	C(4T)1	26(5)
C(31)	Ir(2)	Cl(2)	159.3(5)	C(4S)	C(3S)	C(2S)	116(5)
C(31)	Ir(2)	C(36)	81.5(6)	C(4T)	C(3S)	C(2S)	102(5)
C(32)	Ir(2)	Cl(1)	92.9(4)	C(3S)	C(4S)	C(2S)1	121(8)

C(32)	Ir(2)	Cl(2)	161.9(5)	C(3S)	C(4T)	C(2S)1	106(8)
C(32)	Ir(2)	C(31)	38.8(6)	C(32)	Ir(2)	C(36)	91.1(7)
C(32)	Ir(2)	C(35)	81.7(6)	C(35)	Ir(2)	Cl(1)	159.2(5)

Torsion Angles in ° for AlexOBN.

Atom	**Atom**	**Atom**	**Atom**	**Angle/°**
Ir(1)	N(3)	C(7)	N(2)	2.5(16)
Ir(1)	N(3)	C(7)	C(8)	-175.6(11)
Ir(1)	N(3)	C(11)	C(10)	176.4(11)
Ir(1)	N(6)	C(18)	N(5)	-7.4(15)
Ir(1)	N(6)	C(18)	C(19)	172.7(12)
Ir(1)	N(6)	C(22)	C(21)	-175.1(12)
Ir(1)	C(23)	C(24)	C(25)	101.5(15)
Ir(1)	C(23)	C(30)	C(29)	10.2(16)
Ir(1)	C(24)	C(25)	C(26)	35.9(15)
Ir(1)	C(27)	C(28)	C(29)	102.2(14)
Ir(1)	C(28)	C(29)	C(30)	35.8(16)
N(1)	C(1)	C(2)	N(2)	-0.8(16)
N(1)	C(1)	C(2)	C(3)	-179.9(13)
N(1)	C(1)	C(6)	C(5)	179.4(14)
N(2)	C(2)	C(3)	C(4)	-178.9(16)
N(2)	C(7)	C(8)	C(9)	-179.2(15)
N(3)	C(7)	C(8)	C(9)	-1(2)
N(4)	C(12)	C(13)	N(5)	0.8(15)

N(4)	C(12)	C(13)	C(14)	-178.9(13)
N(4)	C(12)	C(17)	C(16)	178.9(15)
N(5)	C(13)	C(14)	C(15)	-179.1(15)
N(5)	C(18)	C(19)	C(20)	-177.0(16)
N(6)	C(18)	C(19)	C(20)	3(2)
C(1)	N(1)	B(1)	Ir(1)	179.0(15)
C(1)	N(1)	B(1)	N(2)	-4.0(16)
C(1)	C(2)	C(3)	C(4)	0(2)
C(2)	N(2)	C(7)	N(3)	174.3(14)
C(2)	N(2)	C(7)	C(8)	-8(3)
C(2)	N(2)	B(1)	Ir(1)	-178.5(9)
C(2)	N(2)	B(1)	N(1)	3.5(15)
C(2)	C(1)	C(6)	C(5)	-2(2)
C(2)	C(3)	C(4)	C(5)	0(3)
C(3)	C(4)	C(5)	C(6)	-1(3)
C(4)	C(5)	C(6)	C(1)	2(2)
C(6)	C(1)	C(2)	N(2)	-179.6(14)
C(6)	C(1)	C(2)	C(3)	1(2)
C(7)	N(2)	C(2)	C(1)	-176.1(15)
C(7)	N(2)	C(2)	C(3)	3(3)
C(7)	N(2)	B(1)	Ir(1)	-3.2(16)
C(7)	N(2)	B(1)	N(1)	178.8(12)
C(7)	N(3)	C(11)	C(10)	-3(2)

C(7)	C(8)	C(9)	C(10)	-2(2)
C(8)	C(9)	C(10)	C(11)	3(2)
C(9)	C(10)	C(11)	N(3)	-1(2)
C(11)	N(3)	C(7)	N(2)	-178.2(12)
C(11)	N(3)	C(7)	C(8)	4(2)
C(12)	N(4)	B(2)	Ir(1)	-175.6(14)
C(12)	N(4)	B(2)	N(5)	-1.4(16)
C(12)	C(13)	C(14)	C(15)	1(2)
C(13)	N(5)	C(18)	N(6)	-170.4(13)
C(13)	N(5)	C(18)	C(19)	9(2)
C(13)	N(5)	B(2)	Ir(1)	177.8(9)
C(13)	N(5)	B(2)	N(4)	1.9(16)
C(13)	C(12)	C(17)	C(16)	1(2)
C(13)	C(14)	C(15)	C(16)	-1(2)
C(14)	C(15)	C(16)	C(17)	1(3)
C(15)	C(16)	C(17)	C(12)	-1(2)
C(17)	C(12)	C(13)	N(5)	179.0(13)
C(17)	C(12)	C(13)	C(14)	-1(2)
C(18)	N(5)	C(13)	C(12)	172.6(14)
C(18)	N(5)	C(13)	C(14)	-8(3)
C(18)	N(5)	B(2)	Ir(1)	2.9(18)
C(18)	N(5)	B(2)	N(4)	-173.0(12)
C(18)	N(6)	C(22)	C(21)	-1(2)

C(18)	C(19)	C(20)	C(21)	0(3)
C(19)	C(20)	C(21)	C(22)	-2(3)
C(20)	C(21)	C(22)	N(6)	3(2)
C(22)	N(6)	C(18)	N(5)	177.6(12)
C(22)	N(6)	C(18)	C(19)	-2(2)
C(23)	C(24)	C(25)	C(26)	-47(2)
C(24)	C(23)	C(30)	C(29)	90.6(18)
C(24)	C(25)	C(26)	C(27)	-31.7(18)
C(25)	C(26)	C(27)	Ir(1)	10.6(16)
C(25)	C(26)	C(27)	C(28)	92.4(17)
C(26)	C(27)	C(28)	Ir(1)	-106.7(14)
C(26)	C(27)	C(28)	C(29)	-5(2)
C(27)	C(28)	C(29)	C(30)	-45(2)
C(28)	C(29)	C(30)	C(23)	-31.0(19)
C(30)	C(23)	C(24)	Ir(1)	-101.6(13)
C(30)	C(23)	C(24)	C(25)	0(2)
B(1)	N(1)	C(1)	C(2)	3.1(17)
B(1)	N(1)	C(1)	C(6)	-178.1(15)
B(1)	N(2)	C(2)	C(1)	-1.7(16)
B(1)	N(2)	C(2)	C(3)	177.3(16)
B(1)	N(2)	C(7)	N(3)	0.4(19)
B(1)	N(2)	C(7)	C(8)	178.5(14)
B(2)	N(4)	C(12)	C(13)	0.4(16)

B(2)	N(4)	C(12)	C(17)	-177.6(15)
B(2)	N(5)	C(13)	C(12)	-1.6(15)
B(2)	N(5)	C(13)	C(14)	178.0(16)
B(2)	N(5)	C(18)	N(6)	3.2(19)
B(2)	N(5)	C(18)	C(19)	-177.0(15)
Ir(2)	C(31)	C(32)	C(33)	107.8(16)
Ir(2)	C(31)	C(38)	C(37)	-26(2)
Ir(2)	C(32)	C(33)	C(34)	-4(2)
Ir(2)	C(35)	C(36)	C(37)	105.2(15)
Ir(2)	C(36)	C(37)	C(38)	-10(2)
C(31)	C(32)	C(33)	C(34)	-87(2)
C(32)	C(31)	C(38)	C(37)	56(2)
C(32)	C(33)	C(34)	C(35)	19(2)
C(33)	C(34)	C(35)	Ir(2)	-25.4(19)
C(33)	C(34)	C(35)	C(36)	57(2)
C(34)	C(35)	C(36)	Ir(2)	-105.5(15)
C(34)	C(35)	C(36)	C(37)	0(2)
C(35)	C(36)	C(37)	C(38)	-89(2)
C(36)	C(37)	C(38)	C(31)	23(2)
C(38)	C(31)	C(32)	Ir(2)	-106.8(15)
C(38)	C(31)	C(32)	C(33)	1(2)
C(2S)	C(3S)	C(4S)	C(2S)1	20(11)
C(2S)	C(3S)	C(4T)	C(2S)1	72(5)

C(4S)1	C(2S)	C(3S)	C(4S)	-19(11)
C(4T)1	C(2S)	C(3S)	C(4T)	-70(8)

Hydrogen Atom Coordinates (Å×10^4) and Isotropic Displacement Parameters (Å^2×10^3) for AlexOBN. Ueq is defined as 1/3 of the trace of the orthogonalised U_{ij}.

Atom	***x***	***y***	***z***	**U(eq)**
H(1)	7622.81	6489.81	5692.02	32
H(4)	6198.08	7305.1	5932.14	33
H(3)	5463.59	3976.24	4276.65	37
H(4A)	5604.88	4268.12	3057.23	45
H(5)	6512.48	5381.74	2973.96	45
H(6)	7301.16	6277.09	4103.62	31
H(8)	5204.33	3633.76	5251.09	34
H(9)	4693.57	2826.61	6094.37	38
H(10)	5306.75	3072.14	7493.28	36
H(11)	6315.39	4177.03	8007.25	29
H(14)	4506.69	7700.01	7808.74	42
H(15)	3669.8	8838.81	6965.65	44
H(16)	3906.4	9302.1	5830.18	38
H(17)	4937.14	8601.6	5491.41	39
H(19)	5085.52	6759.35	8562.54	40
H(20)	5584.19	6005.11	9781.26	52
H(21)	6837.52	5128.28	10145.82	37
H(22)	7487.83	4962.03	9226.68	35

H(23)	8151.94	4250.47	8510.77	28
H(24)	8112.71	4063.67	7285.83	33
H(25A)	8695.38	4981.48	6587.85	32
H(25B)	9502.08	4788.04	7423.03	32
H(26A)	9207.07	6345.94	6901.91	34
H(26B)	9557.12	6171.14	7861.73	34
H(27)	8026.46	7038.47	6960.82	32
H(28)	7824.83	7263.06	8111.85	33
H(29A)	8425.12	6378.58	9291.77	30
H(29B)	9244.12	6704.99	9112.64	30
H(30A)	9546.16	5360.31	8805.39	33
H(30B)	9134.97	5111.04	9451.4	33
H(31)	9066.12	8589.16	4466.9	34
H(32)	8593.74	7251.88	4111.3	37
H(33A)	7900.91	7737.38	2528.53	51
H(33B)	7810.68	6768.05	2858.05	51
H(34A)	6452.49	6964.81	2643.38	64
H(34B)	6492.16	7752.05	2054.42	64
H(35)	5900.26	8135.88	3138.46	36
H(36)	6379.21	9526.97	3341.02	44
H(37A)	7262.7	9162.65	2362.2	62
H(37B)	7293.91	10098.17	2799.64	62
H(38A)	8663.99	9187.09	3050.88	52

H(38B)	8595.18	9864.25	3716.51	52
H(1SA)	7852.44	7355.45	10309.24	126
H(1SB)	7893.51	8379.49	10553.69	126
H(1SC)	7829.06	7344	10275.94	126
H(1SD)	7939.44	8359.73	10523.95	126
H(2SA)	9154.55	6091.9	5267.99	166
H(2SB)	8965.12	5038.72	5148.41	166
H(2SC)	8946.23	5198.95	5322.95	166
H(2SD)	9273.86	6158.58	5193.49	166
H(3SA)	10719.07	5724.57	5800.22	114
H(3SB)	10250.51	5386.28	6388.85	114
H(3SC)	10592.75	5892.04	5987.2	114
H(3SD)	10174	5118	6329.2	114
H(4SA)	10738.2	4155.15	5942.79	102
H(4SB)	11380.89	4925.32	5919.78	102
H(4TA)	9878.53	4098.39	5592.51	102
H(4TB)	10900.18	4206.52	6138.39	102

Hydrogen Bond information for AlexOBN.

D	**H**	**A**	**d(D-H)/Å**	**d(H-A)/Å**	**d(D-A)/Å**	**D-H-A/deg**
C(11)	H(11)	N(6)	0.95	2.54	3.039(19)	112.7

2.5.5: Reaction Optimizations for ortho CHB

A. KOtBu Additive with 2 mol % BB

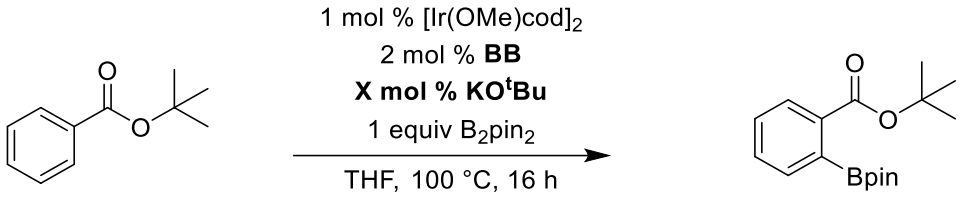

Entry	KO^{t}Bu Loading (mol %)	Conversion (%)	*o*:(*m*+*p*) (%)
1	1	80	1:99
2	2	65	1:99
3	5	16	1:99
4	10	---	---

Reactions run on 0.5 mmol scale of substrate, 0.5 mmol B_2pin_2, 1 mol % $[Ir(OMe)cod]_2$, and 2 mol % **BB** ligand in 1 mL THF. Conversions and selectivity determined by ^{1}H NMR analysis of sample.

B. Decreased BB Pre-ligand Loading

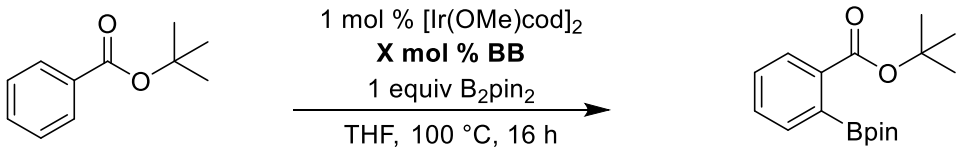

Entry	Ligand Loading (mol %)	Conversion (%)	*o*:(*m**+*p*) (%)
1	2	99	1:99
2	1	80	60:40
3	0.75	74	90:10
4	0.50	67	95:5

Reactions run on 0.5 mmol scale of substrate, 0.5 mmol B_2pin_2, 1 mol % $[Ir(OMe)cod]_2$, and x mol % **BB** ligand in 1 mL THF. Conversions and selectivity determined by ^{1}H NMR analysis of sample. Meta selectivity (m*) includes dimeta-borylated products.

2.5.6: General C–H Borylation Procedures

General Procedure for CHB

Inside a nitrogen-filled glove box, bis(pinacolato)diboron (1 equiv), $[Ir(X)cod]_2$ (1 mol %) (X = OMe or Cl), **BB** pre-ligand (0.5 or 2 mol %), and THF were added to a 3.0 mL wheaton vial

equipped with a stir bar. (Hetero)arene substrate (1 equiv) was added and the vial was sealed with a screw cap and taken outside of the glovebox. The reaction was placed in a 4x4 aluminum heating block on top of a stir plate and stirred at 100 °C for 4-16 hours then cooled to room temperature. The resulting solution was exposed to air and volatiles were removed under reduced pressure. The compound was purified using a small plug of silica gel with 15 mL DCM as eluent. Fractions collected were dried under vacuum and weighed. ^{1}H and GCMS analysis of material confirmed selectivity's of respective borylated compounds. Yields were determined by weight.

Condition A: Chelate-directed CHB with 0.5 mol % **BB**.

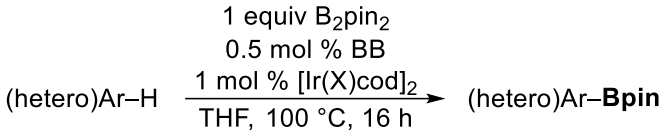

Following the general procedure for CHB using bis(pinacolato)diboron (127 mg, 0.50 mmol, 1 equiv), [IrCl(cod)]$_2$ (3.31 mg, 0.005 mmol, 0.01 equiv) or [Ir(OMe)cod]2 (3.36 mg, 0.005 mmol, 0.01 equiv), **BB** pre-ligand (1 mg, 0.0025 mmol, 0.0005 equiv), and THF (1 mL). Reactions ran for 16 h.

Condition B: Steric-directed CHB with 2 mol % **BB** and [Ir(OMe)cod]$_2$.

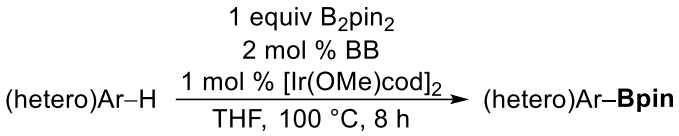

Following the general procedure for CHB using bis(pinacolato)diboron (127 mg, 0.50 mmol, 1 equiv), [Ir(OMe)cod]$_2$ (3.36 mg, 0.005 mmol, 0.01 equiv), **BB** pre-ligand (3.88 mg, 0.01 mmol, 0.02 equiv), and THF (1 mL). Reactions ran for 8 h.

<u>Condition C</u>: Chelate-directed CHB with 2 mol % **BB** and $[IrCl(cod)]_2$.

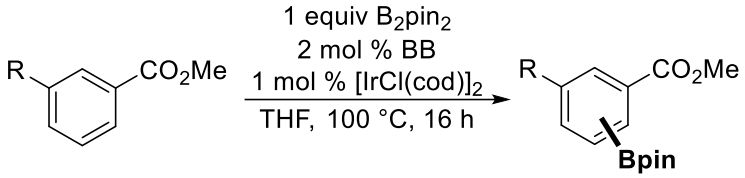

Following the general procedure for CHB using bis(pinacolato)diboron (63.5 mg, 0.25 mmol, 1 equiv), $[IrCl(cod)]_2$ (1.7 mg, 0.0025 mmol, 0.01 equiv), **BB** pre-ligand (1.9 mg, 0.005 mmol, 0.02 equiv), and THF (0.5 mL). Reactions ran for 16 h.

2.5.7: Compound Characterization of Steric and Chelate-Directed Products

Methyl 2-(4,4,5,5-tetramethyl)-1,3,2-dioxaborolan-2-yl)benzoate (2a)

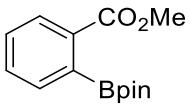

Following general procedure A with methyl benzoate (63 µL, 68 mg, 0.50 mmol) as the substrate, starting material converted to 85% (*o*:(*m*+*p*):di-*o*) = 78:8:14) borylated products. **2a** was obtained as a colorless oil (111 mg, 85%) after passing crude material through a short plug of silica using DCM as eluent. Using $[Ir(OMe)cod]_2$ as the precatalyst, substrate converted 80% (*o*:(*m*+*p*):di-*o*) = 76:8:14) borylated products and yielded 96 mg (73%). ^{1}H NMR (500 MHz, $CDCl_3$) δ 7.95 (dt, *J* = 7.8, 0.9 Hz, 1H), 7.54 – 7.50 (m, 2H), 7.44 – 7.40 (ddd, *J* = 7.8, 6.2, 2.6 Hz, 1H), 3.92 (s, 3H), 1.43 (s, 12H); ^{11}B NMR (160 MHz, $CDCl_3$) δ 31.6 (br, s). Spectral data were in accordance to literature.[29] *See pg. 84 for NMR spectra.*

Methyl 3,5-(4,4,5,5-tetramethyl)-1,3,2-dioxaborolan-2-yl)benzoate (3a)

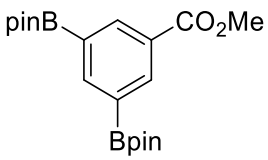

Following general procedure B with methyl benzoate (63 µL, 68 mg, 0.50 mmol) as the susbtrate, was added, starting material converted to 99% (*o*:(*m*+di-*m*):*p*) = (0:70:30) borylated products. **3a** was obtained as a colorless oil (85 mg, 65%) after passing crude material through a short plug of silica using DCM as eluent. ^{1}H NMR (500 MHz, $CDCl_3$) δ 8.56 (d, *J* = 1.3 Hz, 1H), 8.44 (t, *J* = 1.3 Hz, 1H), 4.00 – 3.81 (m, 3H), 1.36 (d, *J* = 4.2 Hz, 12H); ^{11}B NMR (160 MHz, $CDCl_3$) δ 31.4 (br, s). Spectral data were in accordance to literature.[30] *See pg. 86 for NMR spectra.*

***tert*-Butyl 2-(4,4,5,5-tetramethyl)-1,3,2-dioxaborolan-2-yl)benzoate (2b)**

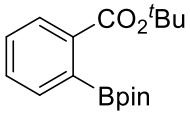

Following general procedure A, with *tert*-butyl benzoate (178 µL, 178 mg, 1.0 mmol) as the substrate, was added, starting material converted to 84% (*o*:(*m*+*p*) = 94:6) borylated products. **2b** was obtained as a white solid (243 mg, 80%) after passing crude material through a short plug of silica using DCM as eluent. ^{1}H NMR (500 MHz, $CDCl_3$) δ 7.82 (dt, *J* = 7.7, 0.9 Hz, 1H), 7.47 – 7.44 (m, 2H), 7.37 – 7.34 (ddd, *J* = 7.7, 6.0, 2.8 Hz, 1H), 1.58 (s, 3H), 1.42 (s, 12H); ^{11}B NMR (160 MHz, $CDCl_3$) δ 31.6 (s). Spectral data were in accordance to literature.[31] *See pg. 87 for NMR spectra.*

***tert*-Butyl 3,5-(4,4,5,5-tetramethyl)-1,3,2-dioxaborolan-2-yl)benzoate (3b)**

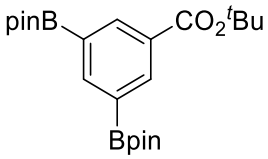

Following general procedure B with *tert*-butyl benzoate (89 µL, 89 mg, 0.5 mmol) as the substrate, starting material converted to 90% (*o*:(*m*+di-*m*):*p* = 0:65:35) products. **3b** was obtained as a colorless oil (89 mg, 58%) after passing crude material through a short plug of silica using

DCM as eluent. ^{1}H NMR (500 MHz, $CDCl_3$) δ 8.40 (dt, *J* = 2.8, 1.5 Hz, 1H), 8.31 (dt, *J* = 7.8, 1.6 Hz, 1H), (d, *J* = 1.4 Hz, 9H), 1.18 (d, *J* = 2.6 Hz, 12H); ^{11}B NMR (160 MHz, $CDCl_3$) δ 30.2 (br, s). Spectral data were in accordance to literature.[31]

***N*,*N*-dimethyl-2-(4,4,5,5-tetramethyl-1,3,2-dioxaborolan-2-yl)benzamide (2c)**

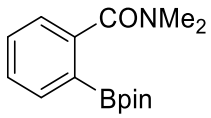

Following general procedure A with *N*,*N*-dimethylbenzamide (74 mg, 0.50 mmol) as the substrate, was added, starting material converted to 95% (*o*:(*m*+*p*) = 96:4) products. **2c** was obtained as a colorless oil (123 mg, 89%) after passing crude material through a short plug of silica using DCM as eluent. ^{1}H NMR (500 MHz, $CDCl_3$) δ 7.81 (ddd, *J* = 7.5, 1.4, 0.6 Hz, 1H), 7.46 (td, *J* = 7.5, 1.4 Hz, 1H), 7.37 (td, *J* = 7.5, 1.2 Hz, 1H), 7.30 (ddd, *J* = 7.6, 1.3, 0.7 Hz, 1H), 3.06 (s, 3H), 2.89 (s, 3H), 1.30 (s, 12H); ^{11}B NMR (160 MHz, $CDCl_3$) δ 29.4 (br, s). Using $[Ir(OMe)cod]_2$ as the precatalyst, starting material converted to 95% (*o*:(*m*+*p*) = 95:5) borylated products. **2c** was obtained as a colorless oil (114 mg, 83%) after passing crude material through a short plug of silica using DCM as eluent. Spectral data were in accordance to literature.[31] *See pg. 110 for NMR spectra.*

***N*,*N*-dimethyl-3,5-(4,4,5,5-tetramethyl-1,3,2-dioxaborolan-2-yl)benzamide (3c)**

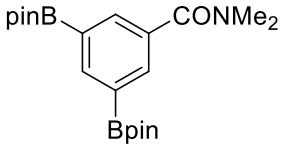

Following general procedure B with *N*,*N*-dimethylbenzamide (75 mg, 0.50 mmol) as the substrate, starting material converted to 99% (*o*:(*m*+di-*m*):*p* = 1:77:22) products. **3c** was obtained as a colorless oil (62 mg, 45%) after passing crude material through a short plug of silica using

DCM as eluent. ^{1}H NMR (500 MHz, $CDCl_3$) δ 8.29 (d, *J* = 1.5 Hz, 1H), 7.93 (d, *J* = 1.2 Hz, 2H), 3.10 (s, 3H), 2.95 (s, 3H), 1.34 (s, 24H); ^{11}B NMR (160 MHz, $CDCl_3$) δ 29.0 (br, s). Spectral data were in accordance to literature.[32] *See pg. 112 for NMR spectra.*

Methyl 5-bromo-2-fluoro-3-(4,4,5,5-tetramethyl-1,3,2-dioxaborolan-2-yl)benzoate (2d)

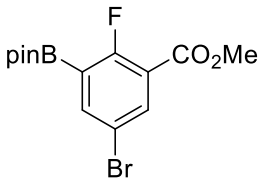

Following general procedure A with methyl 5-bromo-2-fluorobenzoate (116 mg, 0.50 mmol) as the substrate, starting material converted to 96% (3 position:other = >99:1) products. **2d** was obtained as a colorless oil (153 mg, 90%) after passing crude material through a short plug of silica using DCM as eluent. ^{1}H NMR (500 MHz, $CDCl_3$) δ 8.12 (dd, *J* = 6.2, 2.7, 1H), 7.99 (dd, *J* = 4.4, 2.8 Hz, 1H), 3.91 (s, 3H), 1.35 (s, 12H); ^{11}B NMR (160 MHz, $CDCl_3$) δ 28.2 (br, s). Using $[Ir(OMe)cod]_2$ as the precatalyst, starting material converted to 94% (3:other = >99:1) borylated products. **2d** was obtained as a colorless oil (116 mg, 65%) after passing crude material through a short plug of silica using DCM as eluent. Spectral data were in accordance to literature.[33] *See pg. 108 for NMR spectra.*

Methyl 5-bromo-2-fluoro-3-(4,4,5,5-tetramethyl-1,3,2-dioxaborolan-2-yl)benzoate (2d)

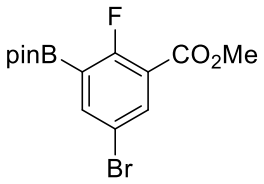

Following general procedure B with methyl 5-bromo-2-fluorobenzoate (116 mg, 0.50 mmol) as the substrate, starting material converted to 98% (3 position:other = >99:1) products. **2d** was obtained as a colorless oil (167 mg, 93%) after passing crude material through a short plug of

silica using DCM as eluent. ^{1}H NMR (500 MHz, $CDCl_3$) δ 8.12 (dd, *J* = 6.2, 2.7, 1H), 7.99 (dd, *J* = 4.4, 2.8 Hz, 1H), 3.91 (s, 3H), 1.35 (s, 12H). ^{11}B NMR (160 MHz, $CDCl_3$) δ 29.9 (br, s). Spectral data were in accordance to literature.[33]

Methyl 3-methoxy-6-(4,4,5,5-tetramethyl)-1,3,2-dioxaborolan-2-yl)benzoate (2e)

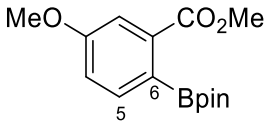

Following general procedure A with methyl 3-methoxybenzoate (73 µL, 83 mg, 0.50 mmol) as the substrate, starting material converted to 79% (*6 position:5 position* = 93:7) borylated products. **2e** was obtained as a colorless oil (104 mg, 71%) after passing crude material through a short plug of silica using DCM as eluent. Using $[Ir(OMe)cod]_2$ as the precatalyst, starting material converted to 67% (*o*:(*m*+*p*) = 95:5) borylated products. **2a** was obtained as a white solid (99 mg, 63%) after passing crude material through a short plug of silica using DCM as eluent, yielding 126 mg (83%) borylated products in the ratio (*6 position:5 position* = 96:4).

Following general procedure C, with methyl 3-methoxybenzoate (36.5 µL, 0.25 mmol) as the substrate, starting material converted to 80% (*6 position:5 position* = 85:15) borylated products. **2e** was obtained as a colorless oil (19 mg, 23%) after passing crude material through a short plug of silica using DCM as eluent. ^{1}H NMR (500 MHz, $CDCl_3$) δ 7.43 (s, 1H), 7.42 (d, *J* = 2.4 Hz, 1H), 7.03 (dd, *J* = 8.1, 2.6 Hz, 1H), 3.91 (d, *J* = 1.3 Hz, 4H), 3.84 (s, 3H), 1.41 (s, 12H).; ^{11}B NMR (160 MHz, $CDCl_3$) δ 31.1 (br, s). Spectral data were in accordance to literature.[31] *See pg. 89 for NMR spectra.*

Methyl 3-methoxy-5-(4,4,5,5-tetramethyl)-1,3,2-dioxaborolan-2-yl)benzoate (3e)

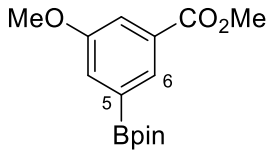

Following general procedure B with methyl 3-methoxybenzoate (73 µL, 83 mg, 0.50 mmol) as the substrate starting material converted to 85% (*6 position:5 position* = 5:95) borylated products. **3e** was obtained as a colorless oil (112 mg, 76%) after passing crude material through a short plug of silica using DCM as eluent. ^{1}H NMR (500 MHz, $CDCl_3$) δ 8.07 (dd, *J* = 1.5, 0.9 Hz, 1H), 7.66 (dd, *J* = 2.7, 1.5 Hz, 1H), 7.52 (dd, *J* = 2.8, 0.9 Hz, 1H), 3.92 (s, 3H), 3.87 (s, 3H), 1.36 (s, 12H); ^{11}B NMR (160 MHz, $CDCl_3$) δ 30.8 (s). Spectral data were in accordance to literature.[34]
See pg. 91 for NMR spectra.

Methyl 3-dimethylamino-6-(4,4,5,5-tetramethyl)-1,3,2-dioxaborolan-2-yl)benzoate (2f)

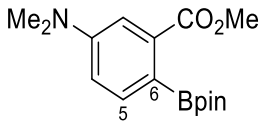

Following general procedure A with methyl 3-(dimethylamino)benzoate (81 µL, 90 mg, 0.50 mmol) as the substrate, starting material converted to 80% (*6 position:5 position* = 91:9) products. **2f** was obtained as a colorless oil (110 mg, 72%) after passing crude material through a short plug of silica using DCM as eluent. Using $[Ir(OMe)cod]_2$ as the precatalyst, starting material converted to 76% (*6 position:5 position* = 84:16) borylated products. **2f** was obtained as a colorless oil after passing crude material through a short plug of silica using DCM as eluent, yielding 90 mg (62%) borylated products in the ratio (*6 position:5 position* = 96:4). ^{1}H NMR (500 MHz, $CDCl_3$) δ 7.44 (d, *J* = 8.3 Hz, 1H), 7.20 (d, *J* = 2.6 Hz, 1H), 6.81 (dd, *J* = 8.3, 2.6 Hz, 1H), 3.89 (s, 3H),

2.99 (s, 6H), 1.38 (s, 12H). ^{11}B NMR (160 MHz, $CDCl_3$) δ 31.9 (br, s). Spectral data were in accordance to literature.[35] *See pg. 93 for NMR spectra.*

Methyl 3-dimethylamino-5-(4,4,5,5-tetramethyl)-1,3,2-dioxaborolan-2-yl)benzoate (3f)

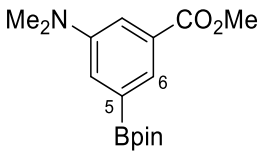

Following general procedure B with methyl 3-(dimethylamino)benzoate (81 µL, 90 mg, 0.50 mmol) as the substrate, was added, starting material converted to 94% (*6 position:5 position* = 1:99) products. **3f** was obtained as a colorless oil (122 mg, 80%) after passing crude material through a short plug of silica using DCM as eluent. ^{1}H NMR (500 MHz, $CDCl_3$) δ 7.82 (dd, *J* = 1.5, 0.9 Hz, 1H), 7.49 (dd, *J* = 2.9, 1.5 Hz, 1H), 7.34 (d, *J* = 2.8 Hz, 1H), 3.89 (s, 3H), 3.01 (s, 6H), 1.35 (s, 12H);); ^{13}C NMR (126 MHz, $CDCl_3$) δ 167.8, 150.0, 130.3, 123.8, 122.7, 115.9, 83.9, 52.0, 40.7, 24.8; ^{11}B NMR (160 MHz, $CDCl_3$) δ 31.1 (br, s); HRMS (ESI+) m/z calcd for $C_{16}H_{24}BNO_4$ $[M + H]^+$ 306.1832, found 306.1888. *See pg. 95 for NMR spectra.*

Methyl 3-bromo-6-(4,4,5,5-tetramethyl)-1,3,2-dioxaborolan-2-yl)benzoate (2g)

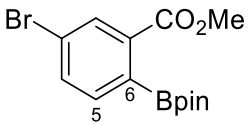

Following general procedure A with methyl 3-bromobenzoate (108 mg, 0.5 mmol) as the substrate, starting material converted to 96% (*6 position:5 position* = 77:23) products. **2g** was obtained as a colorless oil (138 mg, 81%) after passing crude material through a short plug of silica using DCM as eluent. Using $[Ir(OMe)cod]_2$ as the precatalyst, starting material converted to 80% (*6 position:5 position* = 80:20) borylated products. **2g** was obtained as a colorless oil (132 mg, 77%) after passing crude material through a short plug of silica using DCM as eluent.

Following general procedure C with methyl 3-bromobenzoate (54 mg, 0.25 mmol) as the substrate, starting material converted to 88% (*6 position:5 position* = 68:32) products. **2g** was obtained as a colorless oil (64 mg, 87%) after passing crude material through a short plug of silica using DCM as eluent. ^{1}H NMR (500 MHz, $CDCl_3$) δ 8.09 (dd, *J* = 2.0, 0.5 Hz, 1H), 7.62 (dd, *J* = 7.9, 1.9 Hz, 1H), 7.35 (d, *J* = 7.9 Hz, 1H), 3.93 (s, 3H), 1.42 (s, 12H); ^{11}B NMR (160 MHz, $CDCl_3$) δ 30.9 (br, s). Spectral data were in accordance to literature.[35] *See pg. 98 for NMR spectra.*

Methyl 3-bromo-5-(4,4,5,5-tetramethyl)-1,3,2-dioxaborolan-2-yl)benzoate (3g)

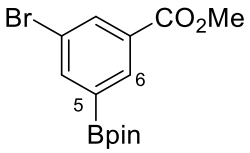

Following general procedure B with methyl 3-bromobenzoate (108 mg, 0.50 mmol) as the substrate, was added, starting material converted to 98% (*6 position:5 position* = 1:99) products. **3g** was obtained as a colorless oil (159 mg, 93%) after passing crude material through a short plug of silica using DCM as eluent. ^{1}H NMR (500 MHz, $CDCl_3$) δ 8.37 (t, *J* = 1.3 Hz, 1H), 8.25 (t, *J* = 1.9 Hz, 1H), 8.10 (dd, *J* = 2.1, 1.0 Hz, 1H), 3.92 (s 3H), 1.35 (s, 12H); ^{11}B NMR (160 MHz, $CDCl_3$) δ 30.4 (br, s). Spectral data were in accordance to literature.[36] *See pg. 100 for NMR spectra.*

Methyl 3-trifluoromethyl-6-(4,4,5,5-tetramethyl)-1,3,2-dioxaborolan-2-yl)benzoate (2h)

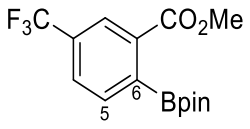

Following general procedure A with methyl 3-(trifluoromethyl)benzoate (79 µL, 102 mg, 0.50 mmol) as the substrate, starting material converted to 87% (*6 position:5 position* = 77:23) products. **2h** was obtained as a colorless oil (138 mg, 81%) after passing crude material through a short plug of silica using DCM as eluent. Using $[Ir(OMe)cod]_2$ as the precatalyst, starting material

converted to 85% (*6 position:5 position* = 73:27) borylated products. **2h** was obtained as a colorless oil (177 mg, 72%) after passing crude material through a short plug of silica using DCM as eluent.

Following general procedure C with methyl 3-(trifluoromethyl)benzoate (39.5 µL, 0.25 mmol) as the substrate, starting material converted to 98% (*6 position:5 position* = 70:30) products. **2h** was obtained as a colorless oil (65 mg, 79%) after passing crude material through a short plug of silica using DCM as eluent. ^{1}H NMR (500 MHz, $CDCl_3$) δ 8.21 (dt, *J* = 1.6, 0.8 Hz, 1H), 7.77 (ddt, *J* = 7.8, 1.8, 0.8 Hz, 1H), 7.63 (dt, *J* = 7.7, 0.7 Hz, 1H), 3.94 (s, 3H), 1.41 (s, 12H); ^{11}B NMR (160 MHz, $CDCl_3$) δ 29.6 (br, s). Spectral data were in accordance to literature.[31] *See pg. 102 for NMR spectra.*

Methyl 3-trifluoromethyl-5-(4,4,5,5-tetramethyl)-1,3,2-dioxaborolan-2-yl)benzoate (3h)

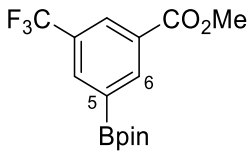

Following general procedure B with methyl 3-(trifluoromethyl)benzoate (79 µL, 102 mg, 0.50 mmol) as the substrate, starting material converted to 93% (*6 position:5 position* = 1:99) products. **3h** was obtained as a colorless oil (145 mg, 88%) after passing crude material through a short plug of silica using DCM as eluent. ^{1}H NMR (500 MHz, $CDCl_3$) δ 8.62 (ddd, *J* = 1.7, 1.2, 0.6 Hz, 1H), 8.37 (tq, *J* = 1.2, 0.6 Hz, 1H), 8.23 (dq, *J* = 1.9, 0.9 Hz, 1H)., 3.95 (s, 3H), 1.36 (s, 12H); ^{13}C NMR (126 MHz, $CDCl_3$) δ 165.9, 138.9, 135.5 (q, *J* = 4.3 Hz), 130.6 (q, *J* = 42 Hz), 130.3, 129.0 (q, *J* = 4.8 Hz), 124.8 (q, *J* = 272.8 Hz), 84.6, 52.4, 24.8, 1.0; ^{19}F NMR (470MHz, $CDCl_3$) δ -62.7 (s); ^{11}B NMR (160 MHz, $CDCl_3$) δ 30.5 (br, s). HRMS (APCI+) m/z calcd for $C_{15}H_{18}BF_3O_4$ $[M + H]^+$ 331.1284, found 331.1315. *See pg. 104 for NMR spectra.*

Methyl 5-(4,4,5,5-tetramethyl-1,3,2-dioxaborolan-2-yl)thiophene-2-carboxylate (2i)

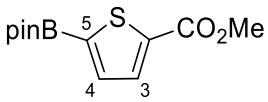

Following general procedure A with methyl thiophene-2-carboxylate (58 µL, 71 mg, 0.50 mmol) as the substrate, starting material converted to 99% (3:5 = 1:99) products. **2i** was obtained as a colorless oil (137 mg, 90%) after passing crude material through a short plug of silica using DCM as eluent. ^{1}H NMR (500 Hz, $CDCl_3$) δ 7.80 (d, *J* = 3.7 Hz, 1H), 7.55 (d, *J* = 3.7 Hz, 1H), 3.88 (s, 3H), 1.34 (s, 12H). ^{11}B NMR (160 MHz, $CDCl_3$) δ 28.9 (br, s). Using $[Ir(OMe)cod]_2$ as the precatalyst, starting material converted to 99% (3:5 = 1:99) borylated products. **2i** was obtained as a colorless oil (118 mg, 90%) after passing crude material through a short plug of silica using DCM as eluent. Spectral data were in accordance to literature.[37] *See pg. 114 for NMR spectra.*

Methyl 5-(4,4,5,5-tetramethyl-1,3,2-dioxaborolan-2-yl)thiophene-2-carboxylate (2i)

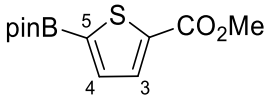

Following general procedure B with methyl thiophene-2-carboxylate (58 µL, 71 mg, 0.50 mmol) as the substrate, starting material converted to 99% (3-position:5-position = 1:99) products. **2i** was obtained as a colorless oil (156 mg, 99%) after passing crude material through a short plug of silica using DCM as eluent. ^{1}H NMR (500 MHz, $CDCl_3$) δ 7.82 (d, *J* = 3.8 Hz, 1H), 7.56 (d, *J* = 3.7 Hz, 1H), 3.90 (s, 3H), 1.36 (s, 12H); ^{11}B NMR (160 MHz, $CDCl_3$) δ 28.9 (br, s). Spectral data were in accordance to literature.[37]

Methyl-5-methyl-3-(4,4,5,5-tetramethyl-1,3,2-dioxaborolan-2-yl)thiophene-2-carboxylate (2j)

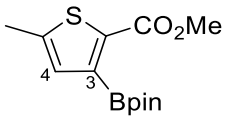

Following general procedure A with methyl 5-methylthiophene-2-carboxylate (66 µL, 78 mg, 0.50 mmol) as the substrate, starting material converted to 88% (3:4 = 94:6) products. **2j** was obtained as a colorless oil (120 mg, 85%) after passing crude material through a short plug of silica using DCM as eluent. ^{1}H NMR (500 MHz, $CDCl_3$) δ 6.86 (q, *J* = 1.0 Hz, 1H), 3.93 (s, 3H), 2.53 (d, *J* = 1.0 Hz, 3H), 1.40 (s, 12H); ^{11}B NMR (160 MHz, $CDCl_3$) δ 28.8 (br, s). Using $[Ir(OMe)cod]_2$ as the precatalyst, starting material converted to 88% ((3:4 = 80:20) borylated products. **2j** was obtained as a colorless oil (78 mg, 55%) after passing crude material through a short plug of silica using DCM as eluent. Spectral data were in accordance to literature.[37] *See pg. 116 for NMR spectra.*

Methyl-4-methyl-3-(4,4,5,5-tetramethyl-1,3,2-dioxaborolan-2-yl)thiophene-2-carboxylate (3j)

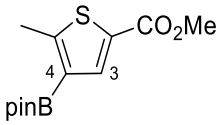

Following general procedure B with methyl 5-methylthiophene-2-carboxylate (66 µL, 78 mg, 0.50 mmol) as the substrate, starting material converted to 99% (3:4 = 1:99) products. **3j** was obtained as a colorless oil (131 mg, 93%) after passing crude material through a short plug of silica using DCM as eluent. ^{1}H NMR (500 MHz, $CDCl_3$) δ 7.93 (s, 1H), 3.83 (s, 3H), 2.69 (s, 3H), 1.30 (s, 12H); ^{11}B NMR (160 MHz, $CDCl_3$) δ 31.0 (br, s). Spectral data were in accordance to literature.[37]

Methyl 5-(4,4,5,5-tetramethyl-1,3,2-dioxaborolan-2-yl)furan-2-carboxylate (2k)

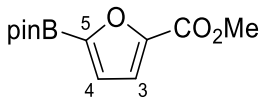

Following general procedure A with methyl furan-2-carboxylate (53 µL, 63 mg, 0.50 mmol) as the substrate, starting material converted to 99% (5:3 = 92:8) products. **2k** was obtained as a colorless oil (103 mg, 82%) after passing crude material through a short plug of silica using DCM as eluent. ^{1}H NMR (500 MHz, $CDCl_3$) δ 7.19 (dd, *J* = 3.5, 0.9 Hz, 1H), 7.08 (dd, *J* = 3.5, 0.9 Hz, 1H), 3.90 (d, *J* = 0.9 Hz, 3H), 1.35 (s, 12H); ^{11}B NMR (160 MHz, $CDCl_3$) δ 30.0 (br, s). Spectral data were in accordance to literature. Spectral data were in accordance to literature. [37] *See pg. 118 for NMR spectra.*

Methyl 5-(4,4,5,5-tetramethyl-1,3,2-dioxaborolan-2-yl)furan-2-carboxylate (2k)

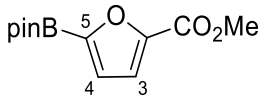

Following general procedure B with methyl furan-2-carboxylate (53 µL, 63 mg, 0.50 mmol) as the substrate, starting material converted to 99% (5:3 = 93:7) products. **2k** was obtained as a colorless oil (125 mg, 99%) after passing crude material through a short plug of silica using DCM as eluent. ^{1}H NMR (500 MHz, $CDCl_3$) δ 7.20 (dd, *J* = 3.5, 0.9 Hz, 1H), 7.09 (dd, *J* = 3.5, 0.9 Hz, 1H), 3.92 (d, *J* = 0.9 Hz, 3H), 1.36 (s, 12H); ^{11}B NMR (160 MHz, $CDCl_3$) δ 30.0 (br, s). Spectral data were in accordance to literature.[37]

Methyl 5-methyl-3-(4,4,5,5-tetramethyl-1,3,2-dioxaborolan-2-yl)furan-2-carboxylate (2l)

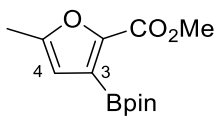

Following general procedure A with methyl 5-methylfuran-2-carboxylate (70 mg, 0.50 mmol) as the substrate, starting material converted to 56% (3:4 = 44:56) products. **2l** was obtained as a colorless oil (35 mg, 47%) after passing crude material through a short plug of silica using DCM as eluent. ^{1}H NMR (500 MHz, $CDCl_3$) δ 7.31 (s, 1H), 3.87 (d, *J* = 0.9 Hz, 3H), 2.54 (s, 3H), 1.32 (d, *J* = 0.9 Hz, 12H); ^{11}B NMR (160 MHz, $CDCl_3$) δ 30.1 (br, s). Spectral data were in accordance to literature.[38]

Methyl 5-methyl-4-(4,4,5,5-tetramethyl-1,3,2-dioxaborolan-2-yl)furan-2-carboxylate (3l)

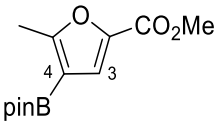

Following general procedure B with methyl 5-methylfuran-2-carboxylate (70 mg, 0.50 mmol) as the substrate, starting material converted to 99% (3:4 = 1:99) products. **3l** was obtained as a colorless oil (98 mg, 74%) after passing crude material through a short plug of silica using DCM as eluent. ^{1}H NMR (500 MHz, $CDCl_3$) δ 7.30 (s, 1H), 3.86 (s, 3H), 2.53 (s, 3H), 1.31 (s, 12H); ^{11}B NMR (160 MHz, $CDCl_3$) δ 30.2 (br, s). Spectral data were in accordance to literature.[38]

2.5.8: Reaction Optimization for Borane Synthesis

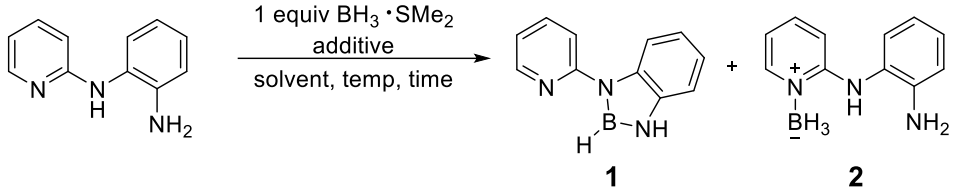

1 **2**

entry	solvent	temp (°C)	time (h)	additive[a]	[M] of rxn	conversion[b]	ratio of **1:2**
1	CH_2Cl_2	rt	24 h	--	0.621	>99%	1:>99
2	CH_2Cl_2	50	5 h	--	0.305	>99%	1:>99
3	CH_2Cl_2	rt	24 h	0.1 equiv HOTf	0.893	>99%	1:>99
4	toluene	115	24 h	--	0.625	32%	94:6
5[c]	toluene	115	24 h	--	0.947	--	--
6	toluene	115	13 h	--	0.089	40%	98:2
7[c,d,e]	toluene	-5 to 115	12 h	--	0.150	--	--
8	THF	-78 to rt	16 h	1.05 equiv *n*BuLi	0.285	>99%	1:>99
9[f]	THF	-78 to rt	12 h	1 equiv $BrBH_2 \cdot SMe_2$ 1.05 equiv *n*BuLi	0.144	>99%	1:>99[g]

[a]$BH_3 \cdot SMe_2$ was used as a 1 M solution in CH_2Cl_2, *n*BuLi was used as a 2.5 M solution in hexanes.[b]Conversion is based on starting material was calculated by the crude ^1H NMR integrations. [c]The aromatic region in the crude ^1H could not give conclusive results, though ^{11}B shows minimal formation of **1** and no unreacted $BH_3 \cdot SMe_2$.[d]Borane was added at -5 °C then refluxed. [e]1.05 equiv of $BH_3 \cdot SMe_2$ was used. [f]$BrBH_2 \cdot SMe_2$ was used as the borane source. [f]Crude reaction mixture contained 30% adduct (**2**) to 70% of an unknown boron compound shown in ^{11}B NMR (C_6D_6) δ 2.5 ppm.

General Reaction Procedure for Entries 1-7

In an oven dried 10 mL Schlenk flask equipped with a stir bar under N_2, N^1-(pyridin-2-yl)benzene-1,2-diamine (1 equiv) was added followed by dry toluene or methylene chloride. The reaction was capped with a rubber septum and stirred until the solid was completely dissolved. Schlenk line tubing under N_2 was fitted on a 3-way adapter connected to a nitrogen bubbler, and the plastic tubing on the last port of the adapter was fitted on the reaction vessel. Plastic tubing was then connected to the N_2 outlet of the bubbler and was submerged in a 100 mL beaker filled with bleach to trap any dimethyl sulfide from the borane reagent. Borane dimethyl sulfide (1 equiv, 1 M solution in methylene chloride) was then added dropwise at rt through the top of the septum using a 12 mL Luer Lock syringe. The dark red solution was then stirred at rt for 10 min. The septum was then replaced with a condenser and the reaction was either refluxed or allowed to stir at rt for

5-24 hours. When refluxed in toluene, the reaction solution turned from dark red to a bright yellow color.

Entry 3: Follows the general reaction procedure with the exception that HOTf (0.1 equiv) was added after the dark red solution stirred at rt for 10 min. *Entry 7:* Follows the general reaction procedure with the exception that the reaction was cooled to 0 °C in an ice bath prior to addition of $BH_3 \cdot SMe_2$, then warmed up to rt.

Procedures for Entry 8-9

In a 50 mL oven dried 3-neck RBF equipped with a stir bar, N^1-(pyridin-2-yl)benzene-1,2-diamine (200 mg, 1.08 mmol, 1 equiv) and dry THF (10 mL) was added and the flask was connected to an N_2 bubbler. The flask was cooled to -78 °C and a 1 M solution of nBuLi in hexanes (0.454 mL, 1.13 mmol, 1.05 equiv) was added dropwise, where the solution turned from yellow to light green. The reaction was allowed to warm to RT after stirring at -78 °C for 1 h, and the solution turned from green to light red. The N_2 bubbler was then connected to a bleach trap and a 1 M solution of $BH_3 \cdot SMe_2$ or $BrBH_2 \cdot SMe_2$ in methylene chloride (1.08 mL, 1.08 mmol, 1 equiv) was added. The reaction solution stirred at rt for 24 h where the color changed from red to bright yellow. *See pg. 120-125 for NMR spectra.*

^{1}H NMR of product 1, entry 6 (500 MHz, $CDCl_3$) δ 8.52 (d, *J* = 5.9 Hz, 1H), 8.25 – 8.21 (m, 1H), 7.72 (t, *J* = 8.3 Hz, 1H), 7.47 – 7.44 (m, 2H), 7.15 – 7.12 (m, 2H), 7.11 – 7.09 (m, 1H), 5.08 (q, *J* = 189.7 Hz, BH), 3.75 (bs, NH).

^{11}B NMR of product 1 (160 MHz, $CDCl_3$) δ 25.4 (d, *J* = 149.9 Hz, BH).

^{1}H NMR of product 2, entry 1 (500 MHz, $CDCl_3$) δ 8.24 (d, *J* = 5.9 Hz, 1H), 7.56 – 7.48 (m, 2H), 7.17 (td, *J* = 7.7, 1.1 Hz, 1H), 7.13 (d, *J* = 7.8 Hz, 1H), 6.84 (dd, *J* = 7.9, 1.1 Hz, 1H), 6.79 (td, *J* = 7.9, 1.1 Hz, 1H), 6.68 (t, *J* = 6.5 Hz, 1H), 6.51 (d, *J* = 8.6 Hz, 1H), 3.86 (bs, 2H), 2.36 (q, *J* = 105.8 Hz, BH_3).

^{11}B NMR of product 2 (160 MHz, $CDCl_3$) δ -17.2 (q, *J* = 89 Hz, BH_3).

2.5.9: Synthesis of $BrBH_2 \cdot SMe_2$

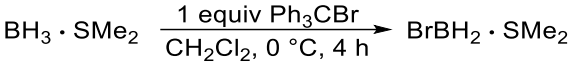

In a dried 10 mL Schlenk flask equipped with stir bar and attached to a N_2 bubbler connected to a bleach trap, trityl bromide (647 mg, 2 mmol, 1 equiv) was added followed by dry methylene chloride (2 mL). The flask was cooled to 0 °C in an ice bath. A 1 M solution of $BH_3 \cdot SMe_2$ in methylene chloride (2 mL, 2 mmol, 1 equiv) was added dropwise and the reaction was stirred at 0 °C for 4 hours where >99% of starting material was converted yielding a 1 M solution of $BrBH_2 \cdot SMe_2$ in methylene chloride. Spectral data were in accordance to literature.[39] *See pg. 126 for NMR spectra.*

^{1}H NMR (500 MHz, C_6D_6) δ 7.11-7.01 (m, 15H), 3.31 (q, J = 131.6 Hz, BH_2), 1.73 (s, 3H), 1.27 (s, 3H).

^{11}B NMR (160 MHz, C_6D_6) δ 10.8 (t, J = 133.2 Hz, BH).

2.5.10: NMR Tube Reaction with Borane and $[IrCl(cod)]_2$

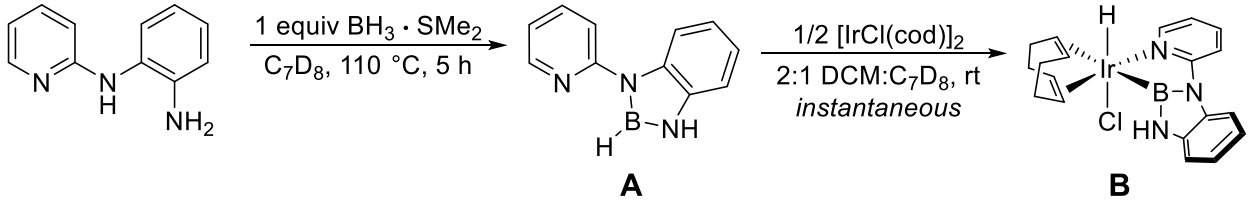

In a 7'' J-young pressure tube purged under N_2, a solution of N^1-(pyridin-2-yl)benzene-1,2-diamine (10 mg, 0.054 mmol, 1 equiv) dissolved in C_7D_8 (0.75 mL) was added, followed by a 1 M solution of $BH_3 \cdot SMe_2$ in methylene chloride (0.054 mL, 0.054 mmol, 1 equiv). A Teflon screw cap was used to seal the tube and the reaction was refluxed at 110 °C and monitored by ^{11}B and ^{1}H NMR. After 5 hours, 92% of starting material was converted to product **A**. After the tube cooled to rt, a solution of $[IrCl(cod)]_2$ (18.1 mg, 0.027 mmol, 0.5 equiv) dissolved in methylene chloride (1.2 mL) was added to yield product **B**. *See pg. 129 for NMR spectra.*

^{1}H NMR of B (500 MHz, C_7D_8) δ 9.04 (d, *J* = 6.1 Hz, 1H), 6.66 – 6.60 (m, 3H), 6.55 (dt, *J* = 7.5, 1.7 Hz, 2H), 6.32 (td, *J* = 6.4, 1.7 Hz, 2H), 6.24 (bs, N–H), 4.22 (t, *J* = 7.1 Hz, 2H), 3.96 (sx, *J* = 4.5 Hz, 1H), 3.45 – 3.39 (m, 2H), 3.03 – 2.97 (m, 1H), 2.84 – 2.74 (m, 1H), 2.03-1.94 (m, 2H), 1.90 – 1.83 (m, 1H), 1.59 – 1.54 (m, 2H), -10.68 (s, Ir–H).

^{11}B NMR of B (160 MHz, C_7D_8) δ 36.7 (bs, Ir–B)

2.5.11: Spectral Data

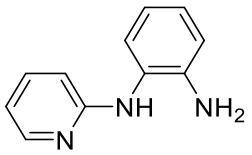

^{1}H NMR

(500 MHz, $CDCl_3$)

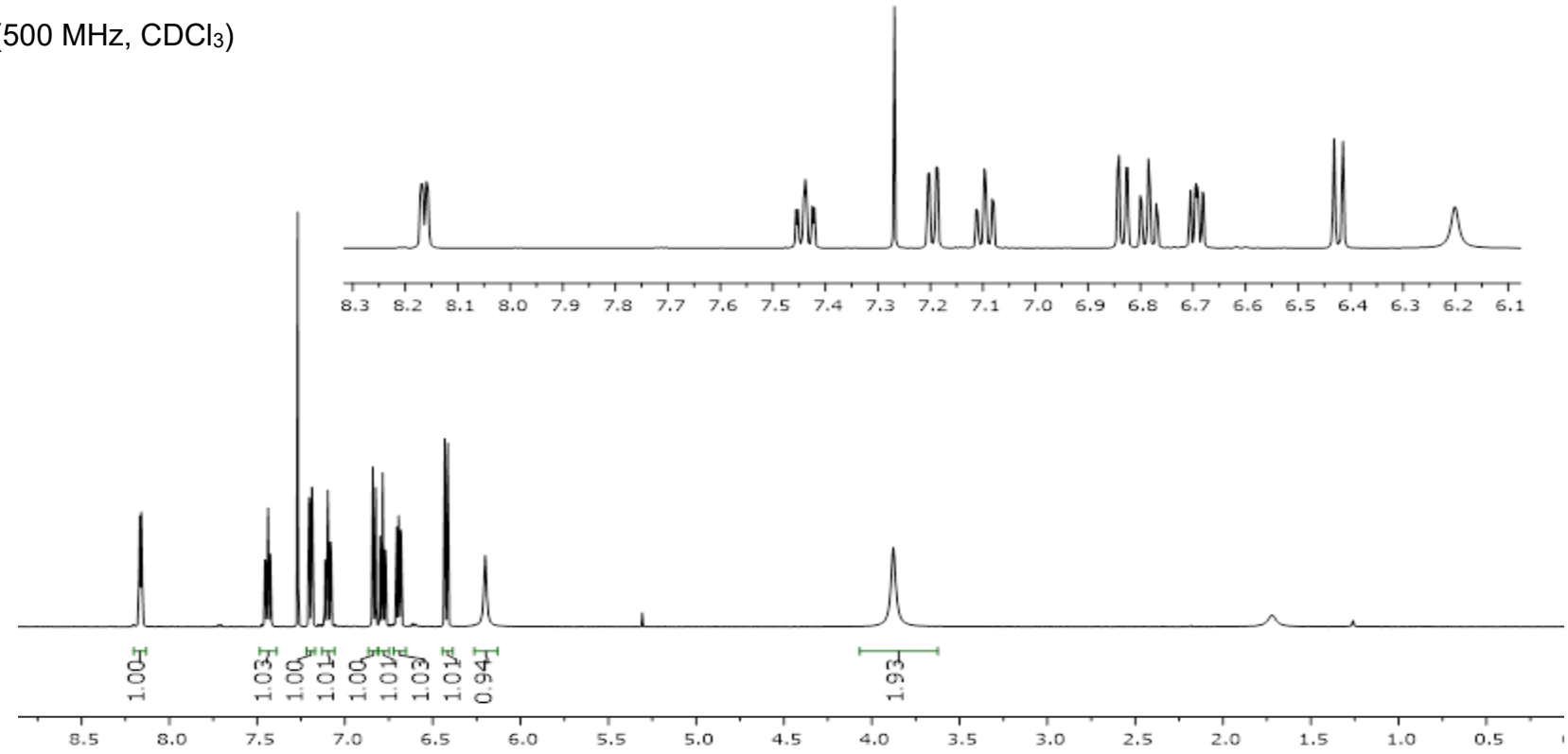

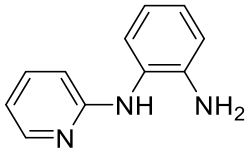

^{13}C NMR

(126 MHz, $CDCl_3$)

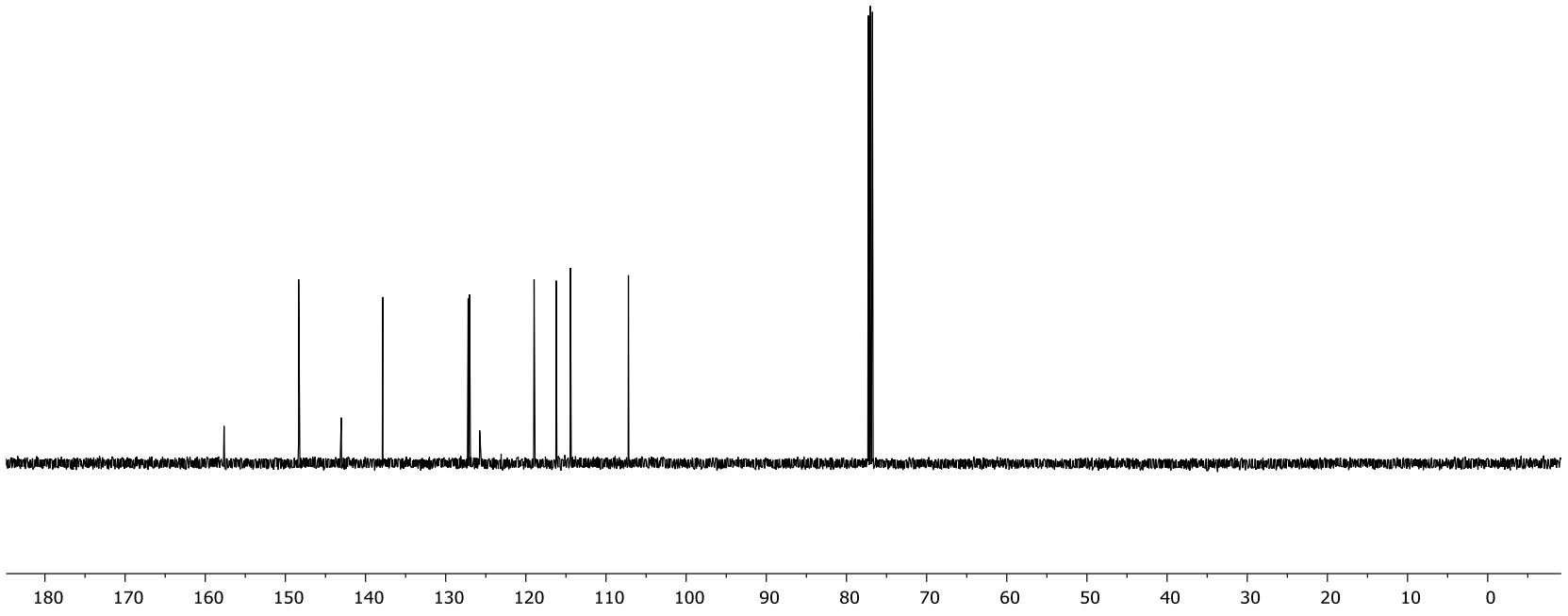

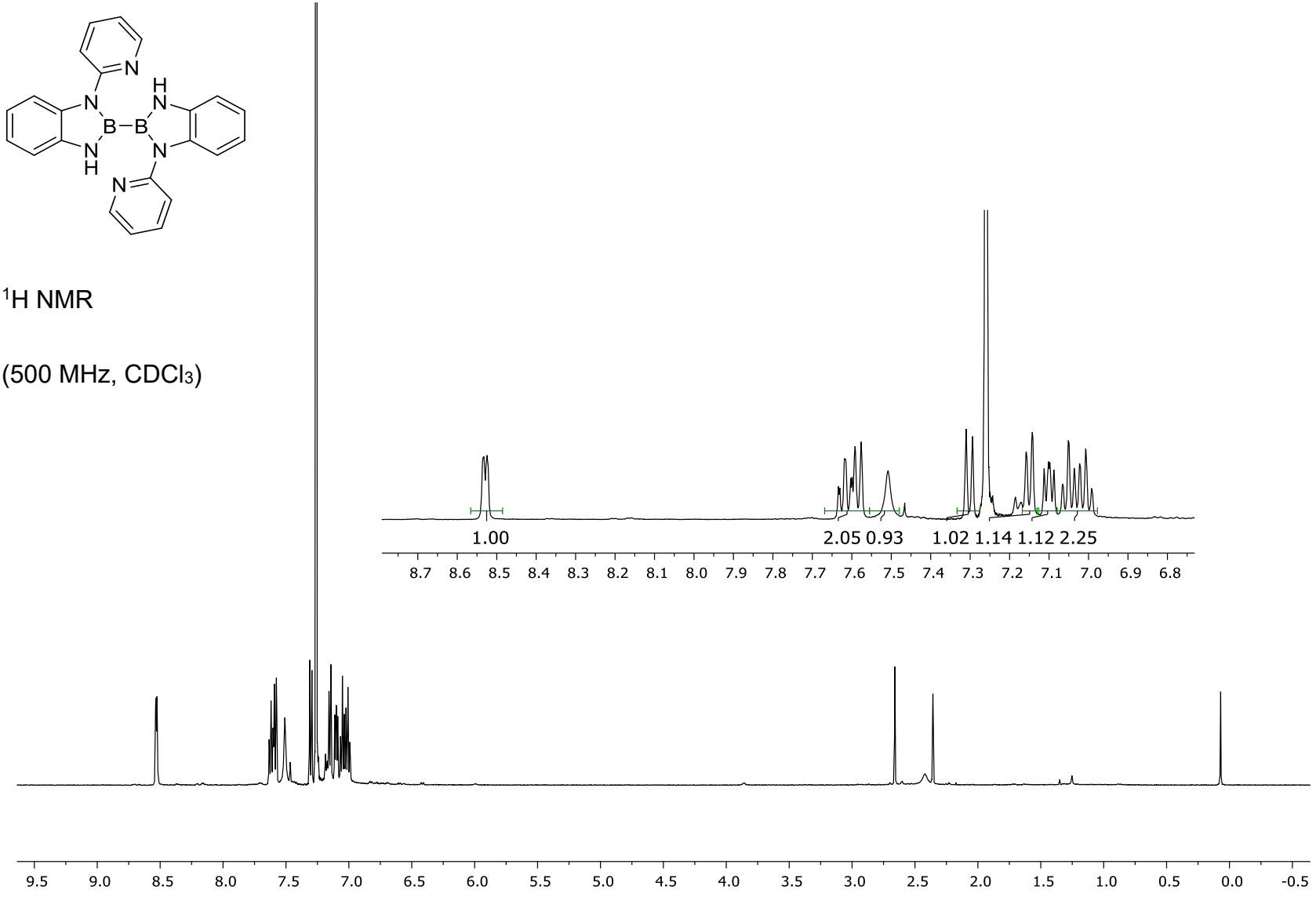

^{1}H NMR

(500 MHz, $CDCl_3$)

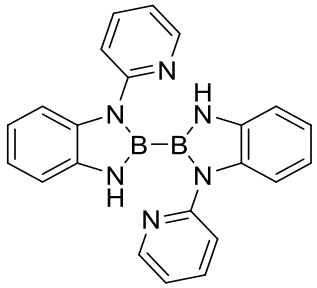

^{13}C NMR

(126 MHz, $CDCl_3$)

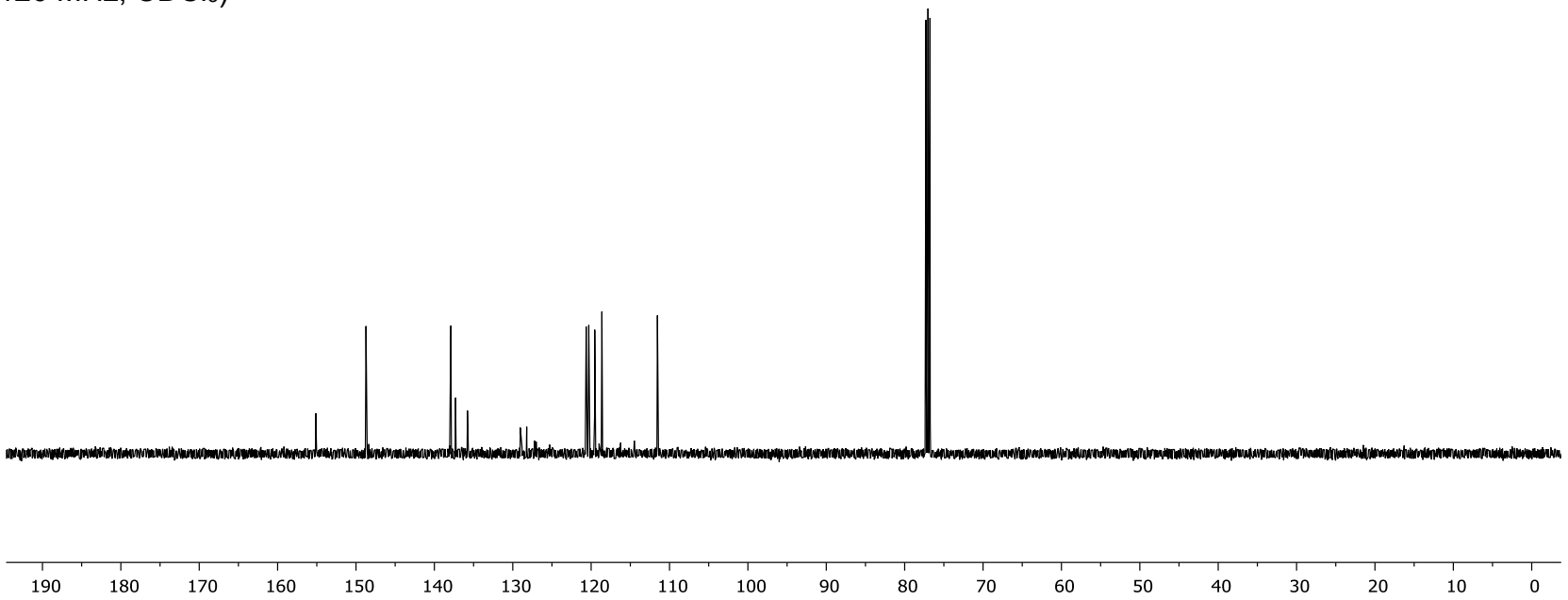

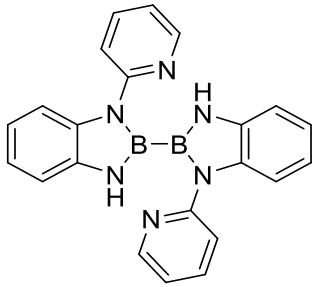

^{11}B NMR

(160 MHz, $CDCl_3$)

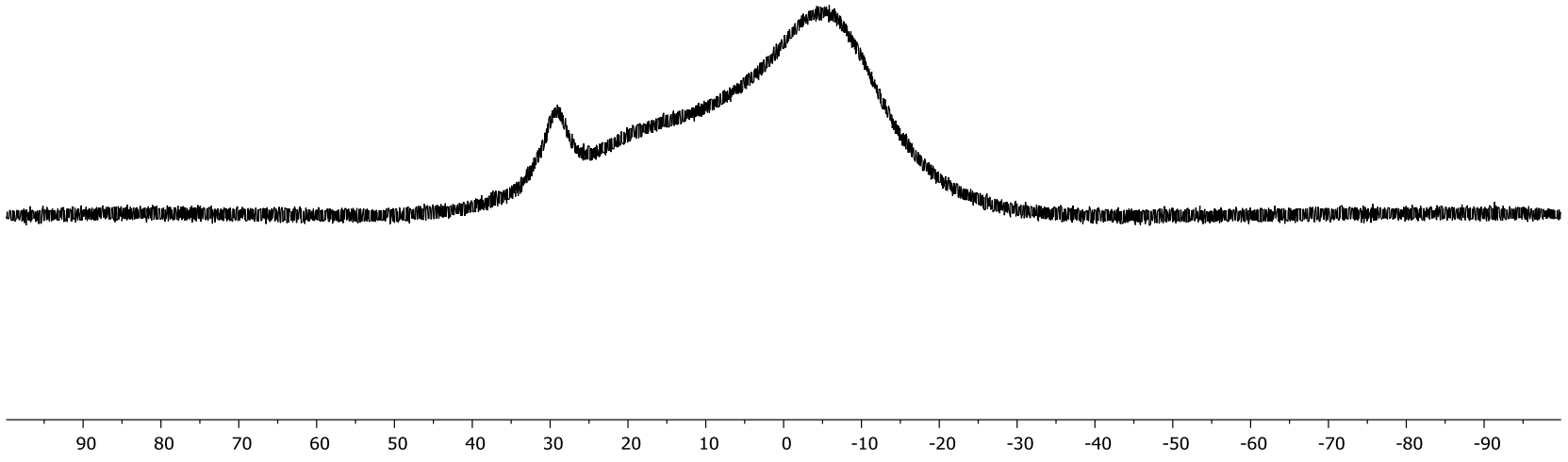

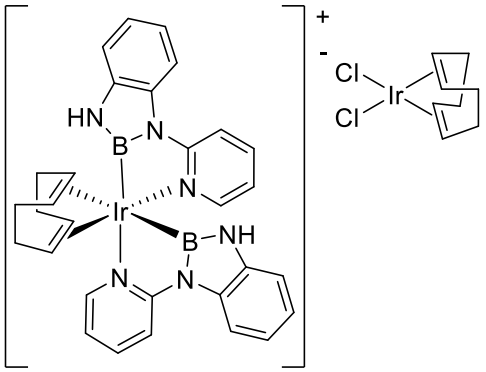

^{1}H NMR

(500 MHz, DMSO-d_6)

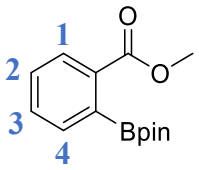

^{1}H NMR

(500 MHz, $CDCl_3$)

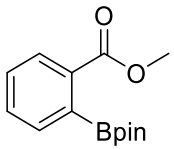

^{11}B NMR

(160 MHz, $CDCl_3$)

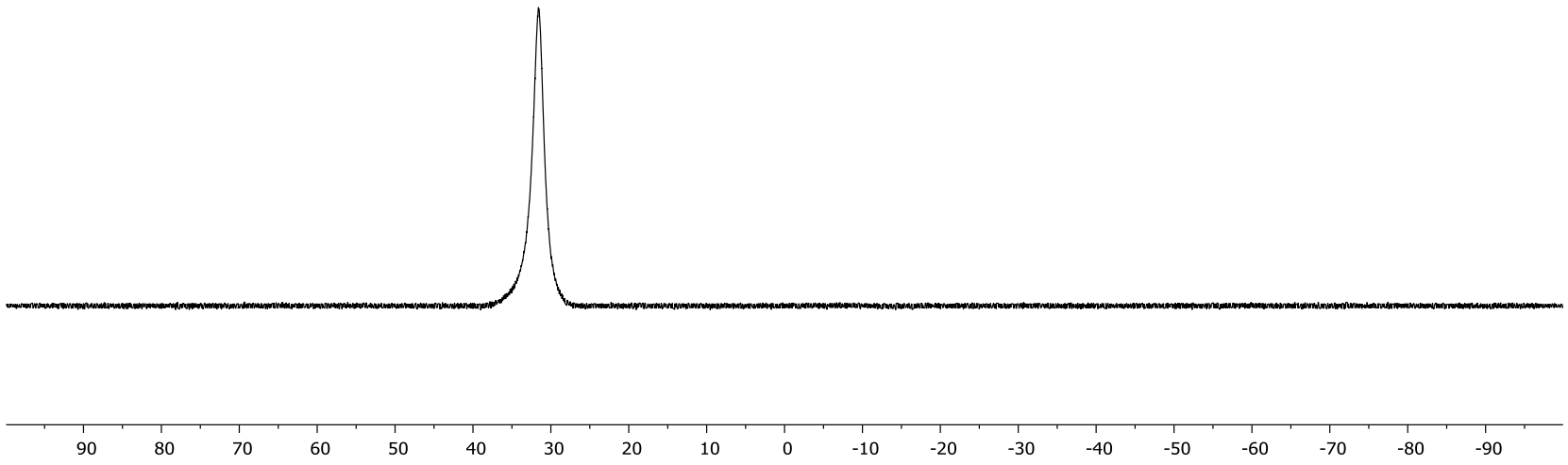

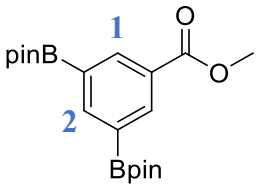

^{1}H NMR

(500 MHz, $CDCl_3$)

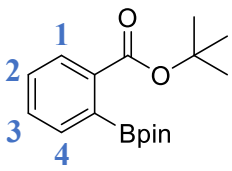

^{1}H NMR

(500 MHz, $CDCl_3$)

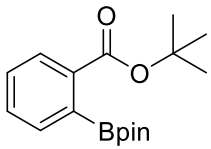

^{11}B NMR

(160 MHz, $CDCl_3$)

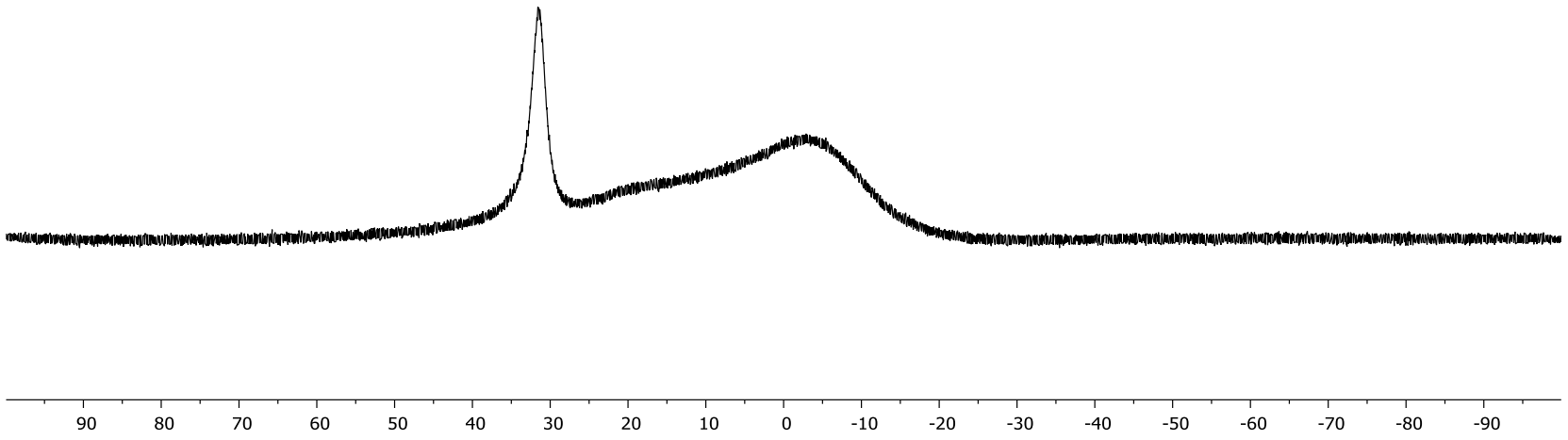

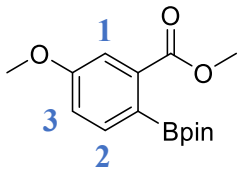

^{1}H NMR

(500 MHz, $CDCl_3$)

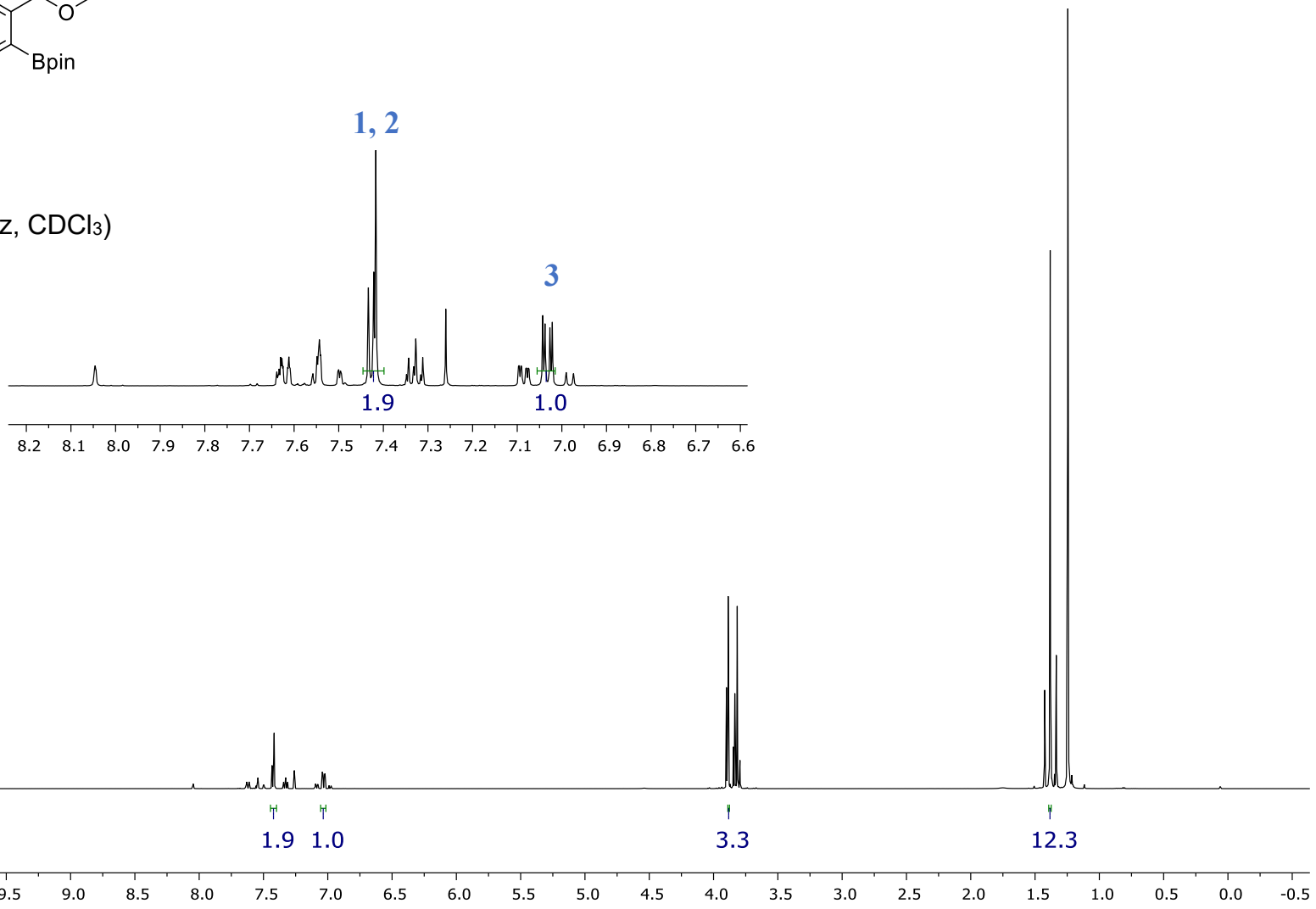

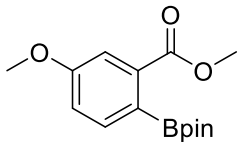

^{11}B NMR

(160 MHz, $CDCl_3$)

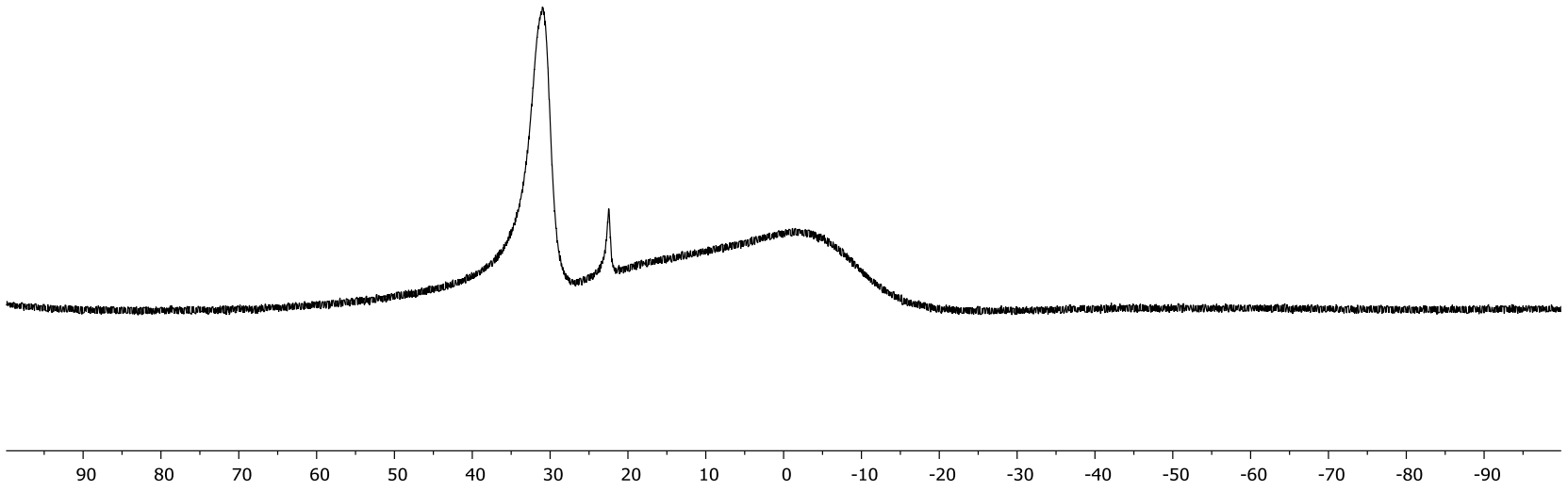

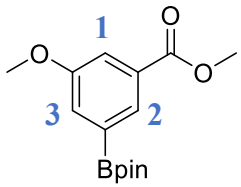

^{1}H NMR

(500 MHz, $CDCl_3$)

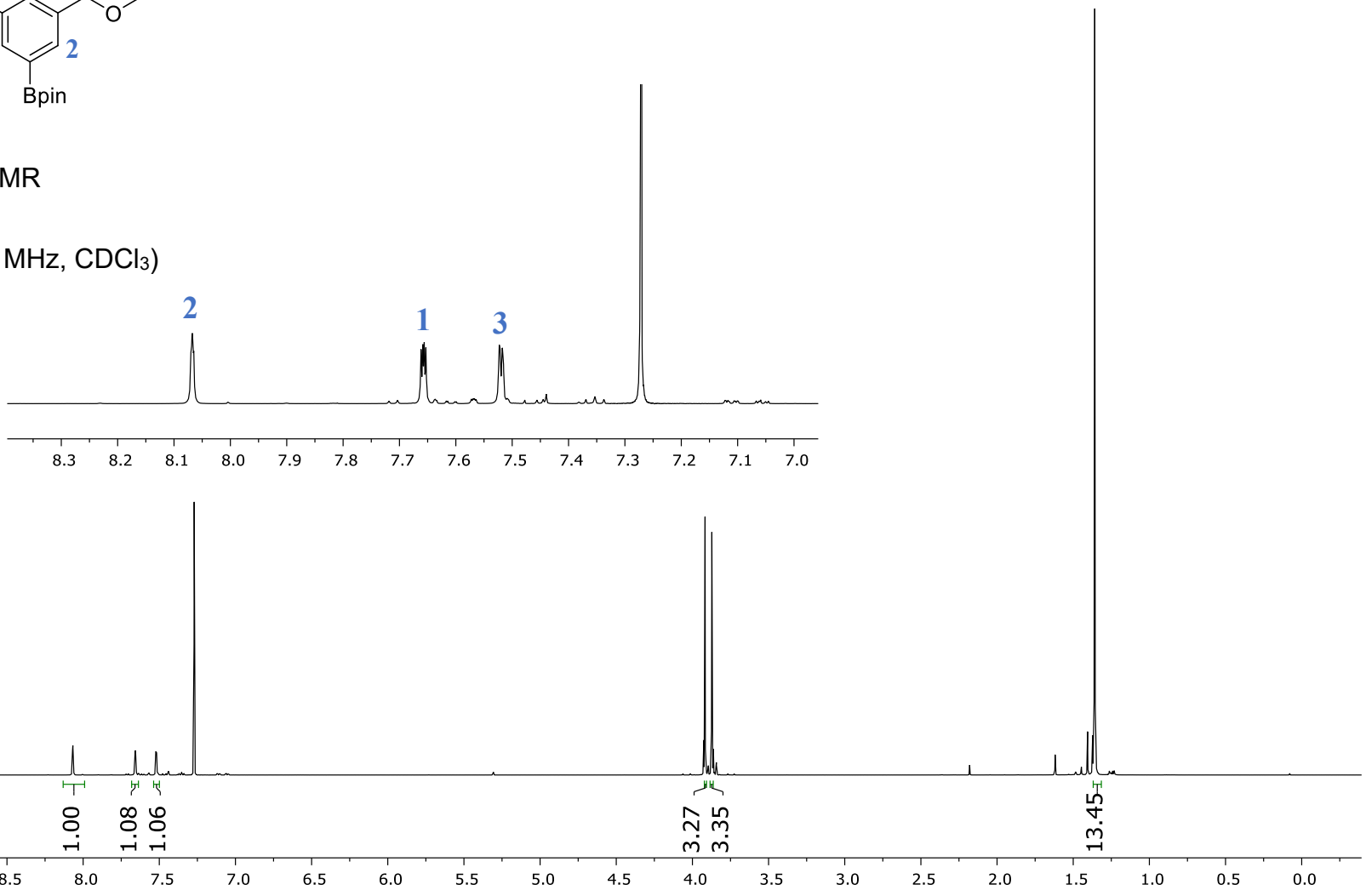

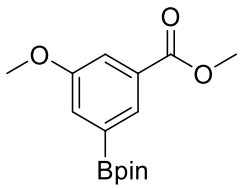

^{11}B NMR

(60 MHz, $CDCl_3$)

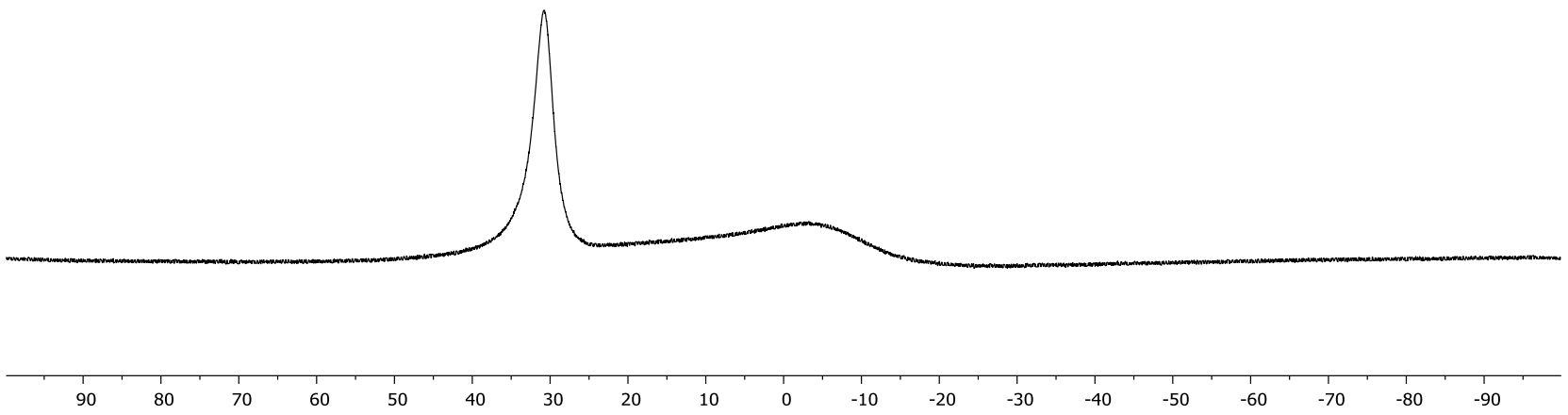

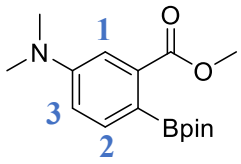

^{1}H NMR

(500 MHz, $CDCl_3$)

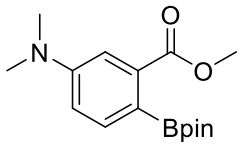

^{11}B NMR

(160 MHz, $CDCl_3$)

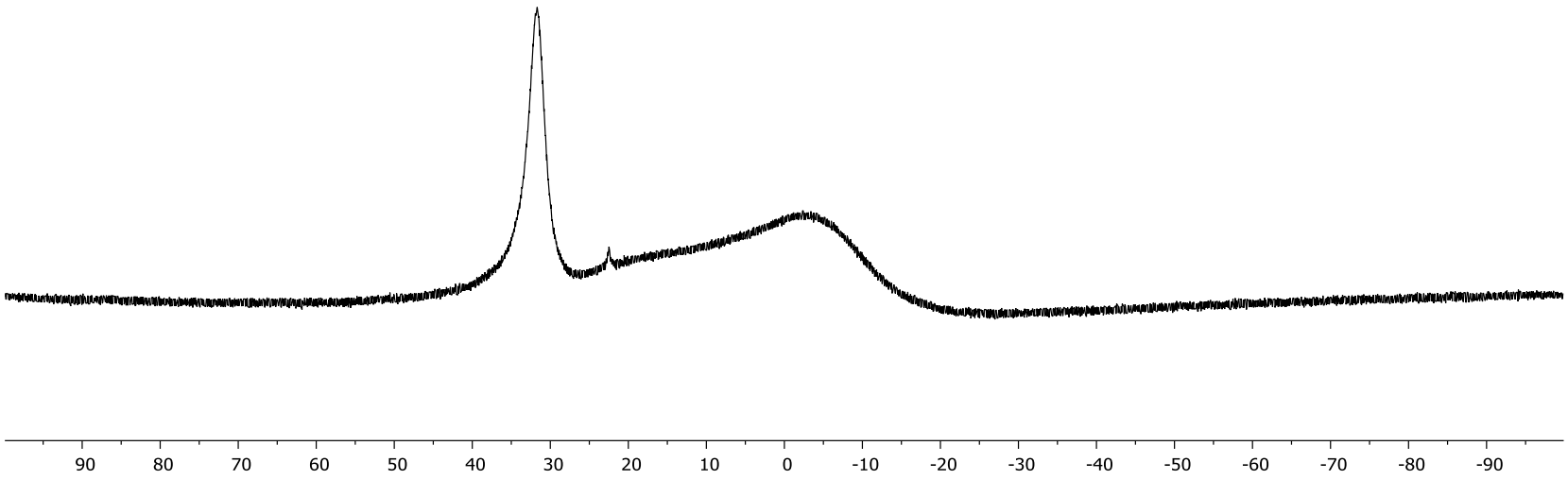

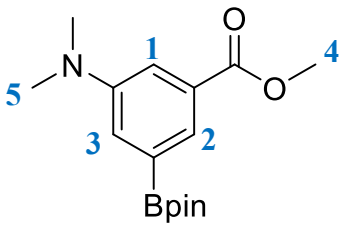

^{1}H NMR

(500 MHz, $CDCl_3$)

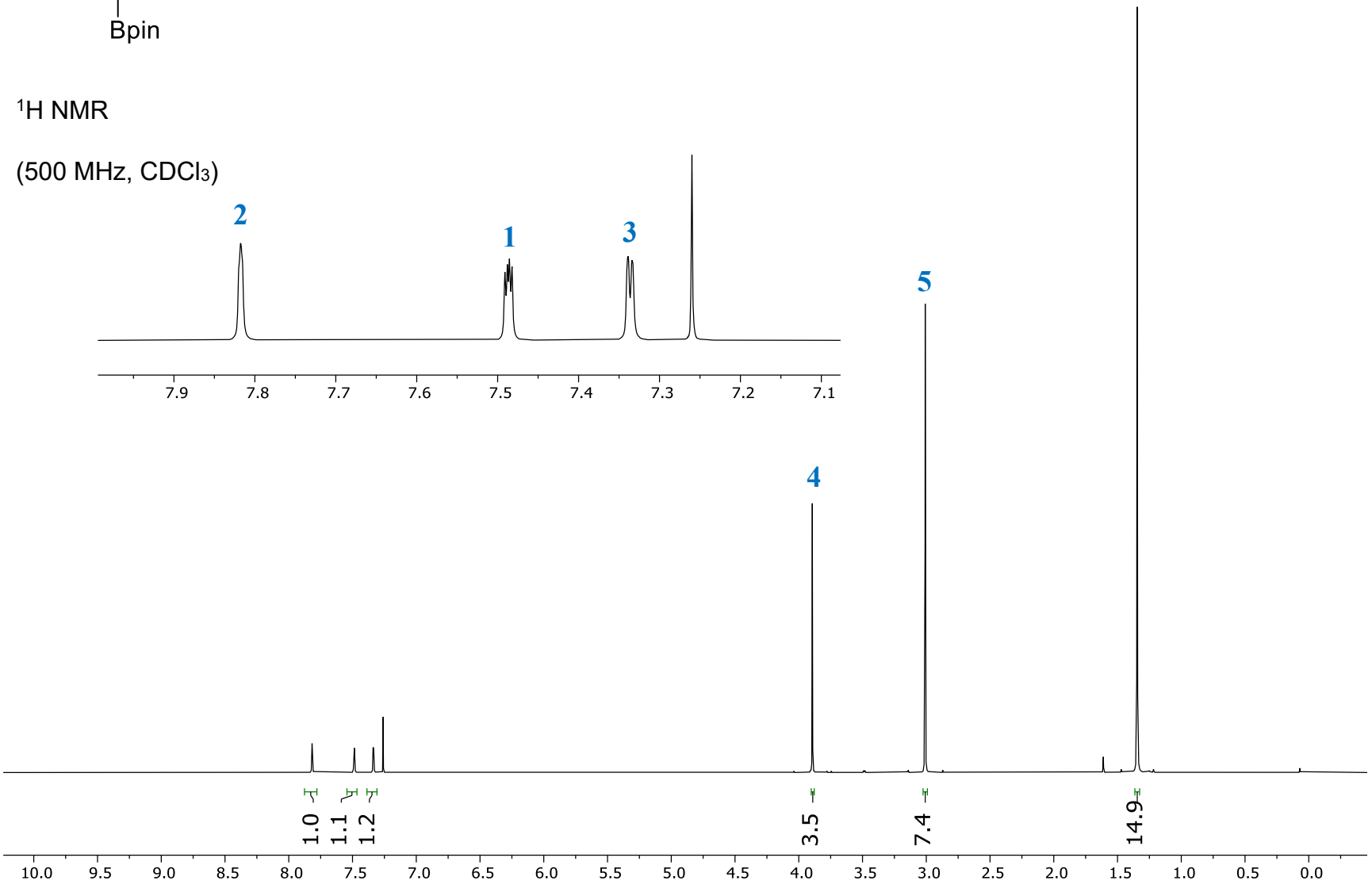

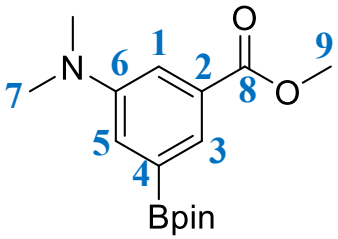

^{13}C NMR

(126 MHz, $CDCl_3$)

Carbon 4 generally not seen due to quadrupolar relaxation of ^{11}B.

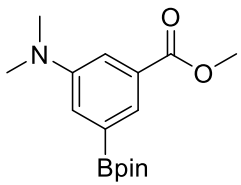

^{11}B NMR

(60 MHz, $CDCl_3$)

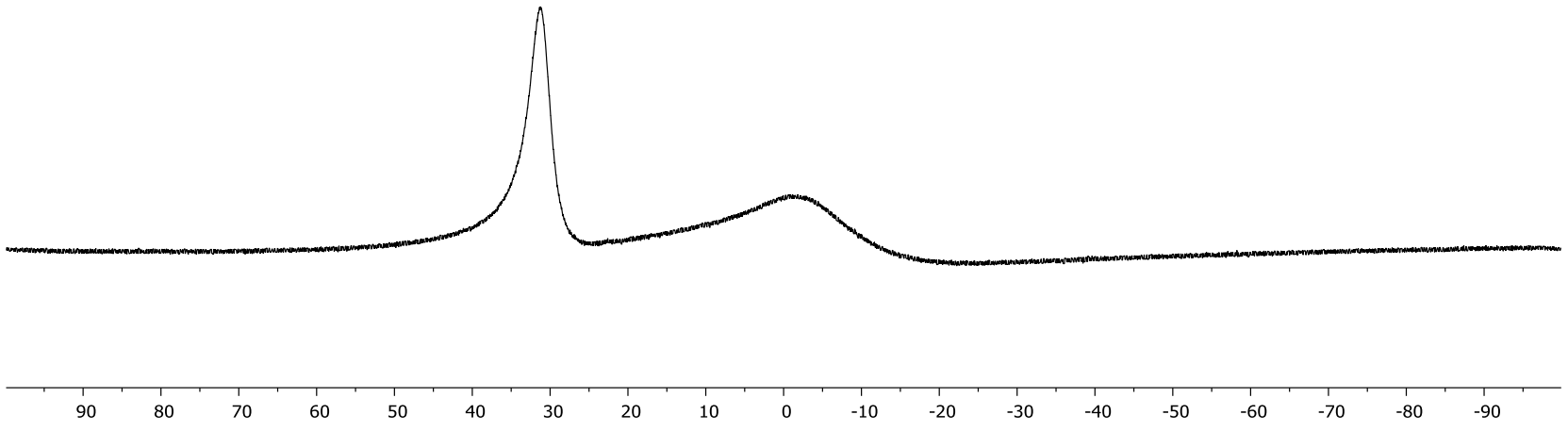

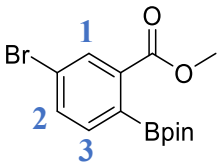

^{1}H NMR

(500 MHz, $CDCl_3$)

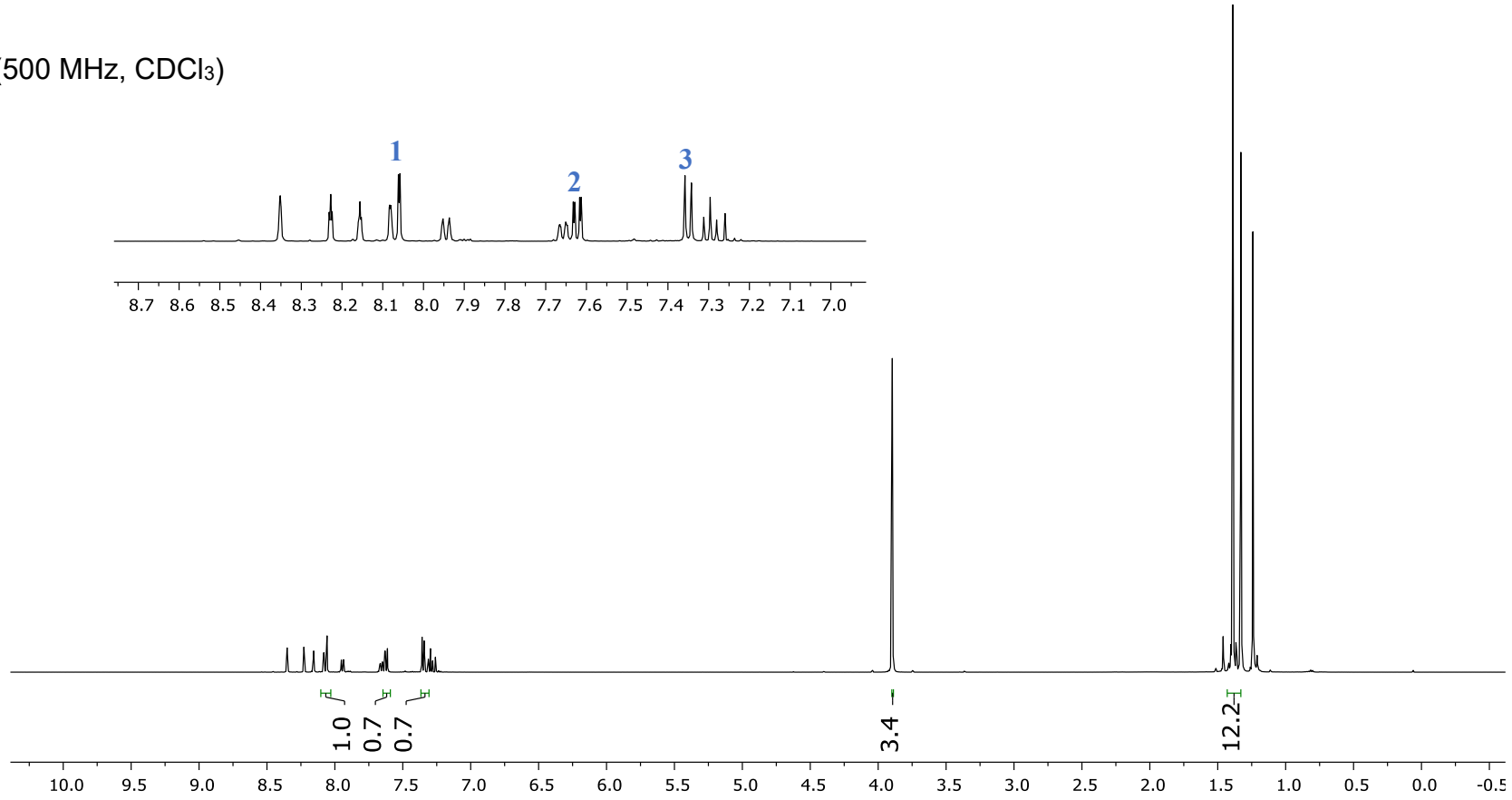

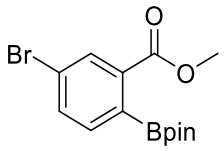

^{11}B NMR

(160 MHz, $CDCl_3$)

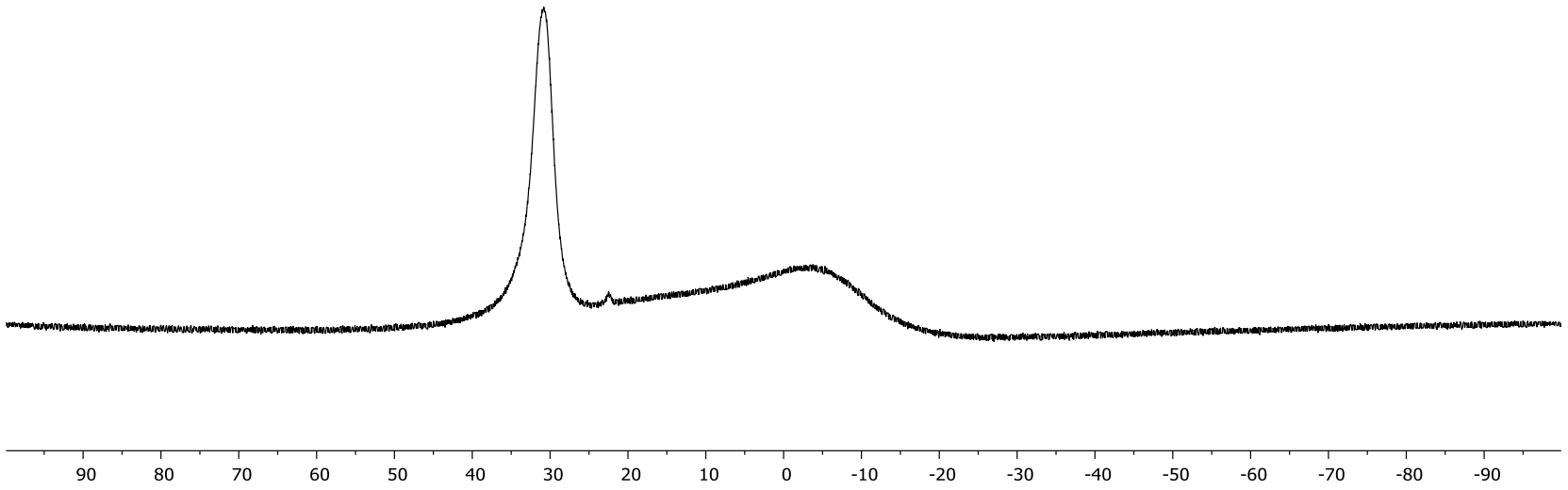

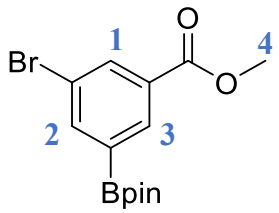

^{1}H NMR

(500 MHz, $CDCl_3$)

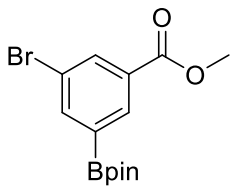

^{11}B NMR

(60 MHz, $CDCl_3$)

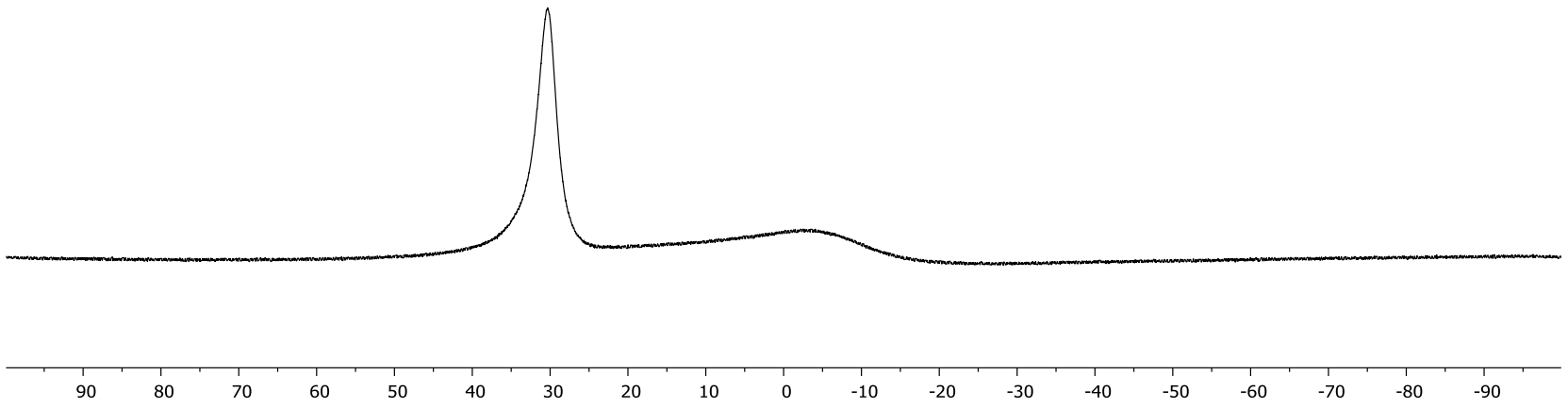

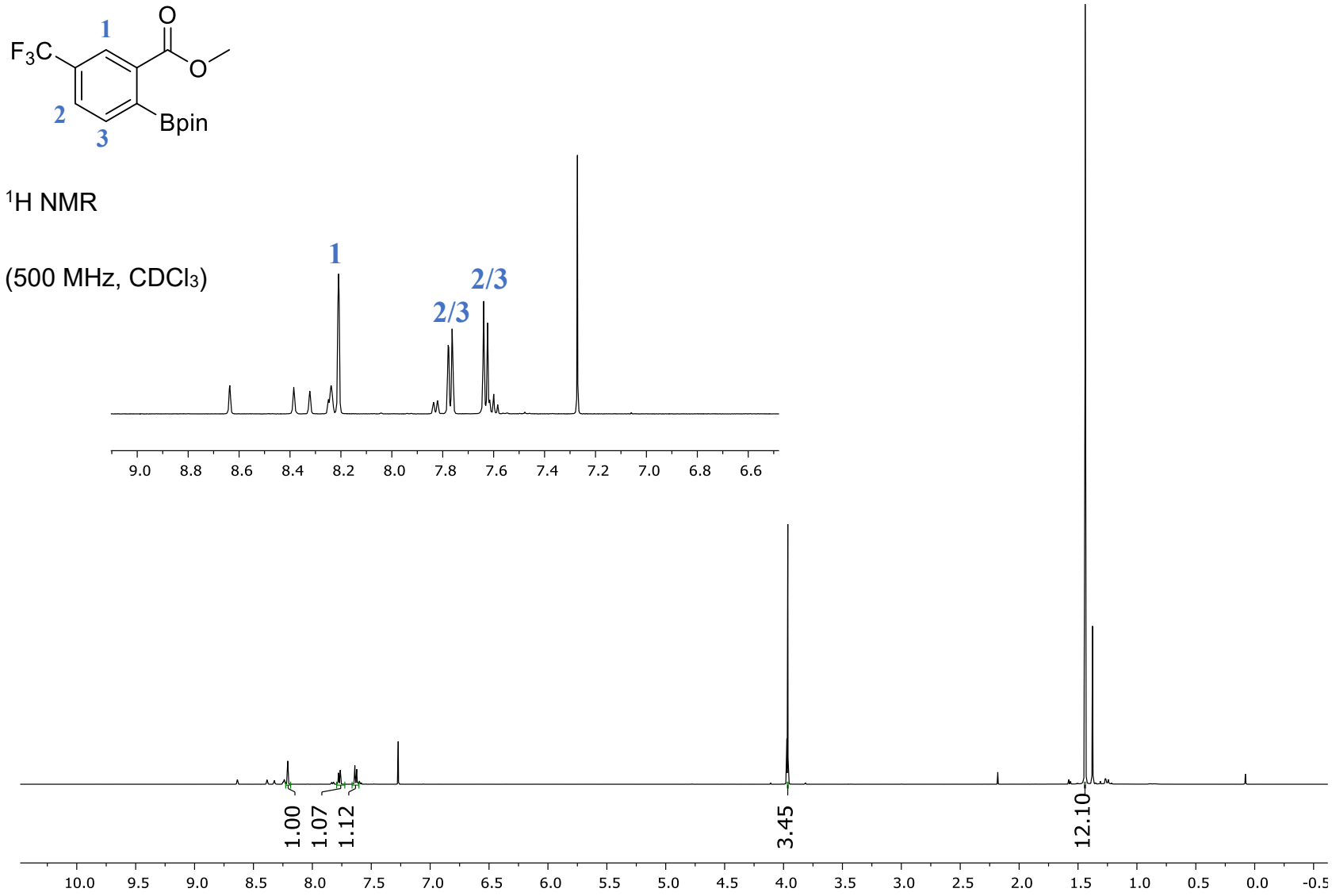
F3C
O
O
Bpin
1
2
3
1H NMR
(500 MHz, CDCl3)
1
2/3
2/3
9.0 8.8 8.6 8.4 8.2 8.0 7.8 7.6 7.4 7.2 7.0 6.8 6.6
1.00
1.07
1.12
3.45
12.10
10.0 9.5 9.0 8.5 8.0 7.5 7.0 6.5 6.0 5.5 5.0 4.5 4.0 3.5 3.0 2.5 2.0 1.5 1.0 0.5 0.0 -0.5

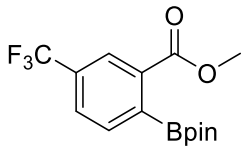

^{11}B NMR

(160 MHz, $CDCl_3$)

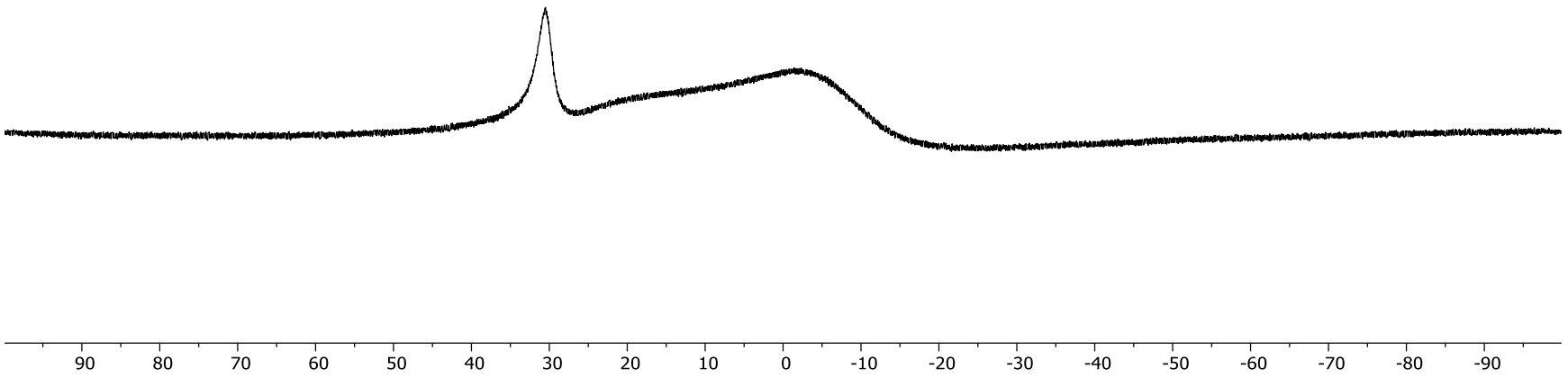

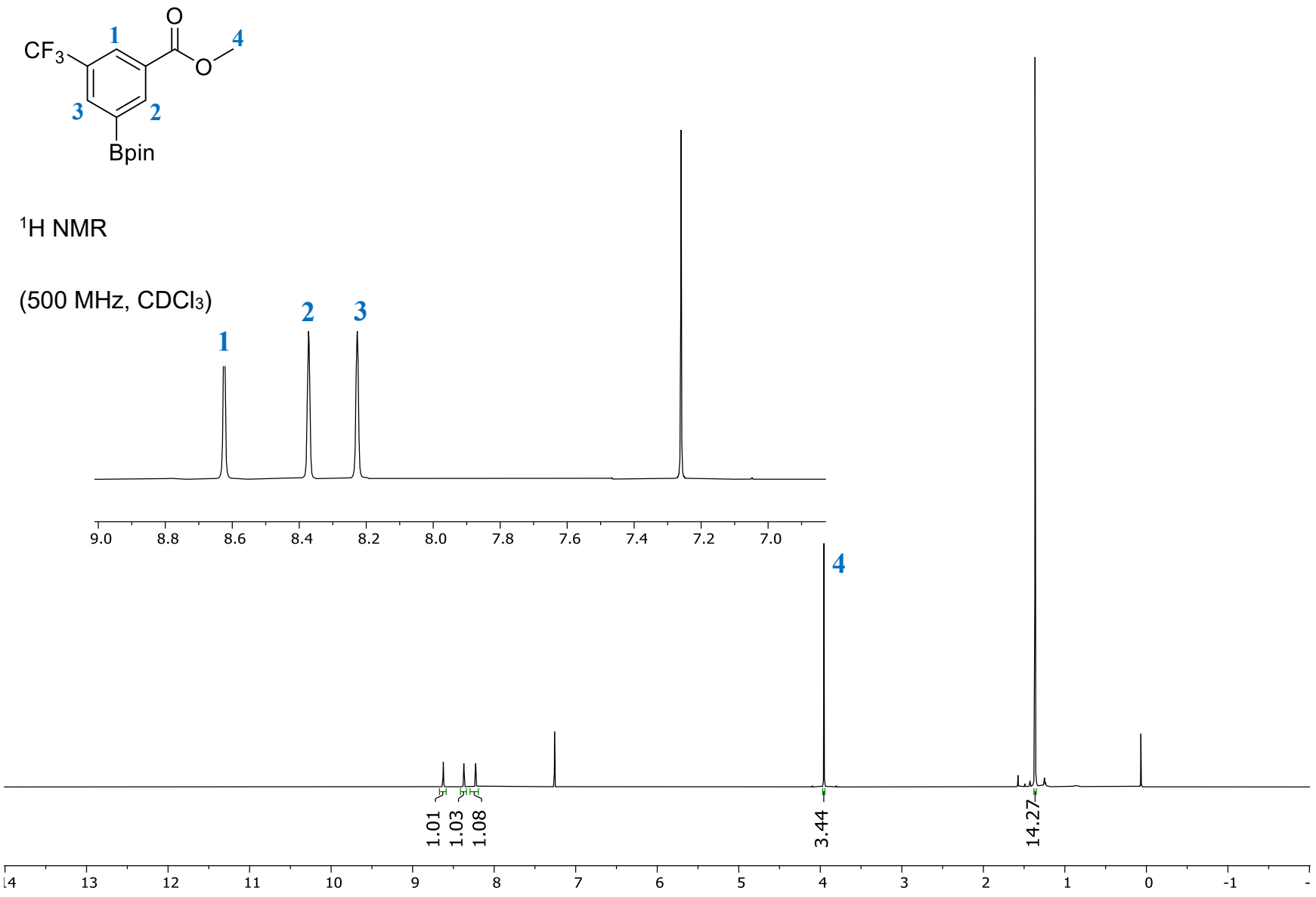
CF3
O
O
1
2
3
4
Bpin
1H NMR
(500 MHz, CDCl3)
1
2
3
4
9.0
8.8
8.6
8.4
8.2
8.0
7.8
7.6
7.4
7.2
7.0
1.01
1.03
1.08
3.44
14.27
13
12
11
10
9
8
7
6
5
4
3
2
1
0
-1

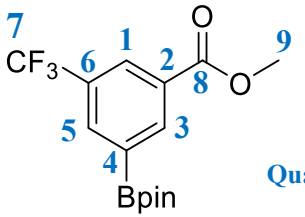

Quaternary carbons 2&4 could not confidently be assigned due to resonances belonging to long range $^{19}F/^{13}C$ coupling between 120-140 ppm.

^{13}C NMR

(126 MHz, $CDCl_3$)

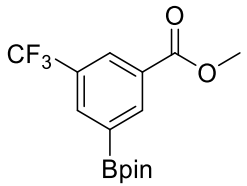

^{19}F NMR

(470 MHz, $CDCl_3$)

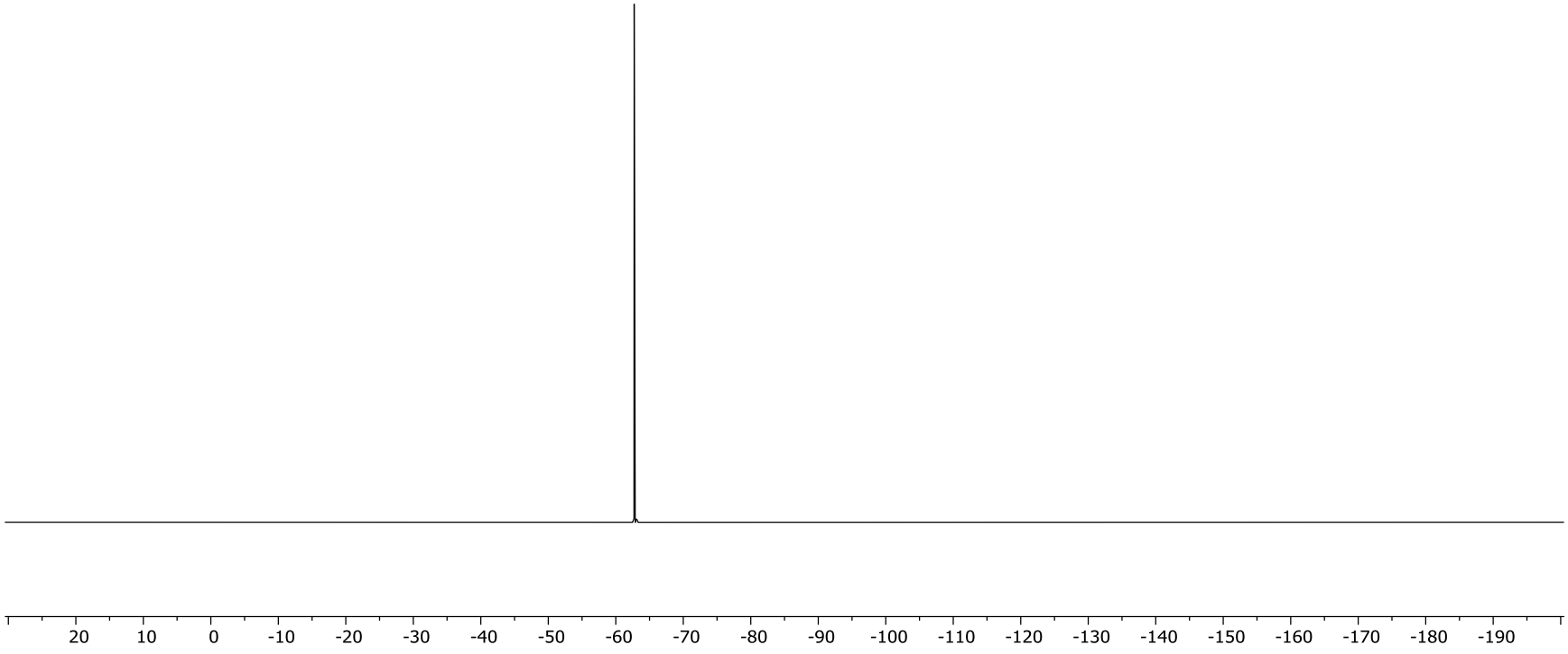

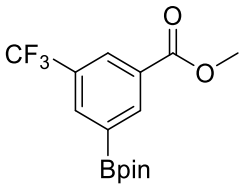

^{11}B NMR

(60 MHz, $CDCl_3$)

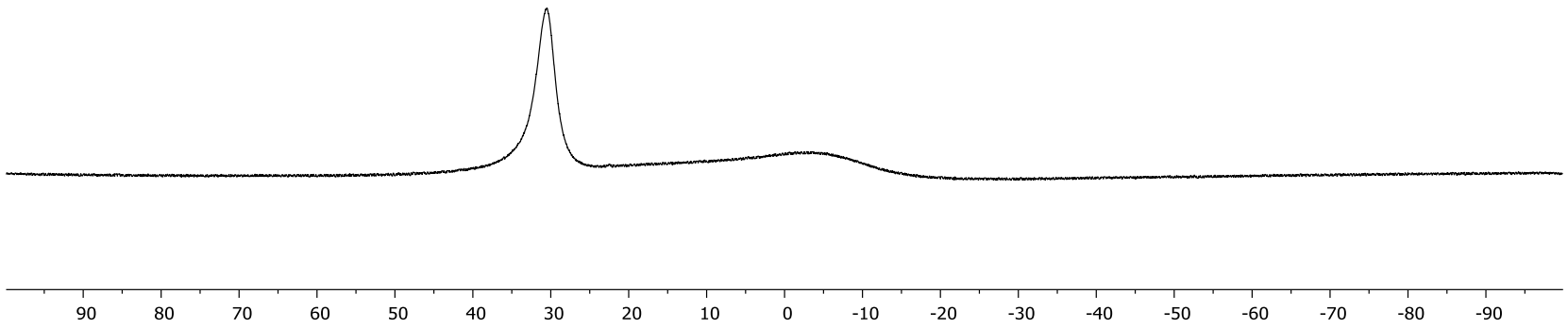

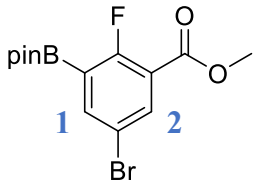

^{1}H NMR

(500 MHz, $CDCl_3$)

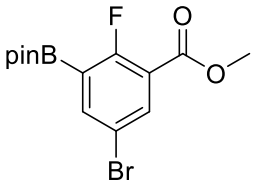

^{11}B NMR

(60 MHz, $CDCl_3$)

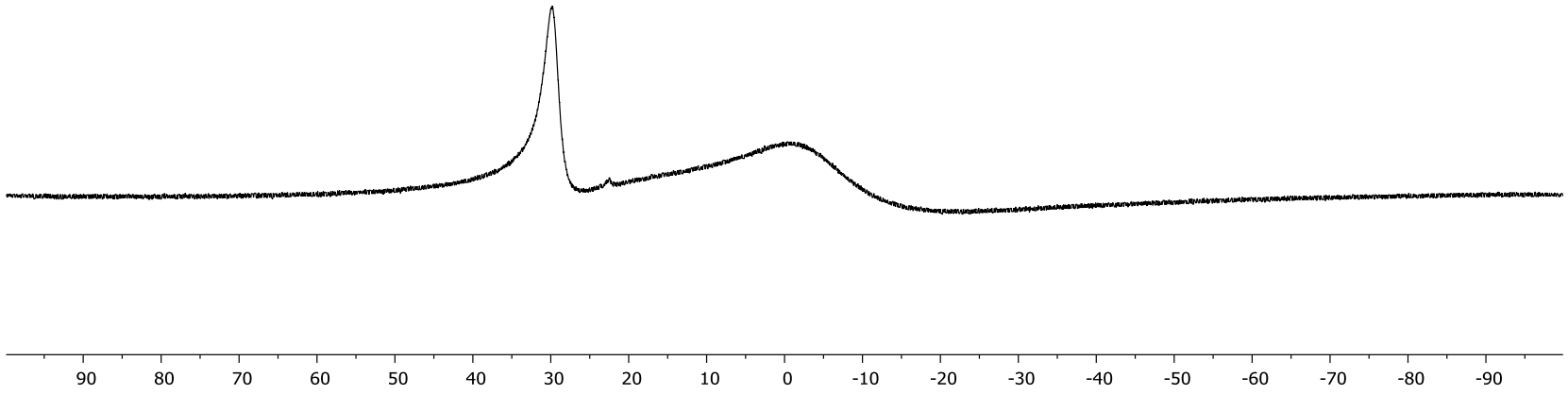

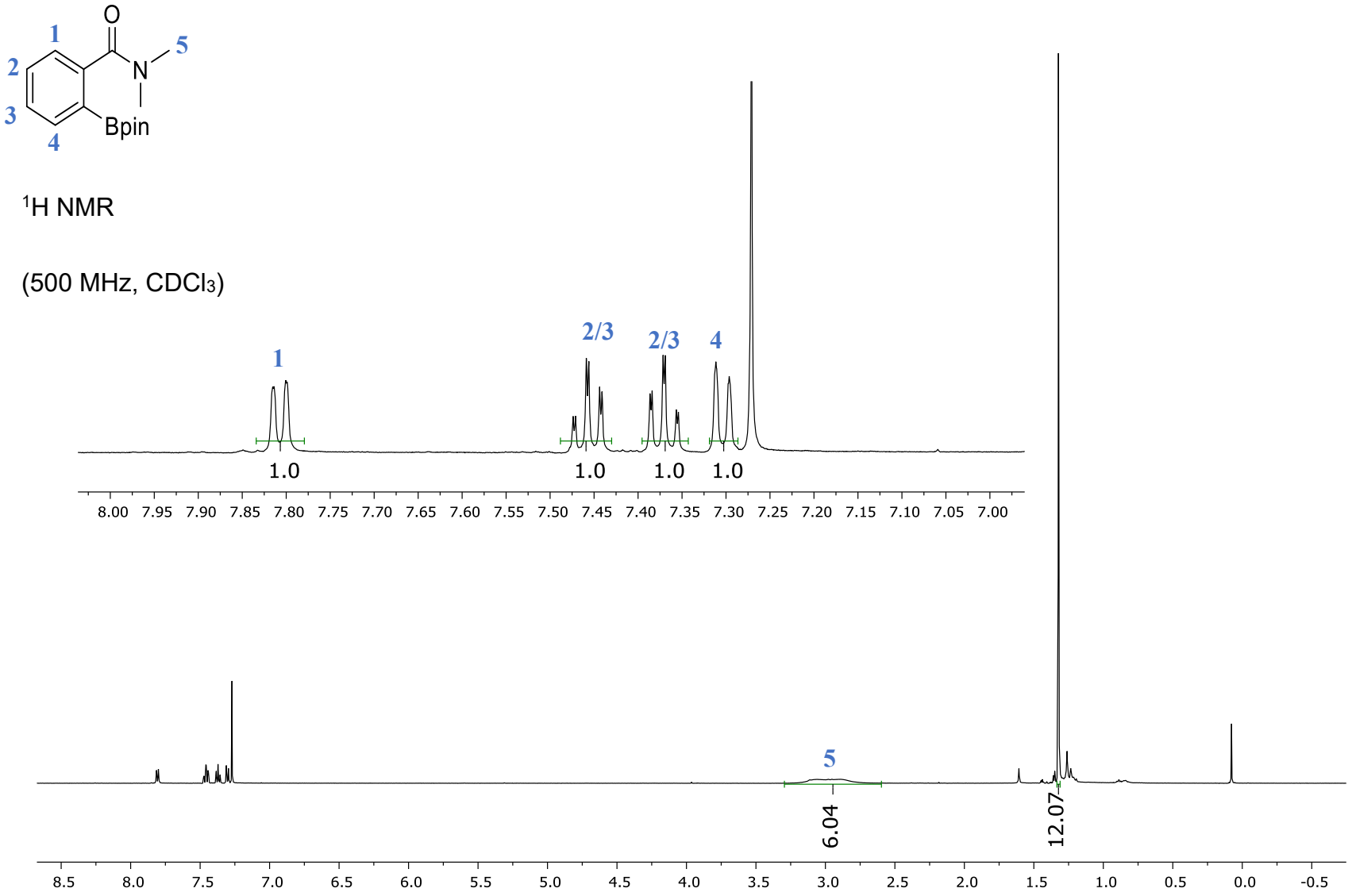
O
1
2
3
4
5
N
Bpin
1H NMR
(500 MHz, CDCl3)
1
2/3
2/3
4
1.0
1.0
1.0
1.0
8.00 7.95 7.90 7.85 7.80 7.75 7.70 7.65 7.60 7.55 7.50 7.45 7.40 7.35 7.30 7.25 7.20 7.15 7.10 7.05 7.00
5
6.04
12.07
8.5 8.0 7.5 7.0 6.5 6.0 5.5 5.0 4.5 4.0 3.5 3.0 2.5 2.0 1.5 1.0 0.5 0.0 -0.5

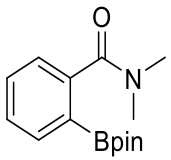

^{11}B NMR

(160 MHz, $CDCl_3$)

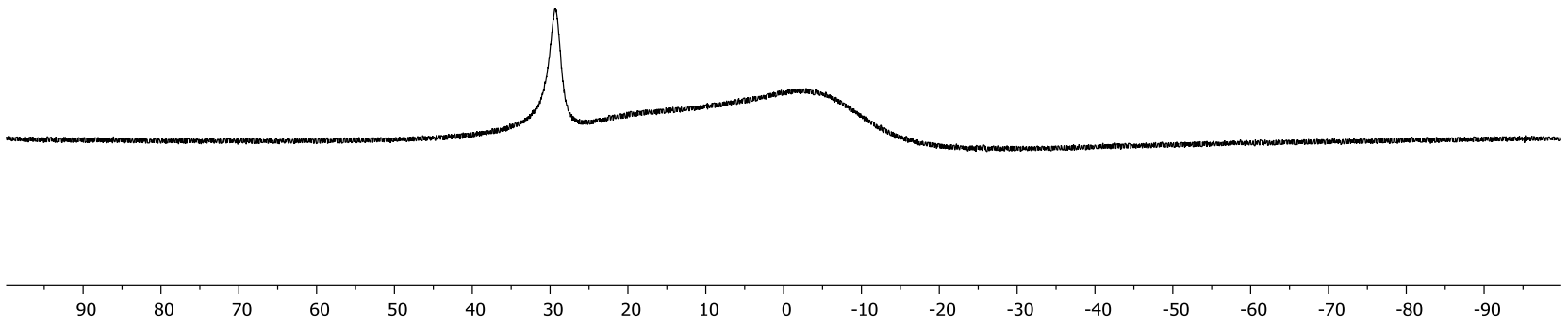

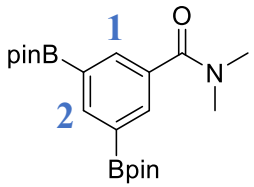

^{1}H NMR

(500 MHz, $CDCl_3$)

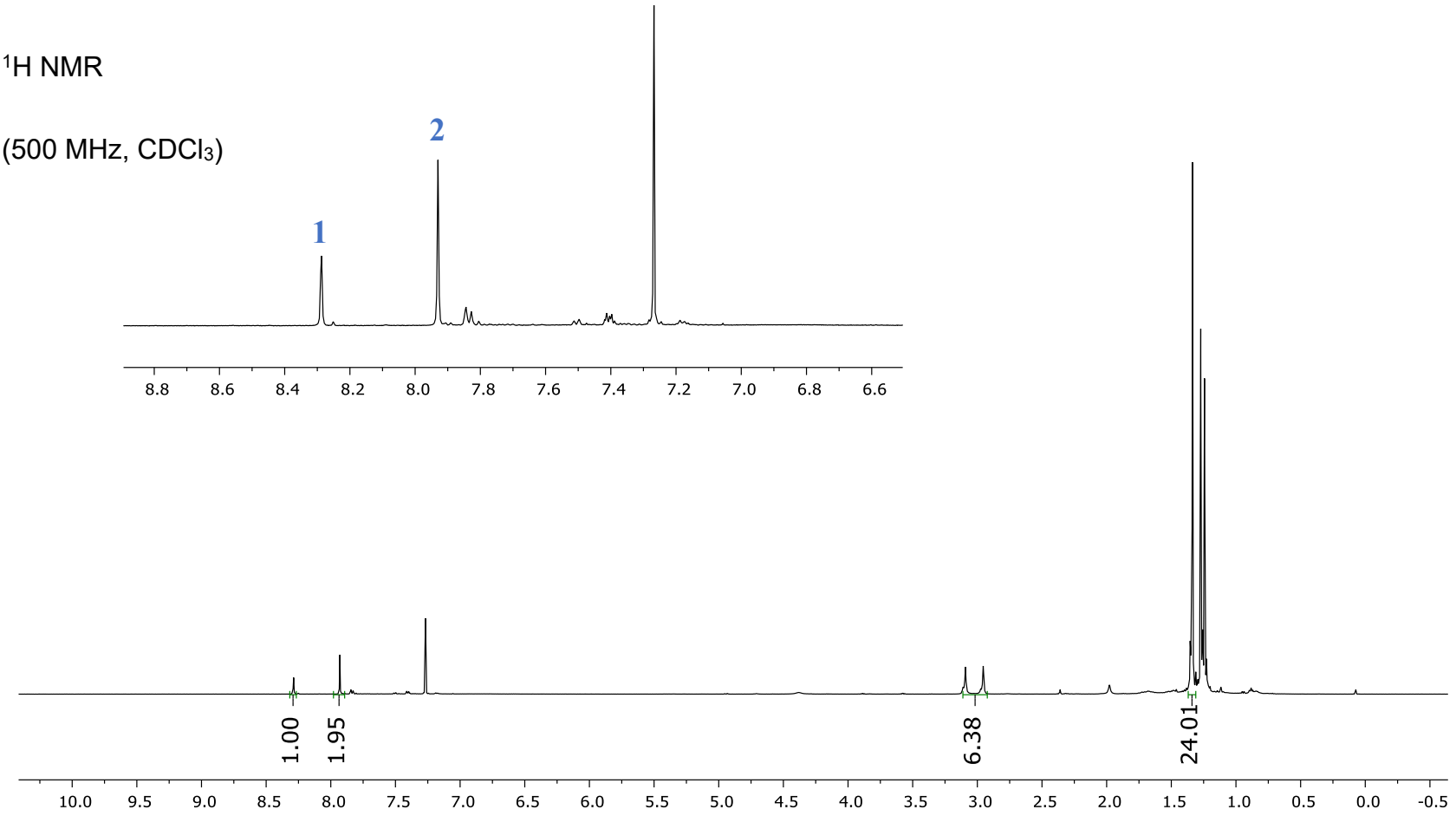

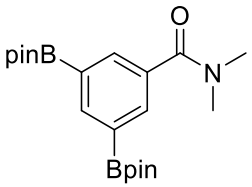

^{11}B NMR

(60 MHz, $CDCl_3$)

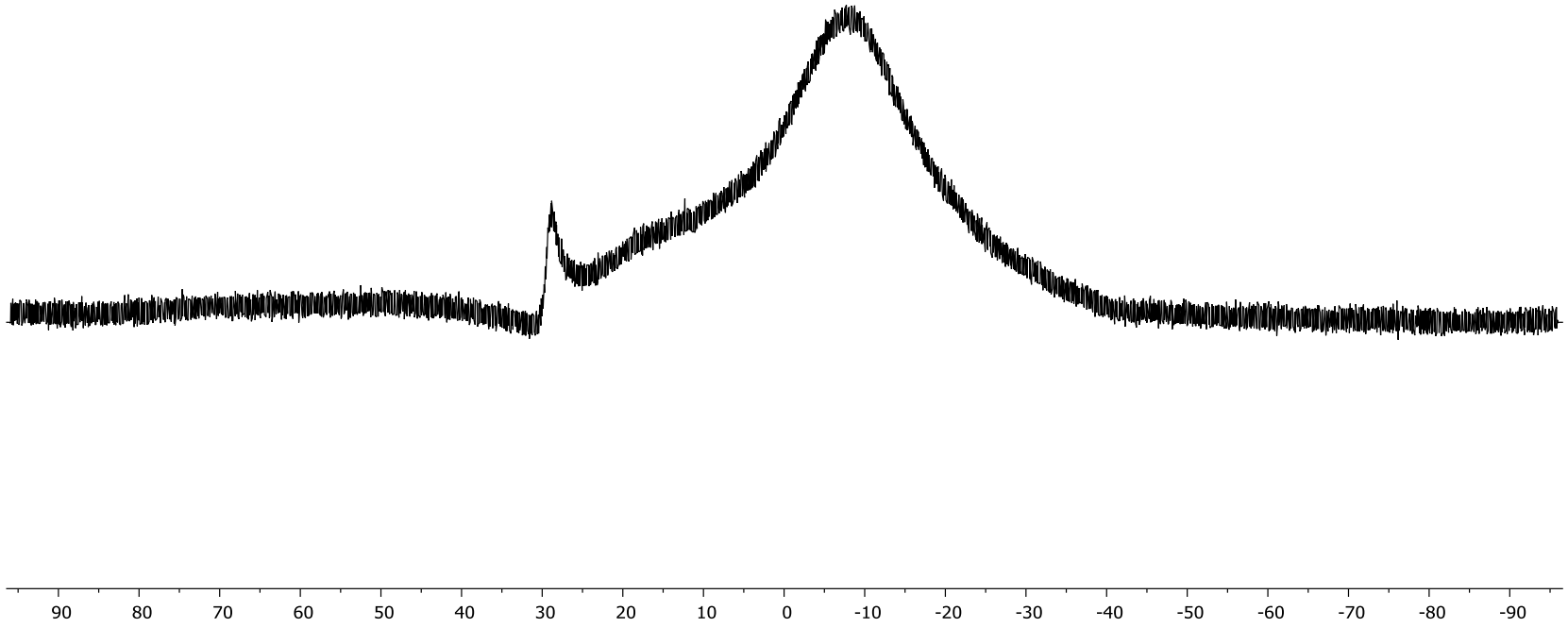

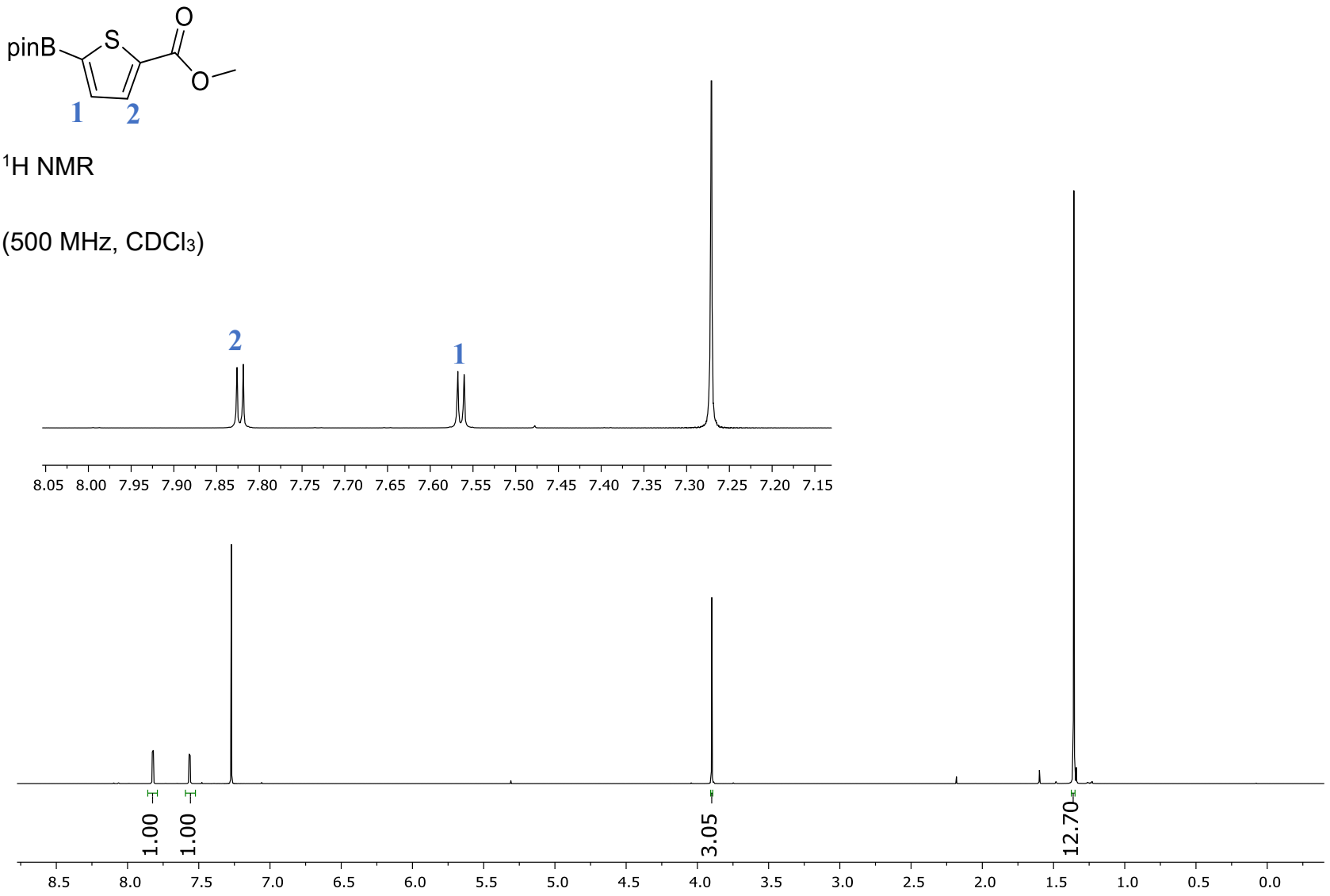
pinB
S
O
O
1
2
1H NMR
(500 MHz, CDCl3)
2
1
8.05 8.00 7.95 7.90 7.85 7.80 7.75 7.70 7.65 7.60 7.55 7.50 7.45 7.40 7.35 7.30 7.25 7.20 7.15
1.00
1.00
3.05
12.70
8.5 8.0 7.5 7.0 6.5 6.0 5.5 5.0 4.5 4.0 3.5 3.0 2.5 2.0 1.5 1.0 0.5 0.0

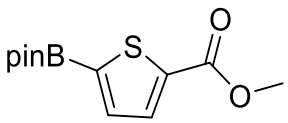

^{11}B NMR

(160 MHz, $CDCl_3$)

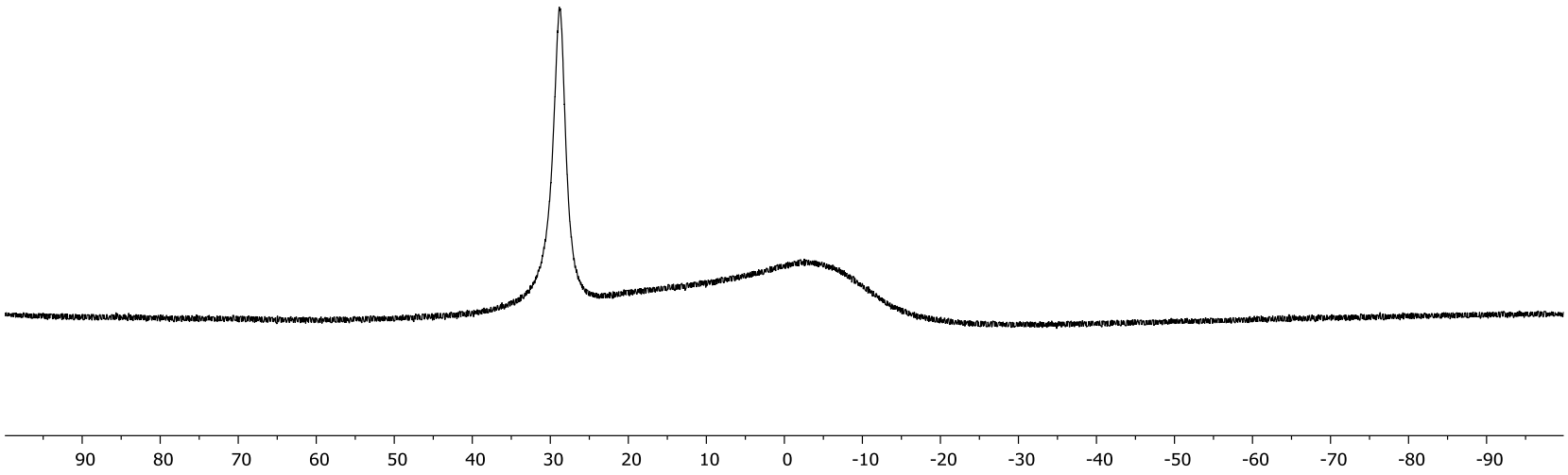

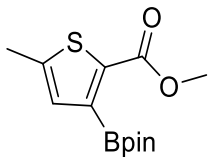

^{1}H NMR

(500 MHz, $CDCl_3$)

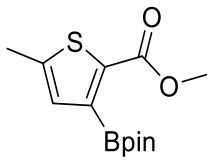

^{11}B NMR

(160 MHz, $CDCl_3$)

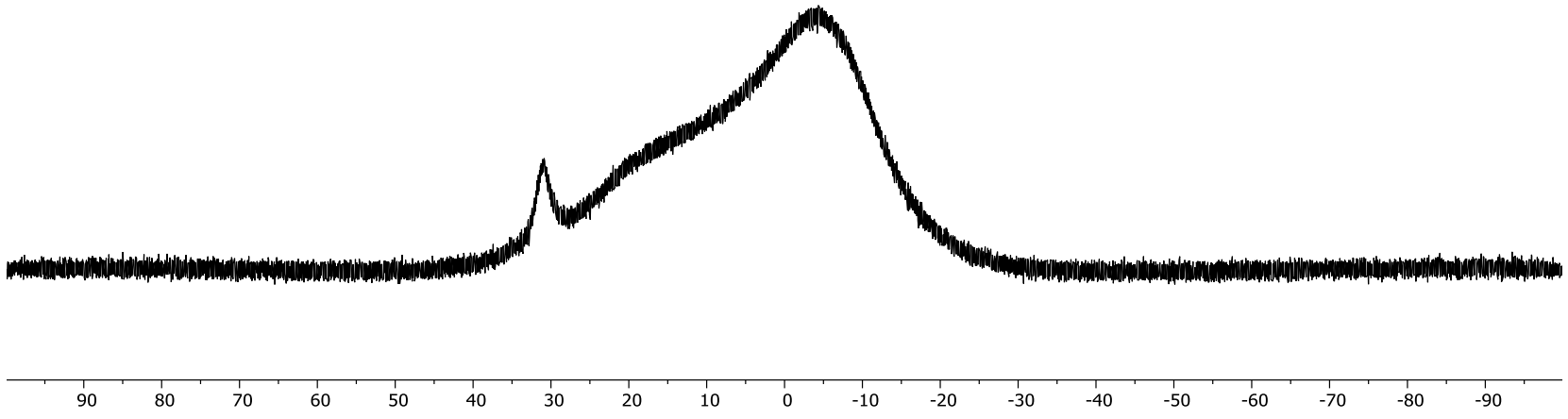

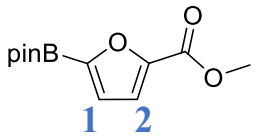

^{1}H NMR

(500 MHz, $CDCl_3$)

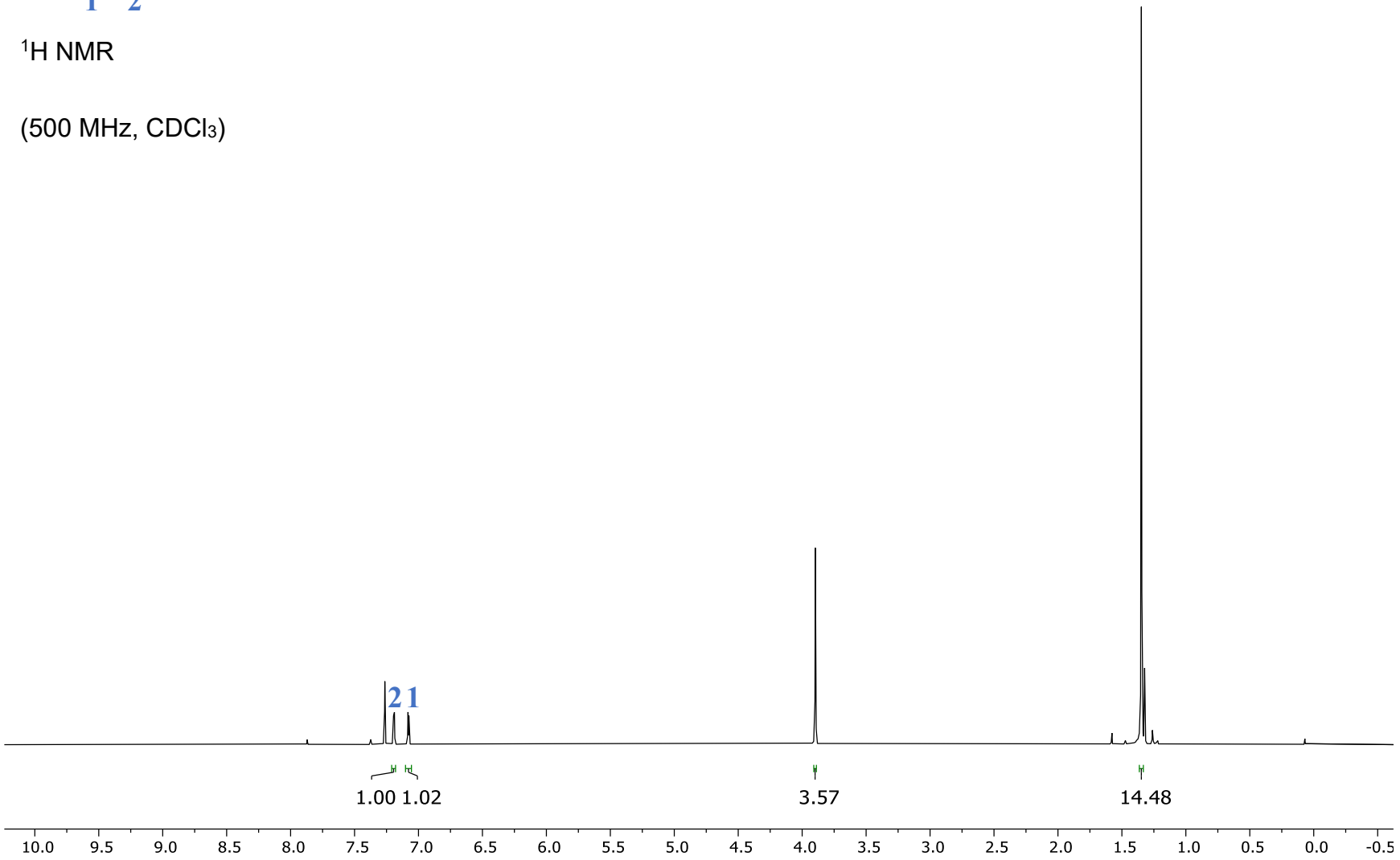

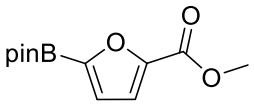

^{11}B NMR

(160 MHz, $CDCl_3$)

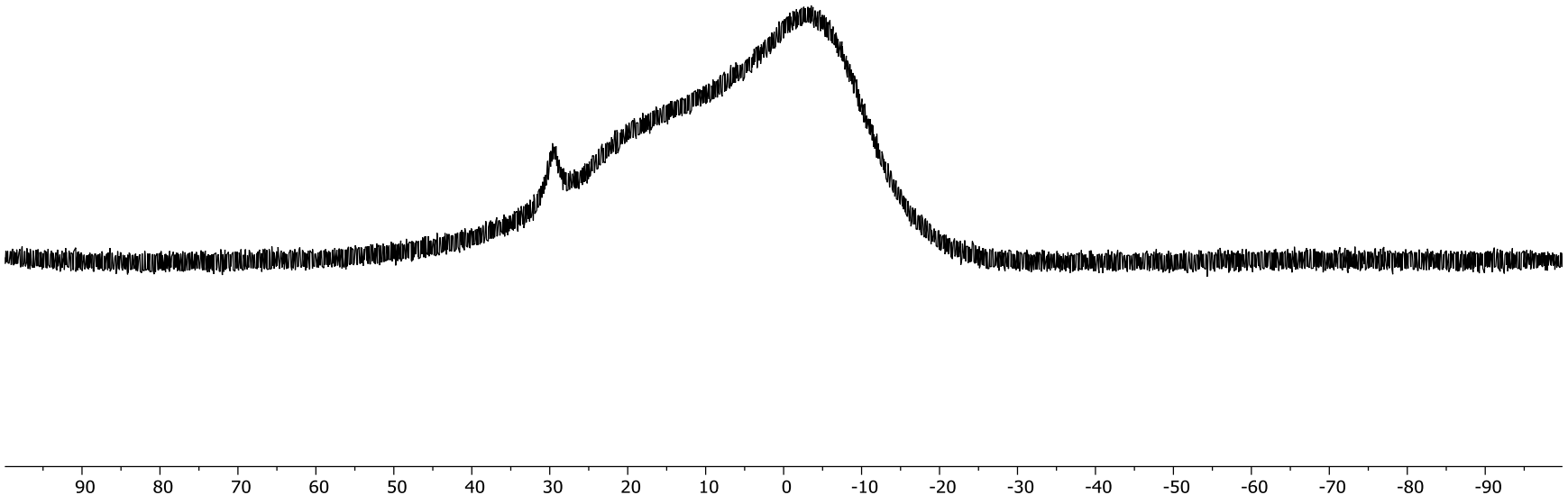

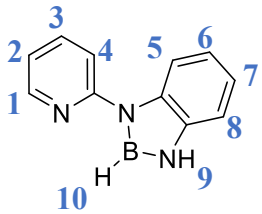

^{1}H NMR, **Entry 6**

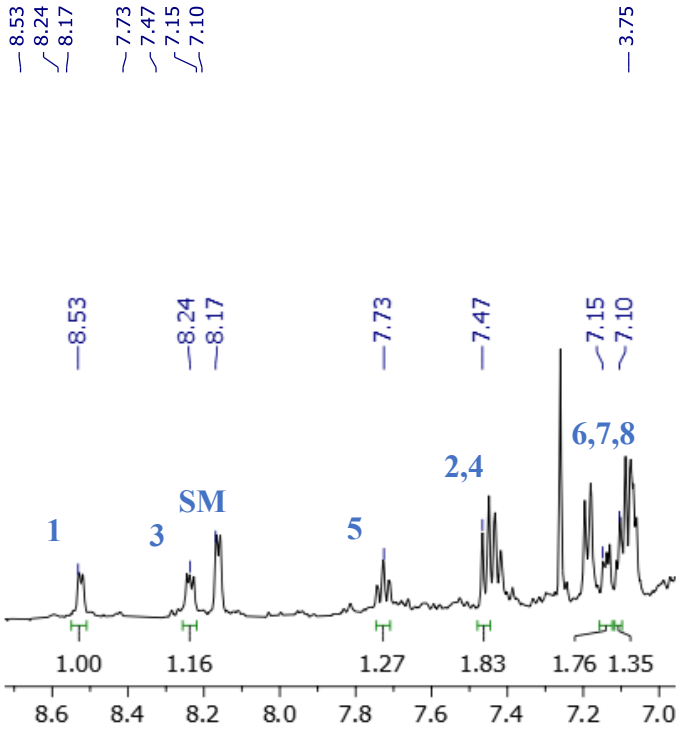

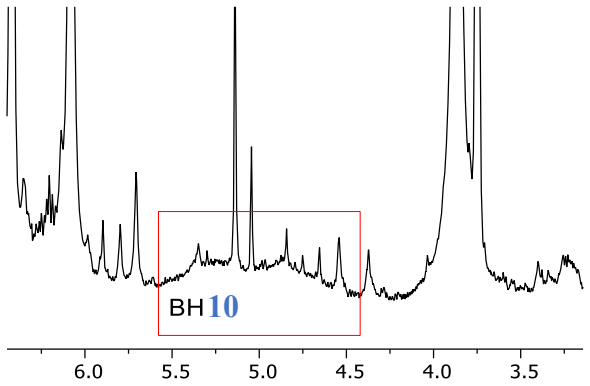

Resonances assigned were <u>not</u> confirmed and are predictions based on splitting and integration.

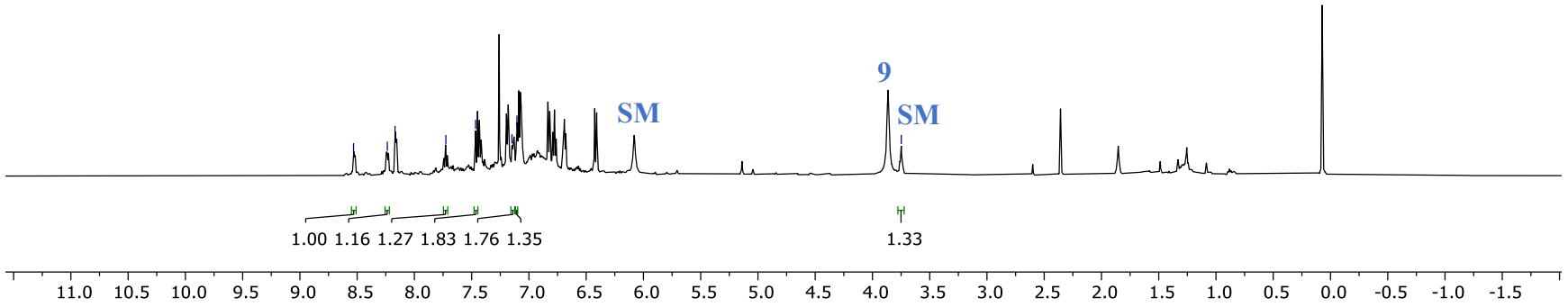

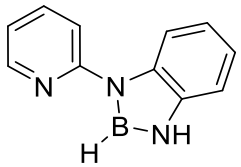

^{11}B NMR, **Entry 6**

(160 MHz, $CDCl_3$)

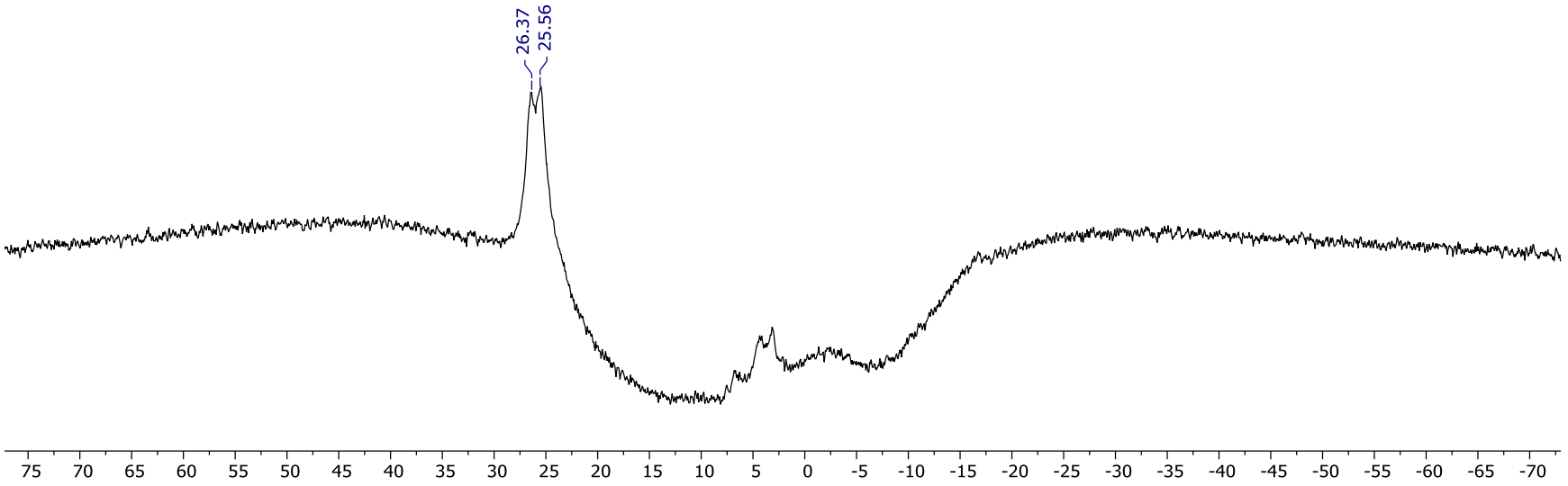

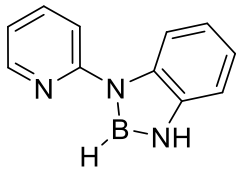

$^{11}B\{H\}$ NMR, **Entry 6**

(160 MHz, $CDCl_3$)

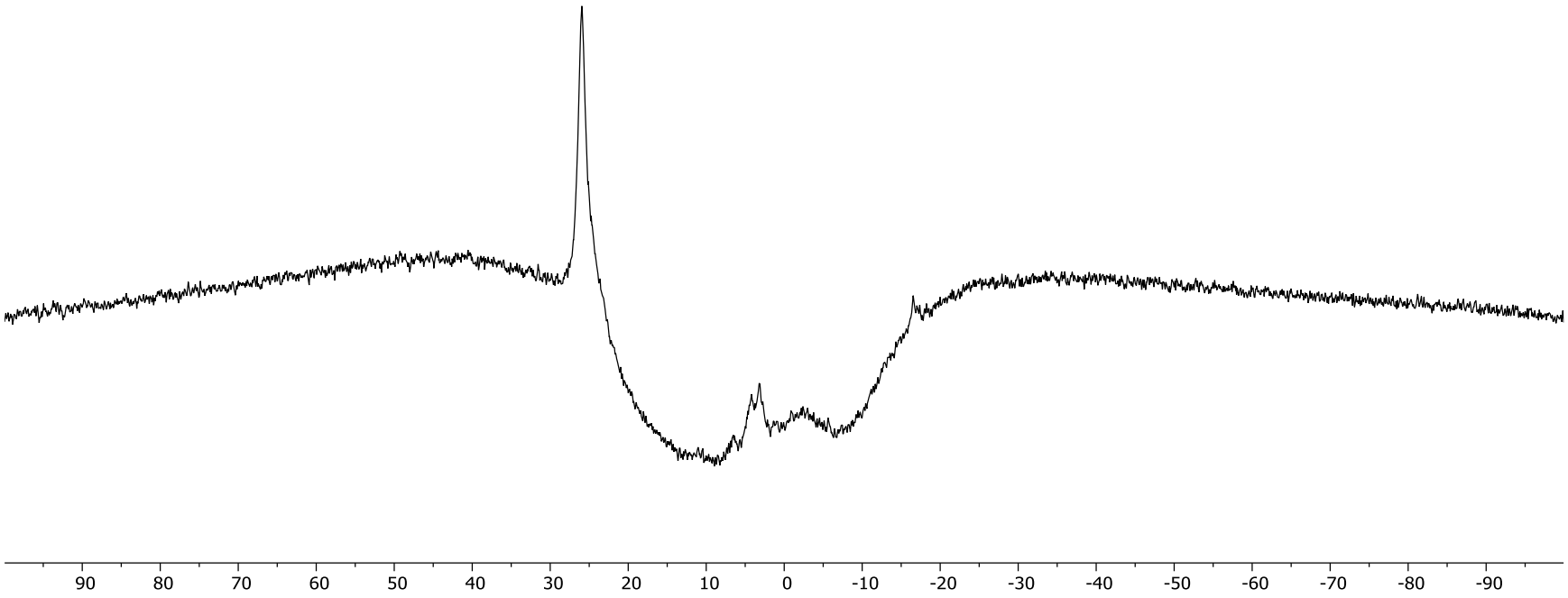

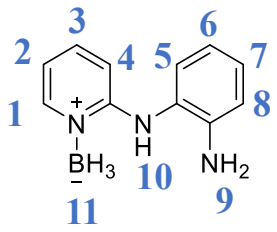

^{1}H NMR

(500 MHz, $CDCl_3$)

Resonances assigned were <u>not</u> confirmed and are predictions based on splitting and integration.

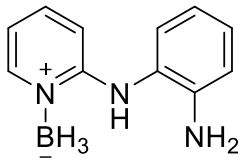

^{11}B NMR

(160 MHz, $CDCl_3$)

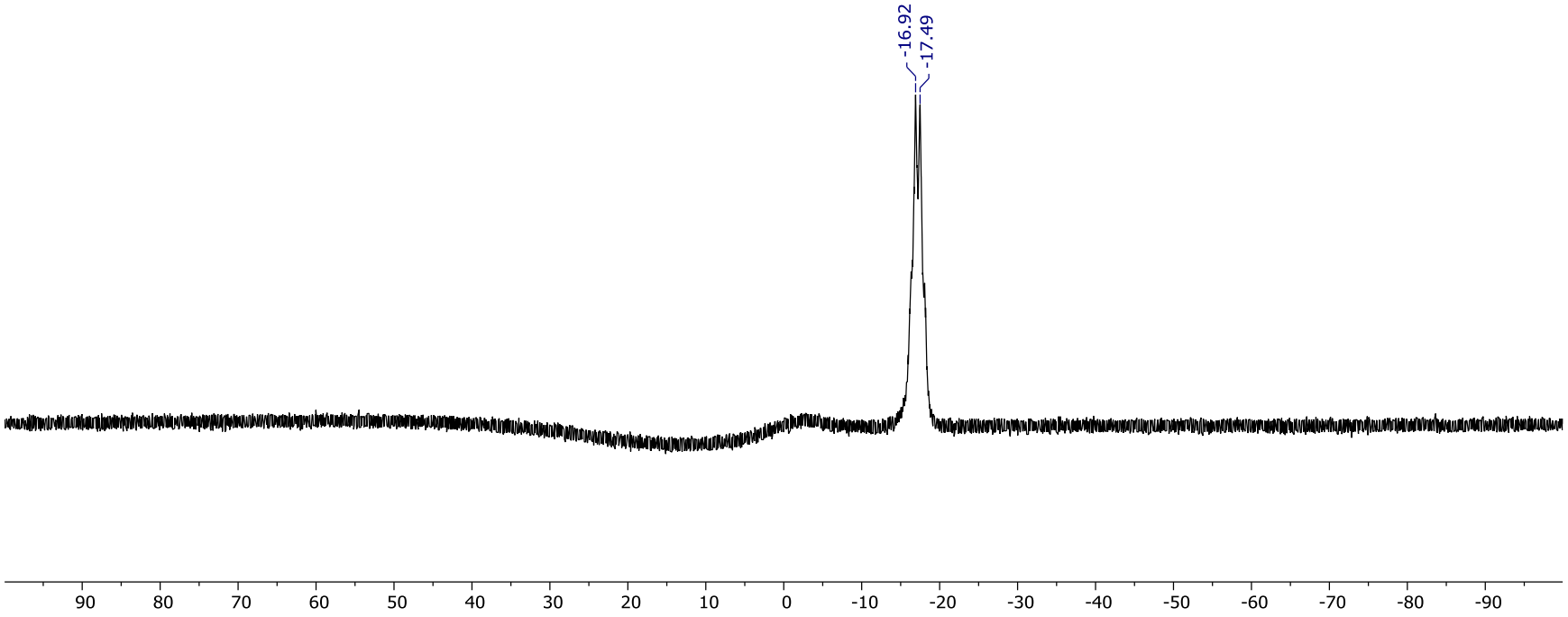

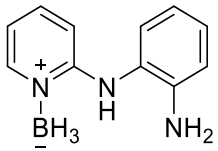

$^{11}B\{H\}$ NMR

(160 MHz, $CDCl_3$)

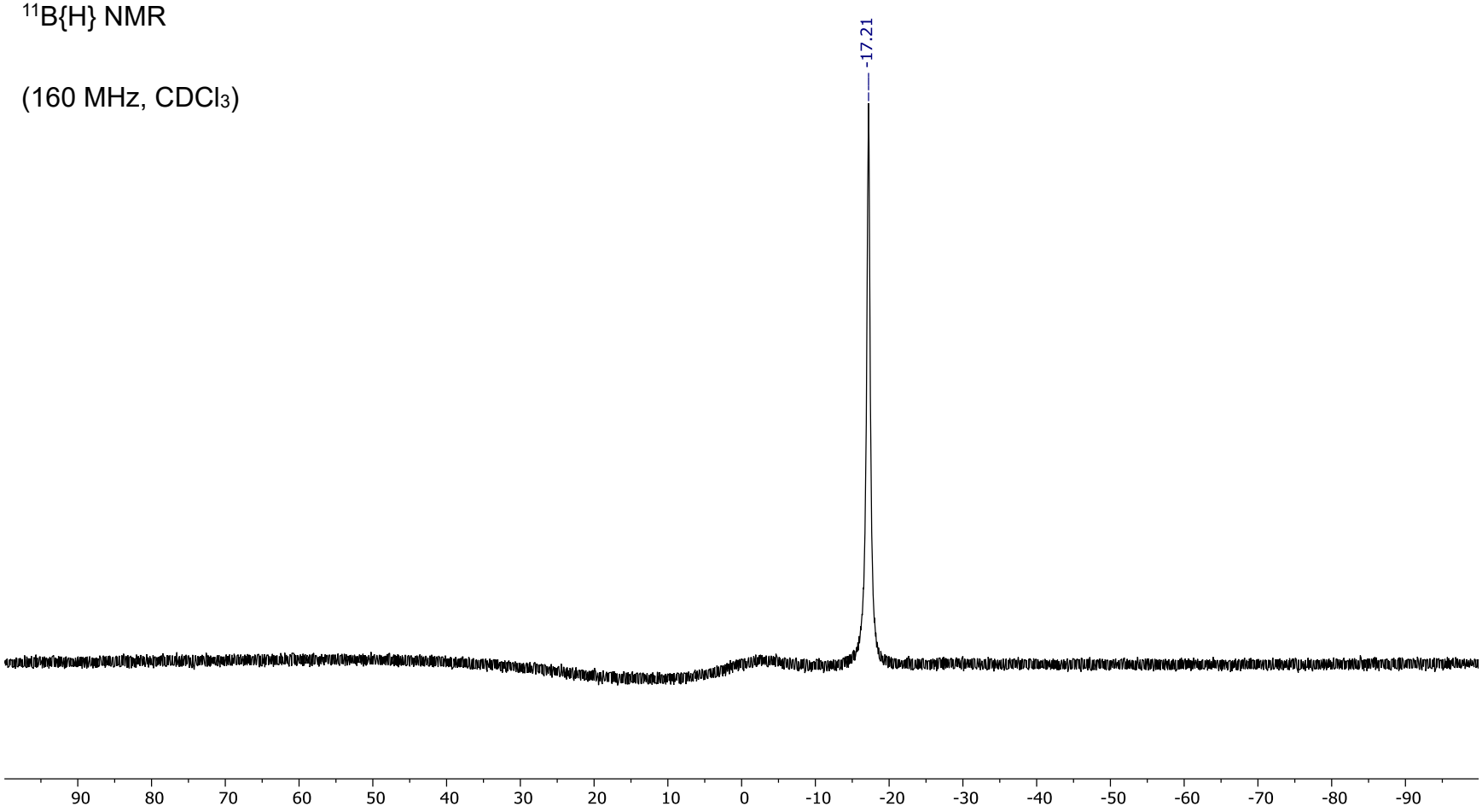

$BrBH_2 \cdot SMe_2$

^1H NMR

(500 MHz, C_6Cl_6)

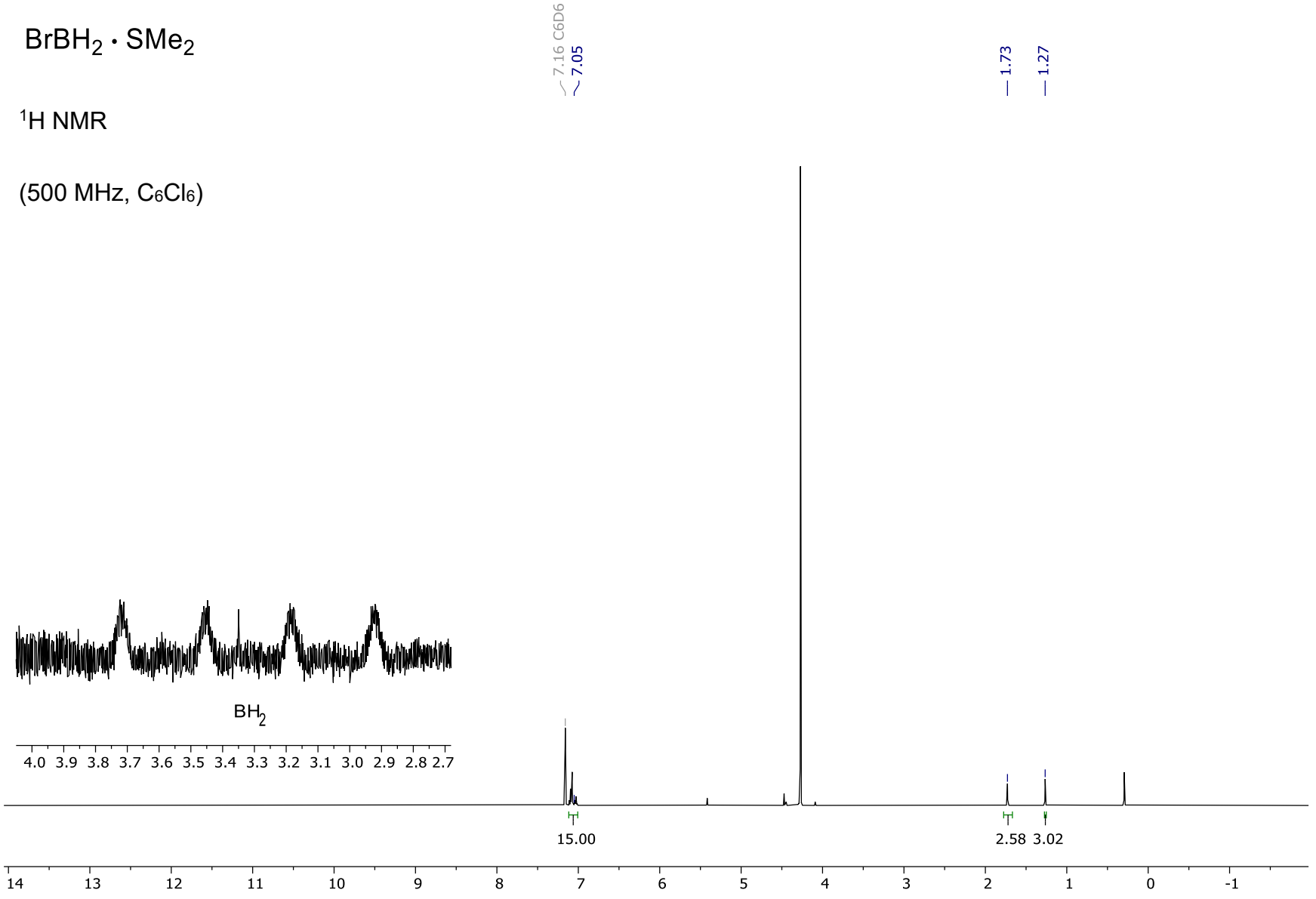

$BrBH_2 \cdot SMe_2$

^{11}B NMR

(160 MHz, C_6Cl_6)

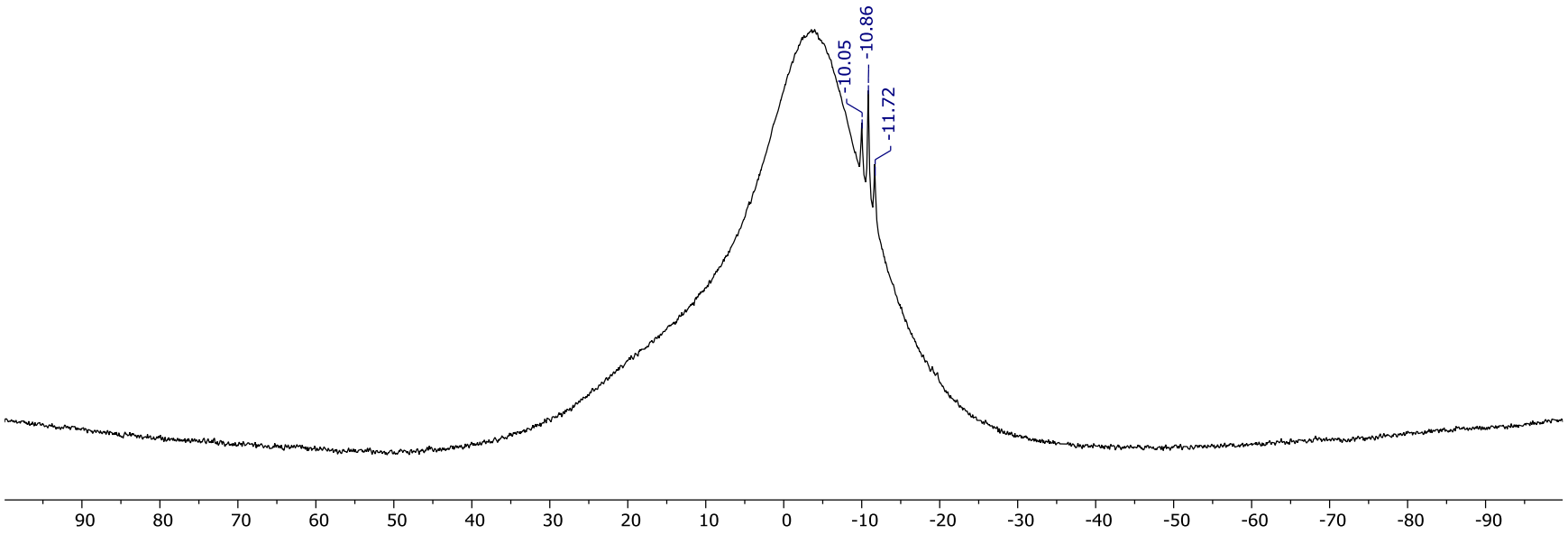

$BrBH_2 \cdot SMe_2$

$^{11}B\{H\}$ NMR

(160 MHz, C_6D_6)

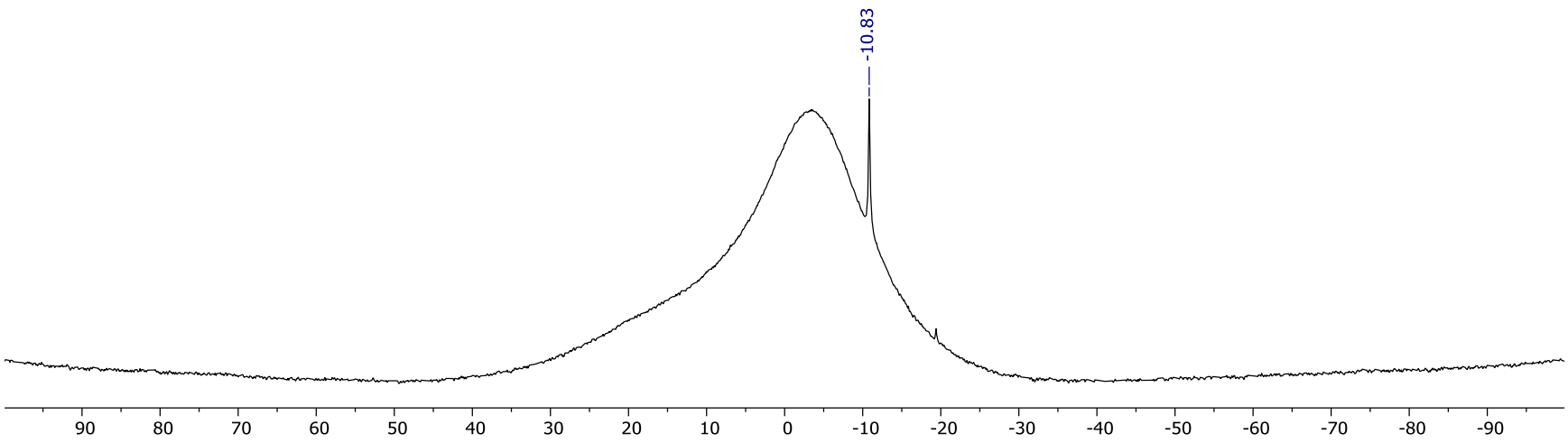

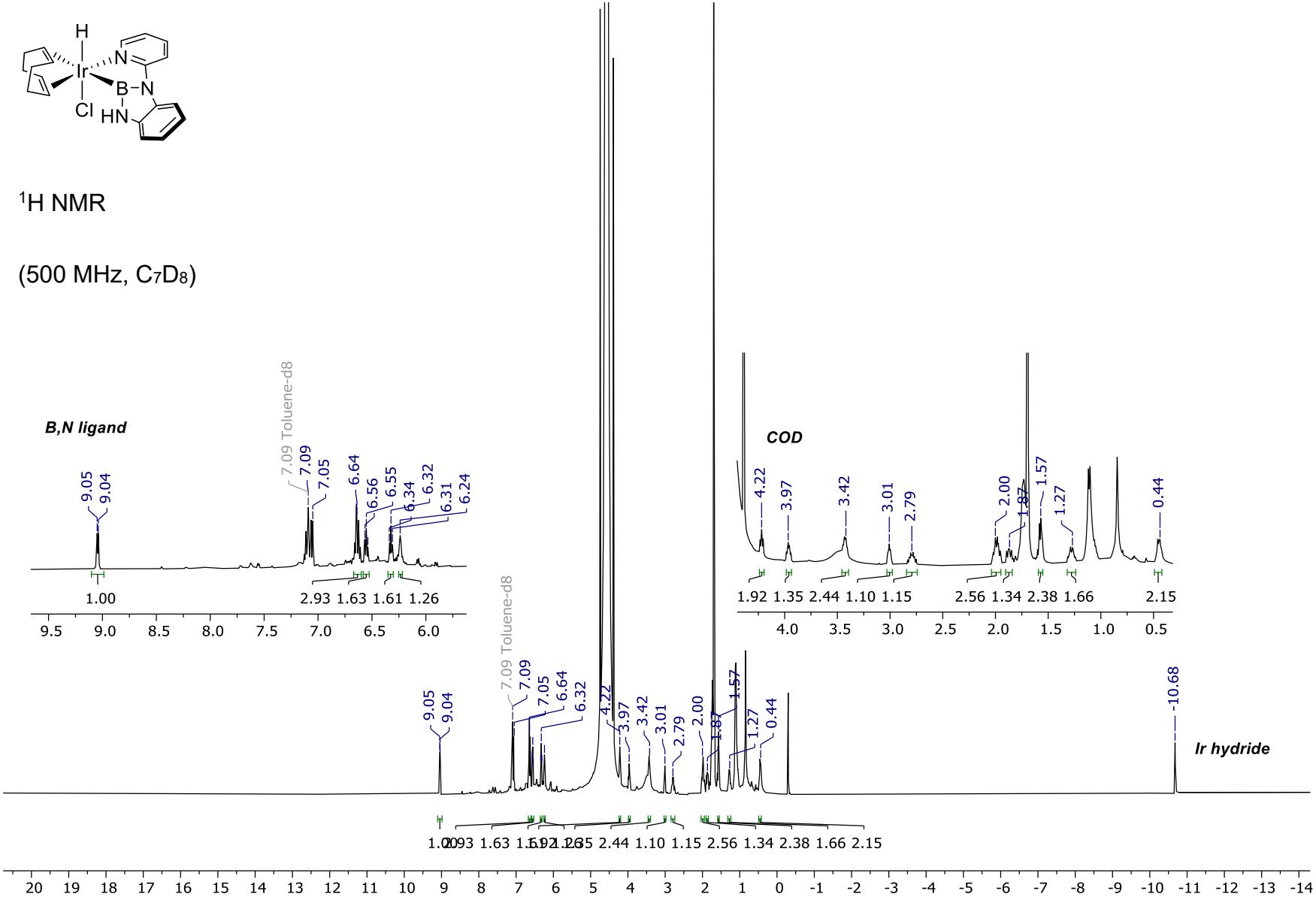
H
Ir
N
B–N
Cl
HN
1H NMR
(500 MHz, C7D8)
B,N ligand
COD
Ir hydride
7.09 Toluene-d8
9.05
9.04
7.09
7.05
6.64
6.56
6.55
6.34
6.32
6.31
6.24
4.22
3.97
3.42
3.01
2.79
2.00
1.87
1.57
1.27
0.44
-10.68
1.00
2.93 1.63 1.61 1.26
1.92 1.35 2.44 1.10 1.15
2.56 1.34 2.38 1.66 2.15

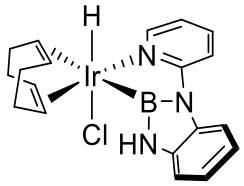

^{11}B NMR

(160 MHz, C_7D_8)

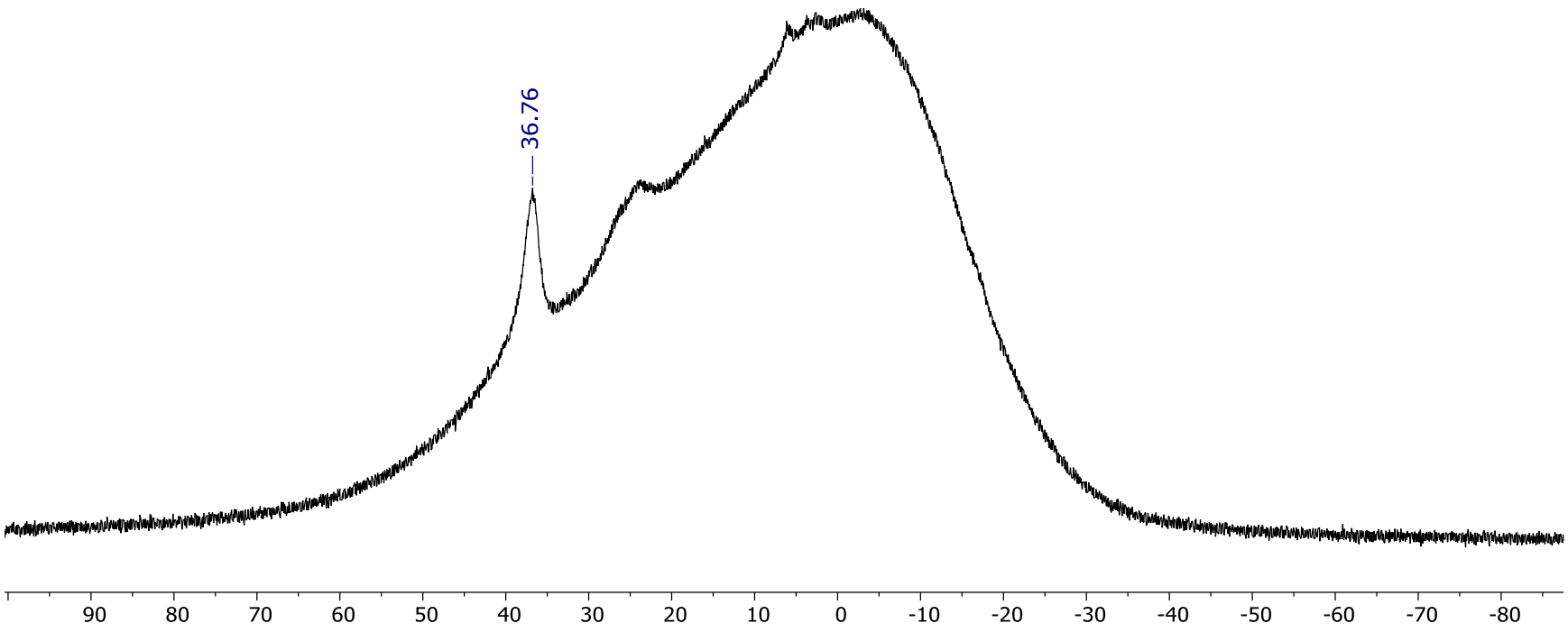

REFERENCES

(1) Hancock, R. D.; Martell, A. E. Chelate Ring Geometry, and the Metal Ion Selectivity of Macrocyclic Ligands. Some Recent Developments. *Supramol. Chem.* **1996**, *6* (3–4), 401–407.

(2) Segawa, Y.; Yamashita, M.; Nozaki, K. Syntheses of PBP Pincer Iridium Complexes: A Supporting Boryl Ligand. *J. Am. Chem. Soc.* **2009**, *131* (26), 9201–9203.

(3) Yamashita, M.; Suzuki, Y.; Segawa, Y.; Nozaki, K. Synthesis, Structure of Borylmagnesium, and Its Reaction with Benzaldehyde to Form Benzoylborane. *J. Am. Chem. Soc.* **2007**, *129* (31), 9570–9571.

(4) Segawa, Y.; Yamashita, M.; Nozaki, K. Boryl Anion Attacks Transition-Metal Chlorides to Form Boryl Complexes: Syntheses, Spectroscopic, and Structural Studies on Group 11 Borylmetal Complexes. *Angew. Chem. Int. Ed Engl.* **2007**, *46* (35), 6710–6713.

(5) Mkhalid, I. A. I.; Barnard, J. H.; Marder, T. B.; Murphy, J. M.; Hartwig, J. F. C-H Activation for the Construction of C-B Bonds. *Chem. Rev.* **2010**, *110* (2), 890–931.

(6) Wang, G.; Xu, L.; Li, P. Double N,B-Type Bidentate Boryl Ligands Enabling a Highly Active Iridium Catalyst for C-H Borylation. *J. Am. Chem. Soc.* **2015**, *137* (25), 8058–8061.

(7) O'Connell, A. C.; Mansour, P. A.; Maleczka, R. E., Jr; Smith, M. R., III. Regiochemical Switching in Ir-Catalyzed C-H Borylation by Altering Ligand Loadings of N,B-Type Diboron Species. *Org. Lett.* **2023**, *25* (45), 8057–8061.

(8) Ishiyama, T.; Takagi, J.; Ishida, K.; Miyaura, N.; Anastasi, N. R.; Hartwig, J. F. Mild Iridium-Catalyzed Borylation of Arenes. High Turnover Numbers, Room Temperature Reactions, and Isolation of a Potential Intermediate. *J. Am. Chem. Soc.* **2002**, *124* (3), 390–391.

(9) Preshlock, S. M.; Ghaffari, B.; Maligres, P. E.; Krska, S. W.; Maleczka, R. E., Jr; Smith, M. R., III. High-Throughput Optimization of Ir-Catalyzed C-H Borylation: A Tutorial for Practical Applications. *J. Am. Chem. Soc.* **2013**, *135* (20), 7572–7582.

(10) Cho, J. Y. Investigation of Stoichiometric and Catalytic B-C Bond Formation by Group 9 Transition Metal Boryl Complexes. Ph.D. Dissertation, Michigan State University, East Lansing, MI, USA, 2002.

(11) Wright, J. S.; Scott, P. J. H.; Steel, P. G. Iridium Catalysed C-H Borylation of Heteroarenes: Balancing Steric and Electronic Regiocontrol. *Angew. Chem. Int. Ed Engl.* **2020**.

(12) Wang, G.; Liu, L.; Wang, H.; Ding, Y.-S.; Zhou, J.; Mao, S.; Li, P. N,B-Bidentate Boryl Ligand-Supported Iridium Catalyst for Efficient Functional-Group-Directed C-H Borylation. *J. Am. Chem. Soc.* **2017**, *139* (1), 91–94.

(13) Zou, X.; Zhao, H.; Li, Y.; Gao, Q.; Ke, Z.; Xu, S. Chiral Bidentate Boryl Ligand Enabled Iridium-Catalyzed Asymmetric C (Sp2)-H Borylation of Diarylmethylamines. *J. Am. Chem. Soc.* **2019**, *141* (13), 5334–5342.

(14) Shi, Y.; Gao, Q.; Xu, S. Chiral Bidentate Boryl Ligand Enabled Iridium-Catalyzed Enantioselective C(Sp3)-H Borylation of Cyclopropanes. *J. Am. Chem. Soc.* **2019**. https://doi.org/10.1021/jacs.9b04549.

(15) Shi, Y.; Gao, Q.; Xu, S. Iridium-Catalyzed Asymmetric C–H Borylation Enabled by Chiral Bidentate Boryl Ligands. *Synlett* **2019**.

(16) Song, P.; Hu, L.; Yu, T.; Jiao, J.; He, Y.; Xu, L.; Li, P. Development of a Tunable Chiral Pyridine Ligand Unit for Enantioselective Iridium-Catalyzed C–H Borylation. *ACS Catal.* **2021**, *11* (12), 7339–7349.

(17) Gao, Q.; Xu, S. Site- and Stereoselective C(Sp3)-H Borylation of Strained (Hetero)Cycloalkanols Enabled by Iridium Catalysis. *Angew. Chem. Int. Ed Engl.* **2023**, *62* (8), e202218025.

(18) Hadebe, S. W.; Sithebe, S.; Robinson, R. S. Microwave-Assisted Suzuki–Miyaura Cross-Coupling of 2-Alkyl and 2-Alkenyl-Benzo-1,3,2-Diazaborolanes. *Tetrahedron* **2011**, *67* (23), 4277–4282.

(19) Oliveri, I. P.; Maccarrone, G.; Di Bella, S. A Lewis Basicity Scale in Dichloromethane for Amines and Common Nonprotogenic Solvents Using a Zinc(II) Schiff-Base Complex as Reference Lewis Acid. *J. Org. Chem.* **2011**, *76* (21), 8879–8884.

(20) Mayer, R. J.; Hampel, N.; Ofial, A. R. Lewis Acidic Boranes, Lewis Bases, and Equilibrium Constants: A Reliable Scaffold for a Quantitative Lewis Acidity/Basicity Scale. *Chemistry* **2021**, *27* (12), 4070–4080.

(21) Nöth, H.; Wrackmeyer, B. *Nuclear Magnetic Resonance Spectroscopy of Boron Compounds*; Springer Science & Business Media, 2012.

(22) Chattopadhyay, B.; Dannatt, J. E.; Andujar-De Sanctis, I. L.; Gore, K. A.; Maleczka, R. E., Jr; Singleton, D. A.; Smith, M. R., III. Ir-Catalyzed *Ortho*-Borylation of Phenols Directed by Substrate-Ligand Electrostatic Interactions: A Combined Experimental/in Silico Strategy for Optimizing Weak Interactions. *J. Am. Chem. Soc.* **2017**, *139* (23), 7864–7871.

(23) Negishi, E. 45.7 - Aliphatic Organoboron Compounds. In *Comprehensive Organometallic Chemistry*; Wilkinson, G., Stone, F. G. A., Abel, E. W., Eds.; Pergamon: Oxford, 1982; pp 265–301.

(24) Muhoro, C. N.; He, X.; Hartwig, J. F. Titanocene Borane σ-Complexes. *J. Am. Chem. Soc.* **1999**, *121* (21), 5033–5046.

(25) Ghaffari, B.; Vanchura, B. A., 2nd; Chotana, G. A.; Staples, R. J.; Holmes, D.; Maleczka, R. E., Jr; Smith, M. R., III. Reversible Borylene Formation from Ring Opening of Pinacolborane

and Other Intermediates Generated from Five-Coordinate Tris-Boryl Complexes: Implications for Catalytic C-H Borylation. *Organometallics* **2015**, *34* (19), 4732–4740.

(26) Weng, W.; Guo, C.; Moura, C.; Yang, L.; Foxman, B. M.; Ozerov, O. V. Competitive Activation of N−C and C−H Bonds of the PNP Framework by Monovalent Rhodium and Iridium. *Organometallics* **2005**, *24* (14), 3487–3499.

(27) Iverson, C. N.; Smith, M. R. Stoichiometric and Catalytic B−C Bond Formation from Unactivated Hydrocarbons and Boranes. *J. Am. Chem. Soc.* **1999**, *121* (33), 7696–7697.

(28) Uson, R.; Oro, L. A.; Cabeza, J. A.; Bryndza, H. E.; Stepro, M. P. Dinuclear Methoxy, Cyclooctadiene, and Barrelene Complexes of Rhodium(I) and Iridium(I): Kirschner/Inorganic. In Inorganic Syntheses. *Kirschner, S., Ed.; Inorganic Syntheses; John Wiley & Sons, Inc.: Hoboken, NJ, USA* **1985**, *231*, 126–130.

(29) Wolan, A.; Zaidlewicz, M. Synthesis of Arylboronates by the Palladium Catalysed Cross-Coupling Reaction in Ionic Liquids. *Org. Biomol. Chem.* **2003**, *1* (19), 3274–3276.

(30) Tajuddin, H.; Harrisson, P.; Bitterlich, B.; Collings, J. C.; Sim, N.; Batsanov, A. S.; Cheung, M. S.; Kawamorita, S.; Maxwell, A. C.; Shukla, L.; Morris, J.; Lin, Z.; Marder, T. B.; Steel, P. G. Iridium-Catalyzed C–H Borylation of Quinolines and Unsymmetrical 1,2-Disubstituted Benzenes: Insights into Steric and Electronic Effects on Selectivity. *Chem. Sci.* **2012**, *3* (12), 3505–3515.

(31) Kawamorita, S.; Ohmiya, H.; Hara, K.; Fukuoka, A.; Sawamura, M. Directed *Ortho* Borylation of Functionalized Arenes Catalyzed by a Silica-Supported Compact Phosphine-Iridium System. *J. Am. Chem. Soc.* **2009**, *131* (14), 5058–5059.

(32) Kuninobu, Y.; Ida, H.; Nishi, M.; Kanai, M. A Meta-Selective C-H Borylation Directed by a Secondary Interaction between Ligand and Substrate. *Nat. Chem.* **2015**, *7* (9), 712–717.

(33) Jayasundara, C. R. K.; Unold, J. M.; Oppenheimer, J.; 3rd, S.; Smith, M. R., III. A Catalytic Borylation/Dehalogenation Route to o-Fluoro Arylboronates. *Org. Lett.* **2014**, *16* (23), 6072–6075.

(34) Hosoya, T.; Yoshida, S.; Nishiyama, Y.; Misawa, Y.; Hazama, Y.; Oya, K. Synthesis of Diverse 3-Azido-5-(Azidomethyl)Benzene Derivatives via Formal C–H Azidation and Functional Group-Selective Transformations. *Heterocycles* **2019**, *99* (0), 1053.

(35) Ishiyama, T.; Isou, H.; Kikuchi, T.; Miyaura, N. *Ortho*-C-H Borylation of Benzoate Esters with Bis(Pinacolato)Diboron Catalyzed by Iridium-Phosphine Complexes. *Chem. Commun.* **2010**, *46* (1), 159–161.

(36) Li, H.; Tang, X.; Pang, J. H.; Wu, X.; Yeow, E. K. L.; Wu, J.; Chiba, S. Polysulfide Anions as Visible Light Photoredox Catalysts for Aryl Cross-Couplings. *J. Am. Chem. Soc.* **2021**, *143* (1), 481–487.

(37) Kawamorita, S.; Ohmiya, H.; Sawamura, M. Ester-Directed Regioselective Borylation of Heteroarenes Catalyzed by a Silica-Supported Iridium Complex. *J. Org. Chem.* **2010**, *75* (11), 3855–3858.

(38) Sasaki, I.; Taguchi, J.; Hiraki, S.; Ito, H.; Ishiyama, T. Catalyst-Controlled Regiodivergent C□H Borylation of Multifunctionalized Heteroarenes by Using Iridium Complexes. *Chem. Eur. J.* **2015**, *21* (25), 9236–9241.

(39) Bolton, R.; Gates, P. N.; Jones, S. A. W. Convenient Preparation of Halogenoborane-Dimethyl Sulfide Complexes. *Aust. J. Chem.* **1987**, *40* (5), 987–989.

CHAPTER 3.

UNPRECEDENTED MODES OF CATALYSIS USING $[IrCl_2(cod)]^-$ SALTS: CATALYTIC C-H BORYLATIONS WITHOUT AN EXTERNAL LIGAND OR DIRECTING GROUP

3.1: Optimizing Reaction Conditions with $[IrCl_2(cod)]^-$

3.1.1: Comparing Catalytic Competency of Ir(I) Pre-catalysts

To understand the role of $[IrCl_2(cod)]^-$ *(abbreviated as [Ir] throughout this chapter)* in catalysis, its salt with $[Li]^+$ as a counterion was synthesized and used independent from any addition ligand in CHB's. Optimization of the reaction was carried out with methyl 3-(trifluoromethyl)benzoate as the substrate to examine regiochemical preference, and with varying mol % and temperatures (**Table 3.1, Entry 1**). Results showed that the reaction was successful using 4 mol % at 100 °C, but was unsuccessful at 50 °C. By ^{19}F NMR analysis, borylation *ortho* to the ester was seen as the major product in entries 2 and 3. Low reactivity was expected based on literature reports published in our group where they show that using $[Ir(Bpin)(PMe_3)]_4$ only yields stoichiometric products due to its oxidation state of 1+, whereas *fac*-$[Ir(Bpin)_3(PMe_3)_3]$ could facilitate catalysis.[1]

In an attempt to increase TON's, $[Ir][NBu_4]$ was synthesized and compared to the $[Li]^+$ salt, and $[IrCl(cod)]_2$ as the control pre-catalyst (**Table 3.1, Entries 2** and **3**). Amazingly, high catalytic activity was observed when the cation was switched from $[Li]^+$ to $[NBu_4]^+$ without the addition of an external donor ligand. It is suspected $[Li]^+$ has a higher binding energy over $[NBu_4]^+$ with $[IrCl_2(cod)]^-$ perhaps disallowing the metal to catalyze the reaction.

Table 3.1: Catalytic Competency of Ir(I) Species in CHB.

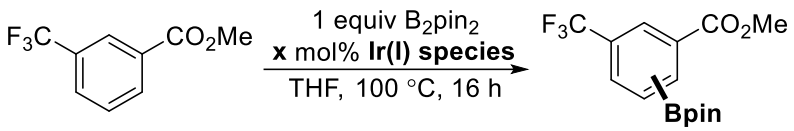

entry	Ir(I) species	x mol %	conversion[a]	selectivity (*o*:*m*)
1	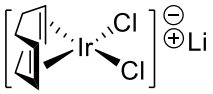	4[b]	13%	94:6
2	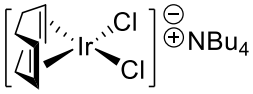	6	82%	49:51
3	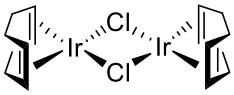	6	12%	59:41

[a]Conversions and selectivities were calculated using ^{1}H NMR of crude reaction mixture.[b]No reaction at 50 °C.

3.1.2: Alkyl Chain Length Effects on Catalysis

Seeing that the initial reactions exhibited a lack of preference for borylation in the least sterically hindered position, we hypothesized that the butyl chain on the cation might be influencing the regioselectivity. In turn, this would broaden the applications of this reaction. Literature reports in our group have described this type of regiocontrol in CHB via ion-pair electrostatic interactions, where the site of C(sp^2)–H activation would be dependent on the alkyl chain length of tetraalkyl ammonium cations paired to sulfate moieties on aromatic derivatives.[2,3] Thus, $[IrCl_2(cod)]^-$ salts with $[N\mathbf{R}_4]^+$ tetraalkylammonium cations, where **R** = Me, Et, Pr, and Bu were synthesized. The salts were then used in CHB reactions with equimolar amounts of the model substrate and B_2pin_2 with varying mol % loadings to see if the length of the chain has effect on the selectivity, and if high conversion would still be achieved at lower pre-catalyst loadings (**Table 3.2**).

The synthesis of [Ir][NMe_4] was unsuccessful due to the poor solubility of NMe_4Cl in solvents such as THF, methylene chloride, and 1,2-dichloroethane, even with prolonged thermolysis. All other salts were successfully made. When testing their catalytic competency in CHB reactions, all were capable of C–H borylating except for [Ir][NEt_4] which showed no conversion of starting material regardless of its high solubility (**Table 3.2, Entry 1**). If electrostatic interactions between the partners in the ion pair is influencing catalysis, we speculate this is the reason for the poor conversion, though this was not the case in our group's ion-pairing work mentioned above.[2]

Table 3.2: Alkyl Chain Length Effects on Selectivity and Reactivity.

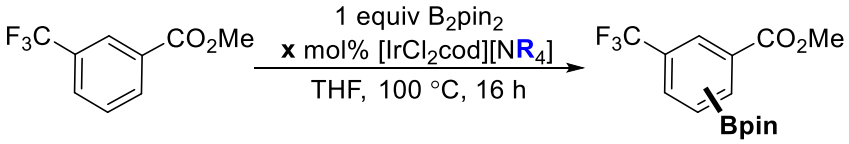

entry	R	x mol%	selectivity (*o*:*m*)	conversion (%)[a]
1	Et	2	---	NR
		6	---	NR
2	Pr	2	71:29	41
		6	64:36	90
3	Bu	2[b,c]	70:30	32
		3[b]	70:30	69
		4	56:44	68
		6	41:59	87
		6[d]	39:61	80
4	Hexyl	6[b]	35:65	84

[a]Conversions and selectivities were calculated by ^{1}H NMR of crude reaction mixture. [b] Pre-catalyst generatred in-situ.[c]Ran for 48 h. [d]Reaction set up in air. NR = no reaction.

Unsurprisingly, using 2 mol % of [Ir][NPr_4] gave poor conversion while increasing the pre-catalyst loading to 6 mol % improved the reactivity from 41% to 90% conversion. (**Table 3.2, Entry 2**). This is similar in the case when using 2 mol % [Ir][NBu_4] as we observe a significant decrease in conversion that only improves as pre-catalyst loadings increase (**Table 3.2, Entry 3**).

Interestingly, we see a clear preference to borylate *ortho* to the ester using 2 and 6 mol % of [Ir][Pr$_4$]. Increasing the alkyl chain length shows that the *ortho* regioisomer is still preferred with [Ir][NBu$_4$]. However, reaching >3 mol % pre-catalyst dramatically increased the amount of *meta* product yielded (**Table 3.2, Entry 3**). To test the robustness of this reaction, CHB of the aryl ester was carried out in air with 6 mol % [Ir][NBu$_4$]. This experiment showed almost identical results with its counterpart. Regardless of this result, all other CHB's were carried out in a nitrogen-filled glovebox as the pre-catalyst does become unstable over time in air (*see section 3.7 for details*) and keeping the THF dry is best to reach optimal conversions.

Experiments were then carried out to address if this may be due to the butyl group on the cation sterically blocking the *ortho* position at higher pre-catalyst loadings. If this were true, then increasing the alkyl chain length should show a decreased preference for *ortho* regioisomers. This was tested with 6 mol % [Ir][N(Hexyl)$_4$] where we observe a minor decrease in *ortho* selectivity in respect to results with 6 mol % [Ir][NBu$_4$] (**Table 3.2, Entry 4**).

To compare all Ir(I) salts in respect to their role of the regiochemical outcome in CHB, the following conclusions can be made: 1) At 6 mol %, there is a clear difference between -Pr and -Bu alkyl chains where the longer the alkyl chain, the lower the *ortho* selectivity preference, 2) when increasing the mol % from 2 to 6, the *ortho* selectivity decreases, though this is more significant when **R** = Bu, as 3) [Ir][NPr$_4$] continues to show its preference for C–H activating *ortho* to the ester regardless of the catalyst loading, likely due to the alkyl chain length being shorter on the cation. These conclusions support the previous hypothesis that the tetraalkylammonium cation does play a role in catalysis, though its interaction with the active catalyst is unknown.

3.2: Substrate Influence on Catalysis

3.2.1: "Ligand Free" CHB's

As mentioned in Chapter 1, Ir-catalyzed CHB reactions typically involve a boron source, an electron rich ligand, and an Ir(I) precatalyst, where $[Ir(X)cod]_2$ (X= Cl, OMe) is most common. As Hartwig demonstrated with dtbpy, these reagents react to form the tris-boryl preassembled complex that begins the Ir^{III}/Ir^{V} catalytic cycle[4] allowing for $C(sp^2)$–H activation on the substrate. This chemical process is homogenous, and reactivity is commonly decided based on electronic properties of the ligand, and the interactions it may have with the transition metal or substrate.

Recent studies suggest that ligand-free borylations are possible (**Scheme 3.1**) when substrates bearing directing groups can coordinate to the metal center enabling catalysis and influencing C–H borylation *ortho* to these directing groups – a concept discussed in Chapter 2. Li and co-workers pioneered this idea in 2017 showing borylation *ortho* to 2-aryl-1,3-dithianes and 1,3-dithiolanes using a 1 : 1.2 : 0.005 equivalence of substrate to B_2pin_2 to $[IrCl(cod)]_2$, respectively.[5] Mechanistic insights were reported in 2022 by Chattopadhyay and Sunoj, where the data followed classical mechanisms, even though no primary KIE was observed. These studies show that the KIE being <1 is likely due to the catalyst-substrate complex having reversible formation, which is not sensitive to isotopic substitution, however the RDS of C–H activation is irreversible (supported by DFT calculations and various control reactions). Though this concept demonstrates that an external ligand (e.g. dtbpy) does not need to be present for reactivity, one can argue that this truly is not "ligand free" if the substrate is playing the role of the ligand, being the key to catalysis and metal activation.

Scheme 3.1: Literature Examples of "Ligand Free" CHB's.[5–8]

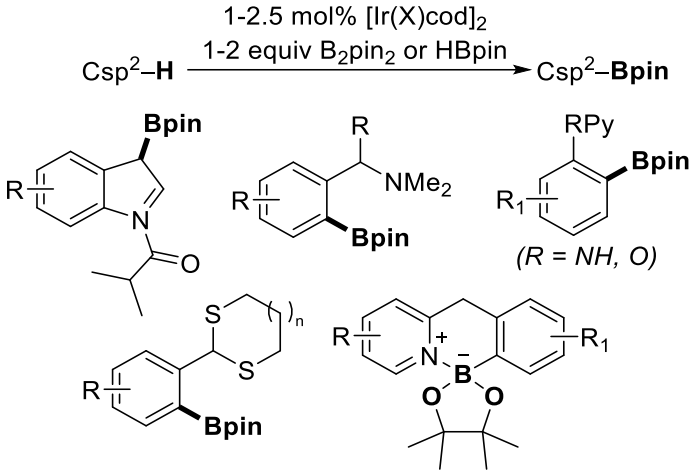

3.2.2: Substrate Scope

To test whether the methyl ester on the substrate used in **Table 3.1** and **3.2** was responsible for catalytic activity through functional group chelation, a variety of substrates that were not bearing such directing groups were tested using 6 mol % $[IrCl_2(cod)][NBu_4]$ and 1 equivalent of B_2pin_2 as the boron source under the optimized reaction conditions (**Scheme 3.2**). Due to complications when working up the crude reaction mixtures containing these products (*see section 3.4.2 for further details*), only moderate to low yields were obtained. Nonetheless, the results show that a directing group is not necessary for catalysis using substrates **3b**, **3c**, and **3f.** This is the first piece of evidence that catalysis can occur without an external source donating electrons into the metal center - an important distinction from other CHB reports and those described to be "ligand-free".

Methyl benzoate derivatives bearing an electron donating group *meta* to the ester resulted in a significant decrease in reactivity. Comparing the weaker donation of –OMe (**3d**) versus $–NMe_2$ (**3e**) showed that stronger donation into the ring system equates to a lower conversion, which is typical in CHB chemistry. However, both substrates yielded a higher percentage of *ortho* borylated

product in comparison to model substrate **3a**, potentially due to induction effects influencing the acidity of the C–H bond.[9]

Scheme 3.2: C(sp^2)–H Borylation of Substrates Using $[IrCl_2(cod)][NBu_4]$.

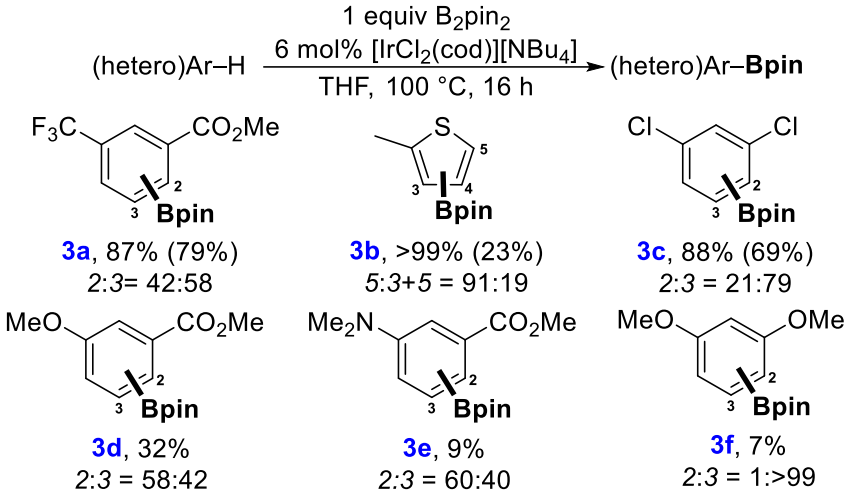

Conversions and selectivities were calculated by ^{1}H NMR of crude reaction mixture. Isolated yields are in paranthese for products **3a-c.**

Testing 1,3-dimethoxybenzene as a highly electron rich substrate with no electron withdrawing groups follows the trend of low reactivity where only 7 % conversion was observed (**3f**). This disadvantage has been overcome by Chattopadhyay who uses ligands designed to improve the geometry and electronics of the metal center.[10] We hypothesize that using $[Ir][NBu_4]$ independent of external ligands is thus expected to give poor TON's on electron rich substrates due to the metal center acting as a poorer nucleophile, in turn making it much more difficult to overcome the kinetic C–H activation barrier.

When analyzing the regiochemical result using 1,3-dichlorobenzene as the substrate (**3c**), a surprising 21:79 ratio of *ortho* to *meta* borylation was observed. These results differ from the prior art as solely *meta* to chlorine borylation is found when using dtbpy. Borylation *ortho* to chlorine could only be achieved at low conversions when forcing borylation to occur on 1,4-

dichlorobenzene.[11,12] A way to borylate *ortho* to chlorine on this substrate has been achieved using a monodentate phosphine ligand where the second coordination site is assumed to be open on the metal for directed CHB to occur.[13] Under simpler conditions, this can more commonly be done with N-heterocycles due to the electronics in the respective π system.[14]

3.2.3: Tri-substituted Aryl Chlorides

Taking advantage of the fact that we do not have a bulky ligand system facilitating these borylations, 1,3,5-trichlorobenzene was tested to see if C–H activation would occur at these sterically hindered sites given the regiochemical result with 1,3-dichlorobenzene. Adding to this idea, 1,3-dichloro-5-fluorobenzene was tested to observe if there would be a selective preference to borylate at the 2-position between the chlorines, or 4-position adjacent to the fluorine.

CHB of 1,3,5-trichlorobenzene showed sluggish reactivity with only 34% conversion of starting material. Mono-borylation was expected, however 82% of the reaction mixture contained a product where the chlorine is displaced with –Bpin (**Table 3.3,** Product **B**). To test if this chemistry was occurring due to Pd or other metal contamination, all Teflon stir bars and Wheaton vials were treated with a simmering solution of aqua regia for 6 hours prior to use. When repeating the CHB's with this glassware, results were consistent and only varied by ± 5 % when comparing the conversions and selectivities (**Table 3.3, Entry 2**).

Table 3.3: C(sp^2)–Cl and C(sp^2)–H Borylation of 1,3,5-trichlorobenzene.

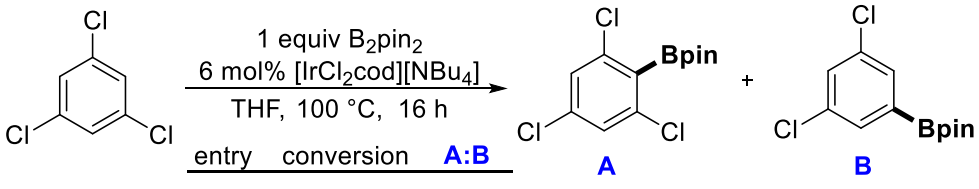

entry	conversion	A:B
1	34%	18:82
2[a]	38%	19:81

[a] Reaction vessel contents were simmered in Aqua Regia, rinsed, then oven dried prior to reaction setup.

Using 1,3-dichloro-5-fluorobenzene as the substrate exhibited similar results (**Table 3.4**), though only 28% of the dechlorinated product was found. Results were again consistent when comparing with the washed glassware (**Table 3.4, Entry 2**). The different ratio of borylated to dechlorinated products may be attributed to the steric differences where the *ortho* to fluorine bonds are more accessible.

Table 3.4: C(sp^2)–Cl and C(sp^2)–H Borylation of 1,3-dichloro-5-fluorobenzene.

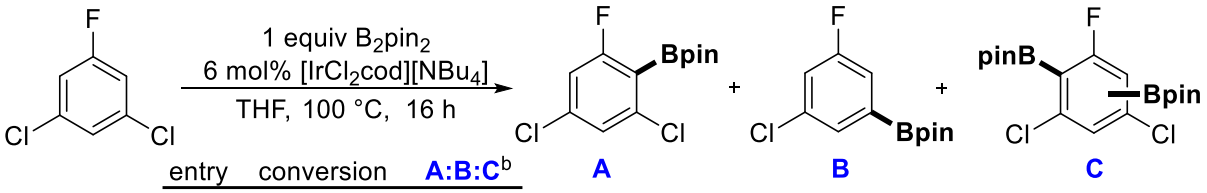

entry	conversion	A:B:C[b]
1	49%	60:28:12
2[a]	50%	65:24:11

[a] Reaction vessel contents were simmered in Aqua Regia, rinsed, then oven dried prior to reaction setup. [b] Product C is a mixture of diborylated products. See experimental for details.

3.2.4: dtbpy Control Reactions

Control reactions with dtbpy were carried out on chlorinated substrates previously tested to see if 1) *ortho* to chlorine borylation could occur with a larger external ligand, and 2) if any chlorines would be displaced with –Bpin **(Scheme 3.3).** Only 3 % *ortho* to chlorine borylation was observed for 1,3-dichlorobenzene, which is significantly different than the 21% yielded with [Ir][NBu4]. When compared to 1,3,5-trichlorobenzene, only 12% conversion of monoborylated product was observed. Using 1,3-dichloro-5-fluorobenzene resulted in 90% conversion of *mono*- and di-borylated product *ortho* to fluorine, where the greater activity in this substrate can be attributed to the smaller size of fluorine, allowing C–H activation sites to be more accessible in positions with less steric hinderance.

Scheme 3.3: Control Reactions with Chlorinated Substrates.

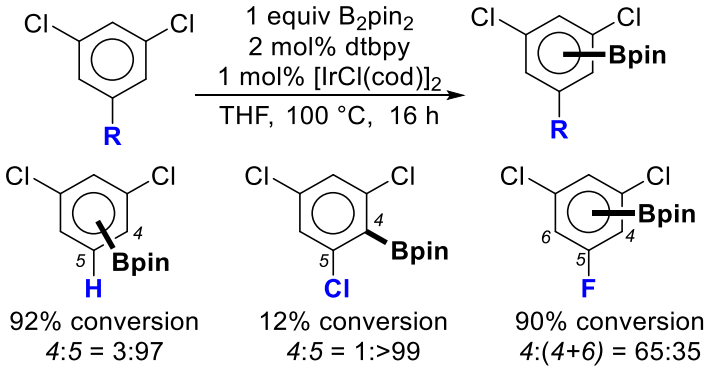

3.2.5: C–Cl Activation Hypotheses

Ir(I) and Ir(III) complexes such as $[Ir(CO)_2Cl_2]^-$,[15] Vaska's complex and analogues, complexes containing PNP pincer ligands,[16] among others have be able to perform C–Cl activation via oxidative addition where sp^2 and sp^3 C–H bonds were present. An example where reaction conditions closely resembled the system in study shows that when using B_2pin_2, dppe, $[IrCl(cod]_2$, and Cs_2CO_3, (Csp^2)–F and –Cl activation of aryl halides yields diaryl ethers.[17]

Generally, aromatic CHB is a method used to replace metalation type reactions as C–H bonds are transformed directly without the use of a haloarene, thus eliminating the initial step of metal-halogen exchange followed by nucleophilic substitution on boron electrophiles.[18] C–H activation occurs over C–Cl activation in CHB due to thermodynamic favorability and respective bond strengths, however, σ complex binding may be more favorable with metal complexes due to the dipole in the C–Cl bond.[19]

Direct C–Cl to C–B bond transformation via oxidative addition on chloroarenes has not been reported in the literature at this time. However, computational studies have been done by the group of Bickelhaupt showing that coordination of a Cl^- anion to Pd(0) catalysts lowers the activation barrier of C–Cl bond activation, calling it "anion assistance".[20] They also report that the

activation enthalpies for oxidative addition are about equal for C–H and C–Cl bonds in this case. Given what has been seen in the NMR kinetic studies discussed in the next chapter, there is a possibility that after decomposition of $[IrCl_2(cod)]^-$, Cl^- may facilitate this type of chemical transformation with Ir(0) catalysts.

As we have seen a mixture of direct C–H activation products versus chlorine displacement with the tri-substituted aryl chlorides, we hypothesize there are competing mechanisms at play, where if the C–H bond is sterically available then direct C–H to C–B transformations will occur. Evidence that supports this claim can be seen where there is no chlorine displacement for 1,3-dichlorobenzene, minor displacement in 1,3-dichloro-5-fluorobenzene, and major displacement for 1,3,5-trichlorobenzene.

3.3: ^{1}H Oil Bath Kinetics With $[IrCl_2(cod)]^-[NBu_4]^+$

3.3.1: Importance

The experimental results collected thus far are distinct from standard CHB reactions. These results consist of catalytic activity i) without an external, complex ligand system or substrate directing groups, ii) having the ability to transform C–Cl bonds to C–Bpin, and iii) with an Ir(I) anionic species with the added advantage of regiocontrol with tetraalkylammonium cations.

Kinetic studies were carried out to seek evidence on if this system is mechanistically different from the accepted Ir^{III}/Ir^{V} homogenous CHB systems. Renowned for his groundbreaking work in experimental design to differentiate between homo- and heterogenous systems, Finke explains that by assessing the overall kinetic reproducibility and curvature of graphical representations of product formation over time, one can distinguish between homo- and heterogeneous systems.[21] Monitoring by NMR also gives further insight into potential reaction

intermediates and reactivity other than C–H activation, all of which improves the hypothesis on how this reaction is occurring.

3.3.2: Kinetic Analysis

Figure 3.1 shows the kinetic data of the optimized reaction, which was heated in an oil bath and monitored by ^{19}F and ^{1}H NMR with 1,3,5-trimethoxybenzene used as the internal standard. Plotting the [M] of substrate over time, a significant induction period is observed. Following this is rapid conversion of starting material to product, where the reaction ends ~ 8 hours. Both points support the hypothesis that this system is a novel CHB process and proceeds through a complex chemical system that is not completely homogeneous, represented by a sigmoidal curve supporting that insoluble pre-catalyst species are responsible for catalyst generation.[21]

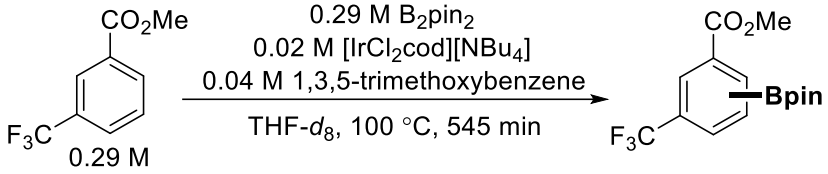

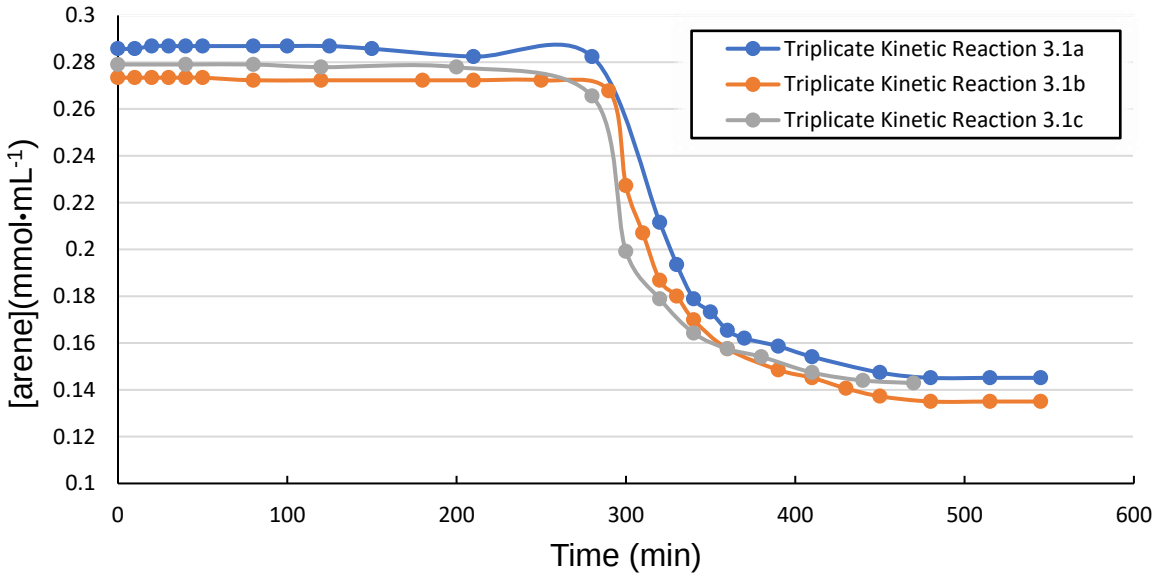

Figure 3.1: Triplicate Kinetic Studies Using [$IrCl_2$(cod)][NBu_4] (*Triplicate Kinetic Reactions 3.1a, 3.1b, and 3.1c*).

Experiments were also carried out with 2-methyl thiophene to test if having a highly reactive substrate without a directing group would affect the kinetics, and directly compared with the aryl ester **(Figure 3.2).** Results show that the active catalyst still takes time to form as indicated by the induction period, though conversion is significantly less rapid. When comparing the experiments of methyl 3-(trifluoromethyl)benzoate in **Figure 3.1** and **3.2**, it is clear that the active catalyst in the latter case was generated significantly faster as the reaction is complete after only 2 hours. It should be noted that both reactions were run using the same batch of pre-catalyst, and we do not have data explaining the difference in reaction rates.

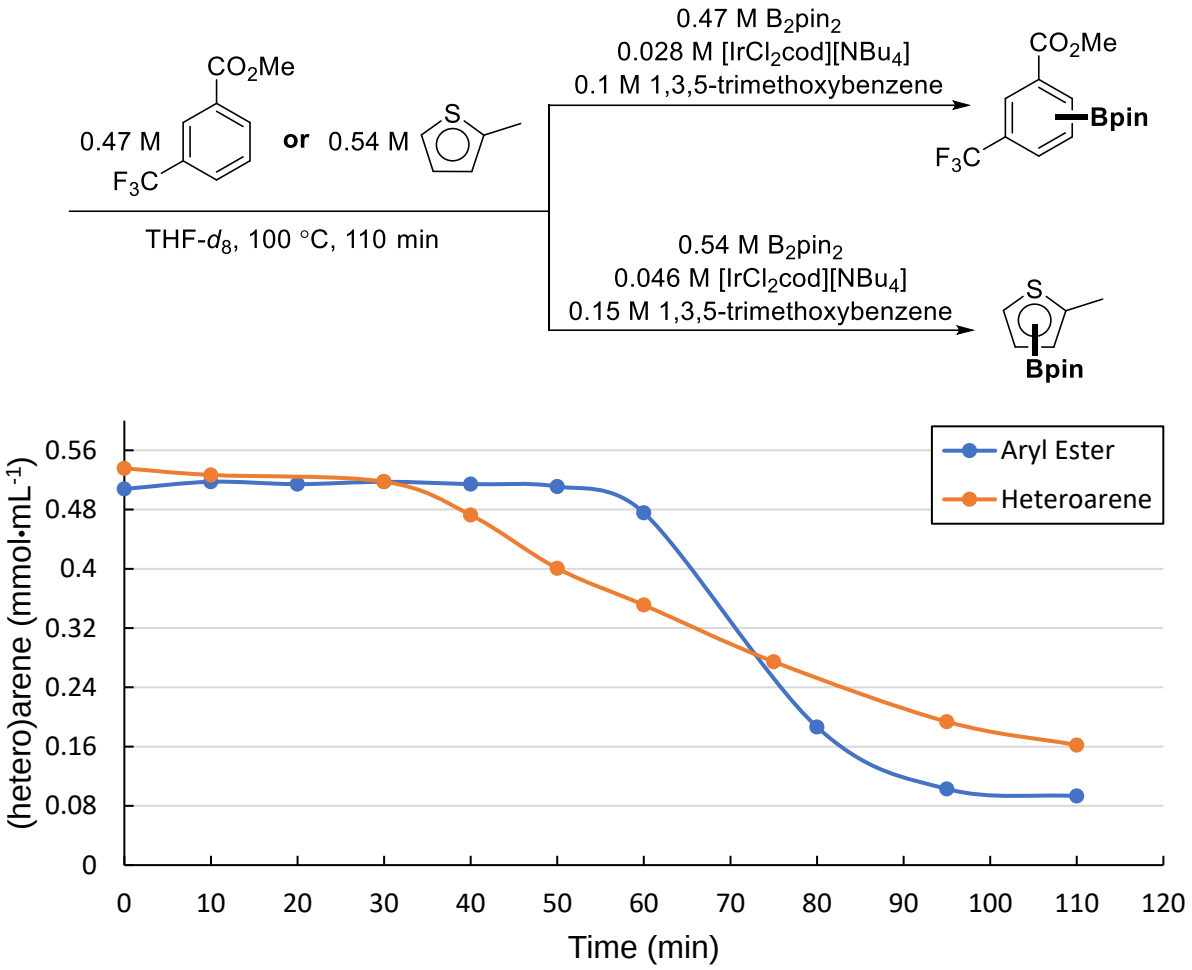

Figure 3.2: Comparing Kinetics of methyl 3-(trifluoromethyl)benzoate (*Kinetic Reaction 3.2*) and 2-methyl thiophene (*Kinetic Reaction 3.3*).

3.3.3: ^{1}H NMR Data Analysis

Shown in **Figure 3.3** is another experiment to test reproducibility (*Kinetic Reaction 3.4)* of the model reaction, where [M] of arene is plotted over time. Below the curve is the hydride region of ^{1}H NMR spectra taken at the plotted time points where Ir–H species are present and changing at specific points of the reaction. No hydrides are present during the induction period (t = 0 to t = 30 min); however, two species appear at -7.8 and -5.0 ppm as soon as starting material is consumed at t = 40 min (**I**). After 15 minutes, two other species are formed at -3.7 and -11.9 ppm (**II**). We see new hydride species forming between -11.0 and -13.5 ppm during rapid catalysis (**III**).

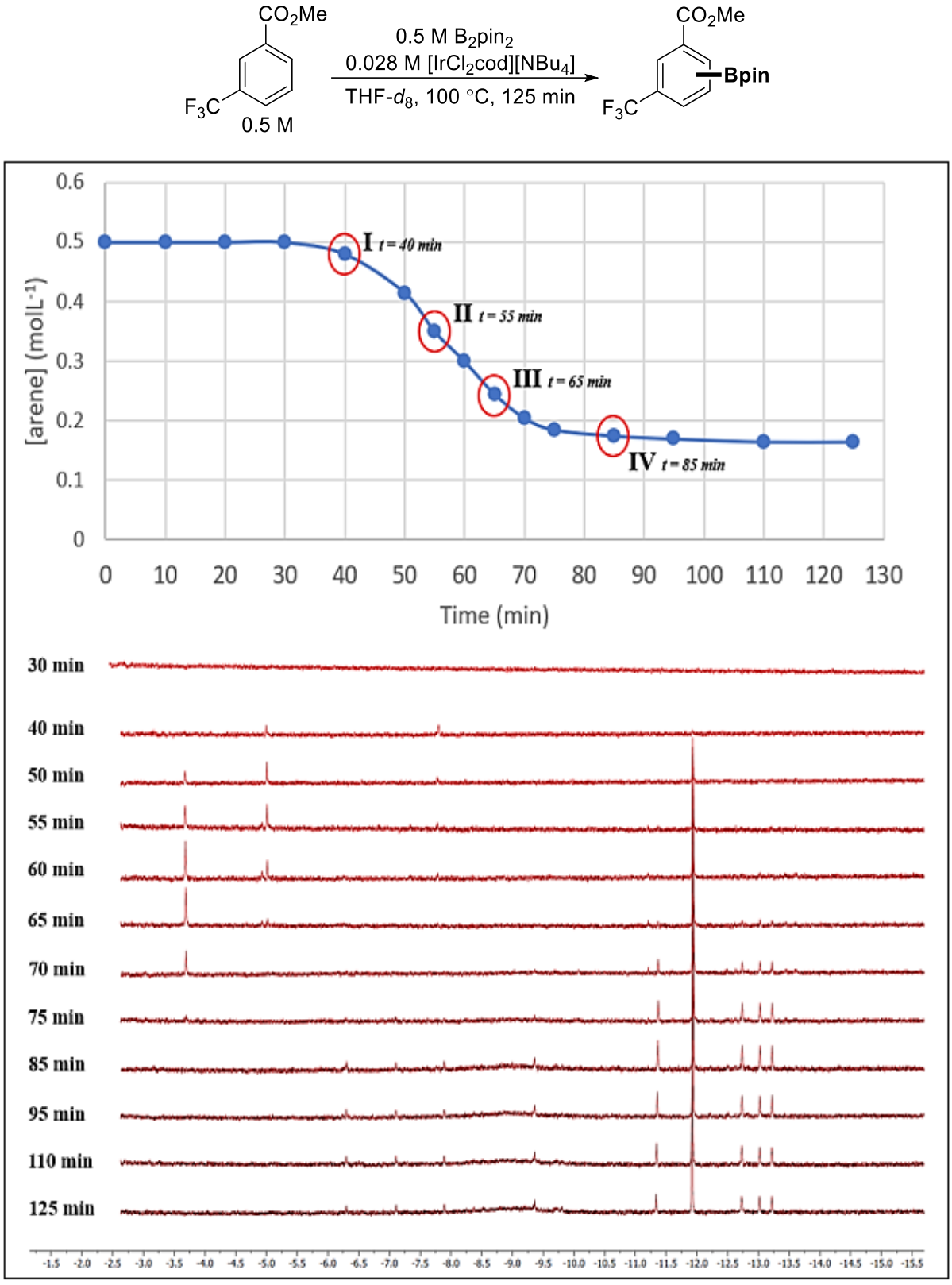

Figure 3.3: Changes in Hydride Region of *Kinetic Reaction 3.4*.

As the reaction slows down between t = 70 and 90 minutes, these species continue to grow while most of the original peaks seen between **I-III** disappear, except for the resonance at -11.9 ppm. At point **IV**, product formation is no longer occurring and the species that represent the peaks most up-field seem to dominate the reaction. VT NMR studies of this sample were carried out at -40 °C to see if we could identify species in equilibrium, however, we were unable to pick out any valuable information due to an overwhelming number of new resonances covering the entire region. Though there were >25 new peaks spanning from -5.5 to -17.5 ppm, they were minor species in comparison to the major upfield peaks shown at the end of the reaction.

To investigate if these species are consistently formed during every CHB reaction, the hydride region of *Triplicate Kinetic Reaction 3.1c* was analyzed and compared (**Figure 3.4**). At the start of catalysis (**I**) no Ir–H resonances are present until 20 minutes later in the middle of rapid conversion (**II**). The chemical shifts of these peaks do not match with those found in *Kinetic Reaction 3.4*, though they do match those from reactions where the same stock solutions were used, being *Triplicate Kinetic Reaction 1a-b*. Additionally, these hydride species disappear once the reaction is over (**III**), which was not observed in the previous case. When comparing the last two studies (*Kinetic Reaction 3.2* and *3.3*), these types of species were formed, but a) did not match the chemical shifts previously observed and b) hydride resonances only appeared when conversion ended and not at the start of conversion.

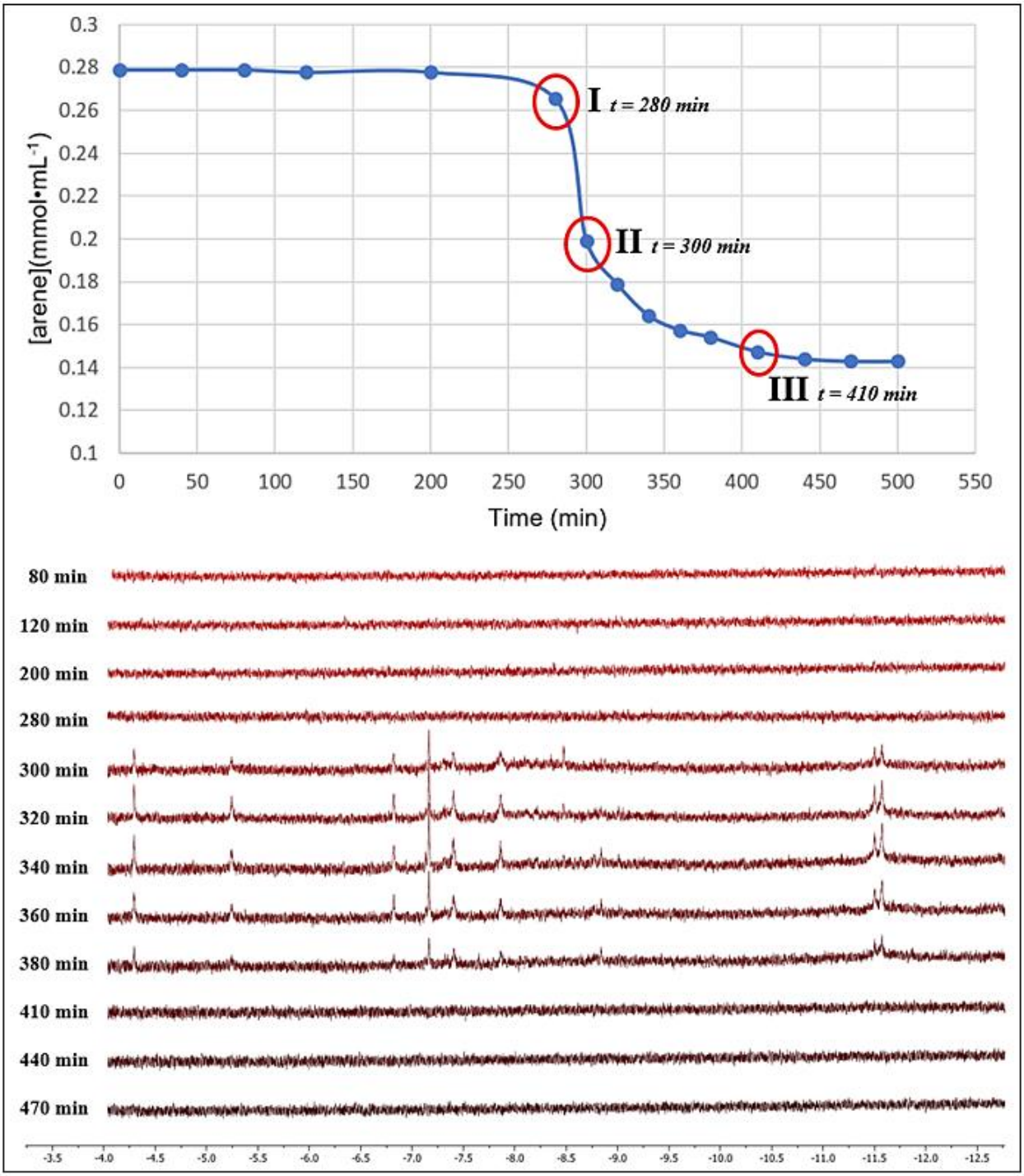

Figure 3.4: Changes in Hydride Region of *Triplicate Kinetic Reaction 3.1c*.

In addition, significant changes over time were seen with the COD and tetrabutylammonium cation resonances of the pre-catalyst (**Figure 3.5**, *Triplicate Kinetic Reaction 3.1b*). Focusing on one representative peak for each species representing by the asterisk, we see that during the induction period the chemical shifts corresponding to the -CH_2 of the alkyl chain ([$IrCl_2$(cod)][N(**CH_2**$CH_2CH_2CH_3$)$_4$], δ 3.4 ppm) and the methylene protons of the COD (δ 2.06 ppm) do not change from t = 0 to t = 250 min. Integrating these peaks during this time frame shows that the [M] of the cation remains consistent while the COD slowly decreases over time (*see section 3.7.10 for the kinetic plot)*. At the point after the induction period (**I**, t = 290), COD completely disappears at t = 360 (**II**) where conversion slows down. We see that the COD was not hydroborylated, but completely hydrogenated. The resonance belonging to the cyclooctane at 1.53 ppm does appear at t = 290 and continues to grow until the COD resonance completely disappears at point **II**, where the hydrogen source is likely from C–H activation but could also be from borane intermediates. Notably, Finke has reported hydrogenation of cyclohexene and benzene with Ir(0) and Rh (0) nanoparticles, respectively.[22,23]

After the induction period at t = 290 min (**I**), we also see that the cation slowly shifts 0.5 ppm downfield while the COD resonance continues to disappear. As catalysis slows down at point **II**, the cation resonance is now shifted 0.12 ppm downfield of its original chemical shift. When catalysis stops completely at t = 450 min (**III**), the cation resonance shifts back up field and continues shifting until the reaction is taken out of the oil bath, moving 0.17 ppm from where it moved at point **II**, and further up field of where it was during the induction period. We hypothesize that these shifts were caused by the tetrabutylammonium cation ion-pairing with possible boryl or iridium anionic species during catalysis, or even a chloride anion that was formed after pre-catalyst decomposition. In addition, there is a significant decrease in the integration corresponding to this

resonance. We are unsure what chemical transformation is occurring, as alkyl or alkenyl species that could be forming from the butyl chain have too low of a boiling point to be observed here.

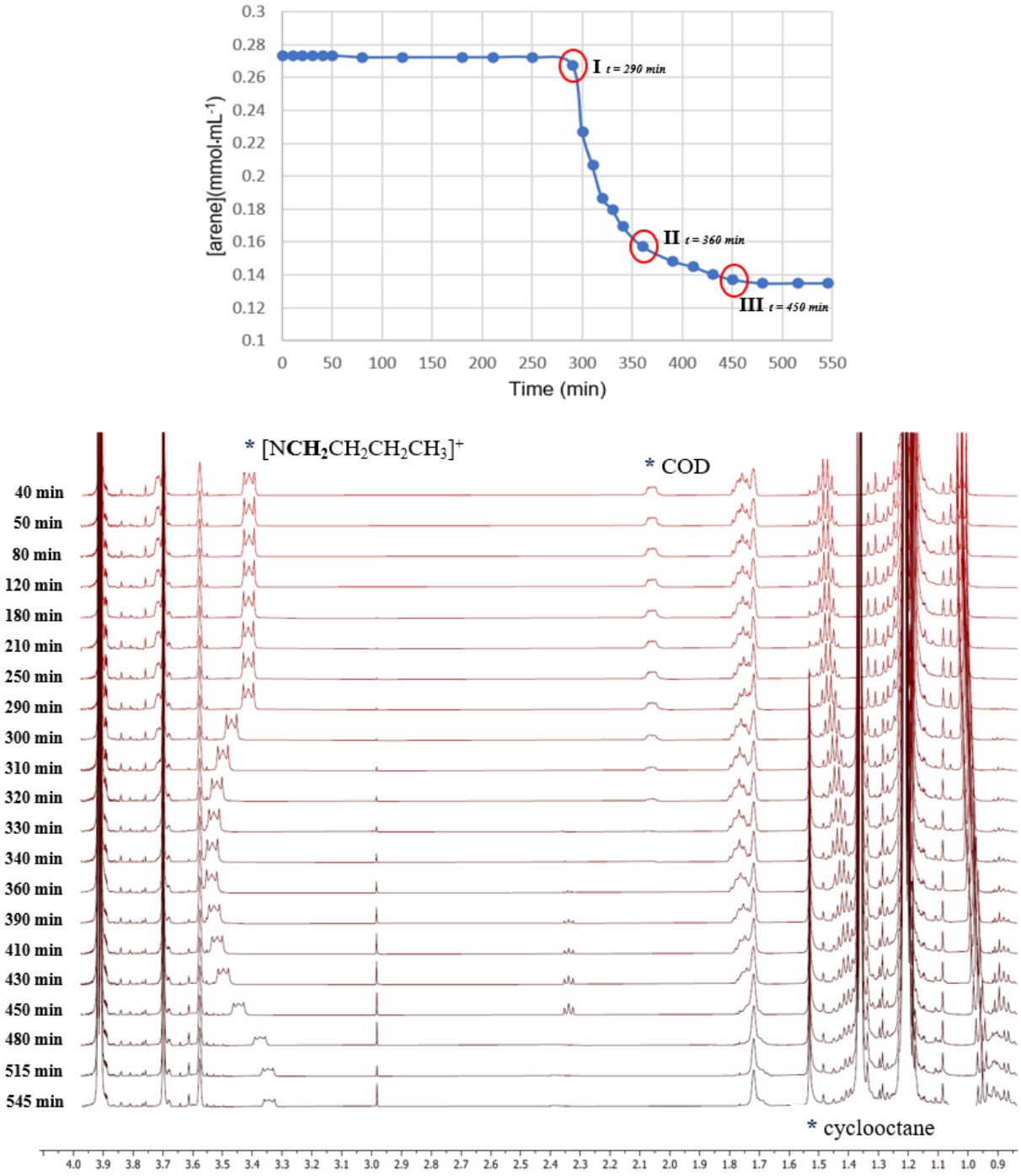

Figure 3.5: Changes in the Up-field Region of COD and $[NBu_4]^+$ for *Triplicate Kinetic Reaction 3.1b*.

3.4: Visual Observations

3.4.1: Reaction Monitoring

Relaying back to Finke's understanding for distinguishing between homo- and heterogenous systems he writes (in a way that I could not do justice re-writing) that *"…. observing a sigmoidal curve is powerful evidence for the in-situ formation of a heterogenous catalyst, assuming that the reaction products – the first step of reliable mechanistic studies- have already been established to be nanoclusters (observed by TEM) or a bulk-metal precipitate (e.g., visual observation)."*[21]

Throughout the course of study testing [Ir][NBu_4] in CHB's, black precipitate was observed during the induction period and in some instances, this solid redissolved back into solution when starting material began converting. To display side-by-side examples where precipitate is formed, **Figure 3.6** shows pictures labeled **A-D** taken during the induction period of numerous reactions that were run under optimized reaction conditions with the model methyl ester substrate, set up in 3 mL Wheaton vials or J-young tubes. As [Ir][NBu_4] is a bright yellow solid, the solution at t = 0 is a homogenous yellow solution (**Figure 3.6**, **A**) where heating the reaction mixture leads to slow generation of precipitate (**B** and **C**). Though the amount of this solid was not quantified, these pictures show the solid crashing out *during* catalyst generation, where one appears darker than the other.

This precipitate was also seen when carrying out the triplicate kinetic studies in **Figure 3.1** (*Kinetic Reactions 3.1a-c*) where copious amounts of black solid were generated after the induction period, and the solution turned black over time (**Figure 3.6**, **E**). When the reaction was complete, the solution was poured out of the J-young tube where a black film adhering to the glass was observed (picture **F**). This film was insoluble in numerous solvents and could only be removed

with a scrub brush and deionized water (this has been observed after most reactions that were set up under similar conditions). It should be noted that this solid was isolated but ^{1}H NMR resonances were not observed. It is likely that this solid was iridium metal, though ICP analysis was not carried out to confirm this. Comparing the observations discussed here supports the hypothesis that this system is heterogeneous and could contain $Ir(0)_x$ nanoclusters from pre-catalyst decomposition that catalyze CHB reactions.

Interestingly, observations from *Kinetic Reaction 3.2* in **Figure 3.2** (where the same aryl ester is used as the substrate) exhibited no signs of this solid during the induction period, but instead the solution darkened in color (**Figure 3.6, D**), eventually turning dark brown. It should be noted that no black solid was observed by the naked eye for *Kinetic Reaction 3.3* with 2-methylthiophene as well.

Figure 3.6: Visual Observations of CHB Solutions with [$IrCl_2$(cod)][NBu_4].

3.4.2: Product Purification

As described in Chapter 2, the most effective way to purify the crude reaction mixture from CHB reactions, separating the Ir and unwanted boron side product (e.g. pinB–OH) is to evaporate the solvent then re-dissolve the mixture and run it through a short silica plug such as the one shown in **Figure 3.7, A**. In the systems using [Ir][NBu_4], the observations differ from homogeneous reactions with dtbpy and an Ir(I) dimer seeing that in our case, the Ir does not sit on top of the silica but travels with the DCM eluent through the powder, leaving tiny insoluble pieces of black

solid in a typically clear solution of soluble organic products (**Figure 3.7, B and C**). This was is not dependent on the substrate as even reactions run in triplicate varied with the amount of black solid that passed through the column. It should be noted that this same barrel of silica was successful in capturing Ir species from crude reaction mixtures with **BB** and other common CHB reaction setups with external ligands.

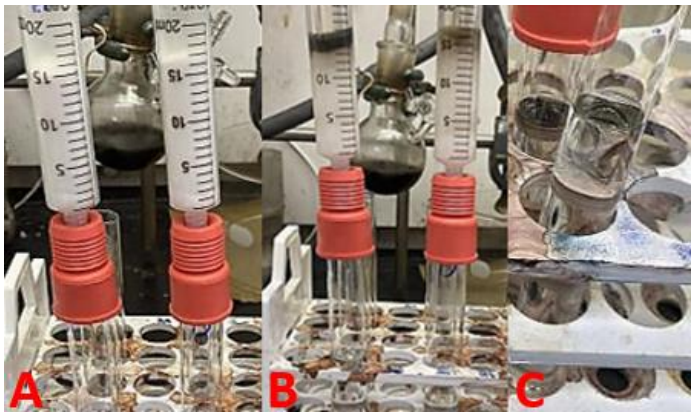

Figure 3.7: Visual Observations During Purification of Crude Reaction Mixtures.

3.5: Mercury Drop Tests

3.5.1: Hg(0) Addition at t = 0

Mercury drop tests are another classical set of experiments used to distinguish between homo- and heterogeneous systems, where if insoluble metal particles are playing a role in catalysis the Hg(0) can amalgamate or adsorb to the surface of these species, "poisoning" them and blocking reactivity.[24] Ir, Rh, and Pt are some of the transition metals that do not form an amalgam with mercury, though poisoning is still obtainable with nanoclusters of the respective metal.[22,25,26] Thus, two types of experiments were carried out with ~30 equivalents of Hg(0) with (hetero)arene substrates where reactions with [Ir][NBu_4] were compared with controls using dtbpy and [IrCl(cod)]$_2$. To obtain accurate conclusions, both sets of reaction conditions were also tested without added mercury.

Under reaction conditions with [Ir][NBu4] (**Table 3.5**), when mercury is added to either the aryl ester or thiophene substrates no reaction is observed. When comparing this to their respective controls with no mercury addition the CHB's were catalytic, and where reaction conversions agreed with previous experiments.

Table 3.5: Mercury Drop Test Experiments with [$IrCl_2$(cod)][NBu_4].

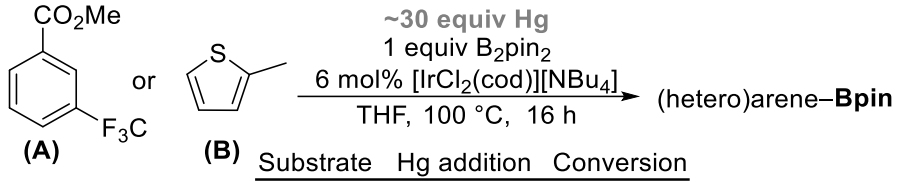

Substrate	Hg addition	Conversion
A	Yes	0%
A	No	88%
B	Yes	0%
B	No	96%

3.5.2: Control Reactions

As Hg(0) was added at t = 0 before heating, the hypothesis was that the mercury was likely poisoning species involved in making the active catalyst, or the active catalyst itself once it was generated. Though unlikely, it's possible that Hg(0) could have directly reacted with the pre-catalyst upon heating to 100 °C, enabling the chance for a species that could catalyze the reaction. To test this, a control reaction was run where a solution of [Ir][NBu_4] and Hg(0) was heated to see if there was any structural change to the pre-catalyst over time (**Scheme 3.4**). It was confirmed by ^{1}H and ^{13}C NMR that the pre-catalyst remained intact, not degrading or undergoing a chemical change from the Hg(0).

Scheme 3.4: Control Reaction with Hg(0) and $[IrCl_2(cod)][NBu_4]$.

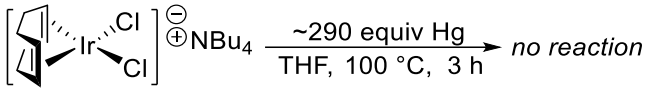

Understanding that CHB reactions using dtbpy and $[IrCl(cod)]_2$ to generate the active catalyst is a homogeneous system, results were unsurprising as the mercury did not poison any reactions where this was added, and conversions of their respective controls without Hg(0) were near identical (**Table 3.6**). This supports the claim that reactions with $[Ir][NBu_4]$ as a pre-catalyst, without an external ligand, are mechanistically different from common CHB reactions.

Table 3.6: Mercury Drop Test Experiments with dtbpy and $[IrCl(cod)]_2$.

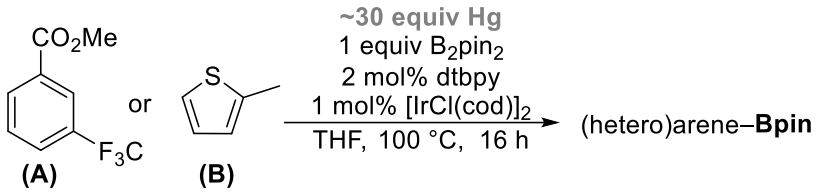

Substrate	Hg addition	Conversion
A	Yes	84%
A	No	88%
B	Yes	>99%
B	No	93%

3.5.3: Hg(0) Addition During Rapid Catalysis

As the initial studies focused on Hg(0) interactions during the induction period, experiments were carried out to test if mercury would have any effect when added to the active catalyst during the stage of rapid catalysis. Similar experiments have been reported in the literature with iridium nanoclusters,[22] aiming to understand if insoluble nano species are catalyzing the reaction, or if the catalyst is soluble in solution and thus will not be disturbed by mercury. The latter could suggest C–H activation is a homogeneous process and give evidence for a system that is partially homogeneous.

Optimized reaction conditions were carried out with 2-methyl thiophene as triplicate control reactions with this substrate show a consistent conversion of >99%. Monitoring by ^{1}H NMR, the reaction vessel was removed from the heated aluminum block at 30% conversion and ~ 30 equivalence of Hg(0) was added once the solution cooled to room temperature (**Table 3.7, A**). Heating the reaction mixture overnight showed the reaction continued to 50% conversion indicating that Hg(0) did inhibit catalysis.

Table 3.7: Addition of Mercury to CHB After Induction Period.

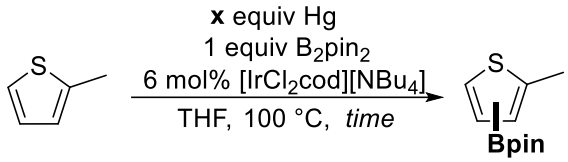

A. 30 equiv Hg

time (h)	conversion
1.5	13%
2	30%
••••• *Hg addition* •••••	
16	50%

B. 310 equiv Hg

time (h)	conversion
2.5	61%
••••• *Hg addition* •••••	
16	88%

It is commonly accepted, but often ignored, that reactions must contain excess Hg(0) and be properly stirred to ensure intimate contact of the Hg(0) beads with potential $Ir(0)_x$ nanoclusters that are catalyzing the reaction in solution. In this way, the most valuable data can be extracted with a higher level of confidence in conclusive results.[21,23] Reports by Finke have shown that when using 2 equivalents of Hg(0) with Rh(0) nanoclusters, catalysis was not poisoned immediately unless an excess of ~310 equivalents Hg (0) was used with vigorous stirring.[23] Running the reaction with excess mercury did not change the results where the reaction continued after Hg(0) addition, as the reaction still did not reach full conversion (**Table 3.7, B**). Air contamination is not believed to be a factor due to the results from the CHB reaction setup in air and the mercury addition experiments at t = 0 (*see section 3.7 for the detailed procedures*). In addition, stopping

the catalysis during rapid conversion was not problematic when monitoring reactions (*section 3.3*) so it is assumed this is not a factor as well.

If opening the vial to add mercury did not affect the reaction, one hypothesis could be that a fraction of the active catalyst is homogenous, or in equilibrium with its heterogeneous counterparts. Another hypothesis could be argued that catalytically active $Ir(0)_x$ nanoclusters were poisoned by Hg(0) depending on their respective size, thus immediate inhibition in this case could be unlikely. Either hypothesis would be difficult to prove with certainty, and synthesis of more well-defined Ir species, ideally with capping agents, would be necessary where subsequent experiments would need to be carried out with extreme precision given the drawback of Hg(0) amalgams with Ir.

There has been a singular report by Maguire showing the possibility of catalytic CHB of **R**–C_6H_5 (**R** = H, Me, OMe, and CF_3) using ionic liquid stabilized Ir(0) nanoparticles and HBpin.[27] Mercury drop test experiments were carried out for that system to study the catalyst and gave similar results to what has been observed in the system with [Ir][NBu_4]. Found were 1) no conversion of substrate when an ionic liquid solution containing nano-Ir(0) and stirred in access mercury was added to benzene and 2) adding excess mercury to an active catalyst solution containing benzene after 8 hours, then continuing the reaction for 14 hours gave only a 30% yield of product – though the conversion before mercury addition was not reported.

3.6: Conclusions

Using $[IrCl_2(cod)][NBu_4]$ independent from an external ligand has proven to be a competent pre-catalyst in transforming C–H to C–B bonds, where the site of C–H activation is influenced by the length of the alkyl chain in the ammonium cation. resulting in a higher amount of *ortho* borylated products. Data shows that this involves a mechanism that is distinct from the classical Ir^{III}/Ir^{V} catalytic cycle where external ligands, including directing groups on substrates, are not necessary for CHB. NMR analysis from oil-bath kinetics show the likelihood of pre-catalyst decomposition into catalytically active $Ir(0)_x$ or IrH_x species, as during rapid conversion of starting material a) COD is hydrogenated to cyclooctane, b) there is a significant chemical shift of the resonance belonging to the NBu_4 cation, and c) new peaks are observed in the Ir–H region. Sigmoidal curves that were produced from NMR kinetics, along with results from mercury drop tests and overall visual observations, signify that this reaction occurs through a complete or partial heterogeneous process. In addition, this system is competent to do direct C–Cl to C–B transformations on tri-substituted aryl chlorides. As these results are novel to CHB chemistry, we hypothesize that a chlorine anion is formed after pre-catalyst decomposition and assists Ir(0) catalytic species to perform both C–H and C–Cl activation.

3.7: Experimental Data

3.7.1: General Information

All reactions were carried out in a nitrogen filled glovebox unless stated otherwise. $[IrCl(cod)]_2$, B_2pin_2, tetraalkyl ammonium salts, and all substrates were obtained commercially. Tetrabutylammonium chloride and lithium chloride was purified according to the literature,[28] where all other alkyl ammonium chloride salts used for $[IrCl_2(cod)]^-$ syntheses were dried under 0.001 Hg vacuum overnight and stored in the glovebox. THF was obtained from a wet still refluxing over sodium benzophenone ketyl. 1,2-dichloroethane and pentane were obtained from

wet stills refluxing over CaH_2. Methyl chloride was obtained from a dry still. All other reagents were used as received unless specified.

Glassware and stir bars were cleaned in a base bath made of KOH and IPA, rinsed with deionized water and acetone, then dried in a 130 °C oven overnight. Standard CHB reactions were set up in 3.0- or 5.0-mL microreactor Wheaton V-vials equipped with a conical stir bar. Reaction vessels were capped with a black phenolic cap, or Kimble Mininert valves when monitoring reaction progress, and transferred to a 4 x 4 aluminum block heated outside of the glovebox. Stock solutions of $[IrCl_2(cod)]^-$ salts in dry THF were freshly prepared for all reactions when generating the compound in-situ or using as an isolated solid. Conversions and selectivity's were calculated based on NMR data of the crude reaction mixture.

All high-resolution mass spectra and NMR data was collected at Michigan State University. NMR data is recorded on a Varian 500 MHz DD2 Spectrometer with a 5 mm Pulsed Field Gradient Probe. Spectra were taken in deuterated solvents that were obtained commercially. $CDCl_3$ was dried with 3 Å molecular sieves that were heated under vacuum before use. Dry THF-d_8 was used directly from an ampule. All dry deuterated solvents were stored in glovebox filled with nitrogen. All NMR spectra presented were processed using MNova software where manual integration, peak picking, and referencing of residual solvent resonance was applied, along with phasing and Berstein Polynomial baseline corrections.

Crude reaction mixtures were concentrated and dissolved in ~ 1.0 mL of methylene chloride before eluting through a short silica plug made in a 12.0 mL Luer lock plastic syringe with ~2-3 g of laboratory grade 230-400 mesh silica. Fractions collected were spotted on 3 x 3-inch silica gel TLC plates and irradiated with ultraviolet light (λ = 254 nm).

In respect to all identical reactions repeated throughout this chapter, note that all conversions and selectivities were obtained for the reaction run under each specific section to ensure reproducibility and accurate comparisons with other experiments at the time reactions were set up.

3.7.2: Synthesis and Characterization of $[IrCl_2(cod)]^-$ Salts

Synthesis of $[IrCl_2(cod)][Li]$.

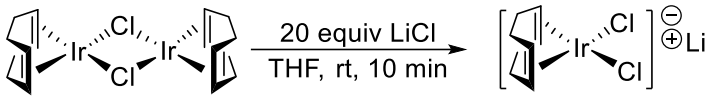

In a 100 mL oven dried Schlenk flask equipped with a stir bar, $[IrCl(cod)]_2$ (1.00 g, 1.49 mmol, 1 equiv) was dissolved in 50 mL of dry THF. LiCl (1.26 g, 29.7 mmol, 20 equiv) was then added and the solution instantly turned from orange to bright yellow. The reaction was stirred at room temperature for 10 minutes then concentrated under vacuum. The resulting solid was washed with dry CH_2Cl_2. After drying under vacuum overnight, $[IrCl_2(cod)][Li]$ was isolated as a bright yellow solid (763 mg, 68%). *See pg. 191 for NMR spectra.*

^{1}H NMR (500 MHz, THF-d_8) δ 4.20 (d, J = 2.7 Hz, 4H), 2.25 (d, J = 10.8 Hz, 4H), 1.55 (q, J = 7.8 Hz, 4H).

^{13}C NMR (126 MHz, THF-d_8) δ 62.73, 32.71.

Synthesis of $[IrCl_2(cod)][NBu_4]$.

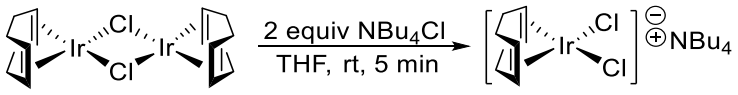

In a 20 mL scintillation vial, $[IrCl(cod)]_2$ (100 mg, 0.149 mmol, 1 equiv) was dissolved in dry THF (5 mL). The solution was transferred to a separate 20 mL scintillation vial charged with NBu_4Cl

(82.8 mg, 0.298 mmol, 2 equiv) and shaken with the cap on for 5 minutes where the solution instantly turned from orange to bright yellow. Using a Pasteur pipette, dry pentane (~10 mL) was added dropwise until the solution became cloudy then placed in a -42 °C glovebox freezer overnight. The top yellow layer was decanted, and the bottom brown layer was washed with additional dry pentane (2 x 10 mL). The pentane layers were collected and concentrated under vacuum to give $[IrCl_2(cod)][NBu_4]$ as a yellow solid (112 mg, 61%). Spectral data are in accordance with literature values.[29] *See pg. 193 for NMR spectra.*

^{1}H NMR (500 MHz, THF-d_8) δ 3.79 (d, *J* = 3.1 Hz, 4H), 3.45 – 3.36 (m, 8H), 2.07 – 2.04 (m, 4H), 1.80 – 1.73 (m, 8H), 1.47 (sx, *J* = 7.5 Hz, 8H), 1.24 (q, *J* = 7.7 Hz, 4H), 1.02 (t, *J* = 7.3 Hz, 12H).

^{13}C NMR (126 MHz, THF-d_8) δ 59.84, 58.32, 33.16, 25.28, 20.93, 14.39.

Synthesis of $[IrCl_2(cod)][NPr_4]$.

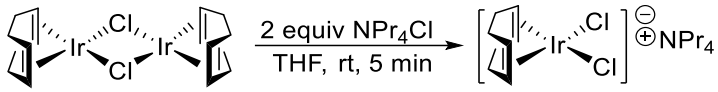

In a 20 mL scintillation vial, $[IrCl(cod)]_2$ (150 mg, 0.223 mmol, 1 equiv) and NPr_4Cl (99.1 mg, 0.447 mmol, 2 equiv) were dissolved in dry CH_2Cl_2 (15 mL) and vigorously shaken with the cap on for 5 minutes. The solvent was evaporated under vacuum to yield a bright yellow solid. The crude material was then dissolved in a minimal amount of dry 1,2-dichloroethane (~3 mL) and dry pentane was layered on top (~7 mL). The vial was then capped and kept at room temperature for 24 hours where a cloudy solution was observed. The vial was then placed in a -42 °C glovebox freezer for an additional 24 hours. The resulting precipitate was filtered and dried under vacuum to yield $[IrCl_2(cod)][NPr_4]$ as a yellow solid (116 mg, 50%). *See pg. 195 for NMR spectra.*

^{1}H NMR (500 MHz, CD_3CN) δ 3.78 (s, 4H), 3.08 – 3.03 (m, 8H), 2.11 (s, 4H), 1.69 – 1.61 (m 8H), 1.28 (s, 4H), 0.94 (t, *J* = 7.3 Hz, 12H).

^{13}C NMR (126 MHz, CD_3CN) δ 60.8 (t, *J* = 2.5 Hz, COD), 59.0 (m, COD), 32.5, 15.9, 10.7 (m, $CH_2CH_2\mathbf{C}H_3$).

Synthesis of [$IrCl_2$(cod)][NEt_4].

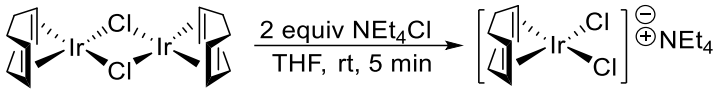

In a 20 mL scintillation vial, [IrCl(cod)]$_2$ (150 mg, 0.223 mmol, 1 equiv) and NEt_4Cl (74 mg, 0.447 mmol, 2 equiv) were dissolved in dry CH_2Cl_2 (15 mL) and vigorously shaken with the cap on for 5 minutes. The solvent was evaporated under vacuum to yield a bright yellow solid. The crude material was then dissolved in a minimal amount of dry 1,2-dichloroethane (~3 mL) and dry pentane was layered on top (~7 mL). The vial was then capped and kept at room temperature for 24 hours where a cloudy solution was observed. The vial was then placed in a -42 °C glovebox freezer for an additional 24 hours. The resulting precipitate was filtered and dried under vacuum to yield [$IrCl_2$(cod)][NEt_4] as a yellow solid (99.4 mg, 44%). *See pg. 197 for NMR spectra.*

^{1}H NMR (500 MHz, CD_3CN) δ 3.78 (s, 4H), 3.16 (q, *J* = 7.3 Hz, 8H), 2.12 (s, 4H), 1.27 (s, 4H), 1.21 (td, *J* = 7.3, 1.9 Hz, 12H).

3.7.3: Ir(I) Pre-catalyst Comparison

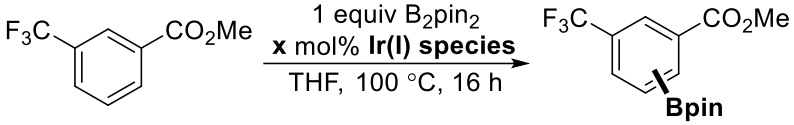

entry	Ir(I) species	x mol %	conversion[a]	selectivity (*o*:*m*)
1	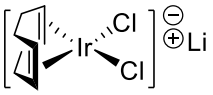	4[b]	13%	94:6
2	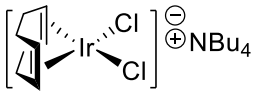	6	82%	49:51
3	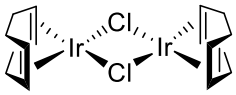	6	12%	59:41

[a]Conversions and selectivities were calculated by ^{1}H NMR of crude reaction mixture.[b]No reaction at 50 °C.

A. [IrCl$_2$(cod)][Li]

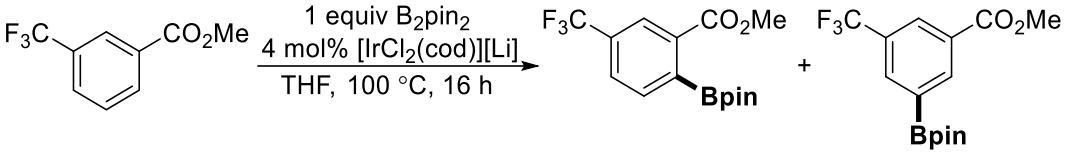

In a 20 mL scintillation vial, [IrCl(cod)]$_2$ (10 mg, 0.015 mmol, 1 equiv) and LiCl (1.3 mg, 0.03 mmol, 2 equiv) was dissolved in dry THF (4.5 mL, 0.0067 M stock solution). The vial was capped and stirred on a hot plate at room temperature for 10 minutes. Separately, a 5.0 mL Wheaton microreactor equipped with a conical stir bar was charged with B$_2$pin$_2$ (0.0635 g, 0.25 mmol, 1 equiv) and dry THF (0.5 mL). The [IrCl$_2$(cod)][Li] stock solution (3.8 mg, 0.01 mmol, 0.04 equiv) was then added, followed by the addition of methyl 3-(trifluoromethyl)benzoate (39.4 µL, 0.25 mmol, 1 equiv) using a glass Micro syringe. The vial was capped then taken out of the glovebox and stirred in a 4 x 4 aluminum block heated to 100 °C for 16 hours. NMR analysis of the crude

reaction mixture showed 13% conversion of starting material to the *ortho* to ester borylated product as the major isomer (*o*:*m* = 94:6).

B. [IrCl(cod)]$_2$

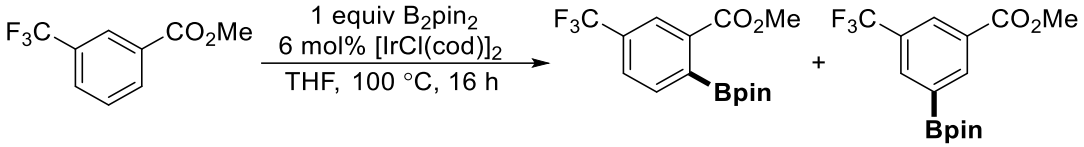

A 5.0 mL Wheaton microreactor equipped with a conical stir bar was charged with B_2pin_2 (0.0635 g, 0.25 mmol, 1 equiv), $[IrCl(cod)]_2$ (10 mg, 0.015 mmol, 0.06 equiv), and dry THF (1 mL). To this solution, methyl 3-(trifluoromethyl)benzoate (39.4 µL, 0.25 mmol, 1 equiv) was added using a glass Micro syringe. The vial was capped then taken out of the glovebox and stirred in a 4 x 4 aluminum block heated to 100 °C for 16 hours. NMR analysis of the crude reaction mixture showed 12% conversion of starting material to the *ortho* to ester borylated product as the major isomer (*o*:*m* = 59:41).

C. [IrCl$_2$(cod)][NBu$_4$]

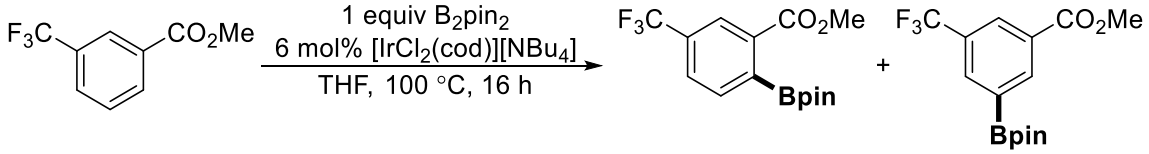

In a 20 mL scintillation vial, $[IrCl(cod)]_2$ (15.1 mg, 0.0224 mmol, 1 equiv) and NBu_4Cl (12.2 mg, 0.0439 mmol, 2 equiv) was dissolved in dry THF (4 mL). The vial was capped and stirred on a hot plate at room temperature for 10 minutes to yield the $[IrCl_2(cod)][NBu_4]$ stock solution (0.0112 M). Separately, a 5.0 mL Wheaton microreactor equipped with a conical stir bar and B_2pin_2 (0.0635 g, 0.25 mmol, 1 equiv) was charged with 1.3 mL of the $[IrCl_2(cod)][NBu_4]$ stock solution (8.9 mg,

0.015 mmol, 0.06 equiv) followed by methyl 3-(trifluoromethyl)benzoate (39.4 µL, 0.25 mmol, 1 equiv). The vial was capped then taken out of the glovebox and stirred in a 4 x 4 aluminum block heated to 100 °C for 16 hours. NMR analysis of the crude reaction mixture showed 82% conversion of starting material to a mixture of *ortho* to ester and *meta* borylated products (*o*:*m* = 49:51).

3.7.4: [IrCl$_2$(cod)][NR$_4$] Pre-catalysts in CHB

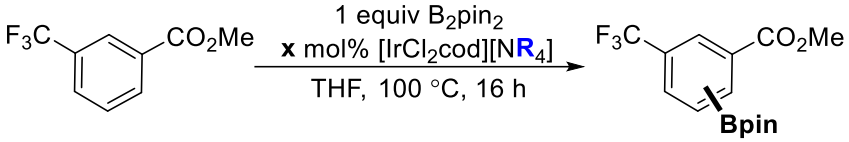

entry	R	x mol%	selectivity (*o*:*m*)	conversion (%)[a]
1	Et	2	---	NR
		6	---	NR
2	Pr	2	71:29	41
		6	64:36	90
3	Bu	2[b,c]	70:30	32
		3[b]	70:30	69
		4	56:44	68
		6	41:59	87
		6[d]	39:61	80
4	Hexyl	6[b]	35:65	84

[a]Conversions and selectivities were calculated by ^{1}H NMR of crude reaction mixture. [b] Pre-catalyst generatred in-situ.[c]Ran for 48 h. [d]Reaction set up in air. NR = no reaction.

Reactions were carried out following the general procedure in *section 3.7.7* below using the respective [IrCl$_2$(cod)][NR$_4$] pre-catalyst shown for each entry, and with the exception that the reaction was scaled down to use 0.25 mmol of substrate and B$_2$pin$_2$. Reactions where the [IrCl$_2$(cod)][NR$_4$] pre-catalyst is generated in-situ follow the procedure described in *section 3.7.3*, ***A*** with the exception that [NR$_4$][Cl] (R = Bu, Hexyl) salt is used instead of LiCl when reacting with [IrCl(cod)]$_2$. The procedure for the CHB reaction set up in air with [IrCl$_2$(cod)][NBu$_4$] as the pre-catalyst is described in *section 3.7.5* below.

3.7.5: CHB Reaction Sensitivity in Air

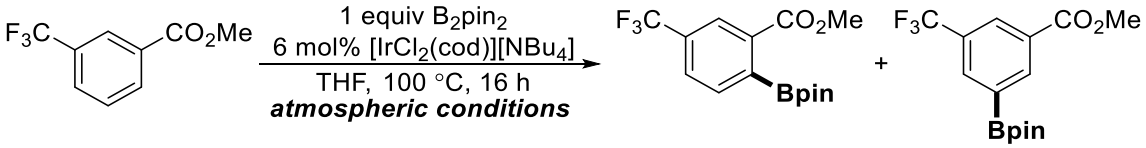

In a nitrogen filled glovebox, $[IrCl_2(cod)][NBu_4]$ (9.2 mg, 0.015 mmol, 0.06 equiv) and dry THF (0.5 mL) was added to a 20 mL scintillation vial and immediately taken out of the glovebox. Using non-oven dried equipment outside of the glovebox, B_2pin_2 (0.0635 g, 0.25 mmol, 1 equiv) was added to a 3.0 mL Wheaton vial. Using a Pasteur pipette, 0.5 mL of the $[IrCl_2(cod)][NBu_4]$ solution was then pipetted into the reaction vessel. 3-(trifluoromethyl)benzoate (39.4 μL, 0.25 mmol, 1 equiv) was then added using a glass micro syringe. The vial was capped then taken out of the glovebox and stirred in a 4 x 4 aluminum block heated to 100 °C for 16 hours. NMR analysis of the crude reaction mixture showed 80% conversion of starting material to a mixture of *ortho* to ester and *meta* borylated products (*o*:*m* = 39:61).

3.7.6: Pre-catalyst Stability

$[IrCl_2(cod)][NBu_4]$ (6.2 mg) solid that was isolated using the procedure described in *section 3.7.2* was added to a 20 mL scintillation vial. The vial was capped and kept on the benchtop for 350 days where the solid turned from bright yellow to dark brown. The ^1H NMR in THF-d_8 suggests that the material was oxidized, evidenced by the major impurities formed over time.

3.7.7: Procedure and Characterization of Borylated (Hetero)arenes

General Procedure for Borylation of (Hetero)arenes

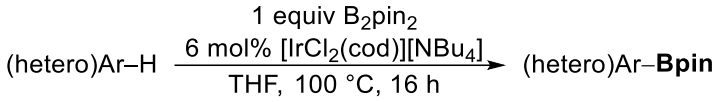

In a nitrogen-filled glovebox, B_2pin_2 (0.1270 g, 0.5 mmol, 1 equiv) was added to a 3.0 mL oven-dry Wheaton microreactor equipped with a conical stir bar. In a separate 20 mL scintillation vial, 0.053 or 0.059 M stock solutions of $[IrCl_2(cod)][NBu_4]$ was made in dry THF (2.0 or 2.2 mL). Using a 1 mL plastic syringe, the $[IrCl_2(cod)][NBu_4]$ stock solution (0.03 mmol, 0.06 equiv) was added followed by substrate (0.5 mmol, 1 equiv). Lastly, dry THF was added to the reaction vessel until the total reaction volume reached 1 mL (1.0 M reaction). The vial was capped then taken out of the glovebox and stirred in a 4 x 4 aluminum block heated to 100 °C for 16 h. After the reaction was complete, appropriate NMR spectra was obtained for the crude reaction mixture and volatiles were removed under vacuum. For isolated products, the crude material was dissolved in methylene chloride and purified by silica gel chromatography. The borylated products were isolated as the regioisomeric mixture.

Borylation of methyl 3-(trifluoromethyl)benzoate (3a)

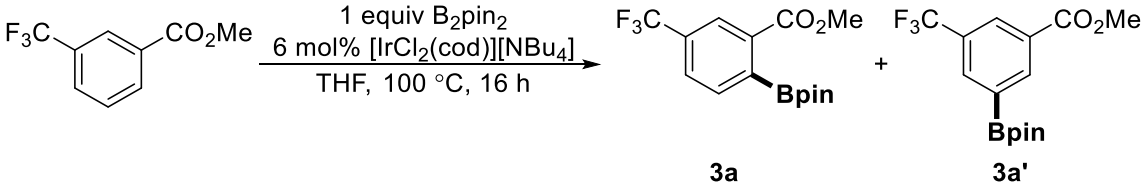

^{19}F NMR analysis of the crude reaction mixture showed 87% conversion of starting material to a mixture of regioisomers (*o*:*m* = 41:59). The material was passed through a short plug of SiO_2 eluting with 1% EtOAc in CH_2Cl_2. Fractions were collected and volatiles were removed under

rotary evaporation to yield a mixture of **3a** and **3a'** (*o*:*m* = 42:58) as a colorless oil (**0.1131 g, 79%**). Spectral data for **3a** are in accordance with literature values.[30] Full compound characterization of isolated **3a'** can be found in Chapter 2, section 2.5.7, pg. 104. *See pg. 198 for NMR spectra of this reaction.*

^{1}H NMR of 3a (500 MHz, $CDCl_3$) δ 8.20 (s, 1H), 7.76 (d, *J* = 7.7 Hz, 1H), 7.62 (d, *J* = 7.9 Hz, 1H), 3.96 (s, 3H), 1.42 (s, 12H).

^{1}H NMR of 3a' (500 MHz, $CDCl_3$) δ 8.62 (s, 1H), 8.37 (s, 1H), 8.23 (s, 1H), 3.96 (s, 3H), 1.36 (s, 12H).

^{19}F NMR of 3a (470 MHz, $CDCl_3$) δ -62.97.

^{19}F NMR of 3a' (470 MHz, $CDCl_3$) δ -62.72.

^{11}B NMR (160 MHz, $CDCl_3$) δ 30.84.

Borylation of 2-methylthiophene (3b)

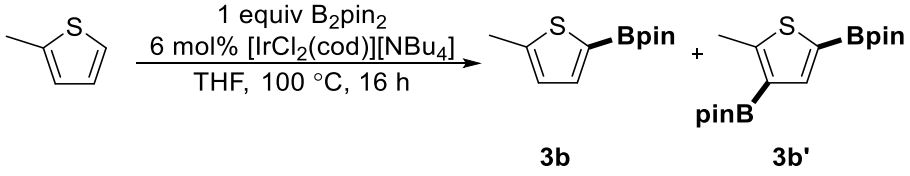

^{1}H NMR analysis of the crude reaction mixture showed >99% conversion of starting material to a mixture of regioisomers (**3b**:**3b'** = 91:9). The material was passed through a short plug of SiO_2 eluting with 1% EtOAc in CH_2Cl_2. Fractions were collected and volatiles were removed under rotary evaporation to yield a mixture of **3a** and **3a'** (**3b**:**3b'** = 58:42) as a colorless oil (**0.0293 g, 23%**). Spectral data are in accordance with literature values.[31,32] *See pg. 201 for NMR spectra.*

^{1}H NMR of 3b (500 MHz, $CDCl_3$) δ 7.44 (s, 1H), 6.84 (s, 1H), 2.53 (s, 1H), 1.30 (s, 12H). *(Sample ran was poorly shimmed for the worked-up mixture of regioisomers. The accurate J-coupling value and spectrum can be found in Chapter 2, sections 2.5.7 and 2.5.11, respectively.)*

^{1}H NMR of 3b' (500 MHz, $CDCl_3$) δ 7.83 (s, 1H), 2.71 (s, 3H), 1.31 (s, 12H), 1.30 (s, 12H).

^{11}B NMR (160 MHz, $CDCl_3$) δ 28.89.

Borylation of 1,3-dichlorobenzene (3c)

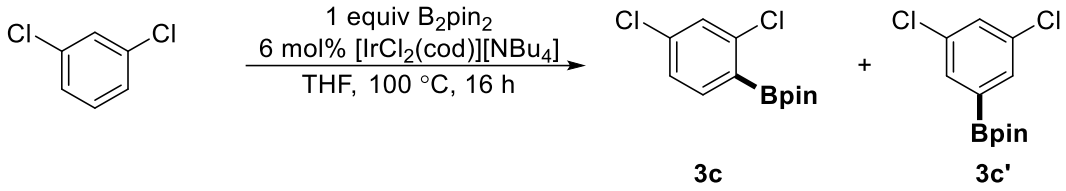

3c **3c'**

^{1}H NMR analysis of the crude reaction mixture showed 88% conversion of starting material to a mixture of regioisomers (**3c**:**3c**' = 21:79). The material was passed through a short plug of SiO_2 eluting with 1% EtOAc in CH_2Cl_2. Fractions were collected and volatiles were removed under rotary evaporation to yield a mixture of borylated products (**3c**:**3c**'=26:74) as a colorless oil (**0.0831 g, 69%**). Spectral data are in accordance with literature values.[33] *See pg. 203 for NMR spectra.*

^{1}H NMR of 3c (500 MHz, $CDCl_3$) δ 7.62 (d, *J* = 2.1 Hz, 1H), 7.37 (t, *J* = 1.9 Hz, 1H), 7.23 – 7.21 (m, 1H), 1.36 (s, 12H).

^{1}H NMR of 3c' (500 MHz, $CDCl_3$) δ 7.65 (s, 2H), 7.43 (d, *J* = 2.1 Hz, 1H), 1.34 (s, 12H).

^{11}B NMR (160 MHz, $CDCl_3$) δ 30.22.

Borylation of methyl 3-methoxybenzoate (3d)

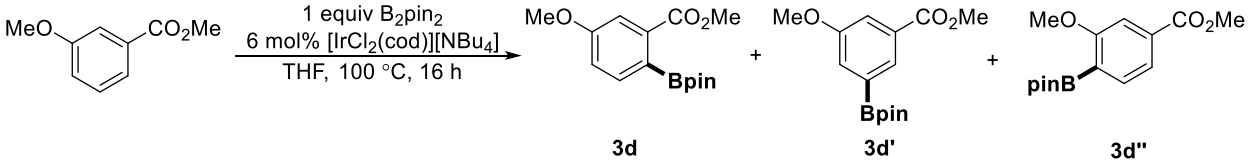

3d **3d'** **3d''**

^{1}H NMR analysis of the crude reaction mixture showed 33% conversion of starting material to a mixture of regioisomers (**3d**:**3d**':**3d"** = 43:36:21) and the reaction solvent was removed under vacuum. Spectral data are in accordance with literature values.[30,34,35] The resonances listed below

are only for the Csp^2–H protons due to the overlapping methyl peaks up-field from the starting material. *See pg. 205 for NMR spectra.*

^{1}H NMR of 3d (500 MHz, $CDCl_3$) δ 7.52-7.48 (m, 2H), 7.37 (t, *J* = 8.1 Hz, 1H), 7.23 – 7.21 (m, 1H), 1.36 (s, 12H).

^{1}H NMR of 3d' (500 MHz, $CDCl_3$) δ 8.05 (s, 1H), 7.51 (s, 1H). *(Csp^2–H resonance at ~7.65 ppm is buried under SM peak and is not reported here. See spectra in section 3.7.11 for details)*

^{1}H NMR of 3d" (500 MHz, $CDCl_3$) δ 7.70 (d, *J* = 9.5 Hz, 1H), 7.60 (d, *J* = 7.5 Hz, 1H), 7.49 (s, 1H)

^{11}B NMR (160 MHz, $CDCl_3$) δ 30.88.

Borylation of methyl 3-methoxybenzoate (3e)

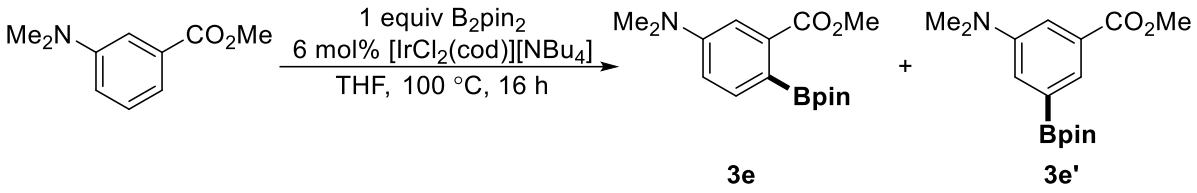

^{1}H NMR analysis of the crude reaction mixture showed 9% conversion of starting material to a mixture of regioisomers (**3e**:**3e'** = 40:60). Spectral data are in accordance with literature values.[36] Due to the low conversion, please refer to the reported values for the isolated regioisomers and the associated spectra in *sections 2.5.7* and *2.5.11*, respectively. *See pg. 207 for crude NMR spectra.*

Borylation of 1,3-dimethoxybenzene (3f)

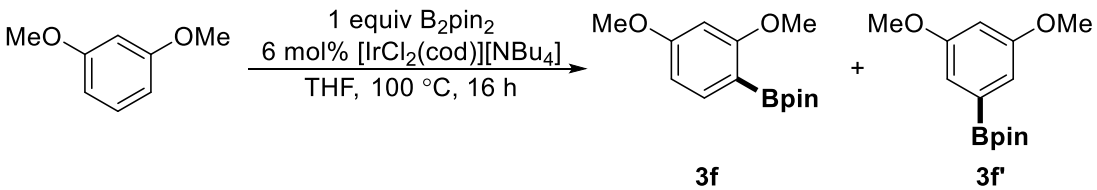

^{1}H NMR analysis of the crude reaction mixture showed 7% conversion of starting material to a mixture of regioisomers (**3f**:**3f'** = 1:>99). Spectral data are in accordance with literature values.[37] The resonances listed below are only for the Csp^2–H protons due to the overlapping methyl peaks up-field from the starting material and low conversion. *See pg. 208 for NMR spectra.*

^{1}H NMR of 3f' (500 MHz, $CDCl_3$) δ 8.05 (s, 1H), 7.51 (s, 1H).

3.7.8: Procedure and Characterization of Tri-Substituted Chlorinated Substrates

Borylation of 1,3,5-trichlorobenzene (3g)

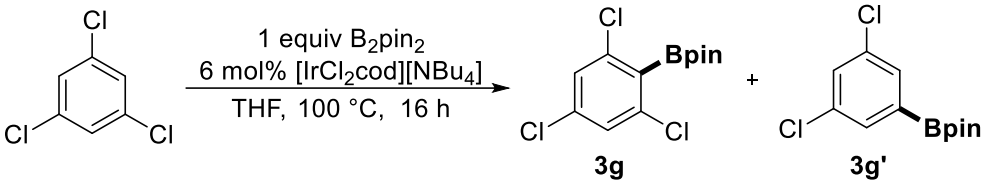

In a nitrogen-filled glovebox, B_2pin_2 (0.070 g, 0.275 mmol, 1 equiv) was added to a 3.0 mL oven-dry Wheaton microreactor equipped with a conical stir bar. In a separate 20 mL scintillation vial, a 0.033 M stock solution of $[IrCl_2(cod)][NBu_4]$ was made in dry THF (1.75 mL). Using a 1 mL plastic syringe, the $[IrCl_2(cod)][NBu_4]$ stock solution (0.5 mL, 0.0165 mmol, 0.06 equiv) was syringed into the reaction vessel followed by 1,3,5-trichlorobenzene (50 mg, 0.275 mmol, 1 equiv) resulting in a 1.13 M solution. The vial was capped then taken out of the glovebox and stirred in a 4 x 4 aluminum block heated to 100 °C for 16 h. After the reaction was complete, ^{1}H NMR spectra was obtained for the crude reaction mixture and volatiles were removed under vacuum. ^{1}H NMR analysis of the crude reaction mixture showed 34% conversion of starting material to a mixture of regioisomers (**3g**:**3g'** = 18:82). Spectral data are in accordance with literature values.[33,37] The ^{1}H NMR resonances listed below are only for the Csp^2–H protons due to the overlapping methyl peaks up-field from the starting material and low conversion. See crude spectra for details.

Note: The starting material had impurities that were found to be 1,3-dichlorobenzene. To highlight this, the ^{1}H NMR of 1,3,5-trichlorobenzene is shown on the crude spectra where the impurities from the SM are present. *See pg. 209 for NMR spectra.*

^{1}H NMR of 3g (500 MHz, C_6D_6) δ 6.82 (s, 2H).

^{1}H NMR of 3g' (500 MHz, C_6D_6) δ 7.85 (d, *J* = 2.1 Hz, 2H), 7.51 (t, *J* = 2.0 Hz, 1H).

^{11}B NMR (160 MHz, C_6D_6) δ 30.26.

Borylation of 1,3-dichloro-5-fluorobenzene (3h)

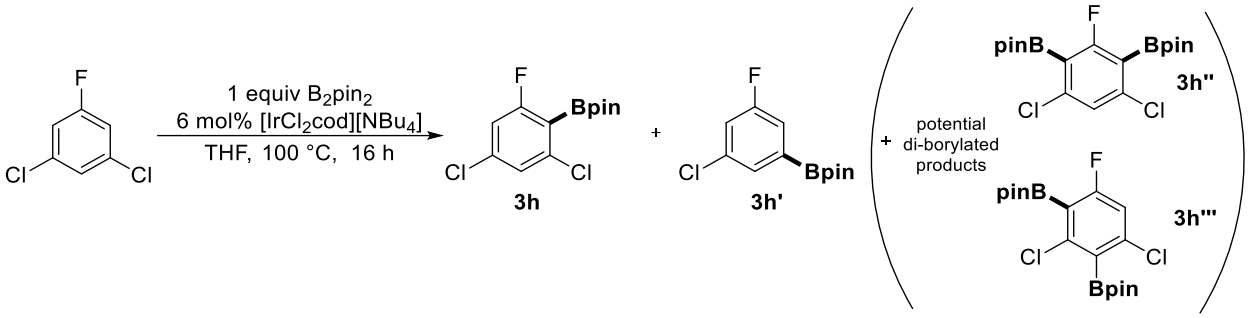

In a nitrogen-filled glovebox, B_2pin_2 (0.070 g, 0.275 mmol, 1 equiv) was added to a 3.0 mL oven-dry Wheaton microreactor equipped with a conical stir bar. In a separate 20 mL scintillation vial, a 0.033 M stock solution of $[IrCl_2(cod)][NBu_4]$ was made in dry THF (1.75 mL). Using a 1 mL plastic syringe, the $[IrCl_2(cod)][NBu_4]$ stock solution (0.5 mL, 0.0165 mmol, 0.06 equiv) was syringed into the reaction vessel followed by 1,3-dichloro-5-fluorobenzene (32 μL, 0.275 mmol, 1 equiv) resulting in a 1.13 M solution. The vial was capped then taken out of the glovebox and stirred in a 4 x 4 aluminum block heated to 100 °C for 16 h. After the reaction was complete, ^{1}H NMR spectra was obtained for the crude reaction mixture and volatiles were removed under vacuum. ^{19}F NMR analysis of the crude reaction mixture showed 49% conversion of starting material to a mixture of regioisomers (**3h**:**3h**':**3h'':3h''':**other = 60:28:3:2:7). Spectral data are in

accordance with literature values for **3h** and **3h'**.[38,39] The ^{1}H NMR resonances listed below are only for the Csp^{2}–H protons due to the overlapping methyl peaks up-field from the starting material and low conversion. See crude spectra for details.

Note: Literature values have not been reported for di-borylated products of **3h"** and **3h'"**. These regioisomers were not isolated to confirm their structural connectivity. Given the relative isotopic abundance of ^{19}F vs ^{1}H, we used the ^{19}F NMR to assign what we believe are regioisomers based on the chemical shift and J-coupling values of the respective regioisomer shown in the scheme above. GC data has proven di-borylated products. In addition, products **3h** and **3h"** are the only products observed in the control reactions listed below with dtbpy for this substrate (as expected), where the ^{19}F resonances match what has been assigned here.

The "other" regioisomer is shown in the ^{19}F NMR at -110.7 (q, J = 7.2 Hz) is unassigned on the spectra and the chemical structure is unknown. We do believe it's likely a product absent of the chlorine atoms on the molecule based on the ^{19}F chemical shifts for regioisomers of borylated and di-borylated fluorobenzene compounds. The closest resemblance to this would be 3,5-Bis(4,4,5,5,-tetramethyl-1,3,2-dioxaborole)fluorobenzene, where in the ^{19}F NMR it is reported to be at -115.6 (t, J = 9.1 Hz) in $CDCl_3$, however the ^{1}H NMR spectra could not be compared due to the low concentration of product in the sample.[40] *See pg. 211 for NMR spectra.*

^{1}H NMR of 3h (500 MHz, C_6D_6) δ *6.82 (dd, J = 1.7, 1.0 Hz, 1H), 6.48 (dd, J = 8.2, 1.7 Hz, 1H).
*Literature reports this to be a triplet. This splitting pattern has been seen in the crude reaction mixture previously. However, this spectra appears to have better shimming and thus am reporting this as a doublet of doublets as shown in the spectra.

^{1}H NMR of 3h' (500 MHz, C_6D_6) δ 7.82 (d, J = 1.6 Hz, 1H), 7.55 (dd, J = 8.3, 2.5 Hz), 6.87 (dt, J = 8.6, 2.2, 1H).

^{19}F NMR of 3h (470 MHz, C_6D_6) δ -100.75 (d, J = 8.3 Hz).

^{19}F NMR of 3h' (470 MHz, C_6D_6) δ -111.43 (t, J = 8.8 Hz).

^{19}F NMR of 3h" (470 MHz, C_6D_6) δ -91.43 (s).

^{19}F NMR of 3h"' (470 MHz, C_6D_6) δ -103.56 (d, *J* = 8.2 Hz).

^{11}B NMR (160 MHz, $CDCl_3$) δ 30.23.

3.7.9: Control Reactions of Chlorinated Substrates

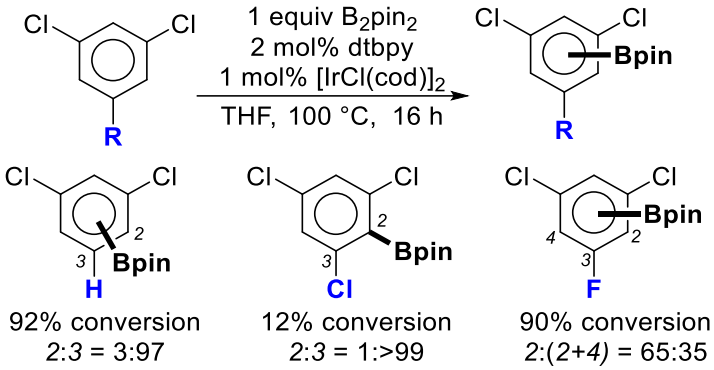

In a nitrogen-filled glovebox, B_2pin_2 (0.070 g, 0.275 mmol, 1 equiv) was added to a 3.0 mL oven-dry Wheaton microreactor equipped with a conical stir bar. In separate 20 mL scintillation vials, stock solutions of dtbpy (0.037 M) and $[IrCl(cod)]_2$ (0.015 M) were made in dry THF. Using a 1 mL plastic syringe, $[IrCl(cod)]_2$ (185 µL, 0.00275 mmol, 0.01 equiv) was syringed into the solution and stirred for 1 minute. To the reaction vessel, dtbpy (147 µL, 0.0055 mmol, 0.02 equiv) was added followed by substrate (0.275 mmol, 1 equiv). Dry THF (0.23 mL) was added to make a 1M solution. The vial was capped then taken out of the glovebox and stirred in a 4 x 4 aluminum block heated to 100 °C for 16 h where the reaction solution turned from dark purple to dark brown. After the reaction was complete, appropriate NMR spectra was obtained for the crude reaction mixture and volatiles were removed under vacuum.

3.7.10: Oil Bath Kinetics

A. Formula to Calculate Molarity from Internal Standard Using ^{1}H NMR

Step 1: Solve for mmols of compound.

$$N_c = [(\frac{\int_C}{H_C}) \div (\frac{\int_{IS}}{H_{IS}})] \text{ x } N_{IS}$$

Step 2: Solve for molarity of the compound in the reaction.

$$[M]_c = \frac{\mathrm{N}_c}{\mathrm{V}}$$

$\int$ = Integration of selected peak in ^{1}H NMR
H = # of protons corresponding to peak integrated
N = # of mmols
C = Compound
IS = Internal stzandard
[M] = Molarity
V = Total volume of the reaction in mL

B. General Procedure and Considerations for Kinetic Experiments

All reactions were carried out in a nitrogen-filled glovebox. Commercially available dry THF-d_8 was taken from the ampule and poured into a round bottom flask. Connected to a high vacuum Schlenk line, the solvent was put under static vacuum and stirred in 3Å molecular sieves overnight. The solution was freeze-pump-thawed x 3 and vacuum transferred to a Schlenk tube to store in the glovebox. The glovebox was purged for 1 hour prior to opening the tube. A Karl Fischer Titrator was used to ensure <5 ppm of water was in the solvent before all reaction setups. All reagents besides the substrate were made as a stock solution in THF-d_8 and added to a 7'' J-young pressure tube with a screw Teflon cap. All stock solutions were made fresh.

The [$IrCl_2$(cod)][NBu_4] was purified and isolated as a solid prior to making the pre-catalyst stock solution. For reactions that used a different batch of pre-catalyst, a standard CHB reaction was set up according to the general procedure. In all cases, the results between both reactions were identical. The internal standard chosen was 1,3,5-trimethoxy benzene as experiments show this

does not undergo chemical transformations under reaction conditions used for kinetic analysis. The internal standard was referenced to 6.04 ppm in the ^{1}H NMR and integrated to 1 prior to spectral analysis. All calculations were based on the mmol amount of the internal standard used in the reaction as shown in the prior section.

All other spectral data was recorded on a Bruker Avance III HD 500 MHz NMR with a 5mm HX double resonance iProbe. For all reactions, an NMR was taken at t = 0 then monitored by heating in a 100 °C oil bath. At all time points during reaction monitoring, the tube was taken out of the oil bath and cleaned with n-hexanes until all excess oil was removed. The tube was able to be held by hand as it had cooled significantly by the time data was ready to be collected. It should be noted that the reaction could not be done by heating the tube in the NMR as the S/N was extremely poor. At the end of the reaction, molarities of COD and the $-CH_2$ of NBu_4 cation are shown as independent species that originated from the pre-catalyst due to the breakdown of $[IrCl_2(cod)][NBu_4]$ after the induction period (*described in section 3.3.3*). All observations regarding black solid generation during the induction period for these reactions can be found in section 3.4.1. ^{19}F NMR data was taken when methyl 3-(trifluoromethyl)benzoate was used as the substrate to ensure integration of the substrate and borylated product matched with the ^{1}H NMR spectra. ^{11}B coupled and decoupled NMR spectra was obtained at the end of each reaction. Valuable data could not be obtained from these spectra as they uniformly showed borylated product, left over B_2pin_2, and boron side products.

C. Chemical Shifts Integrated to Obtain Molarities of Species

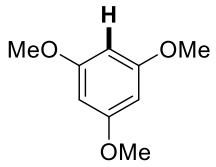

internal standard

H = δ 6.04 (s, 3H)

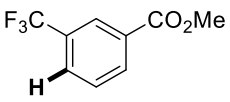

arene starting material

H = δ 7.90 (dt, *J* = Hz, 1H)

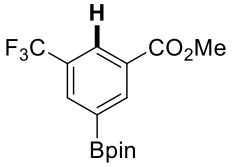

meta borylated product

H = δ 8.58 (s, 1H)

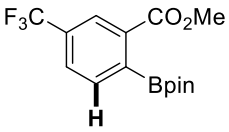

ortho borylated product

H = δ 7.82 (dd, *J* = 7.8, 1 Hz, 1H)

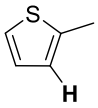

heteroarene starting material

H = δ 6.71 (m, 1H)

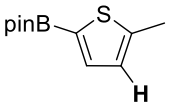

borylated heteroarene

H = δ 7.33 (d, *J* = 2.9 Hz,1H)

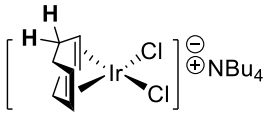

[IrCl$_2$(**cod**)[NBu$_4$]

H = δ 2.05 (m, 4H)

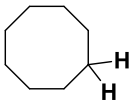

cyclooctane

H = δ 1.53 (m, 16H)

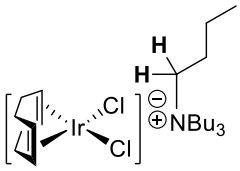

pre-catalyst

H = δ 3.45 - 3.36 (m, 8H)

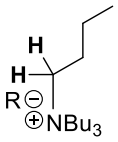

[R][NBu$_4$]*

H = δ 3.45 - 3.36 ± 0.2 (m, 8H)

* Shifting occurs throughout reaction (*see section 3.3.3)*
*Does not overlap with other peaks and can clearly assign based on splitting

D. Triplicate Kinetic Reaction 3.1a *(Corresponding to Figure 3.1)*

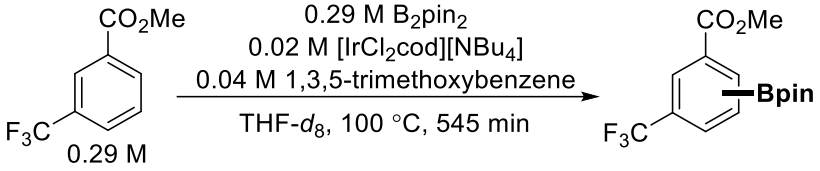

[M] of Reagents at t=0 in 0.6 mL THF-d_8

Reagent	Peak Integration	mmols	[M]
Substrate	2.54	0.171	0.286
[Ir(cod)Cl$_2$][NBu$_4$]	1.45	0.0122	0.0204
Internal Standard	1	0.0225	0.0375

[M] of Reagents and Products at t =545 min

Compound	Peak Integration	mmols	[M]
Substrate	1.29	0.0871	0.145
Internal Standard	1	0.0225	0.0375
[Ir(**cod**)Cl$_2$][NBu$_4$]	0	0	0
[R][**NBu$_4$**]	0.49	0.00413	0.00689
Cyclooctane	1.70	0.00717	0.0120
meta product	0.94	0.0635	0.106
ortho product	0.11	0.00743	0.0124

Conversion = 49%, o:m selectivity = 10:90

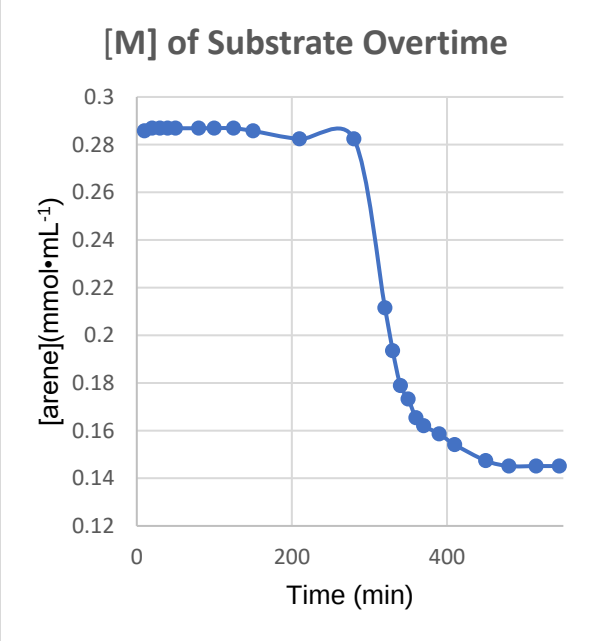

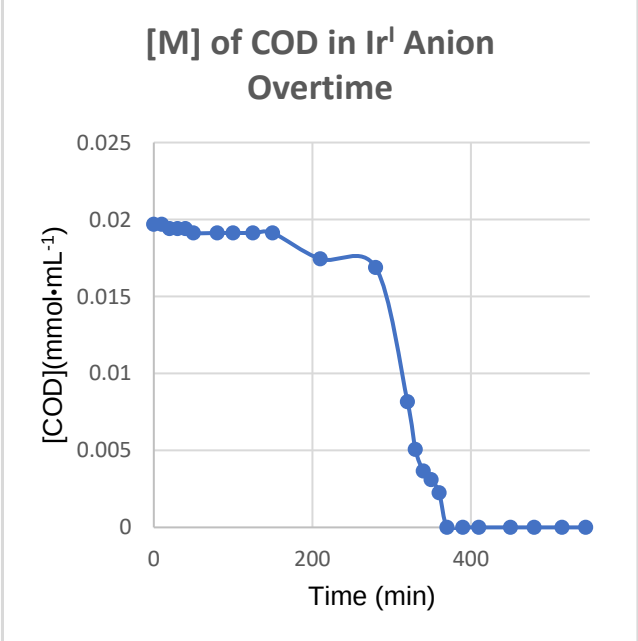

E. Triplicate Kinetic Reaction 3.1b *(Corresponding to Figure 3.1)*

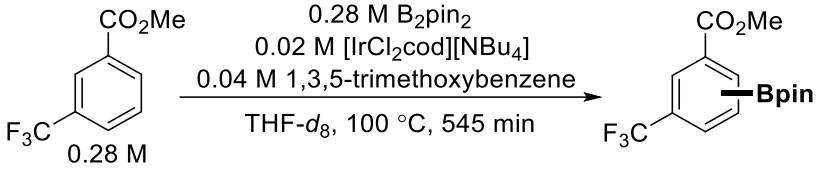

[M] of Reagents at t=0 in 0.6 mL THF-d_8

Reagent	Peak Integration	mmols	[M]
Substrate	2.43	0.164	0.284
[Ir(cod)Cl_2][NBu_4]	1.50	0.0127	0.0211
Internal Standard	1	0.0225	0.0375

[M] of Reagents and Products at t =545 min

Compound	Peak Integration	mmols	[M]
Substrate	1.2	0.0810	0.135
Internal Standard	1	0.0225	0.0375
[Ir(**cod**)Cl_2][NBu_4]	0	0	0
[R][**NBu_4**]	0.54	0.00456	0.00759
Cyclooctane	1.8	0.00759	0.0127
meta product	0.94	0.0635	0.106
ortho product	0.08	0.00540	0.0090

Conversion = 51%, o:m selectivity = 8:92

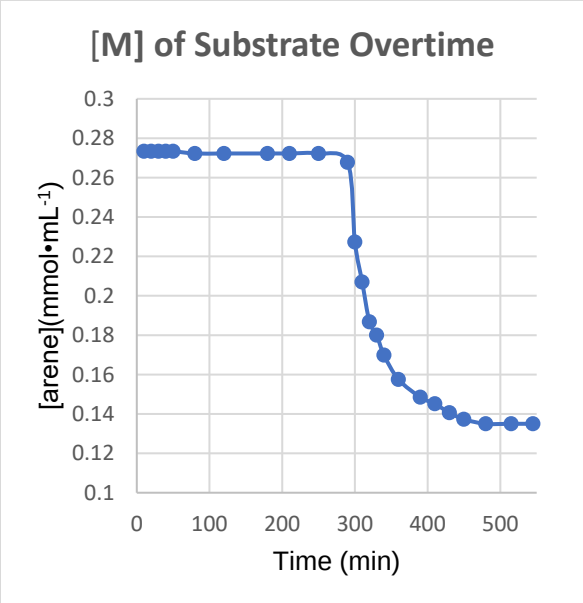

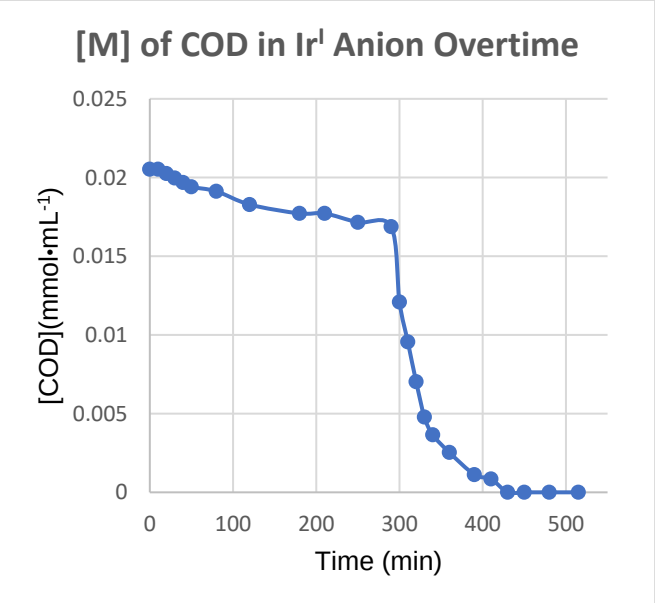

F. Triplicate Kinetic Reaction 3.1c *(Corresponding to Figure 3.1)*

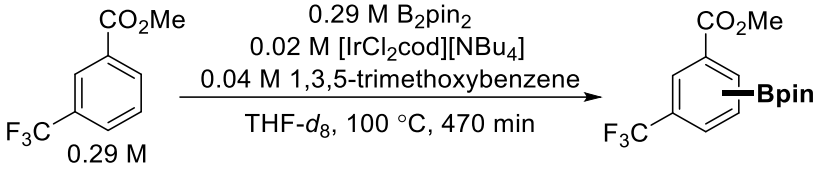

[M] of Reagents at t = 0 in 0.6 mL THF-d_8

Reagent	Peak Integration	mmols	[M]
Substrate	2.48	0.174	0.290
[Ir(cod)Cl_2][NBu_4]	1.46	0.0123	0.0205
Internal Standard	1	0.0225	0.0375

[M] of Reagents and Products at t =475 min

Compound	Peak Integration	mmols	[M]
Substrate	1.27	0.0857	0.143
Internal Standard	1	0.0225	0.0375
[Ir(**cod**)Cl_2][NBu_4]	0	0	0
[R][**NBu_4**]	0.64	0.00540	0.0090
Cyclooctane	1.77	0.00747	0.0124
meta product	0.91	0.0614	0.102
ortho product	0.10	0.00675	0.0113

Conversion = 51%, o:m selectivity = 10:90

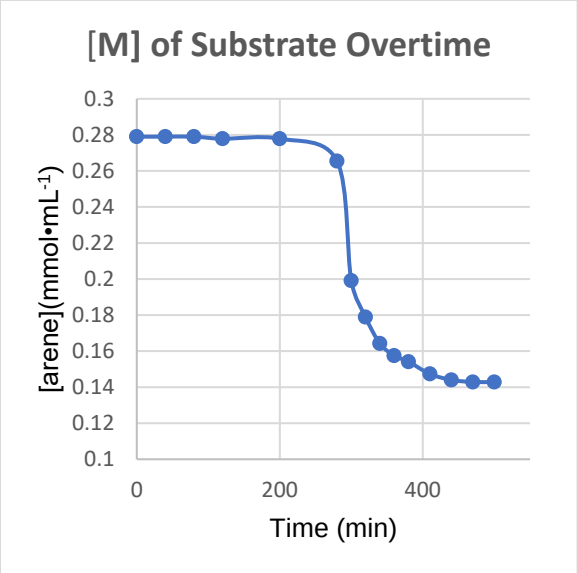

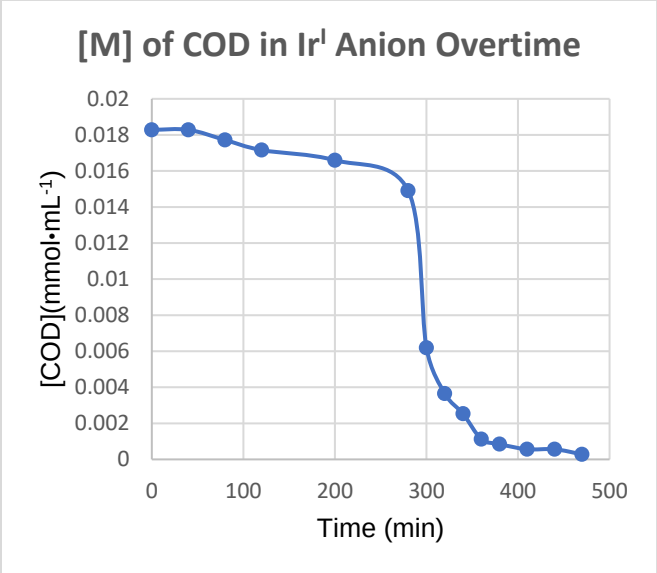

G. Kinetic Reaction 3.2 *(Corresponding to Figure 3.2)*

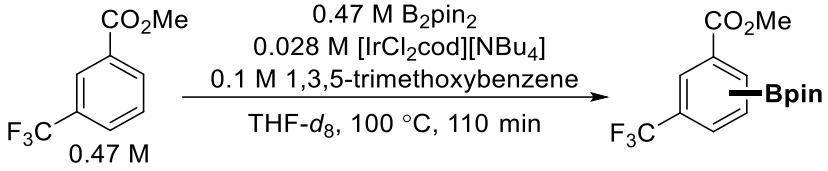

[M] of Reagents at t=0 in 0.75 mL THF-d_8

Reagent	Peak Integration	mmols	[M]
Substrate	1.58	0.356	0.474
[Ir(cod)Cl_2][NBu_4]	0.86	0.0222	0.0278
Internal Standard	1	0.075	0.107

[M] of Reagents and Products at t =110 min

Compound	Peak Integration	mmols	[M]
Substrate	0.29	0.0653	0.087
Internal Standard	1	0.075	0.107
[Ir(**cod**)Cl_2][NBu_4]	0	0	0
[R][**NBu_4**]	0.77	0.0217	0.0289
Cyclooctane	0.98	0.0136	0.0195
meta product	0.54	0.122	0.174
ortho product	0.76	0.160	0.228

Conversion = 82%, o:m selectivity = 57:43

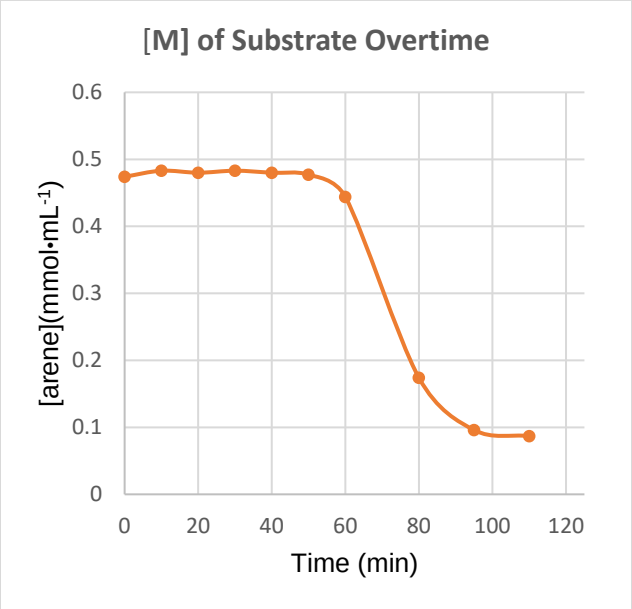

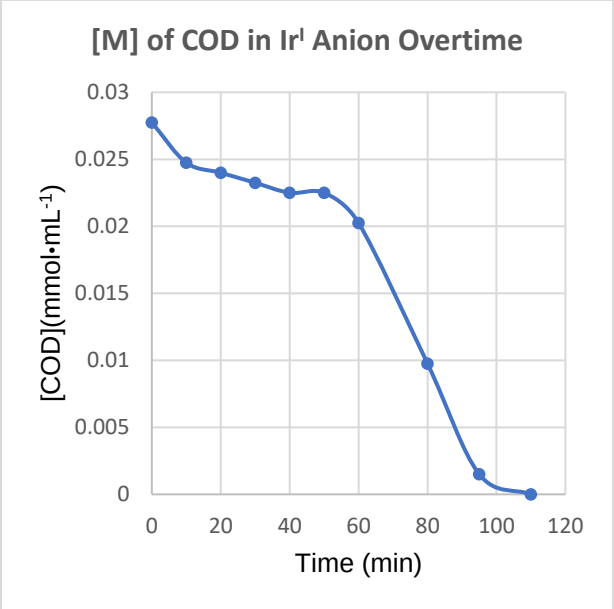

H. Kinetic Reaction 3.3 *(Corresponding to Figure 3.2)*

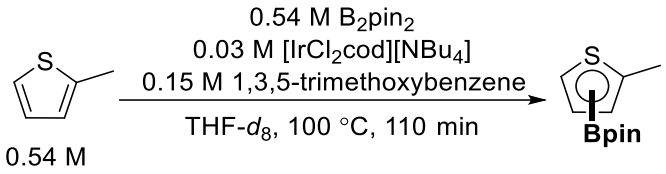

[M] of Reagents at t=0 in 0.70 mL THF-d_8

Reagent	Peak Integration	mmols	[M]
Substrate	1.19	0.375	0.536
[Ir(cod)Cl_2][NBu_4]	0.41	0.0323	0.0461
Internal Standard	1	0.105	0.150

[M] of Reagents and Products at t =110 min

Compound	Peak Integration	mmols	[M]
Substrate	0.31	0.0977	0.140
Internal Standard	1	0.105	0.150
[Ir(**cod**)Cl_2][NBu_4]	0	0	0
[R][**NBu_4**]	0	0	0
Cyclooctane	1.01	0.0199	0.0284
mono-borylated product	0.88	0.277	0.396

Conversion = 74%, mono:di-borylated selectivity = >99:1

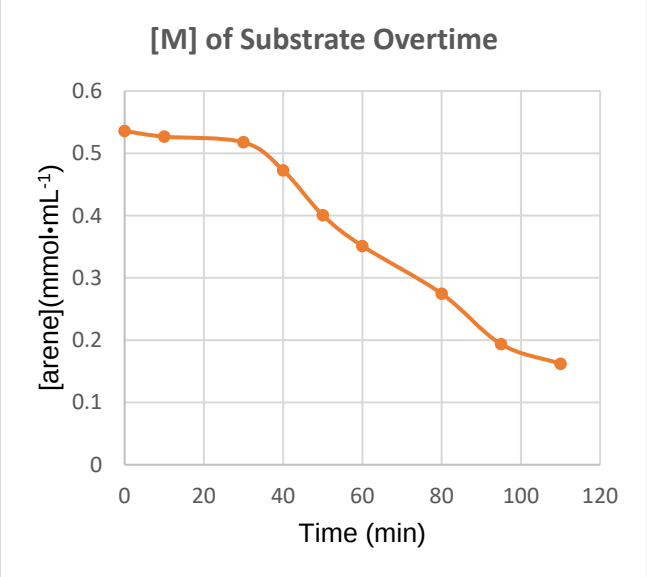

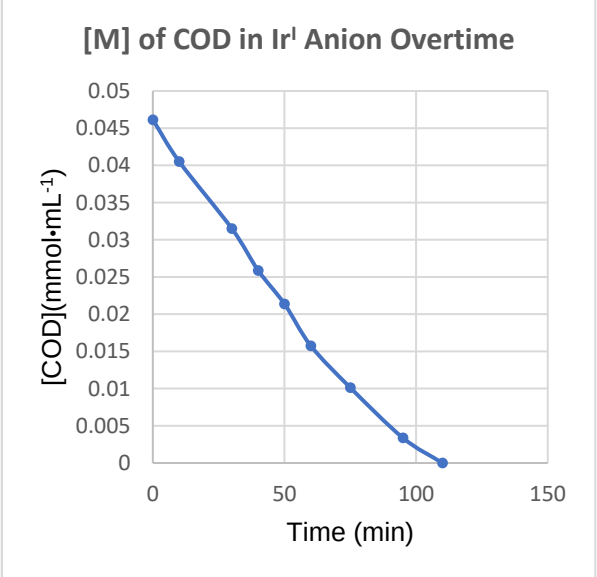

I. Kinetic Reaction 3.4 *(Corresponding to Figure 3.3)*

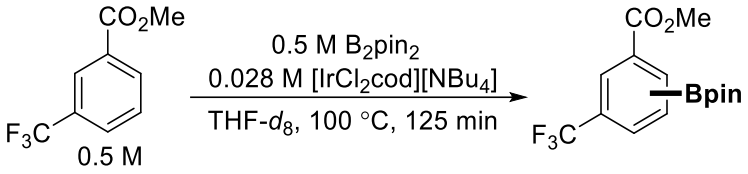

Note: [M] are assumed based on weighed amounts of reagent and conversion to regioisomers.

[M] of Reagents at t = 10 min in 0.75 mL THF-d_8

Reagent	Peak Integration	mmols	[M]
Substrate	1	0.375	0.500
[Ir(cod)Cl$_2$][NBu$_4$]	0.59	0.0277	0.0369

[M] of Reagents and Products at t =125 min

Compound	Peak Integration	mmols	[M]
Substrate	0.67	0.113	0.151
meta product + *ortho* product	1.53	0.263	0.351

Conversion = 70%, o:m selectivity = 65:35

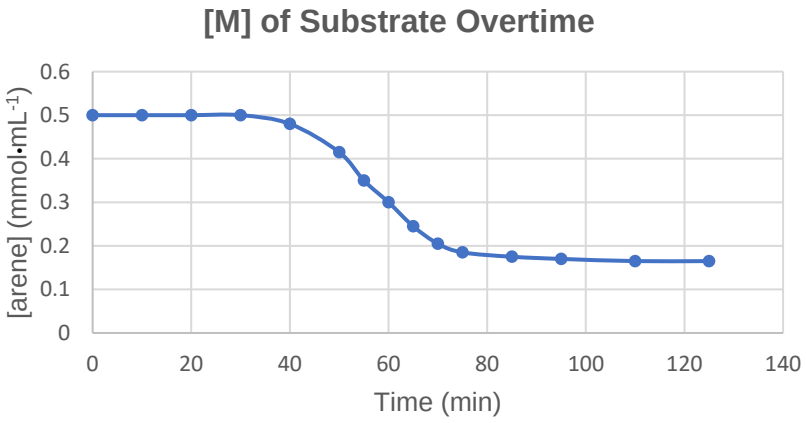

3.7.11: Mercury Drop Tests

A. Addition of Mercury at t = 0 with [$IrCl_2$(cod)][NBu_4]

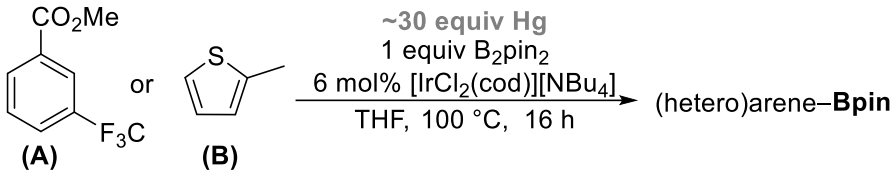

(A) **(B)**

Substrate	Hg addition	Conversion
A	Yes	0%
A	No	88%
B	Yes	0%
B	No	96%

In a nitrogen-filled glovebox, B_2pin_2 (0.0635 g, 0.25 mmol, 1 equiv) was added to a 3.0 mL oven-dry Wheaton microreactor equipped with a conical stir bar. In a separate 20 mL scintillation vial, a 0.024 M stock solution of [$IrCl_2$(cod)][NBu_4] was made in dry THF (3 mL). Using a 1 mL plastic syringe, the [$IrCl_2$(cod)][NBu_4] stock solution (0.615 mL, 0.015 mmol, 0.06 equiv) was added followed by substrate (0.25 mmol, 1 equiv). The vial was capped then taken out of the glovebox. For the reactions *with* mercury, the caps were quickly taken off the vial in air and Hg(0) (0.1 mL, 7.5 mmol, 30 equiv) was added over a 5 second period using a 5 mL Luer Lock syringe with long plastic tubing before recapping the vial. For the reaction without mercury, the cap was taken off and the reaction was exposed to air for ~7 seconds before recapping. All vials were transferred to a 4 x 4 aluminum block heated to 100 °C and stirred for 16 h. After the reaction was complete, appropriate NMR spectra was obtained for the crude reaction mixture.

B. Addition of Mercury at t = 0 with [IrCl(cod)]$_2$ and dtbpy

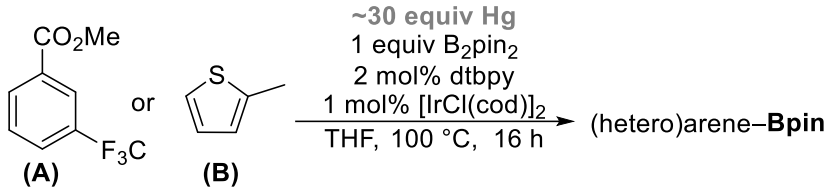

Substrate	Hg addition	Conversion
A	Yes	84%
A	No	88%
B	Yes	>99%
B	No	93%

In a nitrogen-filled glovebox, B_2pin_2 (0.0635 g, 0.25 mmol, 1 equiv) was added to a 3.0 mL oven-dry Wheaton microreactor equipped with a conical stir bar. In a separate 20 mL scintillation vial, stock solutions of [IrCl(cod)]$_2$ (0.01 M) and dtbpy (0.02 M) was made in dry THF. Using a 1 mL plastic syringe, [IrCl(cod)]$_2$ (0.25 mL, 0.0025 mmol, 0.01 equiv) was syringed into the solution and stirred for 1 minute. To the reaction vessel, dtbpy (0.25 µL, 0.005 mmol, 0.02 equiv) was added followed by substrate (0.25 mmol, 1 equiv). The vial was capped then taken out of the glovebox. For the reactions *with* mercury, the caps were quickly taken off the vial in air and Hg(0) (0.1 mL, 7.5 mmol, 30 equiv) was added over a 5 second period using a 5 mL Luer Lock syringe with long plastic tubing before recapping the vial. For the reaction without mercury, the cap was taken off and the reaction was exposed to air for ~7 seconds before recapping. All vials were transferred to a 4 x 4 aluminum block heated to 100 °C and stirred vigorously. After 16 h, ^{1}H or ^{19}F NMR data of the crude reaction mixture was obtained to calculate the conversions displayed in the scheme.

C. Addition of 30-310 equiv Mercury at >30 % Conversion with $[IrCl_2(cod)][NBu_4]$

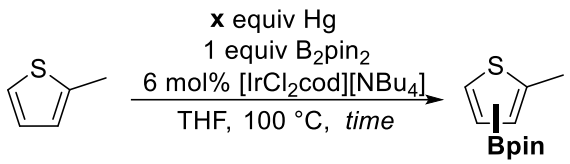

A. 30 equiv Hg

time (h)	conversion
1.5	13%
2	30%
••••• *Hg addition* •••••	
16	50%

B. 310 equiv Hg

time (h)	conversion
2.5	61%
••••• *Hg addition* •••••	
16	88%

Reaction setup follows the general procedure for CHB. Reaction A is set up on a 0.25 mmol scale of substrate in a 3.0 mL Wheaton microreactor with 1 mL of a 0.03 M $[IrCl_2(cod)][NBu_4]$ stock solution. Reaction B is set up on a 0.50 mmol scale of substrate in a 5.0 mL Wheaton microreactor with 0.5 mL of a 0.03 M $[IrCl_2(cod)][NBu_4]$ stock solution. Described below is the addition of mercury **after** the induction period.

After reaction setup, the vial was capped and taken out of the glovebox. All vials were transferred to a 4 x 4 aluminum block heated to 100 °C and monitored by ^{1}H NMR. After reaction was monitored every 20-30 minutes until > 30% conversion was reached. The reaction vessels were then taken off the hot plate and allowed to cool to room temperature. Hg(0) (reaction A = 0.1 mL, 7.5 mmol, 30 equiv / reaction B = 2.3 mL, 155 mmol, 310 equiv) was added over 5-10 seconds and the vial was recapped. The reaction vessels were clamped at a 45° angle over a stir plate and vigorously stirred at room temperature for 10 min to ensure intimate contact of the solution with Hg(0). All vials were transferred back to the 4 x 4 aluminum block heated to 100 °C and stirred for 16 h. After 16 h, ^{1}H NMR data of the crude reaction mixture was obtained to calculate the conversions displayed in the scheme.

D. Control Reaction with [$IrCl_2(cod)$][NBu_4] and Hg(0)

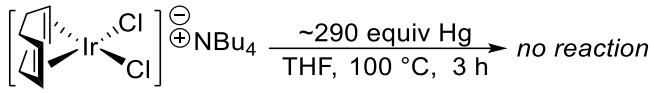

In a nitrogen-filled glovebox, [$IrCl_2(cod)$][NBu_4] (14.1 mg, 0.023 mmol, 1 equiv) was added to a 5.0 mL oven-dry Wheaton microreactor equipped with a conical stir bar. The pre-catalyst was dissolved in dry THF (0.5 mL) then capped and taken out of the glovebox. The cap was quickly removed in air and Hg(0) (0.1 mL, 6.7 mmol, 287 equiv) was added over a 5 second period before recapping the vial. The vial was clamped at a 45° angle and vigorously stirring in an oil bath heated to 100 °C for 3 hours where no color change was observed. After the reaction was complete, the solution was decanted away from the Hg(0) and pumped down under vacuum. The resulting solid was dissolved in ~0.6 mL of THF-d_8 where ^{13}C and ^{1}H NMR data showed no structure change of the anion.

3.7.12: Spectral Data

^{1}H NMR spectrum of [$IrCl_2$(cod)][Li] (500 MHz, THF-d_8)

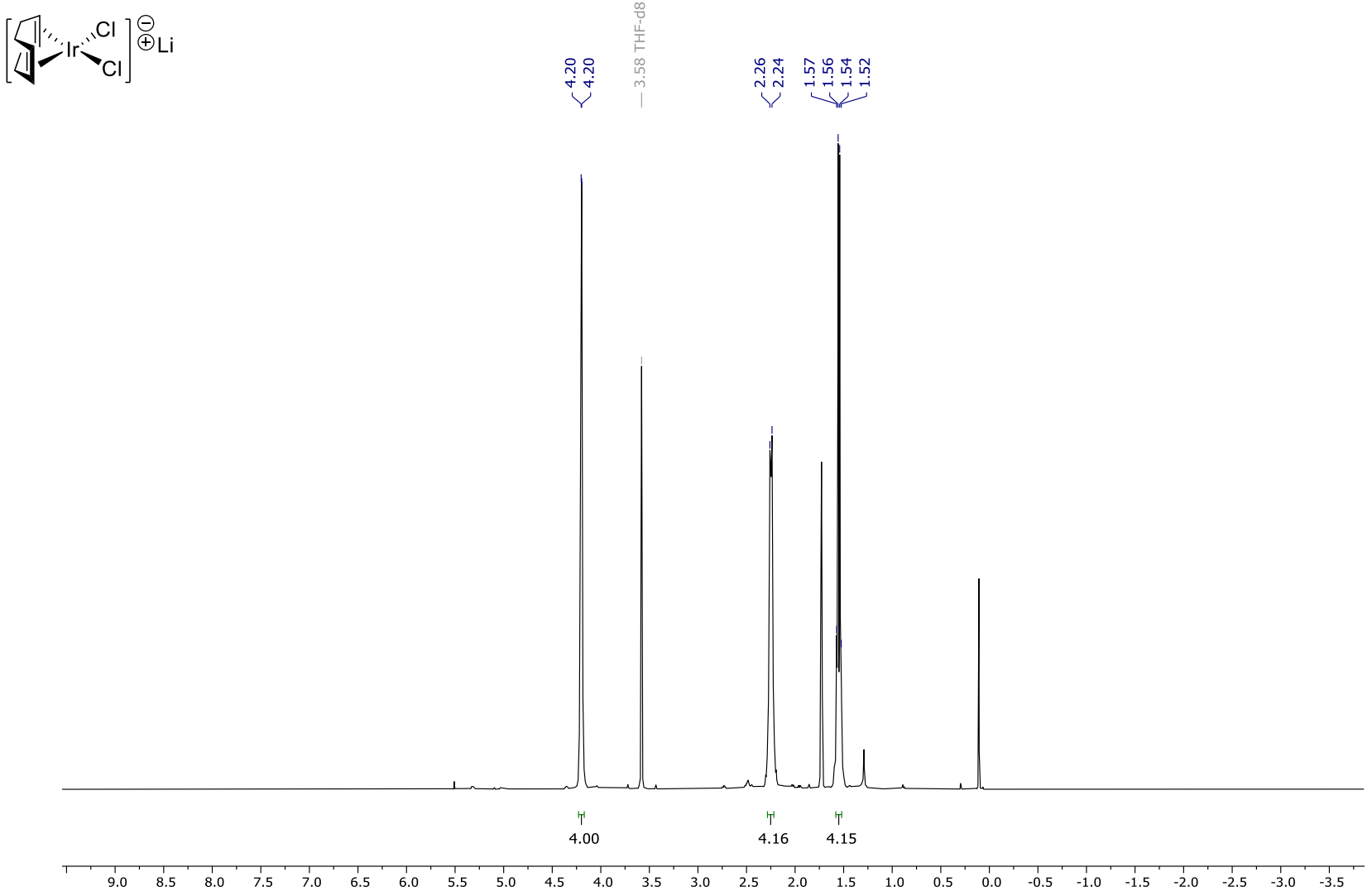

$^{13}C\{^{1}H\}$ NMR spectrum of $[IrCl_2(cod)][Li]$ (126 MHz, THF-d_8)

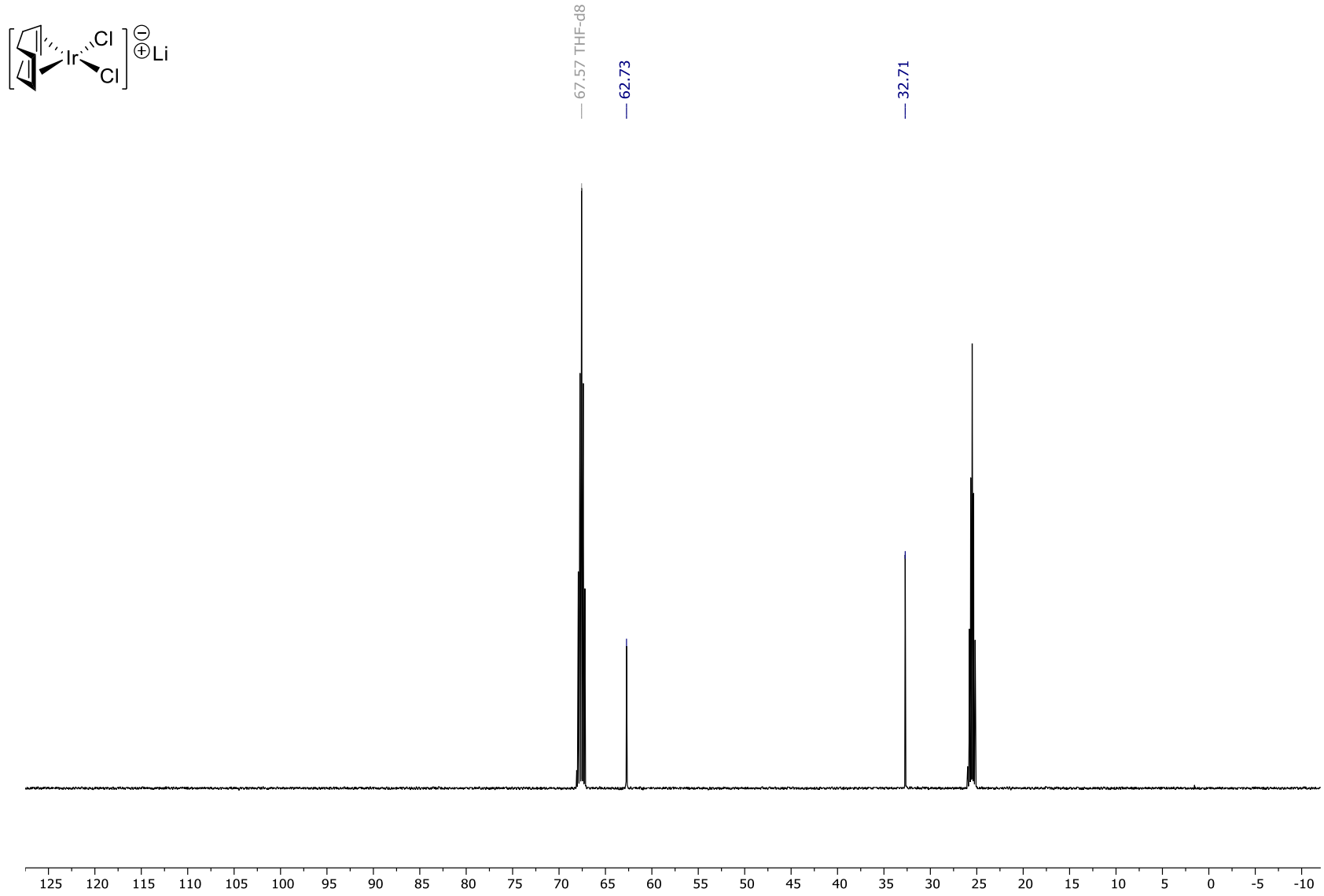

^{1}H NMR spectrum of [$IrCl_2$(cod)][NBu_4] (500 MHz, THF-d_8)

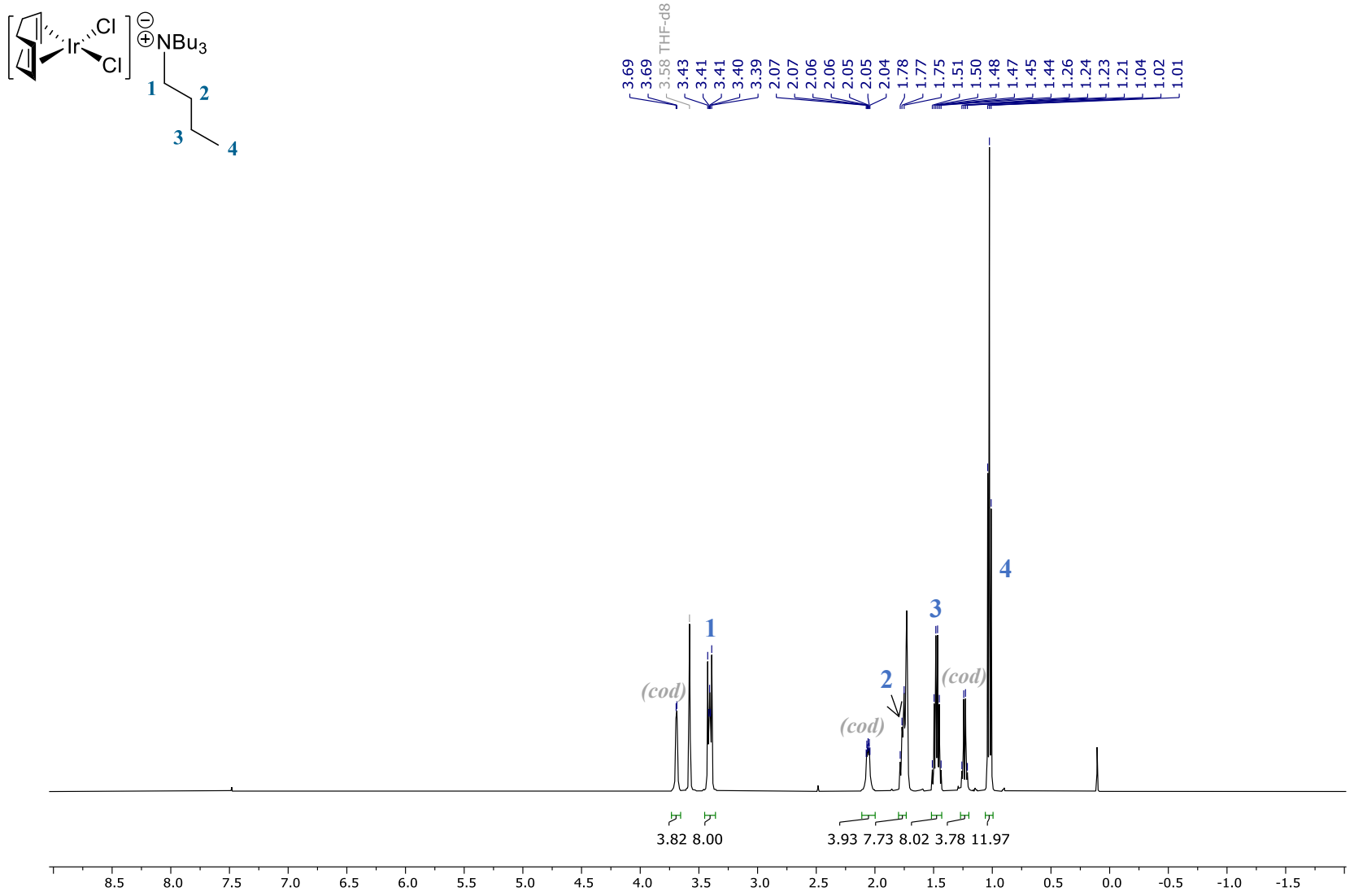

$^{13}C\{^{1}H\}$ NMR spectrum of $[IrCl_2(cod)][NBu_4]$ (126 MHz, THF-d_8)

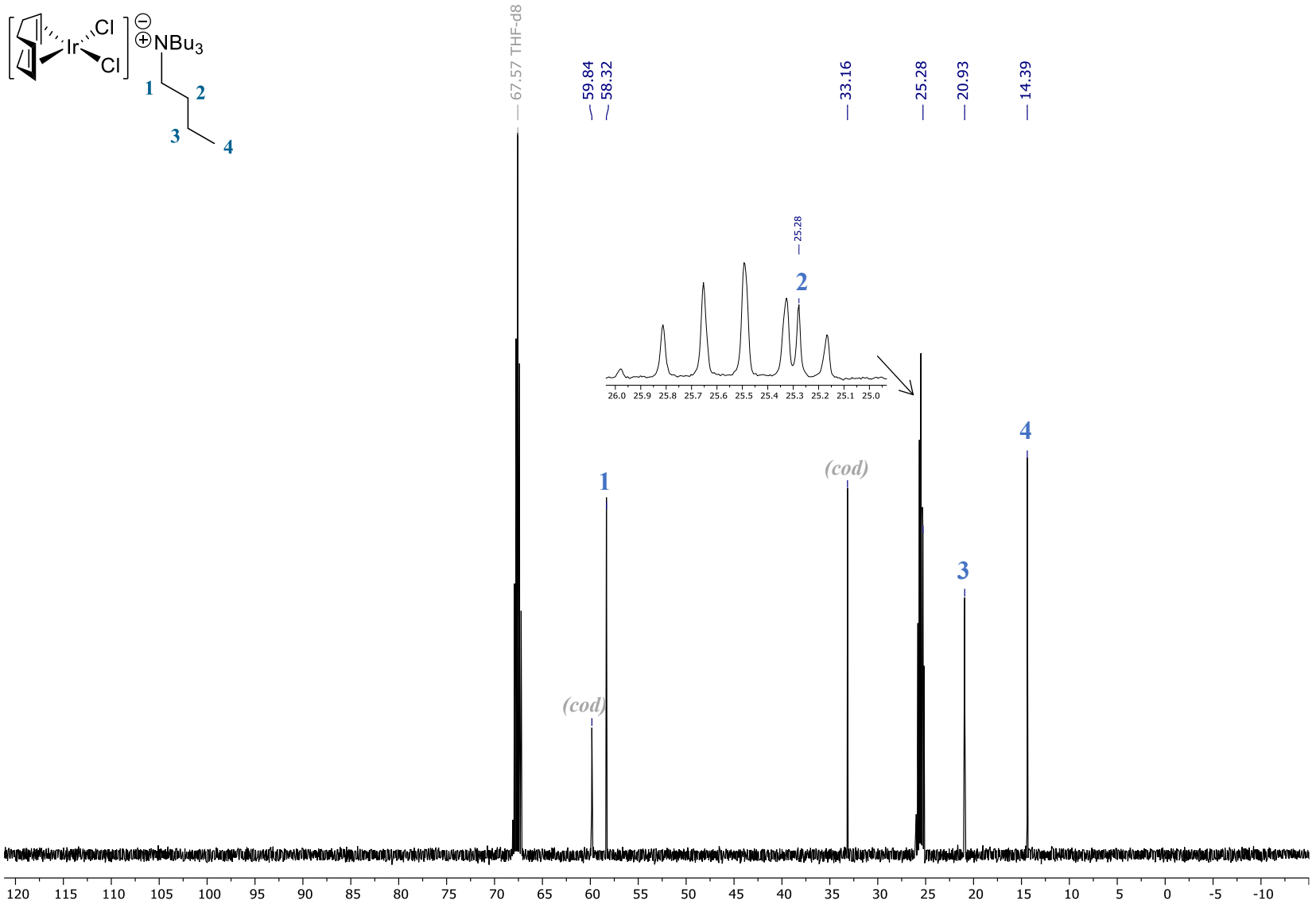

^{1}H NMR spectrum of [$IrCl_2$(cod)][NPr_4] (500 MHz, CD_3CN)

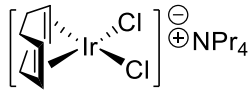

$^{13}C\{^{1}H\}$ NMR spectrum of $[IrCl_2(cod)][NPr_4]$ (126 MHz, CD_3CN)

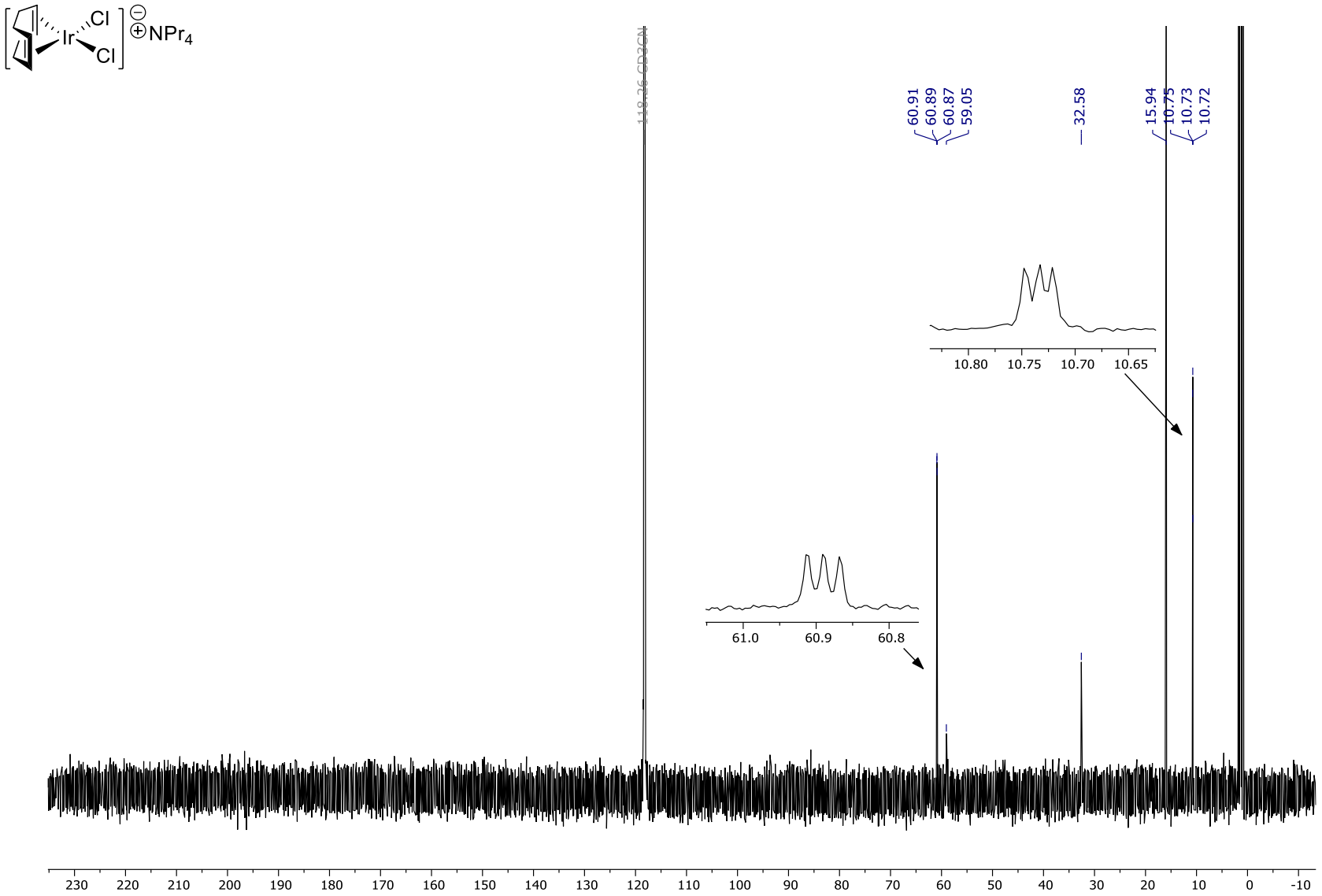

^{1}H NMR spectrum of [$IrCl_2$(cod)][NEt_4] (500 MHz, CD_3CN)

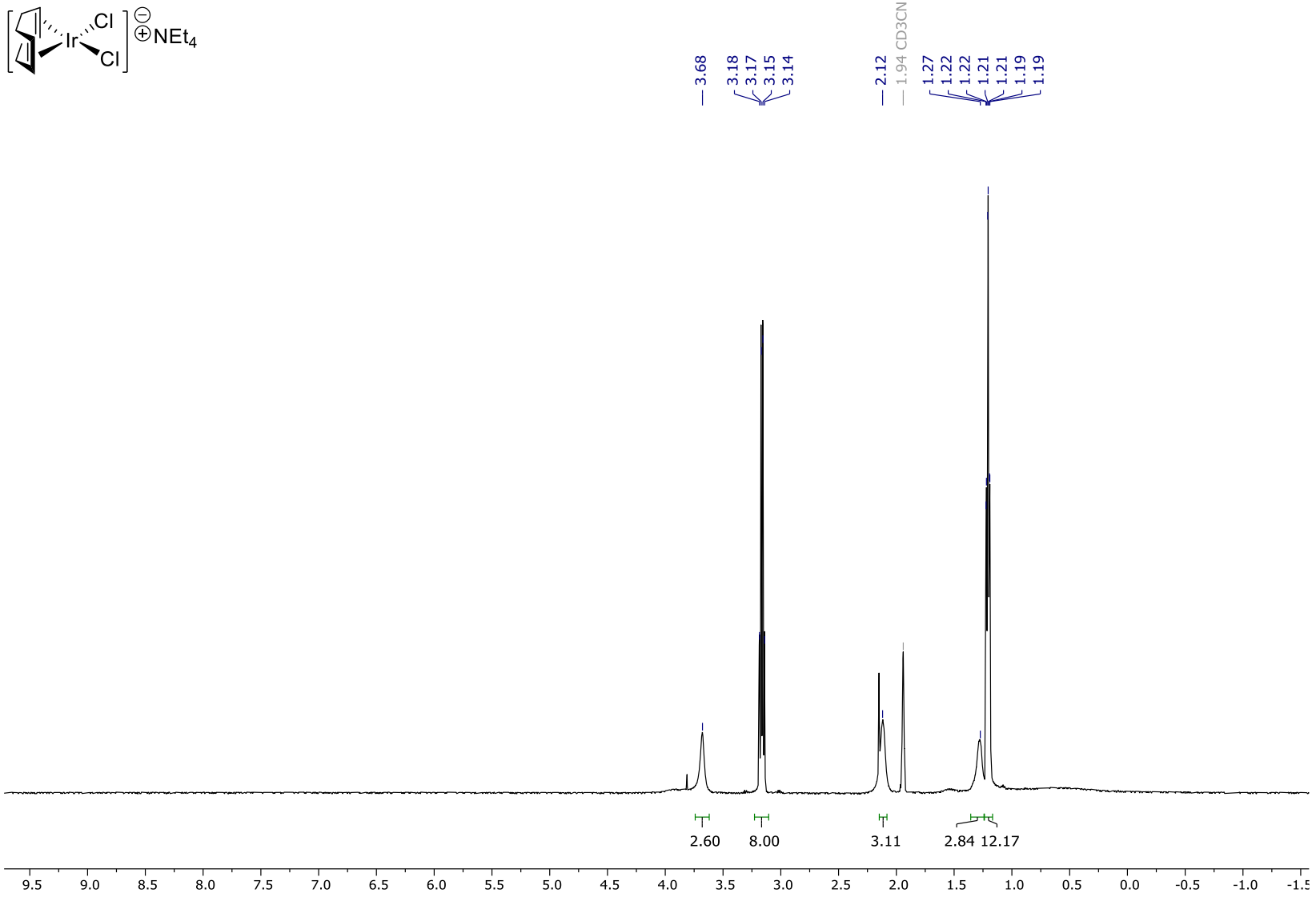

^{1}H NMR spectrum of 3a and 3a' (500 MHz, $CDCl_3$)

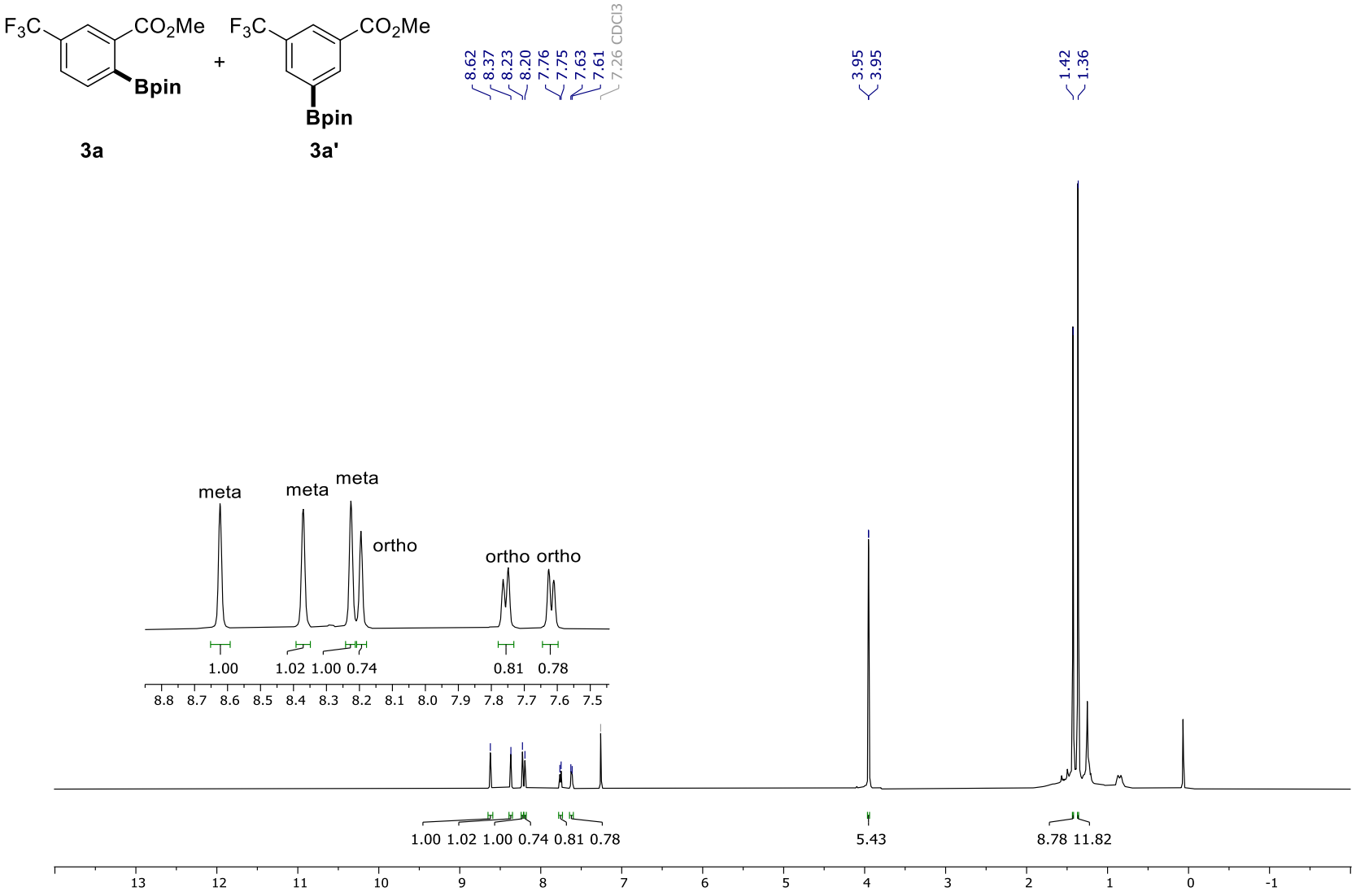

^{19}F NMR spectrum of 3a and 3a' (470 MHz, $CDCl_3$)

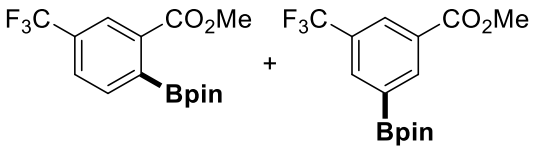

3a 3a'

^{11}B NMR spectrum of 3a and 3a' (160 MHz, $CDCl_3$)

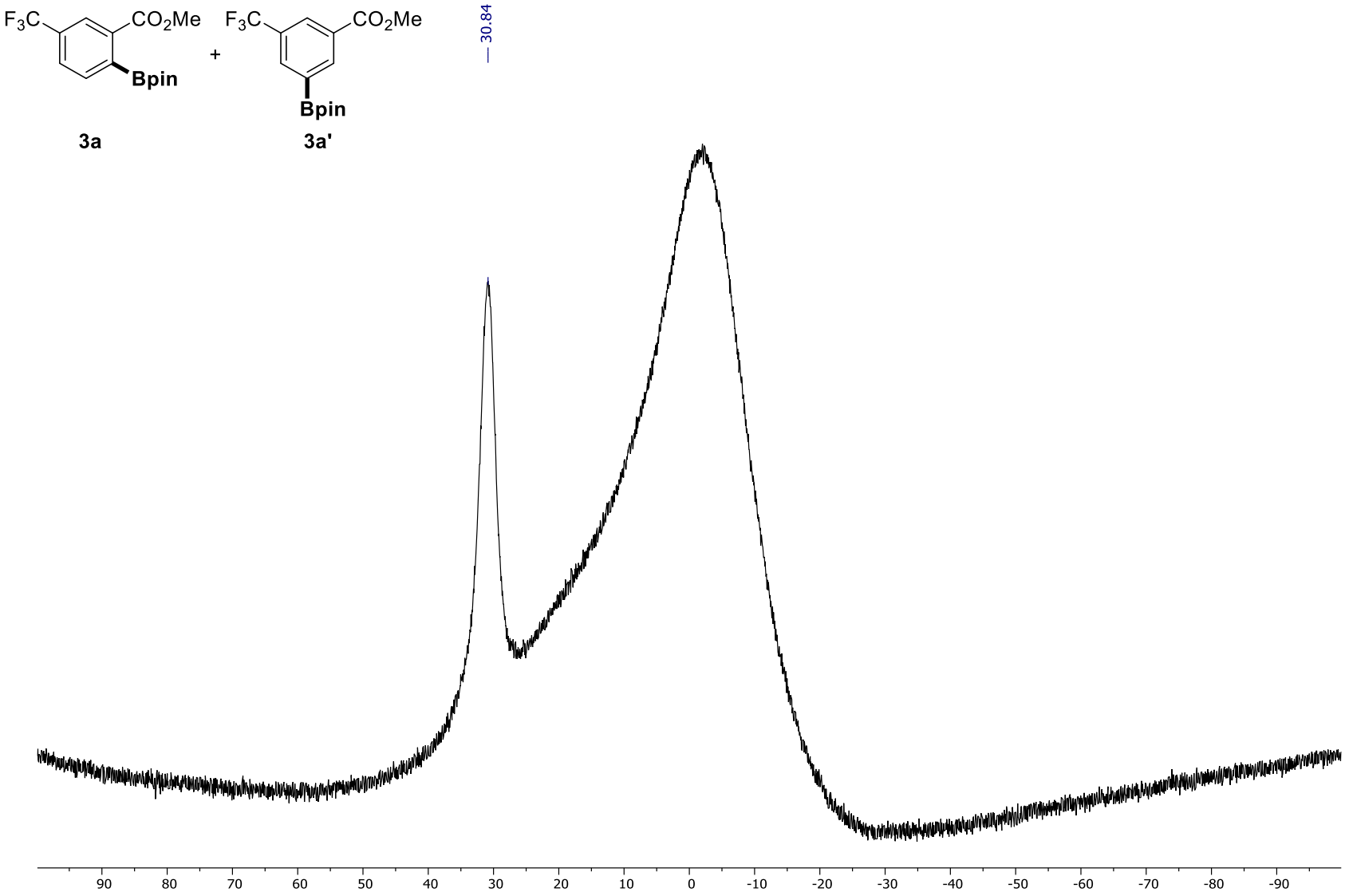

^{1}H NMR spectrum of 3b and 3b' (500 MHz, $CDCl_3$)

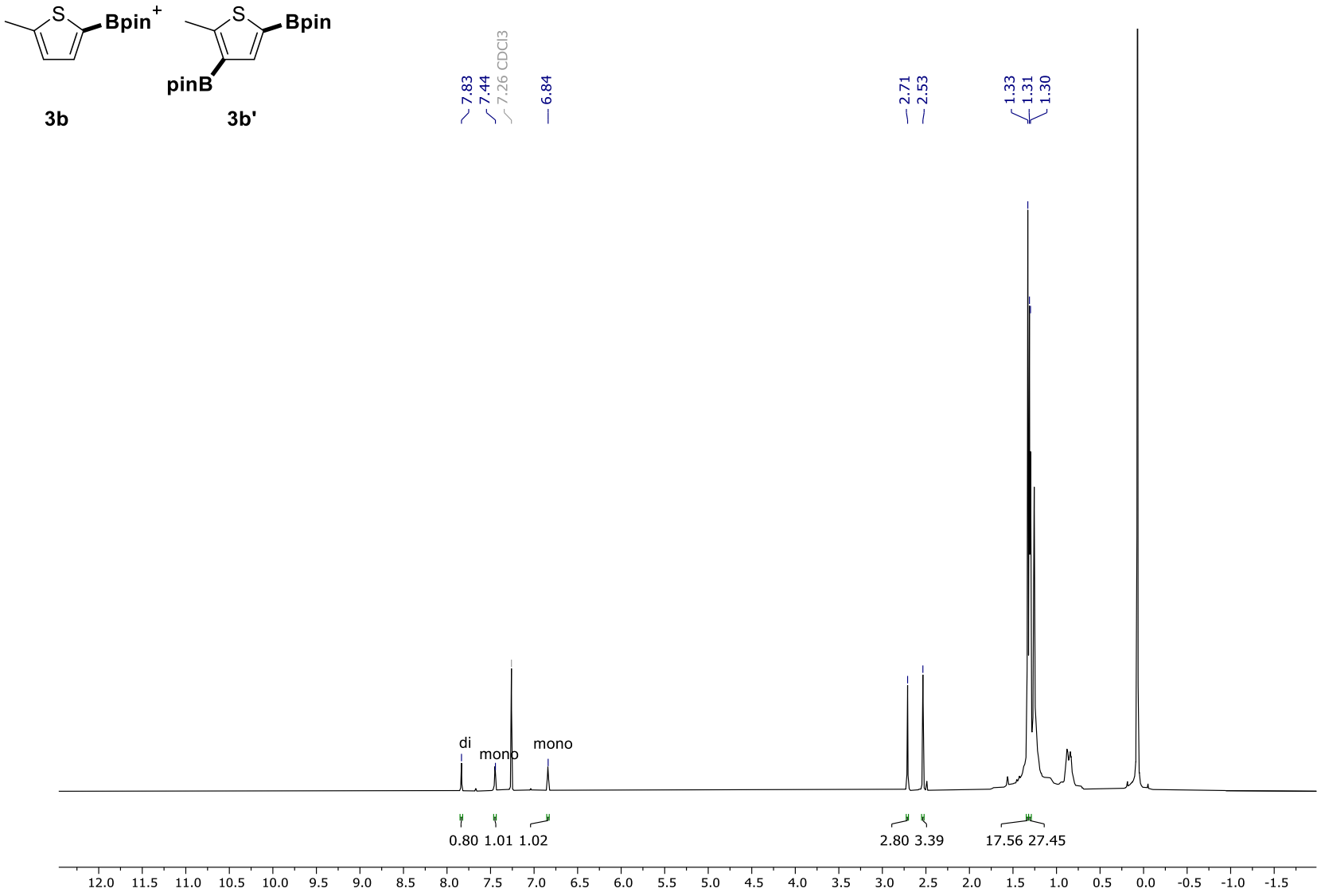

^{11}B NMR spectrum of 3b and 3b' (160 MHz, $CDCl_3$)

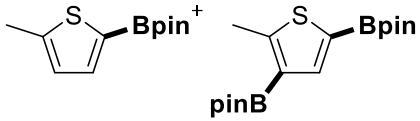

3b

3b'

28.89

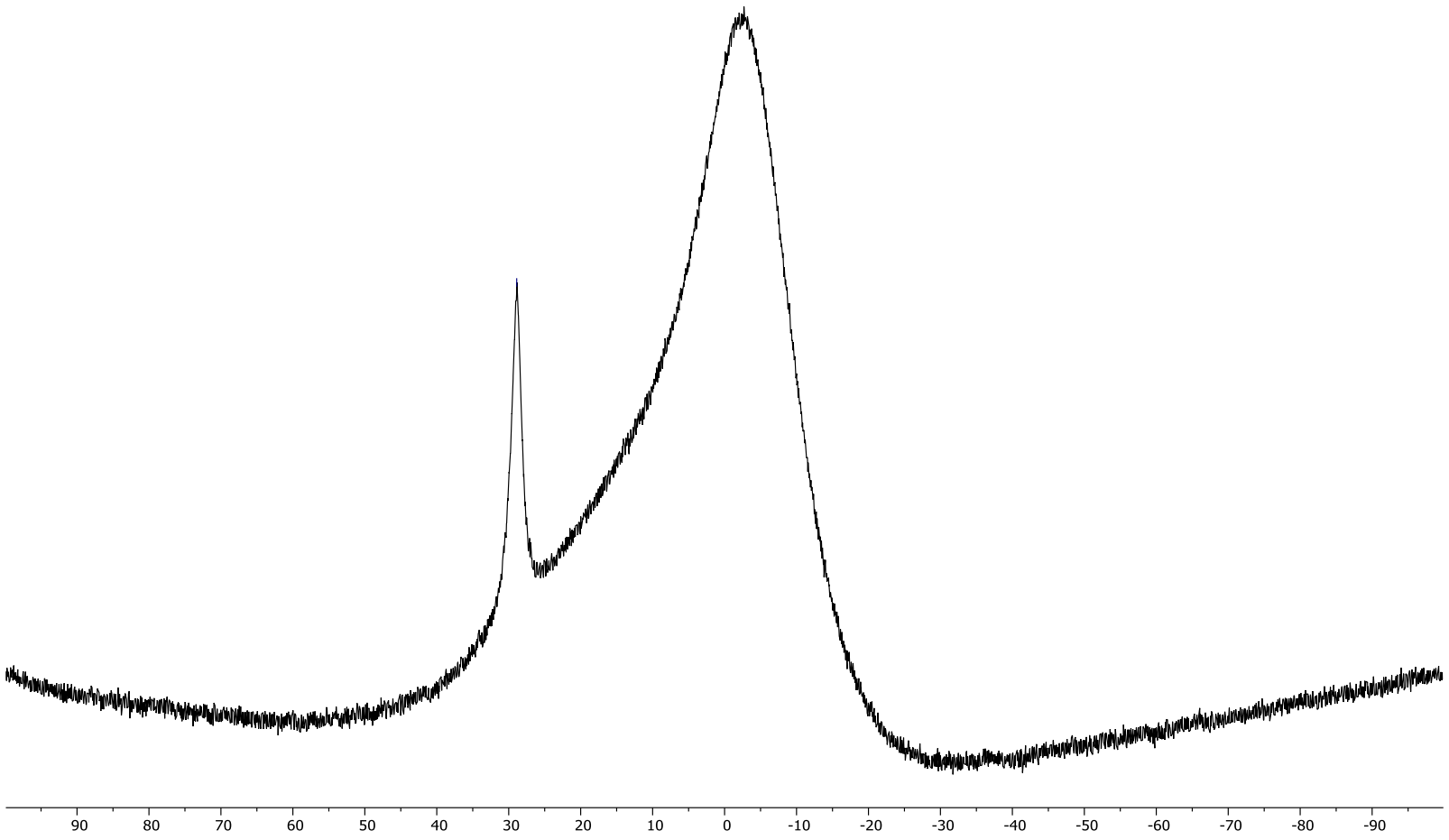

^{1}H NMR spectrum of 3c and 3c' (500 MHz, $CDCl_3$)

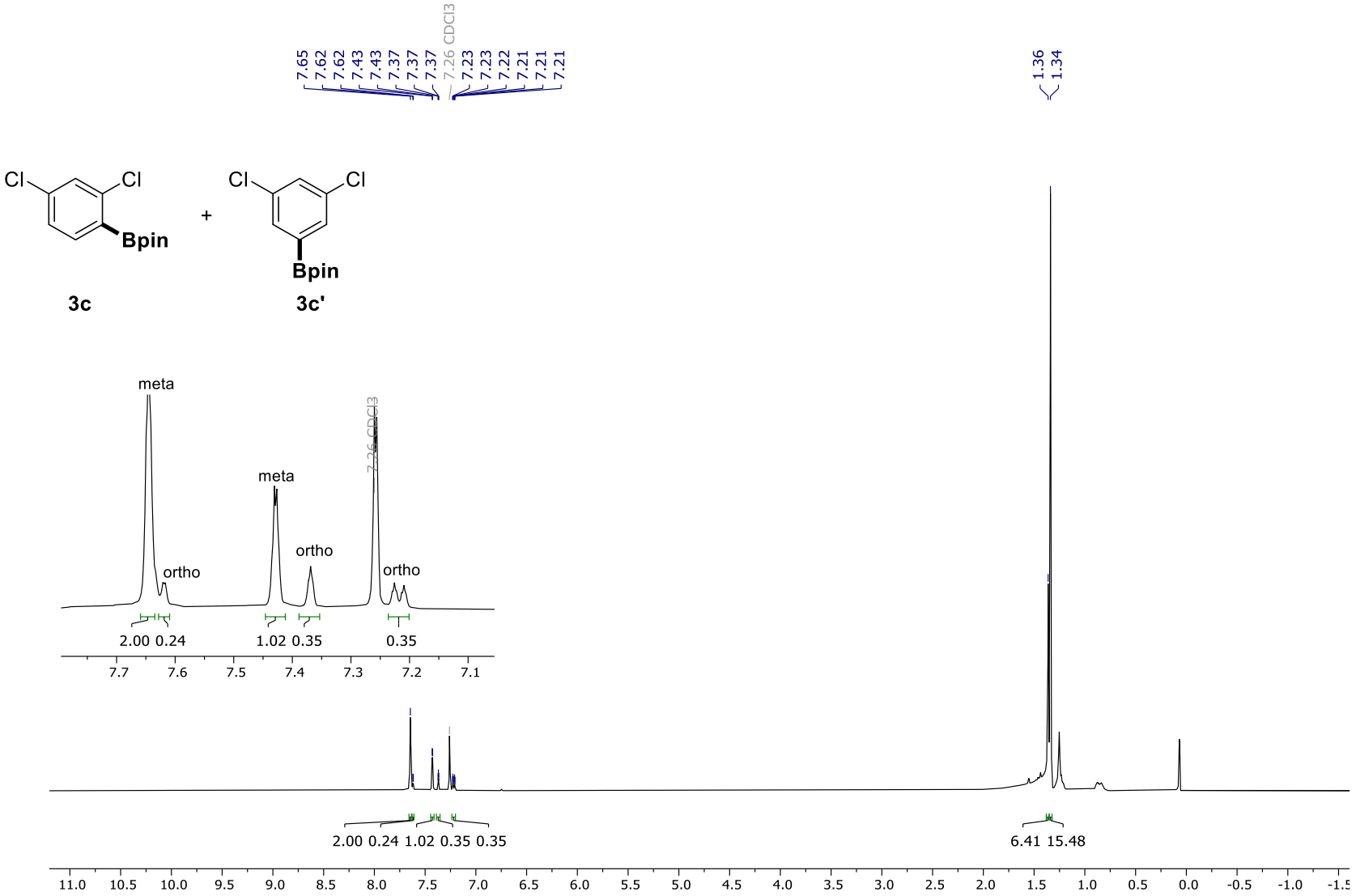

^{11}B NMR spectrum of 3c and 3c' (160 MHz, $CDCl_3$)

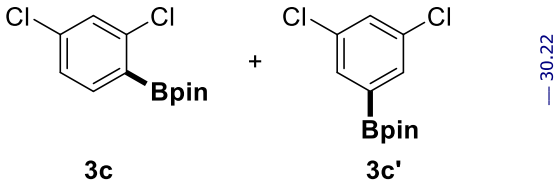

3c 3c'

30.22

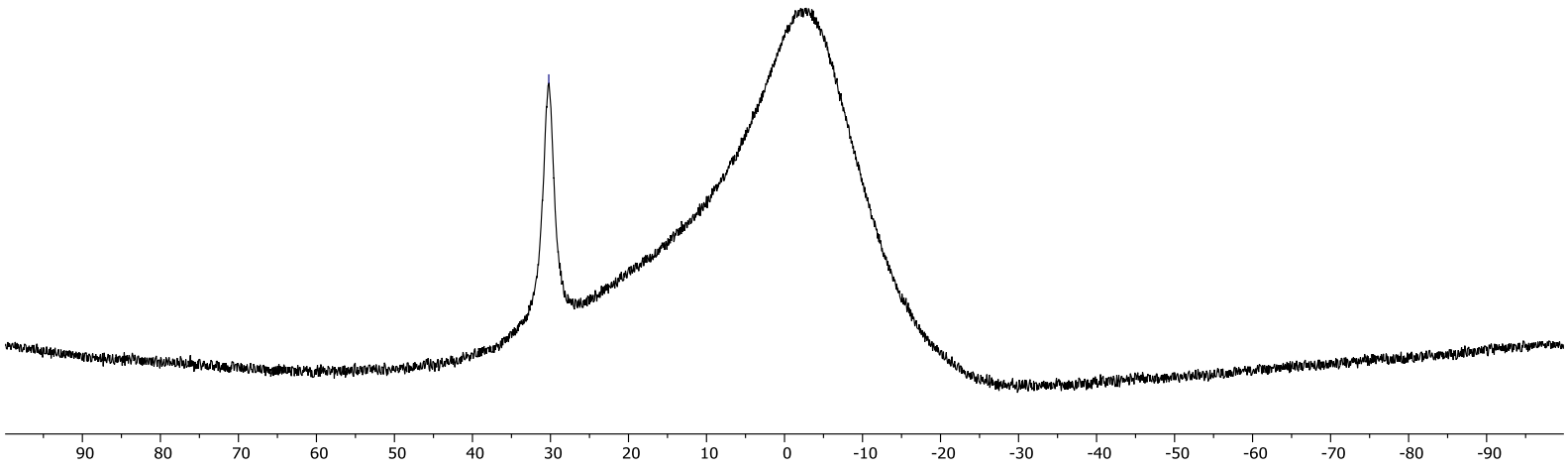

Crude ^{1}H NMR spectrum of 3d and 3d' (500 MHz, $CDCl_3$)

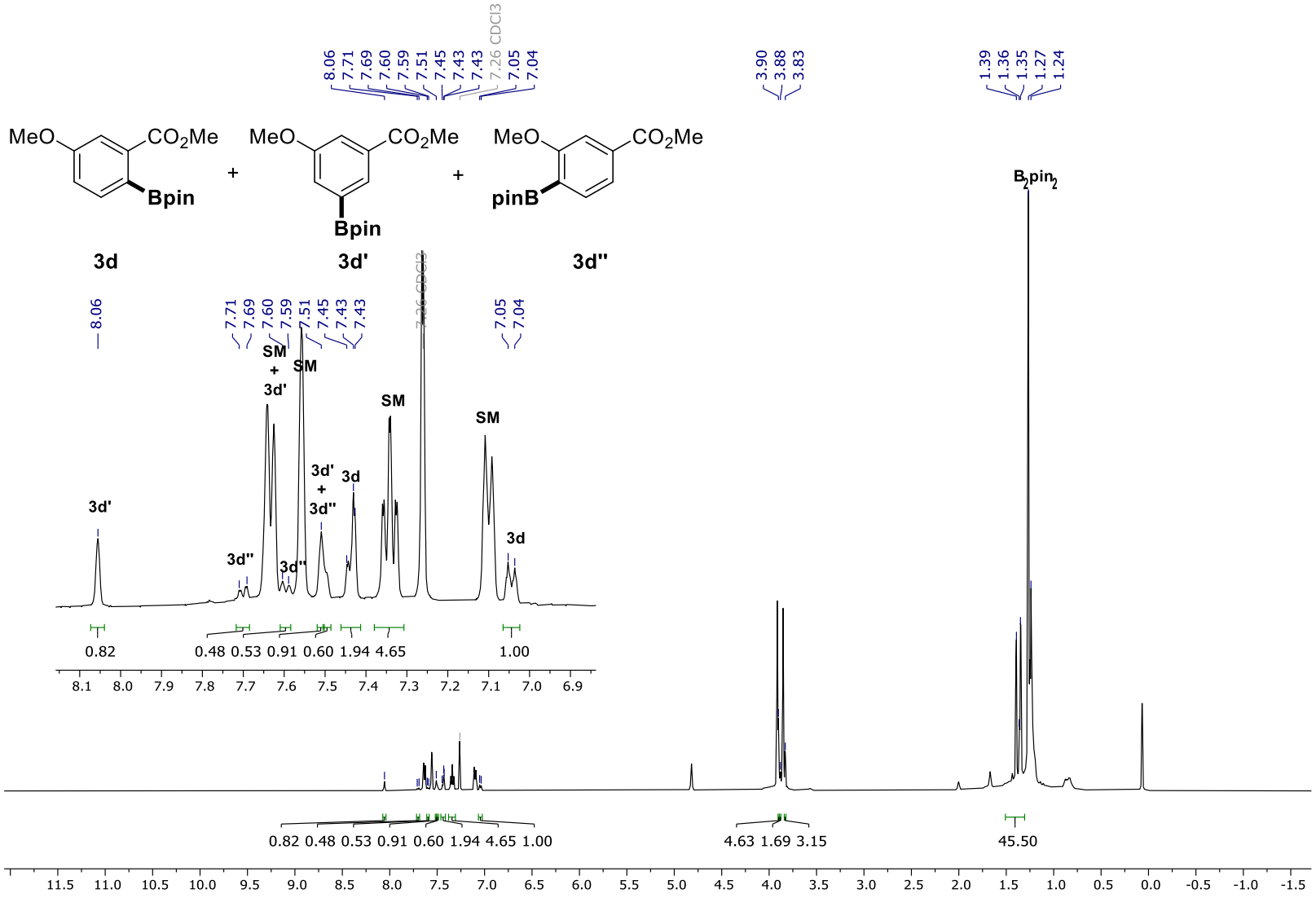

Crude ^{11}B NMR spectrum of 3d, 3d', and 3d" (160 MHz, $CDCl_3$)

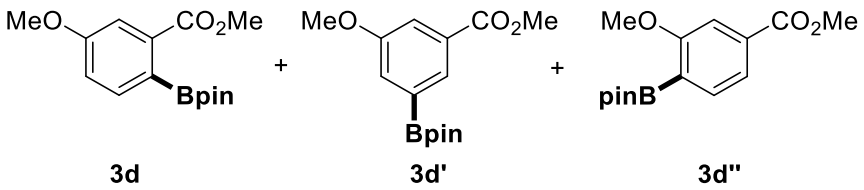

3d 3d' 3d"

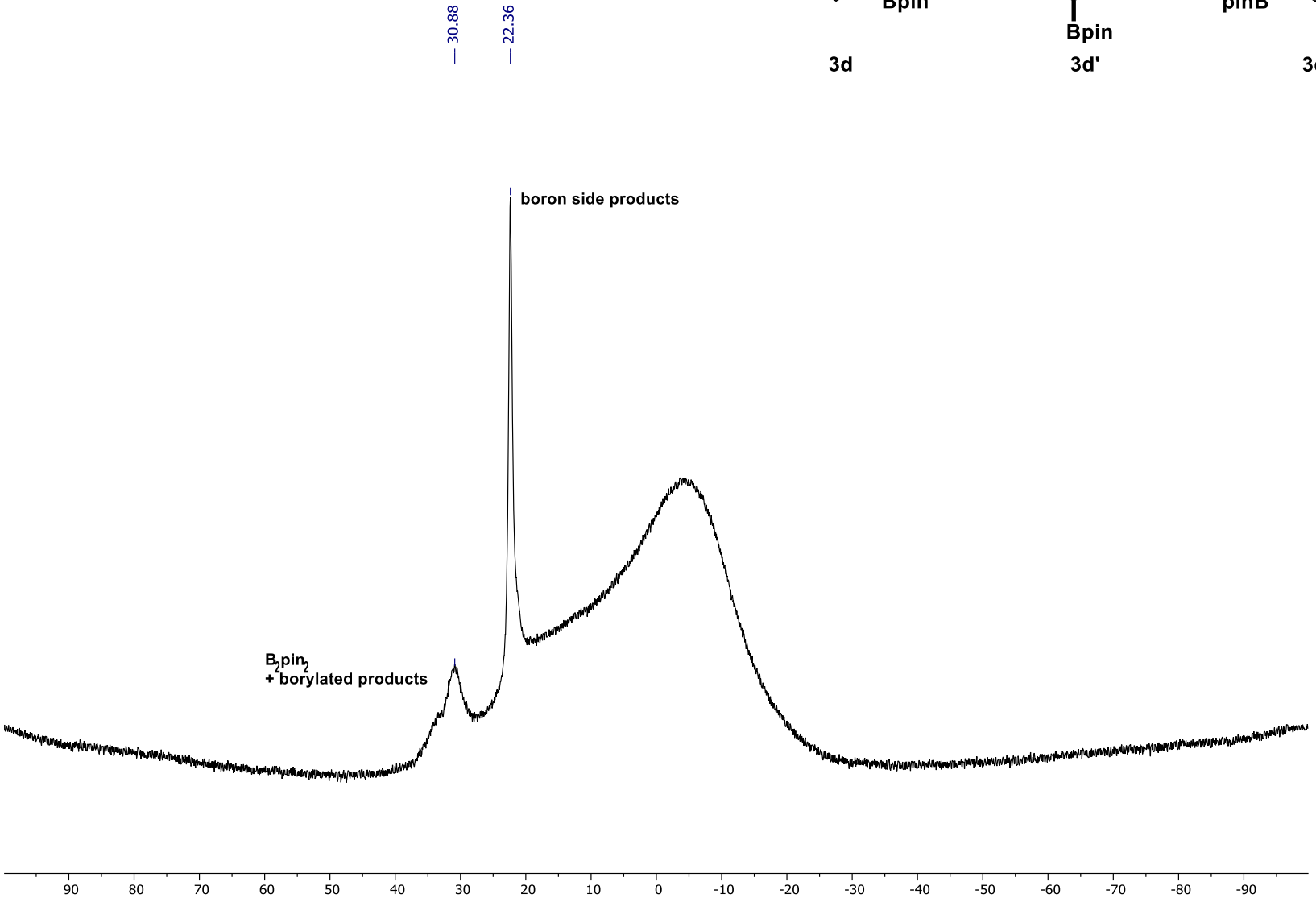

Crude ^{1}H NMR spectrum of 3e and 3e' (500 MHz, $CDCl_3$)

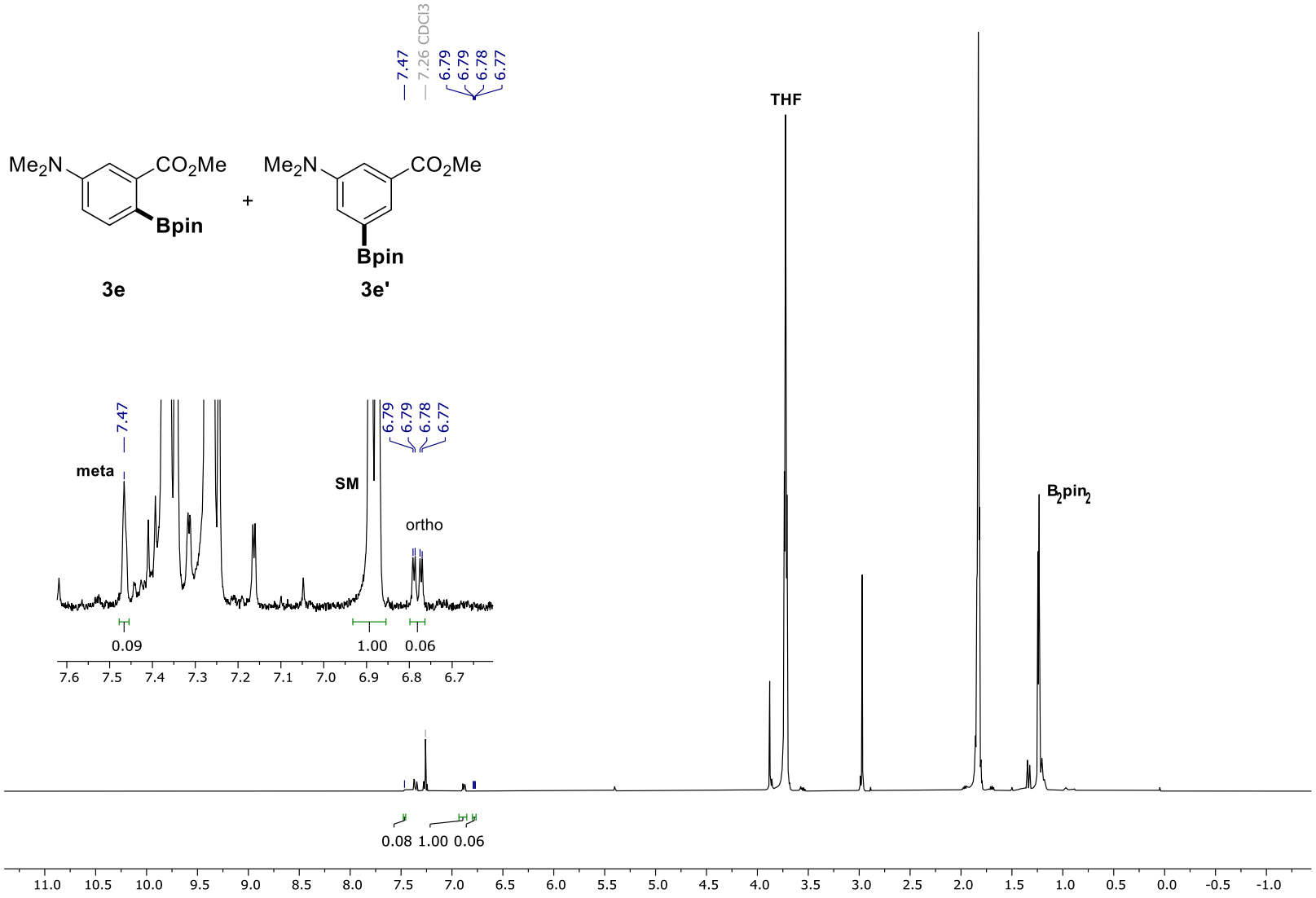

Crude ^{1}H NMR spectrum of 3f' (500 MHz, $CDCl_3$)

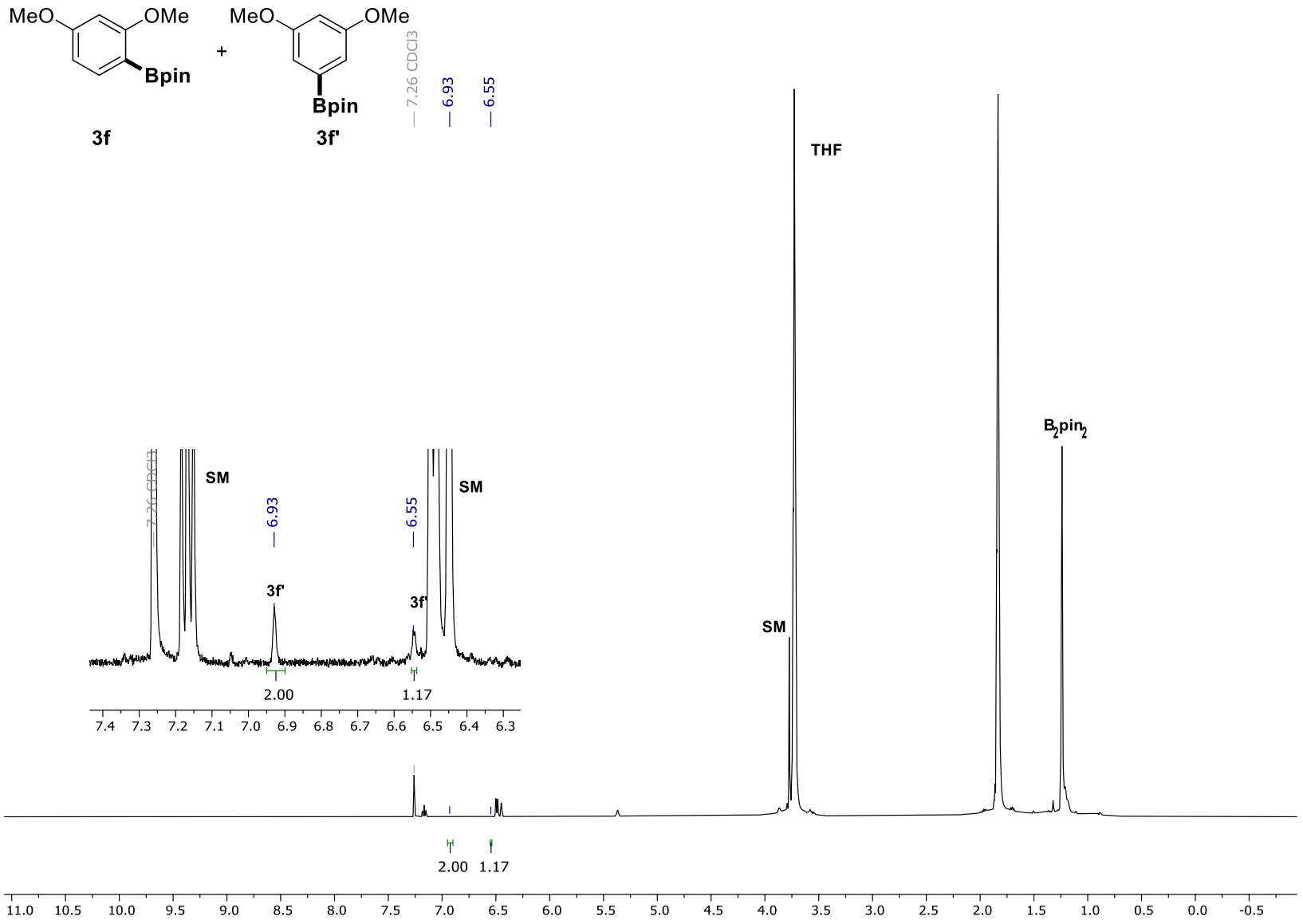

Crude ^{1}H NMR spectrum of 3g and 3g' (500 MHz, $CDCl_3$)

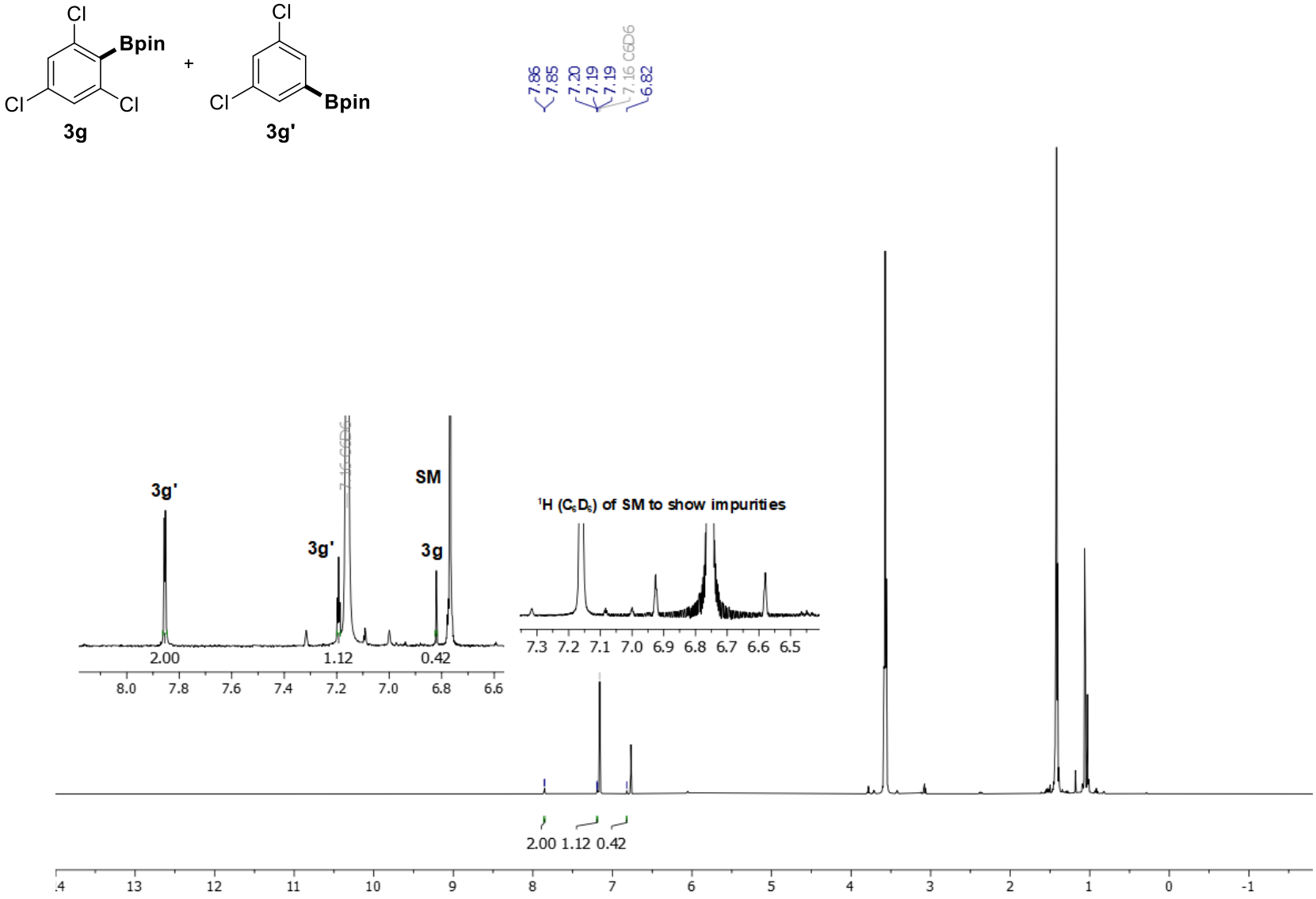

Crude ^{11}B NMR spectrum of 3g and 3g' (160 MHz, C_6D_6)

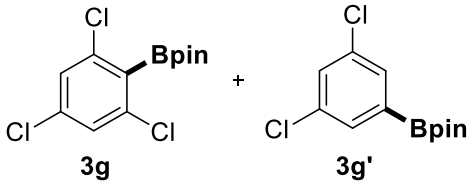

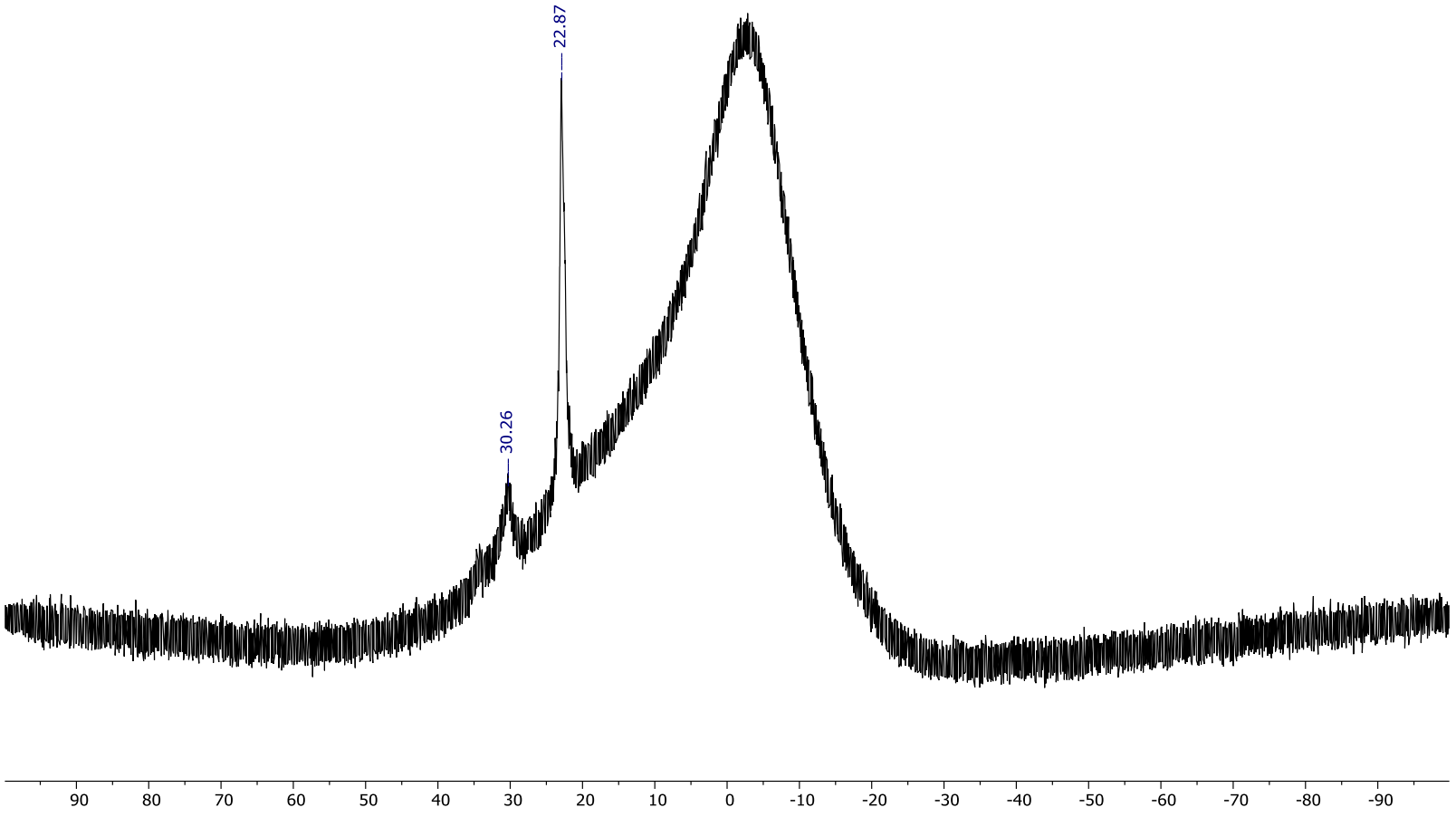

Crude ^{19}F NMR spectrum of 3h, 3h', 3h'', and 3h''' (470 MHz, C_6D_6)

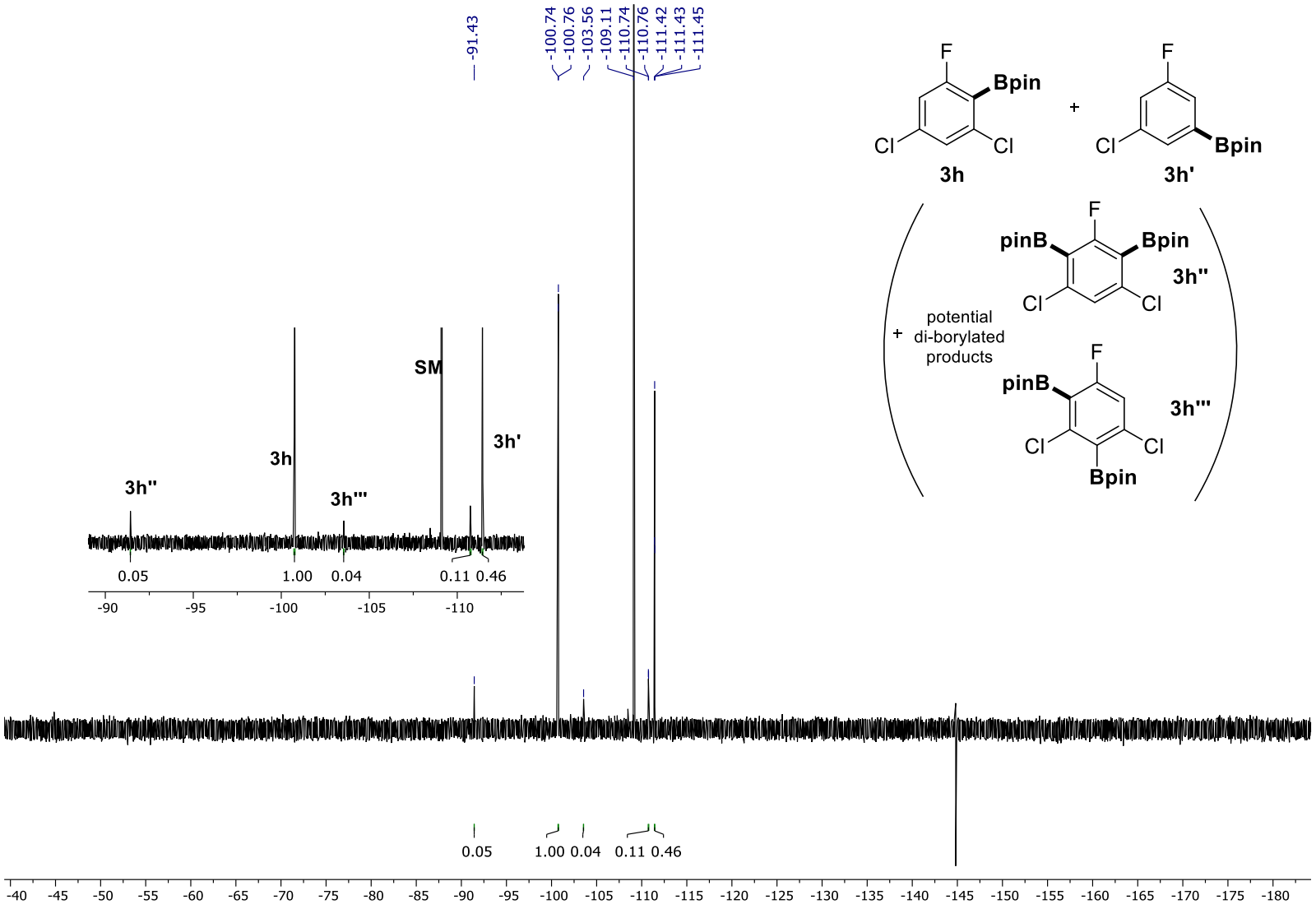

Crude ^{1}H NMR spectrum of 3h, 3h', 3h", and 3h"' (500 MHz, C_6D_6)

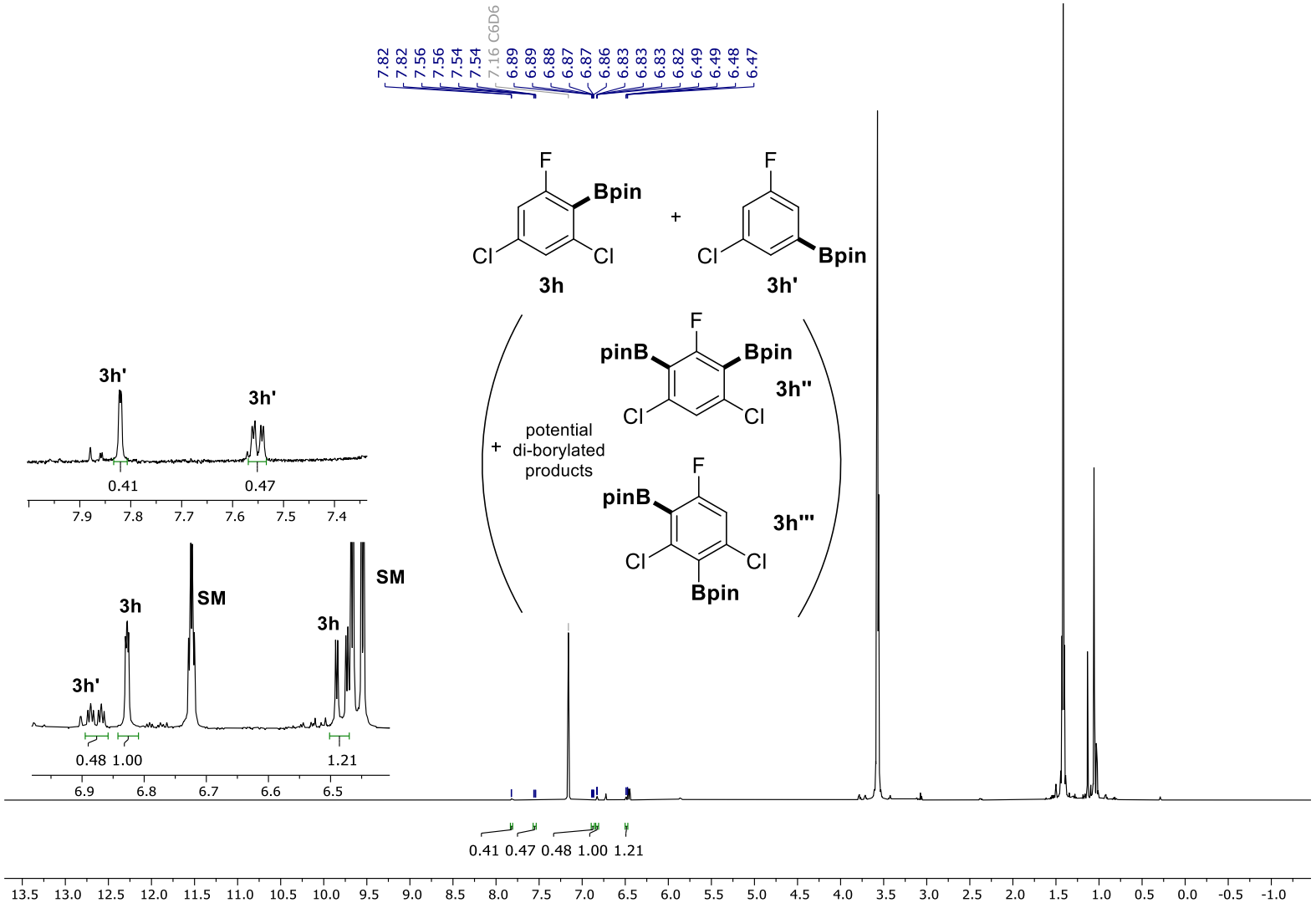

Crude ^{11}B NMR spectrum of 3h, 3h', 3h" and 3h"' (160 MHz, C_6D_6)

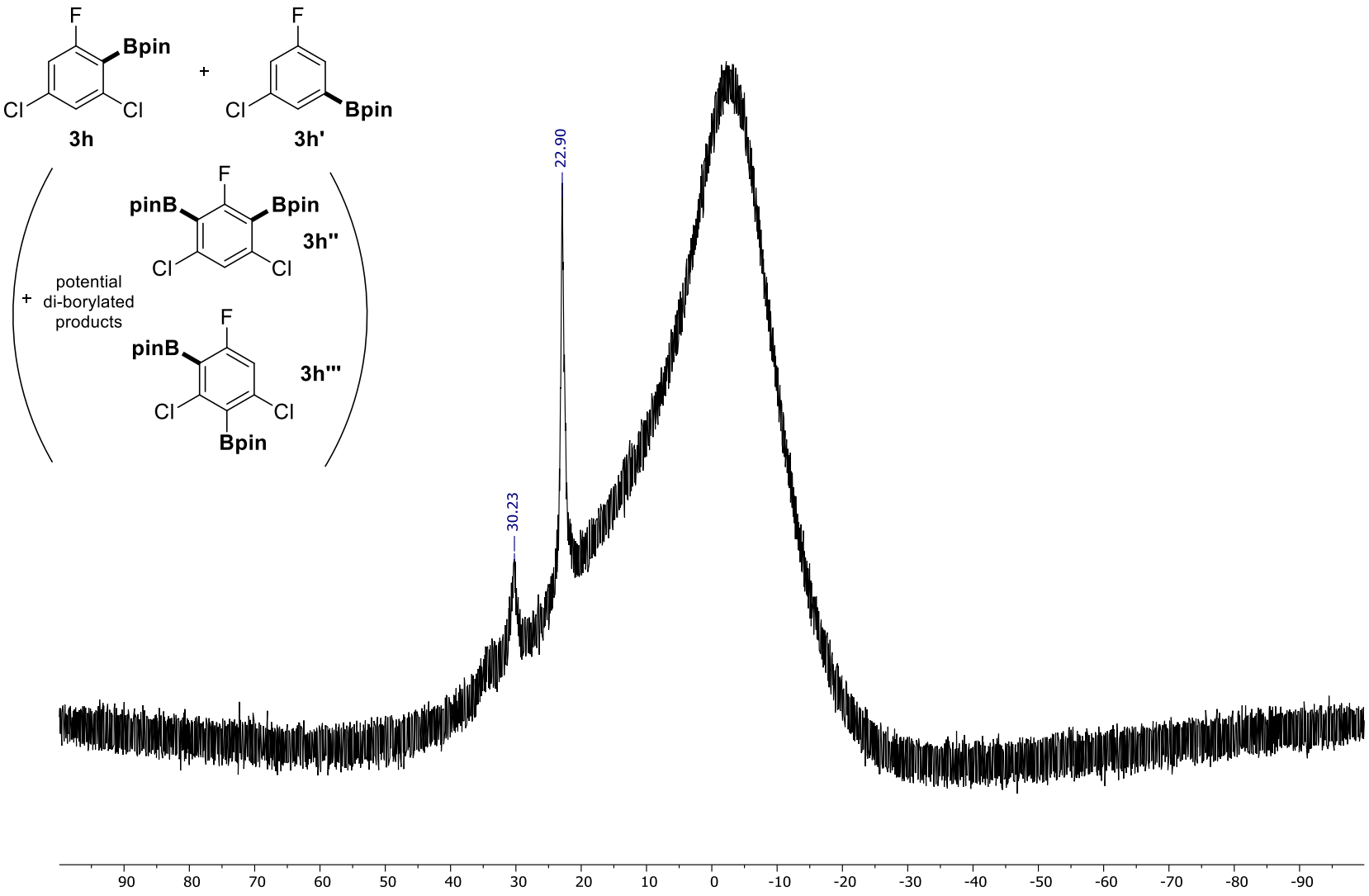

REFERENCES

(1) Cho, J.-Y.; Tse, M. K.; Holmes, D.; Maleczka, R. E., Jr; Smith, M. R., III. Remarkably Selective Iridium Catalysts for the Elaboration of Aromatic C-H Bonds. *Science* **2002**, *295* (5553), 305–308.

(2) Montero Bastidas, J. R.; Oleskey, T. J.; Miller, S. L.; Smith, M. R., III; Maleczka, R. E. Para-Selective, Iridium-Catalyzed C–H Borylations of Sulfated Phenols, Benzyl Alcohols, and Anilines Directed by Ion-Pair Electrostatic Interactions. *J. Am. Chem. Soc.* **2019**, *141* (39), 15483–15487.

(3) Mihai, M. T.; Williams, B. D.; Phipps, R. J. Para-Selective C–H Borylation of Common Arene Building Blocks Enabled by Ion-Pairing with a Bulky Countercation. *J. Am. Chem. Soc.* **2019**, *141* (39), 15477–15482.

(4) Boller, T. M.; Murphy, J. M.; Hapke, M.; Ishiyama, T.; Miyaura, N.; Hartwig, J. F. Mechanism of the Mild Functionalization of Arenes by Diboron Reagents Catalyzed by Iridium Complexes. Intermediacy and Chemistry of Bipyridine-Ligated Iridium Trisboryl Complexes. *J. Am. Chem. Soc.* **2005**, *127* (41), 14263–14278.

(5) Liu, L.; Wang, G.; Jiao, J.; Li, P. Sulfur-Directed Ligand-Free C-H Borylation by Iridium Catalysis. *Org. Lett.* **2017**, *19* (22), 6132–6135.

(6) Mahamudul Hassan, M. M.; Mondal, B.; Singh, S.; Haldar, C.; Chaturvedi, J.; Bisht, R.; Sunoj, R. B.; Chattopadhyay, B. Ir-Catalyzed Ligand-Free Directed C-H Borylation of Arenes and Pharmaceuticals: Detailed Mechanistic Understanding. *J. Org. Chem.* **2022**, *87* (6), 4360–4375.

(7) Yang, Y.; Gao, Q.; Xu, S. Ligand-Free Iridium-Catalyzed Dehydrogenative Ortho C−H Borylation of Benzyl-2-Pyridines at Room Temperature. *Adv. Synth. Catal.* **2019**, *361* (4), 858–862.

(8) Pan, Z.; Liu, L.; Xu, S.; Shen, Z. Ligand-Free Iridium-Catalyzed Regioselective C–H Borylation of Indoles. *RSC Adv.* **2021**, *11* (10), 5487–5490.

(9) Britt A. Vanchura, I. I.; Preshlock, S. M.; Roosen, P. C.; Kallepalli, V. A.; Staples, R. J.; Maleczka, R. E., Jr; Singleton, D. A.; Smith, M. R., III. Electronic Effects in Iridium C–H Borylations: Insights from Unencumbered Substrates and Variation of Boryl Ligand Substituents. *Chem. Commun.* **2010**, *46* (41), 7724–7726.

(10) Hassan, M. M. M.; Guria, S.; Dey, S.; Das, J.; Chattopadhyay, B. Transition Metal-Catalyzed Remote C─H Borylation: An Emerging Synthetic Tool. *Sci Adv* **2023**, *9* (16), eadg3311.

(11) Ishiyama, T.; Nobuta, Y.; Hartwig, J. F.; Miyaura, N. Room Temperature Borylation of Arenes and Heteroarenes Using Stoichiometric Amounts of Pinacolborane Catalyzed by Iridium Complexes in an Inert Solvent. *Chem. Commun.* **2003**, No. 23, 2924–2925.

(12) Wright, J. S.; Scott, P. J. H.; Steel, P. G. Iridium Catalysed C-H Borylation of Heteroarenes: Balancing Steric and Electronic Regiocontrol. *Angew. Chem. Int. Ed Engl.* **2020**.

(13) Kawamorita, S.; Ohmiya, H.; Hara, K.; Fukuoka, A.; Sawamura, M. Directed Ortho Borylation of Functionalized Arenes Catalyzed by a Silica-Supported Compact Phosphine-Iridium System. *J. Am. Chem. Soc.* **2009**, *131* (14), 5058–5059.

(14) Tajuddin, H.; Harrisson, P.; Bitterlich, B.; Collings, J. C.; Sim, N.; Batsanov, A. S.; Cheung, M. S.; Kawamorita, S.; Maxwell, A. C.; Shukla, L.; Morris, J.; Lin, Z.; Marder, T. B.; Steel, P. G. Iridium-Catalyzed C–H Borylation of Quinolines and Unsymmetrical 1,2-Disubstituted Benzenes: Insights into Steric and Electronic Effects on Selectivity. *Chem. Sci.* **2012**, *3* (12), 3505–3515.

(15) Vickers, P. W.; Pearson, J. M.; Ghaffar, T.; Adams, H.; Haynes, A. Kinetics and Thermodynamics of C—Cl Bond Activation by [Ir(CO) 2 Cl 2] −. *J. Phys. Org. Chem.* **2004**, *17* (11), 1007–1016.

(16) Grüger, N.; Wadepohl, H.; Gade, L. H. Iridium Complexes Containing a PNP Pincer Ligand: Syntheses, Structural Chemistry, and Bond Activations. *Eur. J. Inorg. Chem.* **2013**, *2013* (30), 5358–5365.

(17) Chen, J.; Zhao, K.; Ge, B.; Xu, C.; Wang, D.; Ding, Y. Iridium-Catalyzed Synthesis of Diaryl Ethers by Means of Chemoselective C-F Bond Activation and the Formation of B-F Bonds. *Chem. Asian J.* **2015**, *10* (2), 468–473.

(18) Hall, D. G. *Boronic Acids, 2 Volume Set: Preparation and Applications in Organic Synthesis, Medicine and Materials*; Wiley, 2011.

(19) Wu, H.; Hall, M. B. Carbon-Hydrogen vs. Carbon-Halogen Oxidative Addition of Chlorobenzene by a Neutral Iridium Complex Explored by DFT. *Dalton Trans.* **2009**, No. 30, 5933–5942.

(20) Diefenbach, A.; de Jong, G. T.; Bickelhaupt, F. M. Activation of H-H, C-H, C-C and C-Cl Bonds by Pd and PdCl(-). Understanding Anion Assistance in C-X Bond Activation. *J. Chem. Theory Comput.* **2005**, *1* (2), 286–298.

(21) Widegren, J. A.; Finke, R. G. A Review of the Problem of Distinguishing True Homogeneous Catalysis from Soluble or Other Metal-Particle Heterogeneous Catalysis under Reducing Conditions. *J. Mol. Catal. A Chem.* **2003**, *198* (1), 317–341.

(22) Lin, Y.; Finke, R. G. A More General Approach to Distinguishing "Homogeneous" from "Heterogeneous" Catalysis: Discovery of Polyoxoanion- and Bu4N+-Stabilized, Isolable and Redissolvable, High-Reactivity Ir.Apprx.190-450 Nanocluster Catalysts. *Inorg. Chem.* **1994**, *33* (22), 4891–4910.

(23) Weddle, K. S.; Aiken, J. D., III; Finke, R. G. Rh(0) Nanoclusters in Benzene Hydrogenation Catalysis: Kinetic and Mechanistic Evidence That a Putative [(C8H17)3NCH3]+[RhCl4]- Ion- Pair Catalyst Is Actually a Distribution of Cl- and [(C8H17)3NCH3]+ Stabilized Rh(0) Nanoclusters. *J. Am. Chem. Soc.* **1998**, *120* (23), 5653–5666.

(24) Chernyshev, V. M.; Astakhov, A. V.; Chikunov, I. E.; Tyurin, R. V.; Eremin, D. B.; Ranny, G. S.; Khrustalev, V. N.; Ananikov, V. P. Pd and Pt Catalyst Poisoning in the Study of Reaction Mechanisms: What Does the Mercury Test Mean for Catalysis? *ACS Catal.* **2019**, *9* (4), 2984–2995.

(25) Whitesides, G. M.; Hackett, M.; Brainard, R. L.; Lavalleye, J. P. P. M.; Sowinski, A. F.; Izumi, A. N.; Moore, S. S.; Brown, D. W.; Staudt, E. M. Suppression of Unwanted Heterogeneous Platinum(0)-Catalyzed Reactions by Poisoning with Mercury(0) in Systems Involving Competing Homogeneous Reactions of Soluble Organoplatinum Compounds: Thermal Decomposition of Bis(Triethylphosphine)-3,3,4,4-Tetramethylplatinacyclopentane. *Organometallics* **1985**, *4* (10), 1819–1830.

(26) Vargaftik, M. N.; Moiseev, I. I.; Kochubey, D. I.; Zamaraev, K. I. Giant Palladium Clusters: Synthesis and Characterization. *Faraday Discuss.* **1991**, *92* (0), 13–29.

(27) Yinghuai, Z.; Chenyan, K.; Peng, A. T.; Emi, A.; Monalisa, W.; Kui-Jin Louis, L.; Hosmane, N. S.; Maguire, J. A. Catalytic Phenylborylation Reaction by Iridium(0) Nanoparticles Produced from Hydridoiridium Carborane. *Inorg. Chem.* **2008**, *47* (13), 5756–5761.

(28) Armarego, W. L. F.; Chai, C. L. L. Purification of Laboratory Chemicals. Elsevier Inc., Oxford OX2 8DP, UK 2009.

(29) Weng, W.; Guo, C.; Moura, C.; Yang, L.; Foxman, B. M.; Ozerov, O. V. Competitive Activation of N−C and C−H Bonds of the PNP Framework by Monovalent Rhodium and Iridium. *Organometallics* **2005**, *24* (14), 3487–3499.

(30) Ghaffari, B.; Preshlock, S. M.; Plattner, D. L.; Staples, R. J.; Maligres, P. E.; Krska, S. W.; Maleczka, R. E., Jr; Smith, M. R., III. Silyl Phosphorus and Nitrogen Donor Chelates for Homogeneous Ortho Borylation Catalysis. *J. Am. Chem. Soc.* **2014**, *136* (41), 14345–14348.

(31) Kallepalli, V. A.; Gore, K. A.; Shi, F.; Sanchez, L.; Chotana, G. A.; Miller, S. L.; Maleczka, R. E., Jr; Smith, M. R., III. Harnessing C-H Borylation/Deborylation for Selective Deuteration, Synthesis of Boronate Esters, and Late Stage Functionalization. *J. Org. Chem.* **2015**, *80* (16), 8341–8353.

(32) Robbins, D. W.; Hartwig, J. F. A C-H Borylation Approach to Suzuki-Miyaura Coupling of Typically Unstable 2-Heteroaryl and Polyfluorophenyl Boronates. *Org. Lett.* **2012**, *14* (16), 4266–4269.

(33) Takaya, J.; Ito, S.; Nomoto, H.; Saito, N.; Kirai, N.; Iwasawa, N. Fluorine-Controlled C-H Borylation of Arenes Catalyzed by a PSiN-Pincer Platinum Complex. *Chem. Commun.* **2015**, *51* (100), 17662–17665.

(34) Bhatthula, B. K. G.; Kanchani, J. R.; Arava, V. R.; Subha, M. C. S. Total Synthesis of Carbazole Alkaloids. *Tetrahedron* **2019**, *75* (7), 874–887.

(35) Wu, S.; Ren, D.; Zhou, K.; Xia, H.-L.; Liu, X.-Y.; Wang, X.; Li, J. Linker Engineering toward Full-Color Emission of UiO-68 Type Metal-Organic Frameworks. *J. Am. Chem. Soc.* **2021**, *143* (28), 10547–10552.

(36) Ishiyama, T.; Isou, H.; Kikuchi, T.; Miyaura, N. Ortho-C-H Borylation of Benzoate Esters with Bis(Pinacolato)Diboron Catalyzed by Iridium-Phosphine Complexes. *Chem. Commun.* **2010**, *46* (1), 159–161.

(37) Wang, G.; Xu, L.; Li, P. Double N,B-Type Bidentate Boryl Ligands Enabling a Highly Active Iridium Catalyst for C-H Borylation. *J. Am. Chem. Soc.* **2015**, *137* (25), 8058–8061.

(38) Furukawa, T.; Tobisu, M.; Chatani, N. C-H Functionalization at Sterically Congested Positions by the Platinum-Catalyzed Borylation of Arenes. *J. Am. Chem. Soc.* **2015**, *137* (38), 12211–12214.

(39) Miller, S. L.; Chotana, G. A.; Fritz, J. A.; Chattopadhyay, B.; Maleczka, R. E., Jr; Smith, M. R., III. C-H Borylation Catalysts That Distinguish Between Similarly Sized Substituents Like Fluorine and Hydrogen. *Org. Lett.* **2019**, *21* (16), 6388–6392.

(40) Britton, L.; Docherty, J. H.; Nichol, G. S.; Dominey, A. P.; Thomas, S. P. Iron-catalysed C(Sp^2)-H Borylation with Expanded Functional Group Tolerance†. *Chin. J. Chem.* **2022**, *40* (24), 2875–2881.